Chouinard RL, 2018, Surficial geochemical exploration tools for porphyry Cu-Mo mineralization in till-covered terrain, south-central British Columbia, MSc Thesis, UBC, BC, 263 p.

NSERC-CMIC Mineral Exploration Footprints Project Contribution 194.

SURFICIAL GEOCHEMICAL EXPLORATION TOOLS FOR PORPHYRY Cu-Mo MINERALISATION IN TILL-COVERED TERRAIN, SOUTH-CENTRAL BRITISH COLUMBIA

by

Rachel L.M. Chouinard

B.Sc., Brock University, 2014

A THESIS SUBMITTED IN PARTIAL FULFILLMENT OF

THE REQUIREMENTS FOR THE DEGREE OF

MASTER OF SCIENCE

in

THE FACULTY OF GRADUATE AND POSTDOCTORAL STUDIES

(Geological Sciences)

THE UNIVERSITY OF BRITISH COLUMBIA

(Vancouver)

Month 2018

Abstract

The Intermontane Belt of British Columbia is renowned for the endowment of porphyry Cu deposits. As the discovery of porphyry Cu deposits from outcropping mineralised bedrock decreases, mineral exploration is required to adapt new strategies and techniques for exploring deeper. This is especially important in areas with disconnected transported cover, such as the Quaternary glacial sediments that cover much of North America.

Surficial geochemical exploration strategies to detect the presence of known bedrock mineralisation through transported cover were evaluated at two areas of porphyry Cu-Mo mineralisation, Highmont South and J.A., at the Highland Valley Copper property (Teck Resources Limited). The Highmont South target subcrops below 2–10 metres of subglacial till, whereas the J.A. target is concealed by a thick sequence of pre-Quaternary to Holocene sediments, averaging 170 metres and up to 300 metres in thickness. Detailed surficial mapping at both targets followed by upper B horizon soil sampling, physicochemical measurements, profile sampling, biogeochemical and dendrochemical sampling, and installation of passive soil hydrocarbon collector modules was undertaken to characterise the mineralogical and chemical changes that develop in the surficial environment after glacial dispersal and soil development. Soil samples were analysed by ICP-MS following digestion by aqua regia and deionised water leach; and by field-portable X-ray fluorescence. Select anomalous and background samples were subject to sequential selective extractions and/or for Cu isotope analysis to establish the provenance of the geochemical responses. Lodgepole pine needles were digested with aqua regia and analysed by ICP-MS.

Anomalous Cu, Mo, Ag, Bi, Sb, As, and W in upper B horizon soils overlying mineralisation at Highmont South is attributed to local glacial transport of weathered porphyry material. Anomalous Cu, Ag, Sb, and W in upper B horizon soils above the trace of the West Highmont fault, which crosscuts mineralisation, is attributed to metal-bearing groundwater migrating along the fault. Vegetation uptake and cycling is responsible for elevated concentrations of Mo in lodgepole pine needles sampled from trees growing above and proximal to bedrock mineralisation, as well as contributing to elevated soil Mo concentrations in the corresponding area. An additional response of long-chain normal alkane hydrocarbons (C_{12}-C_{15}) is identified in the soil overlying mineralisation and the trace of the West Highmont fault.

There is no evidence for a surficial geochemical response to deeply buried porphyry Cu-Mo mineralised bedrock at J.A. Surficial geochemistry is controlled by differences in several surficial material types, both glacial and post-glacial, as well as hydromorphic processes and potential anthropogenic influences. A clastic response to mineralisation at J.A. is unlikely due to pre-Quaternary cover shielding the mineralised bedrock from glacial erosion during the most recent glaciation. A potential surficial signal generated by vertical ion migration from underlying bedrock could be confounded by a number of factors including: the thickness of cover, low porosity and permeability of the pre-Quaternary sequences, the high variability of surficial material types, and/or anthropogenic influences.

Preface

The author and supervisors Dr. Peter Winterburn and Dr. Martin Ross are responsible for project design and identification of research objectives. Additional research committee members Steve Cook and Dr. Craig Hart, as well as Research Associate Dr. Robert Lee, are credited for providing input at committee meetings and through independent correspondence.

The author is accountable for the following:

- Landscape and surficial material mapping;
- Upper B horizon soil, soil profile, vegetation, and tree core sampling;
- Measurement of soil physicochemical properties;
- Installation and recovery of AGI Sampler hydrocarbon modules;
- Sample selection for Cu isotope analysis, sequential extractions, and dendrochemical analysis;
- Completion of pXRF analysis;
- Interpretation of analytical data.

Soil samples were analysed at Bureau Veritas (BV) Laboratories in Vancouver by aqua regia digest and deionised water leach. Selected soil samples were analysed at ALS Minerals (ALS) in North Vancouver by sequential selection extractions. Copper isotopes were analysed at the Pacific Centre for Isotope and Geochemical Research (PCIGR) at The University of British Columbia in Vancouver. Vegetation samples were analysed at BV by aqua regia digest. Dendrochemical analysis was completed on selected tree core samples at the Queen's Facility for Isotope Research (QFIR) at Queen's University in Kingston, Ontario. Hydrocarbon analysis

from AGI Sampler hydrocarbon modules was completed by Amplified Geochemical Imaging (AGI) in Newark, Delaware, U.S.A.

The author is responsible for interpretation of data from each analysis, under the supervision of Dr. Peter Winterburn. Interpretation of AGI Sampler hydrocarbon module data was provided by AGI and is available in Appendix F, however the author's independent interpretations are also included in this study.

Table of Contents

List of Tables

List of Figures

List of Abbreviations

Soil horizons*:

Ae = eluviated mineral horizon near surface

Aej = juvenile eluviated mineral horizon near surface

Ah = mineral horizon near surface with accumulation of organic matter

B = mineral horizon between A and C horizons, typically illuviated from eluviation of A horizon

BC = mineral horizons undifferentiated

Bm = mineral horizon with colour altered as a result of oxidation

C = mineral horizon unaffected by pedogenic processes operating in A and B horizons

LFH = organic veneer from the accumulation of organic litter (e.g. leaves, twigs, needles)

O = organic horizon developed mainly from decomposed organic material (e.g. moss, wood fibre)

**Refer to: Canadian System for Soil Classification, 3rd Edition (Agriculture Canada, 1998)*

Surficial map units:**

A = undifferentiated alluvial sediments

Af = alluvial fan sediments

Ap = alluvial floodplain sediments

At = alluvial terraced sediments

Cv = colluvial veneer

Cz = landslide deposits

GFb = glaciofluvial sediment blanket

GFh = hummocky glaciofluvial sediments

GFk = glaciofluvial kame terraced sediments

GFp = glaciofluvial outwash plain sediments

GFr = glaciofluvial esker sediments

GFt = glaciofluvial terraced sediments

GL = undifferentiated glaciolacustrine sediments

GLd = glaciolacustrine deltaic sediments

GLv = glaciolacustrine veneer

H = undifferentiated anthropogenic deposits

L = undifferentiated lacustrine sediments

O = undifferentiated organic deposits

Owb = organic bog peat deposits

Owf = organic fen peat deposits

R = undifferentiated bedrock

Tb = till blanket

Th = hummocky till

Ts = streamlined and fluted till

Tv = till veneer

***Refer to: Science language for an integrated Geological Survey of Canada data model for surficial geology maps, version 2.0 (Deblonde et al., 2012)*

Other:

$4A_s$ = four acid (in sequence)

AGI = Amplified Geochemical Imaging

AIF = annual information factsheet

AmA_s = ammonium acetate-acetic acid leach (in sequence)

AMSL = above mean sea level

AR = aqua regia digest

AR_s = aqua regia digest (in sequence)

ARIS = Assessment Report Indexing System

BC = British Columbia

BCGS = British Columbia Geological Survey

BV = Bureau Veritas

CEC = cation exchange capacity

CHH_s = cold hydroxylamine-hydrochloride leach (in sequence)

CMIC = Canadian Mining Innovation Council

CMT = culturally modified tree

C_{org} = organic carbon

CRM = certified reference material

DIW = deionised water leach

DW_s = deionised water leach (in sequence)

EC = electrical conductivity

EGI = Exploration Geochemistry Initiative

GCB = Guichon Creek batholith

GSC = Geological Survey of Canada

HHH_s = hot hydroxylamine-hydrochloride leach (in sequence)

HR-ICP-MS = high resolution inductively coupled plasma-mass spectrometry

HVC = Highland Valley Copper

ICP-AES = inductively coupled plasma-atomic emission spectroscopy

ICP-MS = inductively coupled plasma-mass spectrometry

ICP-OES = inductively coupled plasma-optical emission spectrometry

IDH = Inverse Difference Hydrogen

IP = induced polarisation

IRM = internal reference material

ka = thousand years

Ma = million years

Mt = million tonnes

MDL = minimum detection limit

MDRU = Mineral Deposit Research Unit

MPB = mountain pine beetle

MPD = mean percent difference

Mt = million tonnes

NAD = North American Datum

NaP_s = sodium pyrophosphate leach (in sequence)

NIST = National Institute of Standards and Technology

NRCan = Natural Resources Canada

NSERC = National Science and Engineering Research Council

OREAS = Ore Research and Exploration Pty Ltd.

ORP = oxidation reduction potential

PCIGR = Pacific Centre for Isotopic and Geochemical Research

PIMs = porphyry indicator minerals

pXRF = portable x-ray fluorescence

QA/QC = quality assurance/quality control

Q-ICP-MS = quadrupole inductively coupled-mass spectrometry

REE = rare earth element

RSD = relative standard deviation

SD = standard deviation

SGH = Spatiotemporal Geochemical Hydrocarbon

SOM = soil organic matter

TD-GC/MS = thermal desorption gas chromatography-mass spectrometry

TDS = total dissolved solids

TGI-4 = Targeted Geoscience Initiative 4

UBC = University of British Columbia

UTM = Universal Transverse Mercator

Acknowledgements

First and foremost I would like to extend a heartfelt thank you to my direct supervisor Peter Winterburn. This thesis would just be 200+ bags of soil without his patient guidance, leadership, and encouragement. Peter's commitment to teaching and unwavering support of his students is truly appreciated and has made us all better scientists. Co-supervisor Martin Ross as well as committee members Steve Cook and Craig Hart are thanked for their constructive feedback and support. Research Associate Robert Lee is profusely thanked for all of his support and relentless behind-the-scenes work that made this project possible.

The Teck Resources Limited personnel at Highland Valley Copper are greatly appreciated for allowing access to the site and guidance in the field (Gerald Grubisa, James Stemler, Kevin Byrne, John Ryan, Semyon Martenenko, Miguel Alfaro, Julia Scott, Derek Brillinger). A special thank you is extended to Colin Dunn for his expertise and wonderful generosity in supplying internal reference material for vegetation sampling. Kurt Kyser is greatly appreciated for his support in dendrochemical analysis. His passion for science will be remembered fondly. The MDRU team, especially Sara Jenkins, is thanked for the organisation and technical support. To my fellow Exploration Geochemistry Initiative members Matt Bodnar, Shane Rich, Erika Cayer and Ally Brown: thank you for the discussions and help over the years. Luana Yeung and Darius Kamal are appreciated for their hard work as field assistants.

This study was undertaken as part of the joint Natural Sciences and Engineering Research Council of Canada (NSERC) and Canadian Mining Innovation Council (CMIC) project "Integrated Multi-Parameter Footprints of Ore Systems". Financial support from Bureau Veritas and NSERC made the Exploration Geochemistry Initiative at the MDRU possible. Additional

financial support in the form of scholarships was provided by Geoscience BC and Endeavour Silver Corporation. Contributions of equipment and expertise by Olympus, Reflex Geosciences and AGI are appreciated.

Finally, I would like to thank my family and friends for their love and support. I owe my deepest gratitude to Cameron Green for his patience which carried me through this journey. The true friendship and guidance from Guillaume Lesage will forever be appreciated.

Chapter 1: Introduction

1.1 Rationale for study

South-central British Columbia (BC) is well known for its endowment of porphyry Cu deposits (McMillan and Panteleyev, 1995). These include calc-alkalic porphyry Cu-Mo (±Au) and alkalic porphyry Cu-Au systems (Logan and Schroeter, 2013). The economy of BC has benefited greatly from the development of many of these deposits, mostly discovered from outcropping mineralisation and alteration patterns or from geochemical anomalies produced by subcropping mineralisation under thin till of local provenance. As the number of outcropping and subcropping discoveries declines, exploration geologists must develop techniques to explore for those covered with thicker till or more complex stratigraphy that conceals both mineralised bedrock and locally-derived till.

This project is part of the Porphyry Cu Subproject of the National Sciences and Engineering Research Council (NSERC) and Canadian Mining Innovation Council (CMIC) Mineral Exploration Footprints project. The Porphyry Cu Subproject aims to quantify and identify the footprint of porphyry Cu-(Mo) mineralisation at the Highland Valley Copper (HVC; Teck Resources Limited; "Teck") operation in south-central BC, through a multidisciplinary, integrated geoscience study. The research was undertaken within the Mineral Deposit Research Unit (MDRU) Exploration Geochemistry Initiative, a collaborative research program established at The University of British Columbia (UBC) to develop geochemical exploration models based on the mobility and transport of elements from buried mineralised bedrock to the more easily accessible surface-air interface.

The identified deposits at HVC comprise five main clusters of porphyry-style Cu-Mo mineralisation, whose current state of production ranges from undeveloped to developed. The undeveloped J.A. and Highmont South targets, the subjects of this investigation, comprise two mineralised zones that are buried under variable thicknesses of unconsolidated sediments of various origins. Surficial geochemical studies at these two buried porphyry targets aim to fully characterise mineralogical and chemical changes that develop in the surficial environment after glacial dispersal and soil development. This research will develop surficial geochemical exploration models and practical strategies that may be applied to the search for other buried Cu-(Mo) porphyry mineralisation in recently glaciated environments.

1.2 Thesis objectives

The objectives of this research are to:

- define the surficial response, in a variety of potential common geochemical sampling media, to the presence of buried Cu-Mo porphyry mineralisation at Highland Valley Copper;
- identify the processes contributing to the generation of false anomalies and noise in the geochemical data; and
- evaluate various exploration methods to develop a future framework for surficial geochemical exploration of buried porphyry-Cu deposits in till-covered terrain.

1.3 Thesis structure

This thesis is divided into six chapters, outlined below.

Chapter 1: Introduction

Introduces the rational and objectives of the thesis, provides background information, including geologic setting and glacial history of the project site, and outlines previous surficial geochemical exploration conducted at site.

Chapter 2: Mechanisms of trace element dispersion through transported cover

Presents proposed mechanisms from literature of ion migration from mineralised bedrock upward through young, glacially transported cover.

Chapter 3: Methods

Outlines methodologies employed in the research, including: surficial mapping, collection of geochemical samples, and methods of analysis of these samples in the laboratory.

Chapter 4: Surficial geochemistry of the buried Highmont South target at HVC

Presents results obtained in the surficial geochemical studies conducted in the Highmont South field area at HVC.

Chapter 5: Surficial geochemistry of the buried J.A. target at HVC

Presents results obtained in the surficial geochemical studies conducted in the J.A. field area at HVC.

Chapter 6: Discussion and conclusions

Presents general discussion and conclusions for the results obtained from both field areas and models for formation of surficial geochemical anomalies.

Chapter 7: Exploration implications and recommendations for future work

Provides implications for surficial geochemical exploration strategy and suggests directions for future research.

1.4 Porphyry Cu deposits in south-central British Columbia

British Columbia has a large number of porphyry deposits, related to island-arc magmatism on the fringes of ancestral North America in the early Mesozoic (Logan and Mihalynuk, 2014). The Quesnel terrane, which spans the length of the Canadian Cordillera, represents an island-arc setting in which east-dipping subduction resulted in the formation of both alkalic porphyry Cu-Au and calc-alkalic porphyry Cu-Mo deposits (Logan and Schroeter, 2013). Subduction in the southern Quesnel terrane migrated eastward over time, resulting in a general trend of older calc-alkalic Cu-Mo deposits in the western portion (e.g. Highland Valley Copper, 209–207 Ma; Gibraltar, 212 Ma) to alkalic Cu-Au deposits in the east (e.g. Mount Polley, 205 Ma; New Afton, 201 Ma) (Lee et al., 2017; Logan and Mihalynuk, 2014; Logan and Schroeter, 2013). A second phase of porphyry formation occurred in an intracontinental arc setting in the Late Mesozoic to Cenozoic. This phase is attributed to crustal thickening and decompression melting after the island-arc terranes were accreted onto western North America (Logan and Mihalynuk, 2014).

1.5 Geologic setting of Highland Valley Copper

1.5.1 Regional geologic and tectonic setting

The HVC deposits are located within the Quesnel island arc terrane, which together with the Stikine and Cache Creek terranes comprise the Intermontane Belt of central BC (Logan and Schroeter, 2016). The cluster of porphyry Cu-Mo mineralised centres at HVC is centrally located

within the Late Triassic, calc-alkaline Guichon Creek batholith (Figure 1-1) (Byrne et al., 2013). The batholith was emplaced into the western belt of Late Carnian to Norian volcanic and volcanoclastic rocks of the Nicola Group (D'Angelo et al., 2017). The Nicola Group is comprised of four belts of submarine island-arc volcanic rocks and associated sedimentary rocks that were deposited in a rifted marine basin above an east-dipping subduction zone (Logan, 2013). The batholith, along with several other large plutons in the Quesnel terrane, is likely co-magmatic with the Nicola Group (Logan and Schroeter, 2016). The Guichon Creek batholith is compositionally zoned, consisting of several intrusive facies which, from the margins to the centre, decrease in age and transition from mafic to felsic (Byrne et al., 2013).

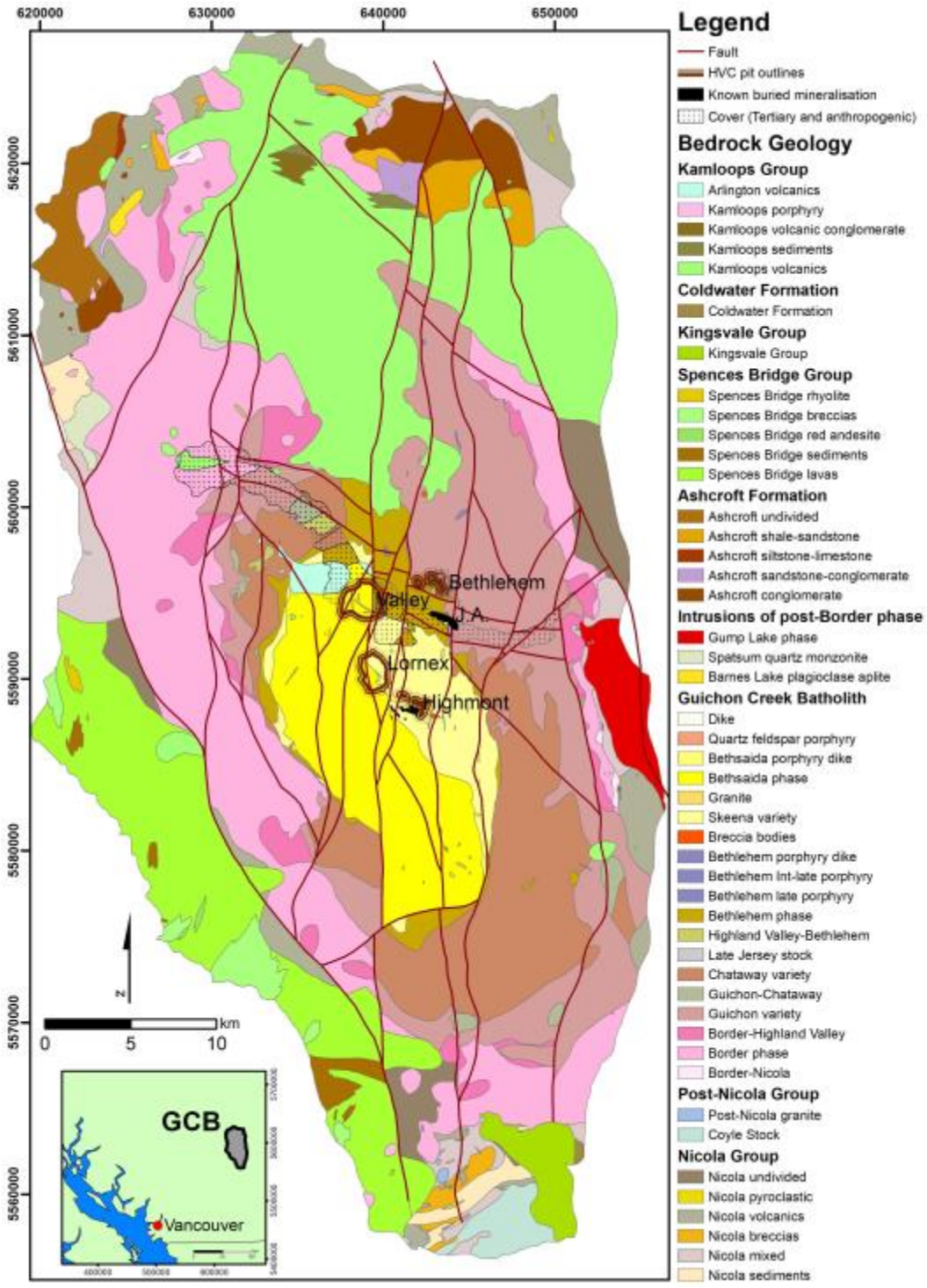

Figure 1-1. Bedrock geology of the Guichon Creek batholith in south-central British Columbia (see inset), with pit outlines and known buried mineralisation at Highland Valley Copper (pers. comm., Teck, 2017). Geology (based on work completed in August 2016 by Teck and CMIC, and modified from McMillan et al. (2009)) is shown with the exception of areas underneath stippling (which represents anthropogenic and Tertiary cover) which are from McMillan et al. (2009).

1.5.2 Local bedrock geology

Highland Valley Copper consists of five known porphyry Cu-Mo mineralised bodies: the currently producing Valley, Lornex, and Highmont pits, the past producing Bethlehem deposit, and the buried and undeveloped J.A. target. The Highland Valley deposits are spatially associated with the younger, coarse-grained porphyritic granodiorite Bethlehem and Bethsaida facies of the Guichon Creek batholith (Byrne et al., 2013).

Two separate porphyry Cu-Mo mineralisation events are inferred at ~209 Ma and 207 Ma (Byrne et al., 2013; D'Angelo et al., 2017). The older event formed the cluster of mineralised centres that comprise the Bethlehem deposit (Iona, Jersey, and Huestis pits), and the younger event formed the more Mo-rich Valley, Lornex, and Highmont deposits, and possibly the J.A. target (Byrne et al., 2013). The north-striking Lornex fault bisects mineralisation, interpreted to have dextrally offset a single centre of mineralisation by 3.5 kilometres, resulting in separation of the Lornex and Valley deposits (Byrne et al., 2013).

1.5.3 Bedrock mineralisation

Each porphyry centre at Highland Valley exhibits the same general trend of Cu-Fe sulphide zoning, grading outwards through a bornite-dominant core to a chalcopyrite > bornite zone to pyrite ± chalcopyrite and pyrite-only zone (Byrne et al., 2013; Lesage et al., 2016). The porphyry deposits are generally high in bornite and low in pyrite. The older pulse of mineralisation that formed the Bethlehem deposits was less Mo-rich than the younger pulse which formed Valley, Lornex, Highmont – and, possibly, J.A. Copper and Mo mineralisation at Bethlehem is associated with quartz veins with K feldspar (± biotite) halos, sulphide-only veins, and fractures or veins with sericite envelopes (Byrne et al., 2013). Common sulphide minerals are

chalcopyrite, bornite, pyrite, and molybdenite, with lesser chalcocite. These are often accompanied by specular hematite and, less often, magnetite. At Valley, Lornex, Highmont, and J.A., mineralisation is typically higher grade in areas of high vein density (Byrne et al., 2013).

As a whole, the HVC deposits contain relatively low grade mineralisation (McMillan, 1985; Byrne et al., 2013). Together, the Valley, Lornex, and Highmont deposits contain proven and probable reserves of 546.6 Mt at 0.29% Cu and 0.008% Mo, calculated with a 0.10% Cu equivalent cut-off (Teck 2017 AIF, February 2018).

1.5.4 Bedrock alteration

Porphyry-related hydrothermal alteration in the Highland Valley district includes mainly potassic alteration (K feldspar ± biotite), sodic-calcic alteration (albite-chlorite-epidote ± actinolite ± diopside ± garnet), coarse-grained white mica alteration, and white mica-chlorite-prehnite alteration (Lesage et al., 2016; 2017). At the Valley and Lornex deposits, Cu mineralisation is strongly associated with quartz veins and fractures with coarse grey muscovite halos. At the Bethlehem deposits, there is a strong association between Cu mineralisation and quartz veins with K feldspar (± biotite) alteration halos. J.A. and Highmont exhibit an association of both Cu and Mo mineralisation with pervasive and vein- and fracture-controlled sericite alteration (± quartz veins) (Byrne et al., 2013).

1.5.5 Surficial geology

Present-day physiography of the study area is strongly influenced by the style of deglaciation that occurred in the region. Rolling uplands and steep-walled, flat-floored valleys characteristic to the field sites are a function of ice retreating northward and the development of ice-contact

and proglacial land systems, including various glaciolacustrine and glaciofluvial deposits (Bobrowsky et al., 2002).

Much of the Highland Valley area is covered by varying thicknesses of glacial sediments, the product of a regional Late Wisconsinan ice-flow trending predominantly south-southeast (Figure 1-2) (Plouffe and Ferbey, 2015a). Bedrock typically outcrops in areas of thin cover, where streams have incised through cover material, and can also be found in areas of thicker cover at the stoss (up ice-flow) ends of glacial features such as crag and tail ridges (Ferbey et al., 2016).

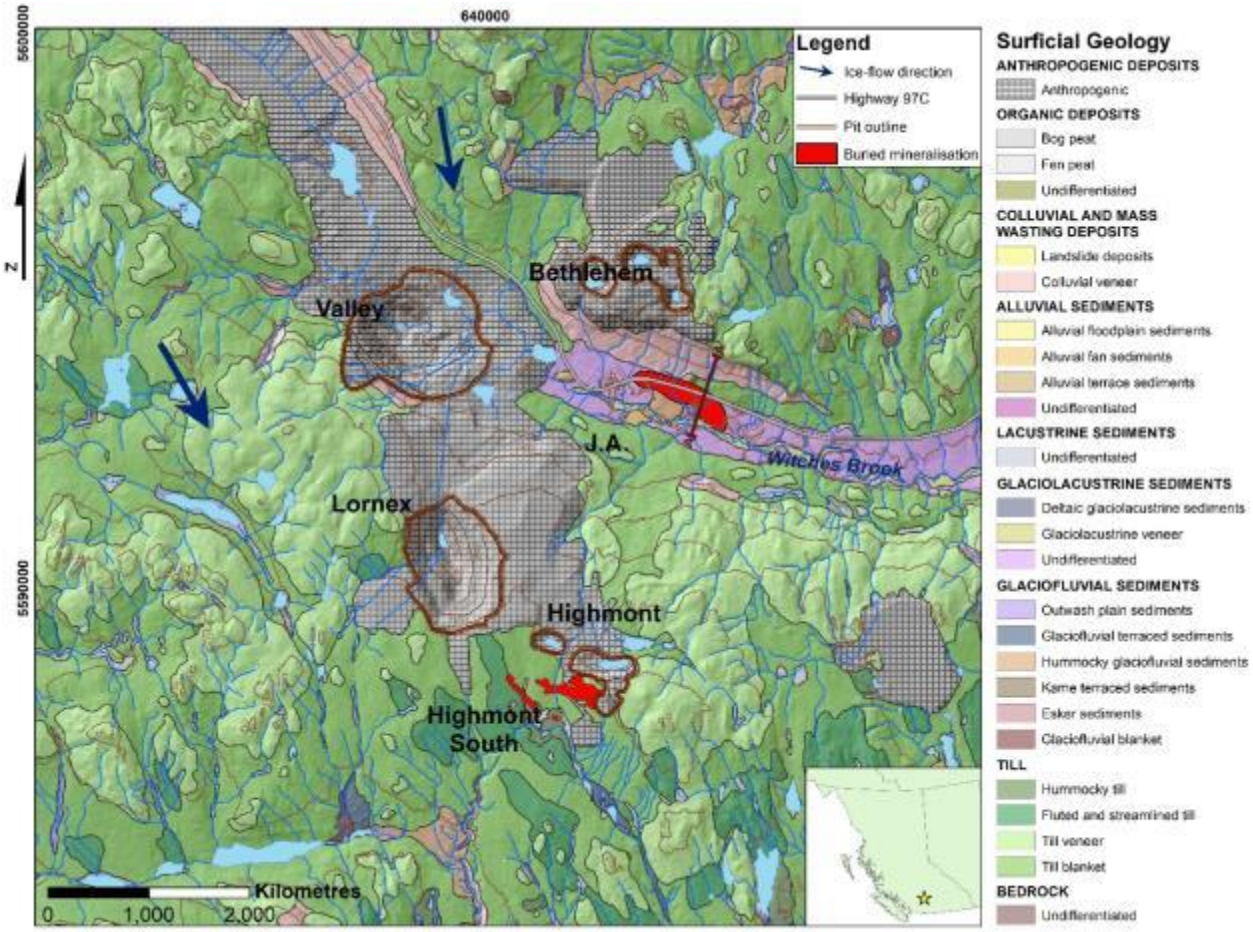

Figure 1-2. Surficial geology of the HVC region (Plouffe and Ferbey, 2015b). A–A' line represents location of cross section depicted in Fig. 1-3. Contours plotted with 100 metre interval spacing. Pit outlines and location of Highmont South buried mineralisation provided by Teck (pers. comm., Teck, 2018); J.A. buried mineralisation from McMillan (1985).

1.5.5.1 Glacial history

The Highland Valley area was most recently glaciated during the Late Wisconsinan (Clague and Ward, 2013). The Cordilleran ice sheet was formed when ice advanced out of northwestern alpine areas of accumulation onto the Interior Plateau (Stumpf et al., 2000). A relatively simple south-southeast ice-flow history was interpreted for the HVC area by Plouffe and Ferbey (2015a) based on glacial landforms such as drumlins, flutings, and crag-and-tails on air photos, and outcrop-scale ice-flow indicators such as striations and grooves from their own mapping, as well as from previous studies (Tipper, 1971a, b; Fulton, 1975; Ryder, 1976; Clague, 1989; Ryder et al., 1991; Bobrowsky et al., 1993, 2002; Plouffe et al., 2011; Ferbey et al., 2013; Plouffe et al., 2013a, b).

The single regional ice-flow phase reconstruction from the surficial mapping effort indicates that the till exposed at surface is likely to have been transported along one dominant ice-flow direction. This should simplify the tracing of till constituents to their respective up-ice bedrock source. Other tills occurring in the subsurface along the buried portion of the valley where thick deposits are known to occur (Bobrowsky, 1993) might record a more complex history not preserved in the surficial record. However, this thesis focuses on till at or close to the surface. For the purpose of this research the surficial till is thus expected to have been mainly transported in a south-southeast direction according to previous work.

1.5.5.2 Glacial diamicton (till) facies

Two facies of glacial diamicton (till) in the Highland Valley mine area are recognised and described by Ferbey et al. (2016): a regionally developed subglacial traction till deposited under moving ice at the glacier/substrate interface; and an overlying locally developed ablation till,

which may comprise sediment transported from within the entire ice column and deposited through melt-out processes (Evans et al., 2006).

The subglacial traction till is described as a well-compacted, massive, and relatively clay-rich cobble-boulder diamicton (Ferbey et al., 2016). Cobbles and boulders mainly comprise local intrusive and occasionally local extrusive lithologies, most of which display striations. The stratigraphically higher ablation till is poorly compacted, poorly sorted, and has less clay content than the subglacial till (Ferbey et al., 2016). The ablation till has a greater proportion of cobbles and boulders than the subglacial till, with the same local lithologies, but rarely displaying striations (Ferbey et al., 2016). The abundance of sand and silt in both till facies is attributed to the glacial incorporation of local Guichon Creek batholith medium-grained granodiorite (Ferbey et al., 2016).

1.5.6 Concealed mineralisation

1.5.6.1 Highmont South

The zone at Highmont South is interpreted to be auxiliary mineralisation to the main Highmont deposits which are located approximately 1 kilometres to the northeast (McMillan et al., 2009; Byrne et al., 2013). The buried Highmont South target subcrops beneath 2–10 metres of subglacial till (averaging 5–6 metres; based on historic drilling, pers. comm., Teck, 2016).

The Highmont South targets consist of small northwest-trending lobes near and subparallel to the lithological boundary between the Skeena variety quartz diorite and the Bethsaida facies quartz monzonite (Reed and Jambor, 1976; McMillan, 1985). A large composite quartz-feldspar porphyry dike was emplaced to the north of Highmont South and is interpreted to have had a significant influence on the development of the Highmont deposits as a whole, specifically by

controlling sulphide zoning (Byrne et al., 2013). This porphyry dike, as well as the lithological contact between the Skeena variety and Bethsaida phase, is cut by the north-striking West Highmont fault causing an apparent horizontal left-lateral displacement of 54 metres (Reed and Jambor, 1976; McMillan, 1985).

Sulphide mineralisation at Highmont South is not well understood and thus inferences must be made from the main Highmont deposits. Common sulphide minerals at Highmont are chalcopyrite, bornite, and molybdenite (McMillan, 1985). Mineralisation mainly occurs in veins and as minor disseminations, and zones outwards from the composite dike as bornite > chalcopyrite, to mainly chalcopyrite, to pyrite-chalcopyrite ± bornite (Byrne et al., 2013). Pyrite is not abundant (McMillan, 1985). Molybdenite occurs in zones with and without Cu mineralisation, and overall there is poor spatial correlation between Mo and Cu. Copper mineralisation is correlated with domains of intense sericite alteration (Byrne et al., 2013).

Intensity of hydrothermal alteration at Highmont is lower than the Valley-Lornex deposits (McMillan, 1985). Quartz/sericite alteration is typically fracture-controlled rather than pervasive and overprints broad domains of biotite alteration (Byrne et al., 2013). Abundances of tourmaline and specular hematite increase towards the composite dike and form crackle breccias within the dike. Oxidation of the Highmont deposits is minor, increasing significantly along faults (Reed and Jambor, 1976).

1.5.6.2 J.A.

The J.A. porphyry system is a blind target named after the chairman of the Bethlehem Copper Corporation, J.A. McClelland (McMillan, 1976). Concealing the mineralised bedrock at J.A. is a thick sequence of preglacial and glacial sediments, averaging 170 metres and locally up to 300

metres in thickness (based on historic drilling, pers. comm., Teck, 2016). Local accumulations of unconsolidated preglacial sediments shielded the mineralised bedrock from erosion during the last glaciation (Plouffe and Ferbey, 2015a).

The J.A. target is located in a down-dropped fault block, straddling the contact between the Bethlehem granodiorite and the quartz diorite to granodiorite of the Guichon sub-facies (Figure 1-3). Down-dropping of the fault block occurred post-mineralisation during the block-faulting that produced the Witches Brook valley (McMillan, 1976). The body of mineralisation is elongated along a northwest-trending axis and appears to divide into two zones at depth (Byrne et al., 2013). The Guichon-Bethlehem contact in the southern portion of the deposit is cut by a quartz-plagioclase porphyry stock, interpreted as an offshoot to the Bethsaida facies (McMillan, 1976). The highest Cu grades occur adjacent to the Guichon-Bethlehem contact directly north of the porphyry stock in a densely fractured zone which acted as a porous trap for mineralising fluids. Mineralised quartz veins and mineralised quartz-sericite zones only locally influence grades (Byrne et al., 2013).

The economically important sulphide minerals in the J.A. target are chalcopyrite, bornite and molybdenite, with pyrite (McMillan, 1976). Alteration consists of intense sericite-kaolinite zoning northward and moderate to weak feldspar alteration more abundant in the country rock than the porphyry stock (McMillan, 1976; Byrne et al., 2013). The deposit is structurally controlled within a framework of high-angle west-northwest-striking faults interpreted to be post-emplacement of the Guichon Creek batholith, however prior to mineralisation (Byrne et al., 2013).

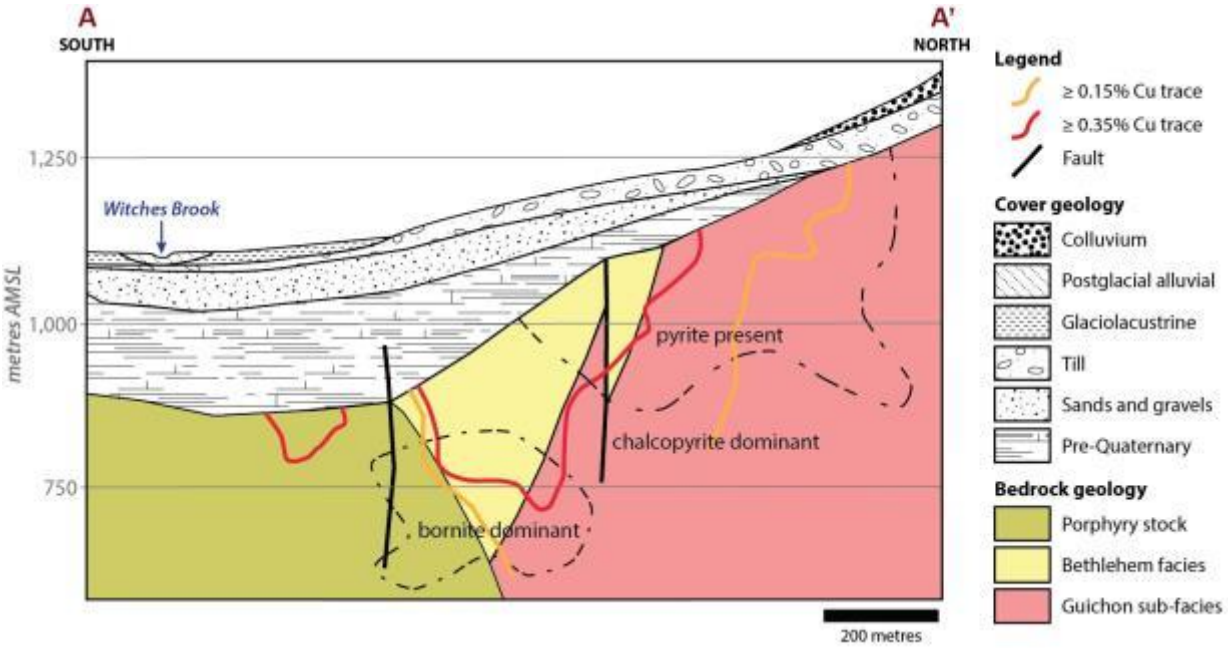

Figure 1-3. Simplified cross section of bedrock geology, mineralisation, and cover types at the J.A. target. Location of section indicated in Fig. 1-2. Modified after Byrne et al. (2013). Pre-Quaternary cover includes bedrock and unconsolidated sediment sequences (Bobrowsky, 1993). Cover sequence is approximate and is based on drilling results (pers. comm., Teck and CMIC, 2016).

1.5.7 History of discoveries

Discovery of the Highmont deposit occurred in the 1930s from outcropping Cu and Mo sulphide mineralisation located on nearby higher ground. This led to prolonged exploration of the Highmont area, which included percussion and diamond drilling, IP surveys, and an adit for underground bulk sampling (Reed and Jambor, 1976). The main Highmont orebodies were delineated by Teck in 1966 through an IP survey and step-out drilling. Production at the main Highmont deposit spanned from the period 1980 to 1984, and resumed in 2005 (Byrne et al., 2013). The smaller auxiliary sulphide bodies at Highmont South are buried targets and remain subject to further exploration. The main Highmont deposit's total measured and indicated resources are 110.9 Mt at 0.14 % Cu and 0.014 % Mo, with proven and probable reserves of 55

Mt as of 2013, calculated with 0.1% Cu equivalent cut-offs (Byrne et al., 2013, and references therein).

J.A. was discovered in 1971 by Bethlehem Copper Corporation by step-out drilling on the north margin of Highland Valley while following a weak IP anomaly (McMillan 1976; Casselman et al., 1995). Estimates based on diamond drilling in the 1970s give the J.A. target a non-NI 43-101-compliant historic resource of 260 million tonnes at 0.43% Cu and 0.017% Mo (McMillan, 1976).

1.6 Previous surficial geochemical exploration

Previous surficial geochemical exploration within the Guichon Creek batholith includes soil, stream sediment, and till sampling (Figure 1-4).

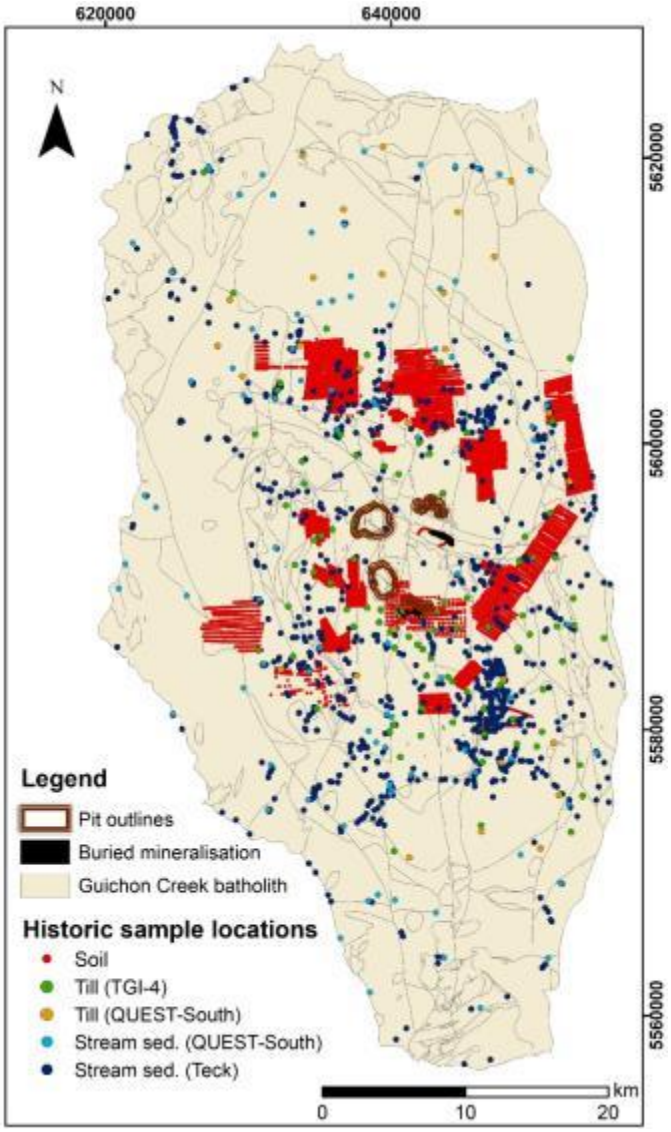

Figure 1-4. Locations of past soil (1958–2014), till (2009–2015), and stream sediment (1979–2009) samples in the Guichon Creek batholith (Teck and CMIC compilations, pers. comm., Robert Lee, 2016; Geoscience BC, 2010; Plouffe and Ferbey, 2015a). Pit outlines and Highmont South buried mineralisation provided by Teck (pers. comm., Teck, 2018); J.A. buried mineralisation from McMillan (1985); Guichon Creek batholith modified from McMillan et al. (2009).

1.6.1 Soil sampling

Soil sampling surveys in the Highland Valley district date back to 1958, with approximately 16,513 reported soil samples from 23 different surveys (Teck and CMIC compilation, pers. comm., Robert Lee, 2016). Most surveys reported the B horizon as a target for soil sample

material, however some sampled A or C horizon material. Analytical data available to the author report soil concentrations of the elements Cu, Mo, and Ag.

A soil sampling survey in the Highmont area was conducted by Kennco Explorations Ltd. in 1959. This consisted of a reconnaissance survey of an 800 feet by 800 feet grid of soil samples across the entire area, after which samples were taken at 100 feet spacing along transects based on initial anomalous soil or geophysical results (Stevenson, 1959). Soil sampling targeted B horizon soil where possible. Copper (Figures 1-5, 1-6), the only element analysed, was determined by hot nitric acid extraction (instrumentation unreported) at the UBC geochemical laboratory (Stevenson, 1959). In the context of known surficial geology and bedrock mineralisation (Figure 1-5), the soil sampling was moderately successful over the Highmont South field area. Results over the main Highmont bodies are variable however anomalous Cu up to 3,100 ppm was detected.

Copper results from the 1959 Kennco soil survey are comparable to the results from this study as well as those from a survey conducted by Teck in 2014 (Figure 1-6).

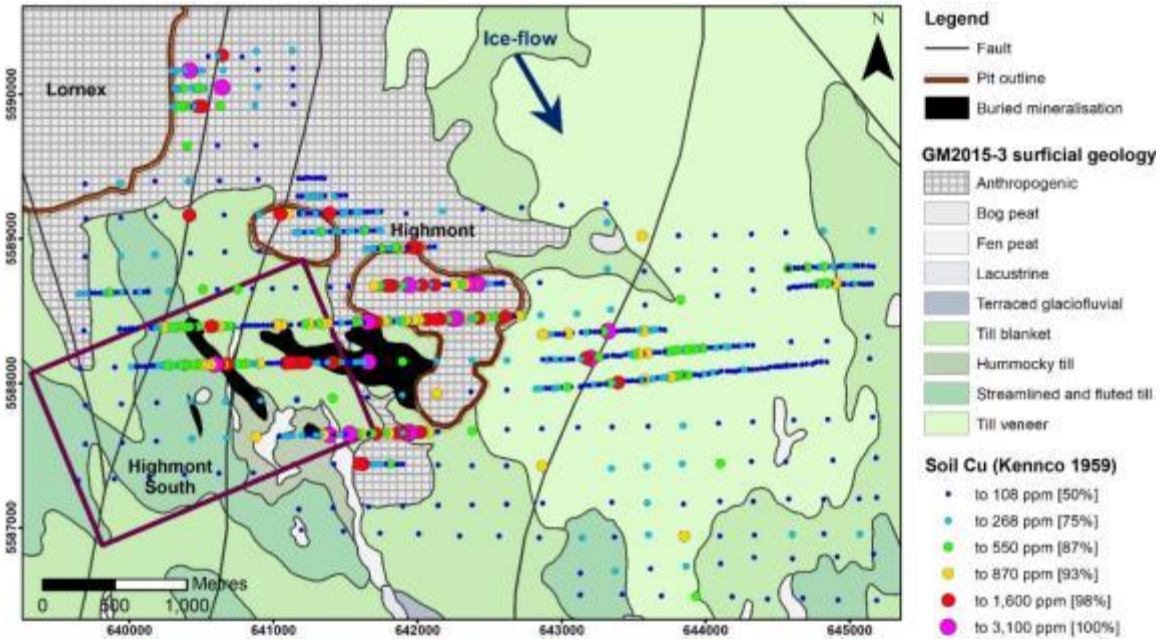

Figure 1-5. Soil Cu results from Kennco Explorations' 1959 geochemical survey are plotted over modern surficial geology (Plouffe and Ferbey, 2015b) with known buried bedrock mineralisation (pers. comm., Teck, 2018). Data plotted by simple percentile intervals. Note: anthropogenic deposits were not present in 1959 as shown in current map, and the Highmont deposit had not been exposed by mining activities. Faults based on work completed in August 2016 by Teck and CMIC, and modified from McMillan et al. (2009). Purple box shows Highmont South field mapping area for this study.

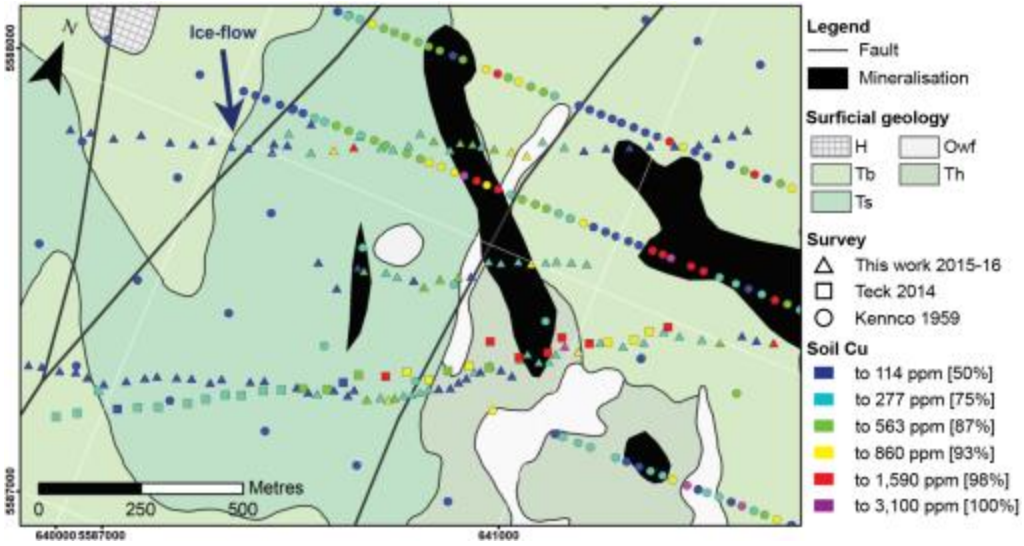

Figure 1-6. Highmont South soil Cu results from this study (2015–16), Teck's 2014 survey, and Kennco Explorations' 1959 survey. Results are plotted over modern surficial geology (Plouffe and Ferbey, 2015b) with buried bedrock mineralisation (pers. comm., Teck, 2017). Data plotted by simple percentile intervals. Note: anthropogenic deposits were not present in 1959 as shown in the current map. Faults based on work completed in August 2016 by Teck and CMIC, and modified from McMillan et al. (2009). Abbreviations: H = anthropogenic; Owf = fen peat; Tb = till blanket; Th = hummocky till; Ts = streamlined and fluted till.

A geochemical orientation survey was conducted by Teck in 2014 over the J.A. and Highmont South areas of buried mineralisation. Seventy-five B horizon soil samples were collected and processed with separate sodium pyrophosphate leach, aqua regia digest, and Ionic Leach™, all analysed by inductively coupled plasma-mass spectrometry (ICP-MS) at ALS Laboratories in Vancouver, BC. The survey included pH and acidified pH measurements of soil-deionised water slurries 1:1 by volume at each sample site. All survey metadata and analytical results were made available to the author.

The author planned a soil sampling transect at Highmont South to closely match that of Teck's in order to compare geochemical results. Soil analysis by aqua regia digest with ICP-MS finish yielded similar results between the two studies. Teck's data shows Cu (Figure 1-7), Mo, Ag, and Bi anomalies in soils overlying bedrock mineralisation at Highmont South in similar locations to this study.

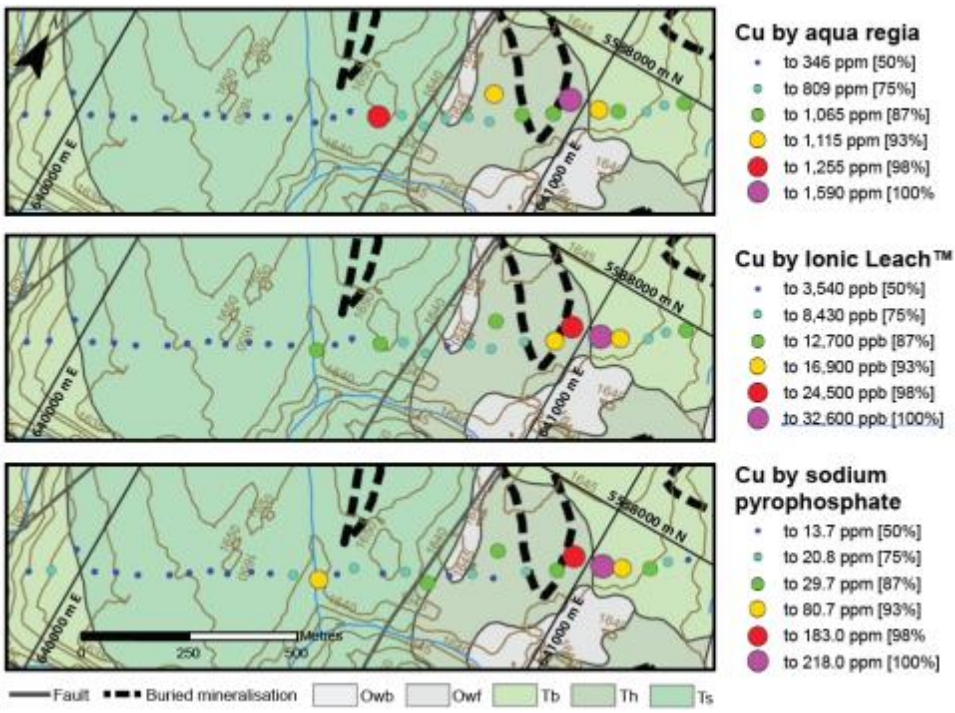

Figure 1-7. Teck 2014 B horizon soil Cu results for separate aqua regia, Ionic Leach™, and sodium pyrophosphate extractions with ICP-MS finish. Data plotted by simple percentile intervals. Contours plotted with 5 metre interval spacing. Surficial geology from Plouffe and Ferbey (2015b); faults modified from McMillan et al. (2009); known buried mineralisation from Teck (pers. comm., Teck, 2017). Abbreviations same as Fig. 1-6, and: Owb = bog peat.

1.6.2 Stream sediment sampling

Past stream sediment surveys, compiled in 2009 as part of the QUEST-South survey by Geoscience BC, have reported anomalous Cu values in the district, increasing in concentration towards the centre of the Guichon Creek batholith where the HVC deposits occur (Figure 1-8) (Arne and Bluemel, 2011, and references therein). A compilation by Teck and CMIC of historical stream sediment samples collected by various past exploration companies indicate a broad trend of increasing Cu and Mo concentrations toward the centre of the batholith (Figure 1-9). The patterns of Cu-Mo-(Ag-Bi) enrichment in stream sediment samples is shifted south (Figures 1-8 and 1-9), likely due to the overall southward movement of water in this portion of the Thompson River basin (Johnsen and Brennand, 2004).

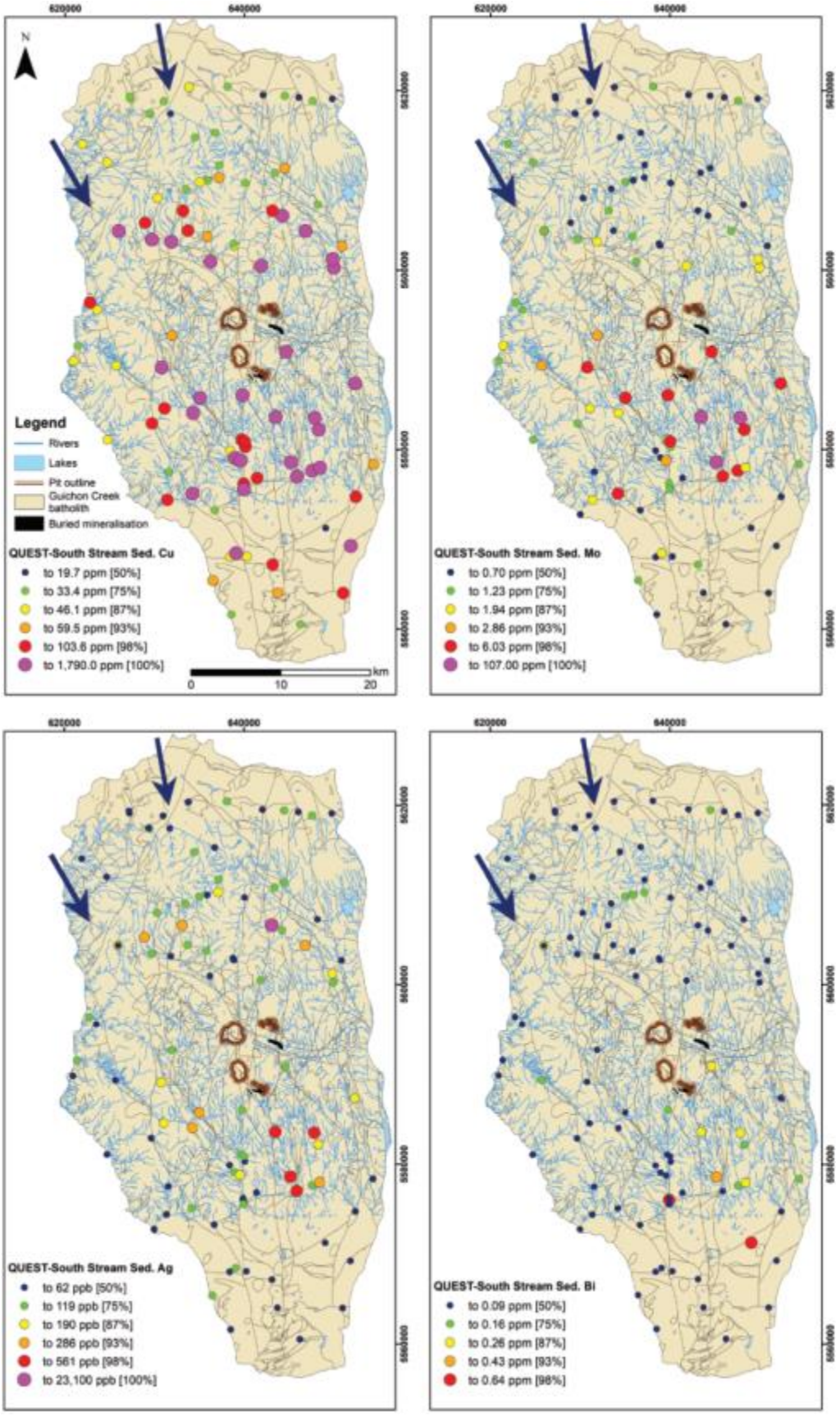
620000
640000
N
Legend
Rivers
Lakes
Pit outline
Guichon Creek batholith
Buried mineralisation
QUEST-South Stream Sed. Cu
to 19.7 ppm [50%]
to 33.4 ppm [75%]
to 46.1 ppm [87%]
to 59.5 ppm [93%]
to 103.6 ppm [98%]
to 1,790.0 ppm [100%]
0
10
20
km
QUEST-South Stream Sed. Mo
to 0.70 ppm [50%]
to 1.23 ppm [75%]
to 1.94 ppm [87%]
to 2.86 ppm [93%]
to 6.03 ppm [98%]
to 107.00 ppm [100%]
QUEST-South Stream Sed. Ag
to 62 ppb [50%]
to 119 ppb [75%]
to 190 ppb [87%]
to 286 ppb [93%]
to 561 ppb [98%]
to 23,100 ppb [100%]
QUEST-South Stream Sed. Bi
to 0.09 ppm [50%]
to 0.16 ppm [75%]
to 0.26 ppm [87%]
to 0.43 ppm [93%]
to 0.64 ppm [98%]

Figure 1-8 (*overleaf*). Concentrations of Cu, Mo, and Ag (aqua regia, ICP-MS) in QUEST-South stream sediment samples (Geoscience BC, 2010) generally increase toward the mineralised centre of the batholith. Elevated Cu, Mo, Ag, and Bi concentrations in stream sediments increase in the dominant southern direction of water flow (Johnsen and Brennand, 2004). Pit outlines and Highmont South buried mineralisation from Teck (pers. comm., Teck, 2017); J.A. buried mineralisation from McMillan (1985); Guichon Creek batholith modified from McMillan et al. (2009).

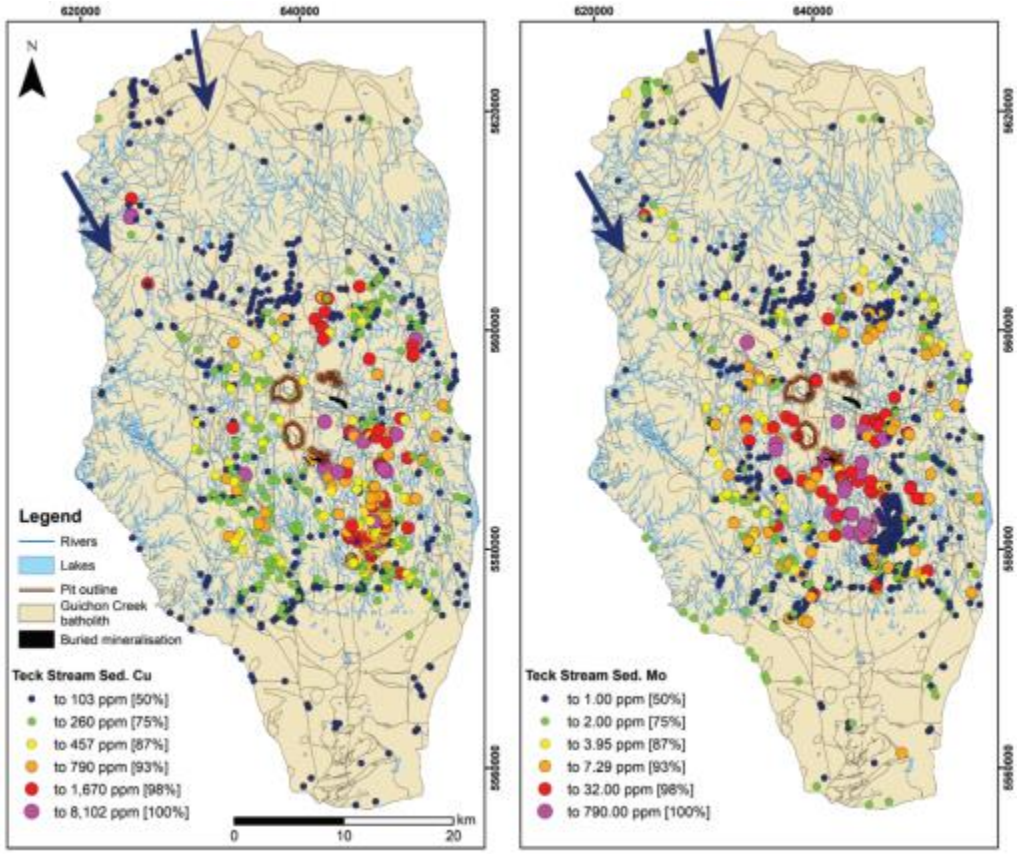

Figure 1-9. Historical stream sediment sample results for Cu and Mo in the Guichon Creek batholith, compiled by Teck Resources Limited and CMIC (pers. comm., Robert Lee, 2017). Enrichment in Cu and Mo increases towards the centre of the batholith and in the dominant southern direction of water flow (Johnsen and Brennand, 2004). Stream sediment samples from 1992 processed with HCl-HNO_3-H_2O partial leach/ICP-OES (ARIS 22373) and from 2012 processed with aqua regia digest/ICP-MS (ARIS 33522). Pit outlines and Highmont South buried mineralisation from Teck (pers. comm., Teck, 2017); J.A. buried mineralisation from McMillan (1985); Guichon Creek batholith modified from McMillan et al. (2009).

1.6.3 Till surveys and porphyry indicator mineral studies

Quaternary geology and geomorphology studies of the region date back to the 1960s (Fulton, 1965; 1967; 1969). The stratigraphic study of a succession of Quaternary sediments in the

Merritt area reports deposits from four different glaciations and two inter-glaciations (Fulton et al., 1992). Sediment sequences mapped in the Valley pit, which are also present in the rest of the valley including over the J.A. target, include preglacial and glaciolacustrine sediments in the lowest parts of the sequence (Bobrowsky, 1993). These investigations, along with regional ice-flow pattern studies, provide an important framework for drift prospecting and surficial exploration in the region. Despite these subsurface stratigraphic complexities, a simple ice-flow history for the uppermost till results in the relatively straightforward provenance analysis for the surficial till (Ferbey et al., 2016). Till sampling for mineral potential in southern British Columbia has a long history including more than 20 years of surficial surveys by the British Columbia Geological Survey (BCGS) and Geological Survey of Canada (GSC) (Anderson et al., 2012).

The GSC produced a surficial map of the Highland Valley district (Plouffe and Ferbey, 2015b) using aerial photography, measured ice-flow indicators, and characterised till mineralogy and geochemistry as part of the Targeted Geoscience Initiative 4 (TGI-4) program and funded by the NSERC-CMIC Exploration Footprints project. The purpose of this five-year program was to assess the use of glacial vectoring and till sampling for mineralogical and geochemical indicators of porphyry Cu mineralisation (Anderson et al., 2012). Detrital porphyry indicator minerals (PIMs) such as green epidote and chalcopyrite (Figure 1-9) were detected, and porphyry Cu-related geochemical signatures reported in tills over several kilometres from the mineralised centres at HVC (Figure 1-10) (Plouffe and Ferbey, 2015b).

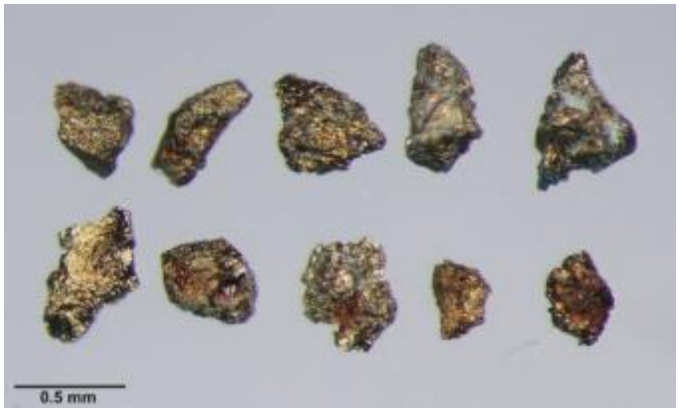

Figure 1-10. Chalcopyrite grains (0.25–0.5 millimetres) recovered from till sampled from the HVC region as part of the Geological Survey of Canada's TGI-4 program (modified from Plouffe et al., 2013a).

Geochemical data from this study shows a regional dispersal pattern of porphyry-related elements Cu, Mo, and Bi in the clay and silt sized fraction (<0.063 millimetres) of tills down-ice from the HVC deposits (Figure 1-10). It is important to note that the author's two study areas (Figure 1-10) exist within a much larger geochemical dispersal pattern. This gives context to the distinction between 'background' and 'local background' geochemistry, where local background reported in the author's study areas could be considered anomalous in the context of 'normal' regional background geochemistry in a nonmineralised region.

The detailed stratigraphy of the pre-glacial and glacial sediment cover is not a part of this research and is being separately undertaken as part of the NSERC-CMIC Exploration Footprints project's Porphyry Cu Subproject by a M.Sc. candidate at the University of Western Ontario (Reman et al., 2017).

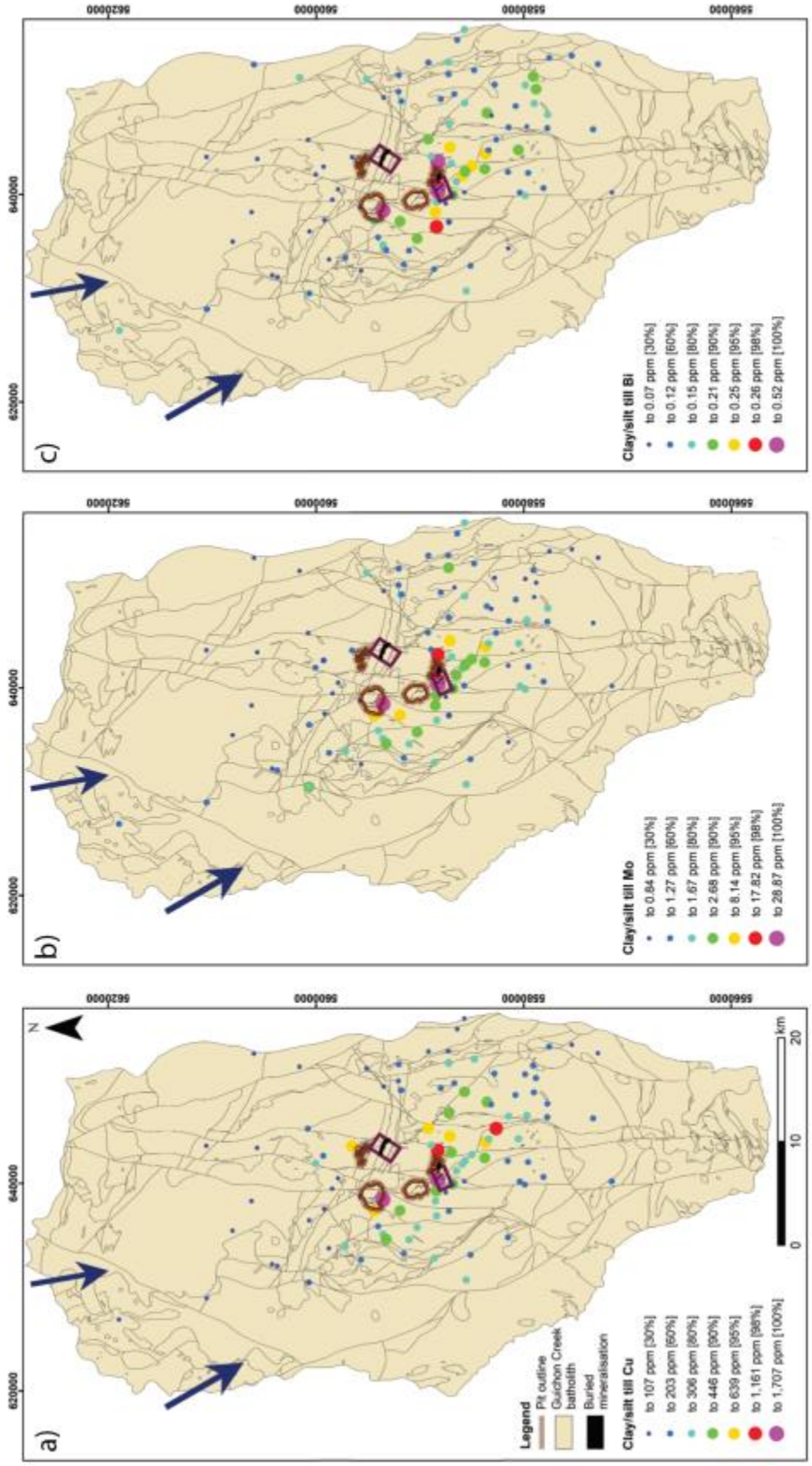

Figure 1-11. Geological Survey of Canada's TGI-4 till sampling results from samples within the Guichon Creek batholith for: a) copper, b) molybdenum, and c) bismuth. Results (aqua regia, ICP-MS) show a geochemical dispersal pattern of porphyry-related elements for several kilometres in the down-ice direction from the HVC deposits (Ferbey et al., 2016). Purple boxes outline field areas for this study. Results plotted by simple percentile intervals. Ice-flow direction from Plouffe and Ferbey (2015b); Pit outlines and Highmont South buried mineralisation from Teck (pers. comm., Teck, 2017); J.A. buried mineralisation from McMillan (1985); Guichon Creek batholith modified from McMillan et al. (2009).

Chapter 2: Mechanisms of trace element dispersion through transported glacial cover

2.1 Introduction

Mechanisms contributing to a surficial geochemical anomaly over mineralised bedrock must be operative within the relatively short Holocene time frame since the deposition of glacial sediments. The majority of glacial deposits in Canada are between 12 ka and 8 ka in age (Hamilton, 2000).

Clastic dispersion can occur in the deposition of glacial sediments, where the glacial erosion of mineralised bedrock and subsequent transport and deposition of mineralised fragments results in a dispersal plume in the down-ice direction from source (Flint, 1971; Miller, 1984). This is an important primary mechanism of anomaly formation in the till-covered glaciated environment, after which secondary processes listed below may operate to further redistribute elements. In regions where multiple centres of mineralisation occur, such as clustered calc-alkalic porphyry deposits in south-central BC, glacial dispersal trains containing mineralised fragments from multiple deposits may overlap one another. Comprehension of factors such as glacial history, stratigraphy, and surrounding geology and mineralisation can contribute to the contrast and refinement of identified local geochemical anomalies compared to more regional signatures.

Weathering and oxidation of buried sulphide mineralisation releases ionic species into the surficial environment that, over time, may migrate away from source and result in the development of a secondary geochemical dispersion halo in the overlying cover (Cameron et al., 2004). Conceptual models exist (e.g. Aspandiar et al., 2006) for the mechanisms of ion migration

in arid and semi-arid environments in the presence of residual regolith and transported overburden, such as those in Australia. The effects of lateral hydromorphic transport of metals is well understood, but there is limited published research on the modelling of vertical ion migration through young, transported glacial cover in the northern hemisphere. Proposed vertical dispersion mechanisms of ions through till include: advective (flow-related) transport and convection within the phreatic zone; diffusion and capillary rise in the vadose zone; electrochemical dispersion in the phreatic zone; dilatancy or barometric pumping; and uptake by vegetation (Figure 2-1) (Hamilton, 2007). An understanding of the ion migration processes in the surficial environment may facilitate predictive geochemical sampling techniques for mineral exploration.

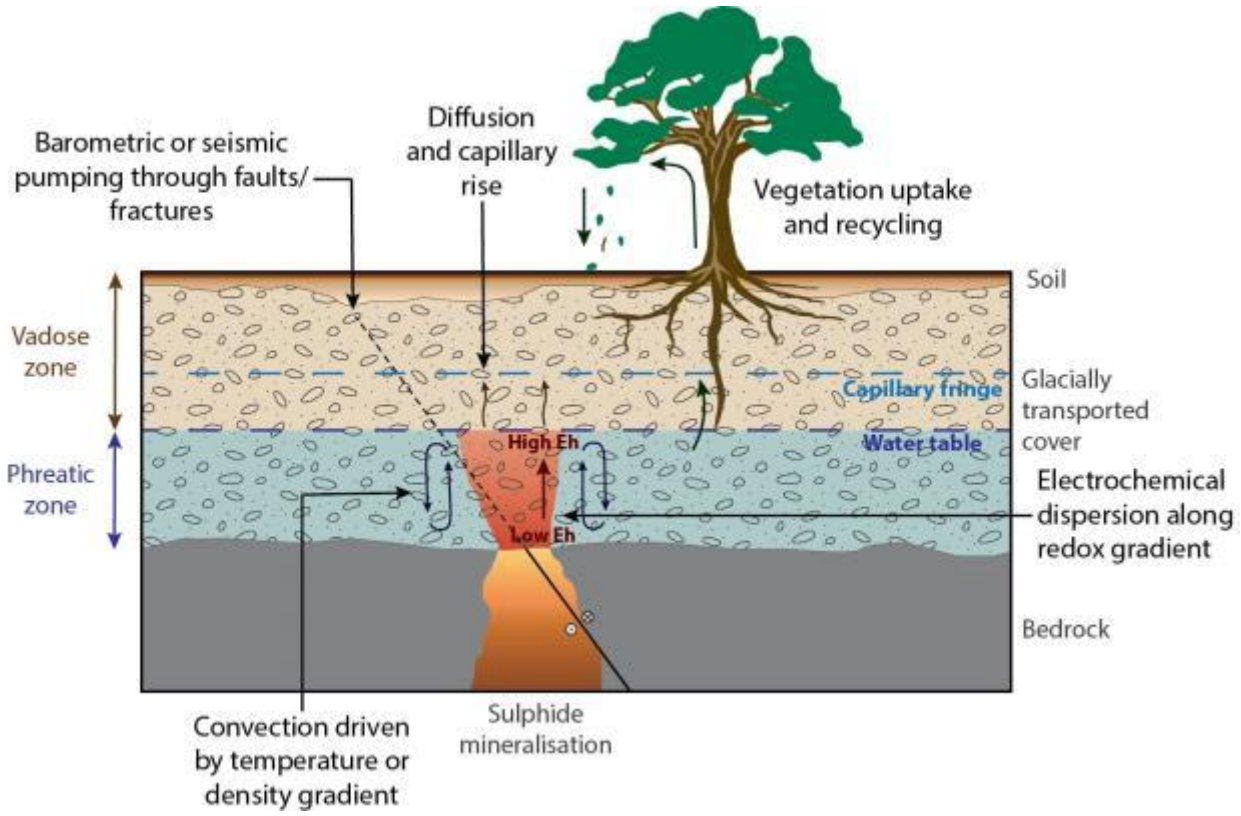

Figure 2-1. Schematic diagram of theorised mechanisms of trace element dispersion in a setting with bedrock mineralisation underlying young glacially transported cover.

2.2 Mechanical dispersion mechanisms

2.2.1 Glacial clastic transport and formation of dispersal plumes

Glacial dispersion involves the physical erosion, entrainment, transport, and deposition of material (Miller, 1984). Glacially-transported fragments of mineralised bedrock can exist as boulders and clasts, produced by quarrying, to sands, silts, and clays, produced by abrasion (Hooke et al., 2013). Microscopic single mineral grains which can be related back to, and are characteristic of, the source deposit's mineralogy are called 'indicator minerals' (Flint, 1971).

Key influences on glacial dispersal patterns include the lithology of the eroded bedrock source, topography of the dispersal area, deposition and transportation modes of glacial debris, and changes in patterns of deposition and erosion (e.g. near an ice divide) (Brushett, 2014). Single-direction ice-flow results in simple ribbon-shaped dispersal trains (Figure 2-2) (McCleneghan et al., 1997). More complicated, multi-direction ice-flow histories can result in fan or 'palimpsest' shaped dispersal plumes which present greater difficulty in tracing back to source. (McCleneghan et al., 1997).

For simple dispersal plumes the distance of the surficial anomaly from its bedrock source is typically a function of cover thickness (Lett, 2001). Dispersal plumes within thin till cover (e.g. <3 metres) will be expressed at surface much closer than those within thick till cover (Figure 2-2) (Lett, 2001).

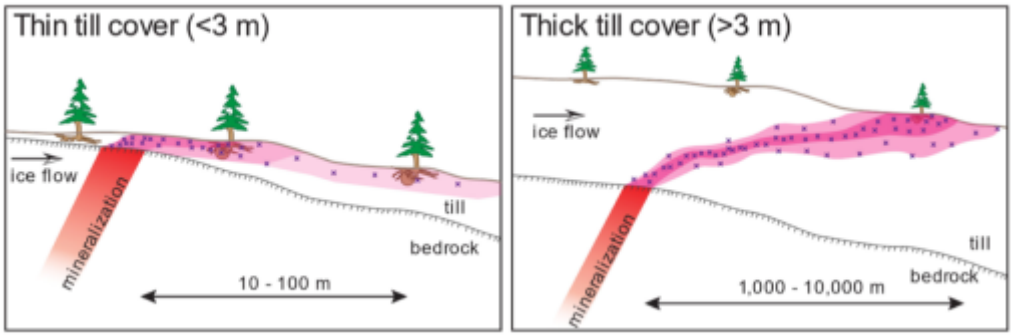

Figure 2-2. Comparison of the effect of till thickness on the distance of the surficial expression of a dispersal plume from its bedrock source (Lett, 2002).

2.3 Chemical dispersion mechanisms

2.3.1 Hydromorphic transport

Element ions liberated from a sulphide body in contact with groundwater can migrate in solution with flowing groundwater (advection) or within a zone of saturation by convection (Cameron et al., 2004; Aspandiar et al., 2006). Although most flow-related transport with groundwater occurs laterally (Hamilton, 2007), vertical flow (upwelling) of groundwater can occur by means of groundwater recharge (Bolviken and Logn, 1975; Smee 1983). The upward migration of groundwater and dissolved constituents is limited compared to rates of lateral hydrodynamic dispersion (Aspandiar et al., 2006).

Upward convection of element ions in solution in groundwater can occur as a result of differences in temperature around a mineral deposit, caused by processes such as exothermic sulphide oxidation reactions at the bedrock mineralisation-overburden interface (Mann et al., 2005). In addition to temperature differences, gradients in the phreatic zone can be generated by differences in salinity and solute content (Freeze and Cherry, 1979). These differences can produce density or buoyancy gradients which carry dissolved elements away from mineralisation at depth (Domenico and Schwartz, 1998).

The hydromorphic mechanisms discussed herein are proposed to result in the accumulation of migrating elements at the water table and are thus more significant to anomaly formation in areas with shallow (near-surface) water tables (Aspandiar et al., 2006).

At higher levels, within the vadose zone, it is proposed that ion migration can be achieved through diffusion or capillary rise (Smee, 1979; Mann et al., 2005). Diffusion of elements along a concentration gradient in glacial sediments is not a quick enough process to account for most observed surficial geochemical anomalies (Smee, 1979). In the 12 ka to 8 ka timeframe allowed by most Canadian glacial sediments, ions cannot vertically diffuse through glacial clay greater than 10 metres (Smee, 1979; Hamilton, 1998). The exception is the H^+ ion which is able to diffuse approximately three times the distance of other ions (Smee, 1979; Hamilton, 1998).

Capillary rise is the movement of groundwater upwards through pore space in the vadose zone by surface tension generated at the air-water interface of the water table (Gillham, 1984). This mechanism depends directly on the porosity and permeability of materials, and is considered unlikely to be very significant in well-compacted tills (i.e. very low pore space and permeability) such as those of the Highland Valley. Additionally, the rate at with capillary rise mobilises ions upwards from the water table must be faster than lateral dispersion/diffusion (Mann et al., 2005).

As with ionic transport, both diffusion and capillary rise have more potential to contribute to surficial geochemical anomaly formation in areas of thin cover (e.g. $\leq$ 10 metres) with substantial porosity and permeability.

2.3.2 Dilatancy and barometric pumping

Dilatancy pumping occurs when groundwater is transferred to surface from the subsurface through a pathway such as a fracture or fault (Aspandiar et al., 2006). This process is typically

referred to as seismic pumping when driven by seismic activity (Nur, 1974), or as barometric pumping when achieved by pressure differentials. Movement of groundwater in contact with mineralisation through a fault or fracture network is proposed to be a very efficient mechanism of metal transfer to the surficial environment (Aspandiar et al., 2006).

2.3.3 Electrochemical dispersion

Electrochemical dispersion of ions was proposed in the late 1990s to explain element migration through transported cover (e.g. Hamilton, 1998, 1999, 2000). However, these models have conceptual difficulties explaining how ions are actually carried to surface.

The most recent model for electrochemical dispersion proposes that an electrochemical cell is generated above an electrically conductive body of sulphide mineralisation (Hamilton, 1999). Reduced species propagate upward through glacial cover along a redox gradient, away from lower Eh conditions at the bedrock surface and toward higher Eh environment at the till-air interface (Hamilton, 1998). This process generates a 'reduced column' over the body of mineralisation (Figure 2-2) which may form a response at the surface (Hamilton, 1998). An 'acidic cap' may be produced by the oxidation of Fe^{2+} and production of H^{+} ions towards the top of the reduced column at the air-water interface (Hamilton, 1998). Here, pH-sensitive ions in solution such as Ca and Mg migrate away from the zone of high H^{+} ion concentration and precipitate at the edges of the column where pH may become less acidic, generating a 'twin peak' geochemical anomaly in section or profile (Hamilton, 1998). In addition to surficial geochemistry, physicochemical parameters may detect the reduced column (e.g. soil oxidation-reduction potential, or ORP) and acidic cap (soil pH) (Hamilton, 2000). Electrochemical cells

generated around an oxidising sulphide body may also be detected by a negative spontaneous potential (SP) response (Sato and Mooney, 1960).

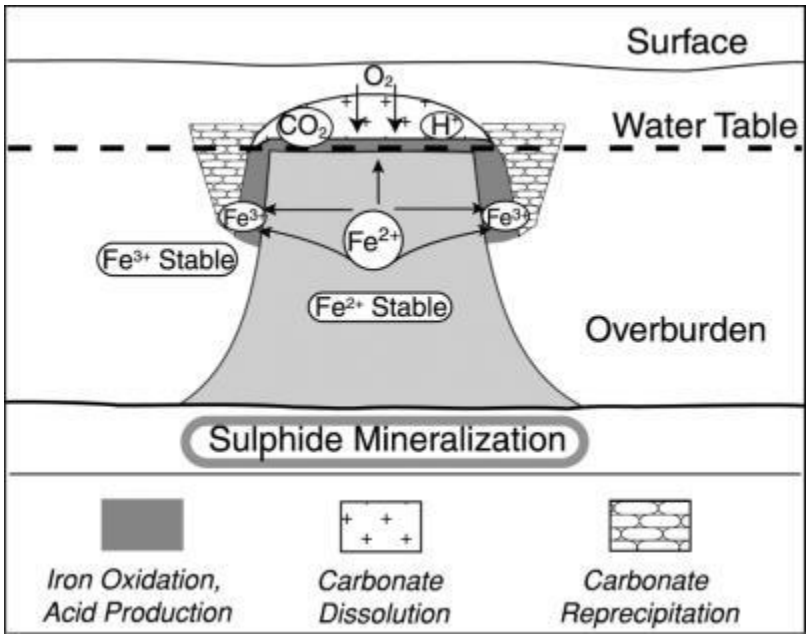

Figure 2-3. Conceptual model of Hamilton (1999) showing the electrochemical dispersion of ionic species through glacial overburden from sulphide mineralisation at depth.

The model for electrochemical dispersion is another example of a mechanism that is more significant to anomaly formation in areas with shallow (near-surface) water tables (Figure 2-3). There remains no explanation for the migration of ions from the water table to surface.

2.4 Biological dispersion mechanisms

2.4.1 Uptake by vegetation

Plant functions can result in the transport of trace elements to surface by processes such as hydraulic lift or uptake and recycling (Brooks et al., 1995). Hydraulic lift is the drawing upwards of groundwater and dissolved constituents by plant roots (Horton and Hart, 1998). Plants absorb elements from the material in which they grow and distribute them as needed throughout their

various tissues. Trees specifically can have deep-penetrating root systems which can tap into material and groundwater containing metals from buried mineralisation (Brooks et al., 1995). The decomposition of vegetation and subsequent incorporation of organic matter into soil ultimately results in the recycling of these metals to the surficial environment (Dunn, 2007). This provides a mechanism for transport of elements from the water table and/or capillary fringe to the surface, and is thought feasible in environments where the water table is up to about 50 metres below the surface (Dunn, 2007; Phillips, 1963). Therefore uptake and cycling by vegetation in the vadose zone combined with dispersion mechanisms operating in the phreatic zone has the potential to generate a surficial geochemical response. Conversely, formation of surficial geochemical anomalies related to buried mineralisation solely as a result of uptake by vegetation is not likely in areas of very thick cover and/or areas with water tables deeper than approximately 50 metres (Dunn, 2007; Phillips, 1963).

2.5 Summary of current knowledge

Research is increasingly being directed at explanation of the mechanisms of vertical trace element dispersion through young, transported glacial cover (Winterburn et al., 2017). Mechanisms proposed include: advective (flow-related) transport and convection within the phreatic zone; diffusion and capillary rise in the vadose zone; electrochemical dispersion; dilatancy or barometric pumping; and uptake by vegetation (Hamilton, 2007). A major shortfall of most of these proposed mechanisms is that they are typically only relevant in environments with thin cover (e.g. $\leq$ 10 metres) and/or shallow (near-surface) water tables (Smee, 1979; Aspandiar et al., 2006). The specific mechanisms for near-surface detection of more deeply-buried mineral deposits have defied explanation.

Chapter 3: Methods

3.1 Surficial mapping

Detailed surficial mapping of the Highmont South and J.A. field areas was conducted to select the most suitable sample sites, and to take into account the different surficial units and processes in the interpretation of geochemical results. The field areas were traversed and mapping was completed at a 1:2,500 scale, recording details in the field such as surficial material types, geomorphology, hydromorphic features, vegetation types, forest fire evidence, road access and anthropogenic features that would influence sample site selection. Surficial geology (UTM NAD83 datum, zone 10N) was remapped at a 1:10,000 scale (Chouinard et al., 2017) following mapping of Plouffe and Ferbey (2015b), using the Geological Survey of Canada's data model for surficial geology (version 2.0; Deblonde et al., 2014). Full details regarding mapping procedure and equipment used are detailed in Appendix A.

3.2 Soil sampling

3.2.1 Upper B horizon soil sampling

In July 2015 two soil transects (transects #1 and #2, Fig. 4-3) were sampled perpendicular to the strike of mineralisation at Highmont South, with 25 metre site spacing close to and over top of the targets, and 50 metre site spacing out into background areas. An infill transect (transect #3, Fig. 4-3) was sampled in June 2016 between the previous two sampling transects, in the same

orientation perpendicular to strike of the mineralisation. A total of 123 upper B horizon soil samples were collected across Highmont South; 98 samples from 93 sites in the 2015 field season and 25 samples from 23 sites in the 2016 field season.

Four soil transects (940 to 1,720 metres in length) were sampled crossing the buried J.A. target perpendicular to the strike of mineralisation (Fig. 5-3), with 50 metre site spacing and approximately 200 to 300 metre spacing between transects. A total of 89 upper B horizon soil samples were collected from 85 sites across J.A. in 2015.

The upper B horizon was the targeted soil horizon for sampling. Ah and Ae horizon soils which have been the object of other studies in British Columbia (e.g. Bissig, Heberlein and Dunn, 2013; Heberlein and Samson, 2010) was not a viable sample medium due to the high potential for anthropogenic inputs and surficial disturbance in the area and; typical soil profiles in both study areas (Figs. 4-4 and 5-5) often did not contain sufficient A horizon material.

At each site, a detailed description of the sampling site and soil profile was recorded and in situ physicochemical measurements (electrical conductivity, pH, and moisture) were conducted for each soil horizon identified. The upper 10 centimetres of the B horizon was targeted for the soil sample, avoiding the topmost 1 centimetre of the B horizon to prevent cross-mixing from the overlying A horizons. Soil was screened in the field through a <6.3 millimetre stainless steel mesh sieve and the following samples were collected from the sieved material:

- 1 kilogram sample for multielement geochemical analyses;
- 300 gram sample transported in a cooler with ice packs, and stored in a freezer at -80°C at UBC for a separate soil microbial study; and
- 300 gram sample for ‘Spatiotemporal Geochemical Hydrocarbon’ (SGH) analysis at ActLabs, Ancaster, Ontario.

Large clasts and organic matter were removed by hand, with clean gloves, for soil which was too wet to sieve. The SGH analysis was not completed. ActLabs declined to analyse the soil samples on the basis that their technique is “not for the purpose of research”.

Sampling procedures and equipment used are detailed in Appendix A. Quality assurance/quality control (QA/QC) practices are reported in Appendix B.

3.2.2 Soil profile sampling

Soil profile sampling sites were selected based on where the upper B horizon soil samples were spatially coincident with Teck’s 2014 upper B horizon soil samples, and significant differences were noted between results from the surveys. Six soil profile sample sites were chosen; 2 at Highmont South and 4 at J.A., which yielded a total of 33 individual soil samples (not inclusive of duplicate samples).

At each site, vegetation was carefully removed from the surface and a hole was dug down to approximately 40 centimetres to expose soil horizons developed on the till. A detailed description was recorded of each horizon and samples were collected at approximately 5 centimetre intervals to at least 10 centimetres below the upper B horizon interval. Sampling intervals were increased or decreased by up to 2 centimetres if necessary to ensure that no contacts were crossed within one interval. In situ physicochemical measurements were conducted for each sampling interval. Beginning from the topmost sampling interval, approximately 200 gram samples were collected for multi-element geochemical analysis by laterally extending the hole. Soil was not screened in the field. Slurry tests were conducted on the material sampled from each interval, as outlined below. Sampling procedures and equipment used are detailed in Appendix A. QA/QC practices are reported in Appendix B.

3.3 Field analyses

In situ measurements in all soil horizons at each soil sampling site were conducted using handheld probes for:

- electrical conductivity (Hanna HI98331 Soil Test EC & Temperature Meter);
- soil moisture (ExTech Instruments MO750 Soil Moisture Meter); and
- pH (Bluelab Soil pH Pen).

Slurry tests using the sampled soil and de-ionised water in a 1:1 volumetric ratio were conducted using handheld probes to measure:

- oxidation reduction potential (Oakton Waterproof ORP Testr® 10 Meter with Ag/AgCl electrode);
- electrical conductivity, pH and acidified pH (Oakton Multi-Parameter PTTestr® 35 pH & TDS Meter); and
- free chlorine content (ExTech CL200 ExStik® Chlorine Meter and activation tablets).

Calibration methods for each probe are detailed in Appendix A. (Note: chlorine measurement results are reported in Appendix D, however they are not discussed in this thesis).

3.4 Conversion of ORP to Eh

Soil ORP measurements were converted to Eh using the following equation:

$$Eh = E_m + E_{ref} \quad (1)$$

Where E_m is the ORP measurement value and E_{ref} is determined by the type of reference cell used. In this case, the probe used to measure ORP used an Ag/AgCl electrode. At 25°C the reference value (E_{ref}) is 222 mV (Bezbaruah and Zhang, 2004).

3.5 Inverse Difference Hydrogen

Inverse Difference Hydrogen (IDH) identifies a soil's buffering capacity due to the presence of $CaCO_3$ (Smee, 2003). IDH is calculated using the following formula:

$$IDH = 1 / ([H^+] - [H^+]_a) \quad (2)$$

Where $[H^+]$ is the concentration of hydrogen ions (given by $[H^+] = 10^{-pH}$), and $[H^+]_a$ is the concentration of hydrogen ions after the addition of one drop of 10% hydrochloric acid to the 1:1 by volume soil-deionised water slurry. Large IDH values will occur when acid neutralising compounds present in the soil act to buffer the acid.

3.6 Laboratory soil analyses

3.6.1 Sample preparation

All soil samples (upper B horizon and soil profile) were submitted to Bureau Veritas Laboratories (BV) in Vancouver, Canada where they were split into two portions – one to archive and one to be processed for further analyses. The portion for analysis was dried at <60°C and sieved to <180 microns using stainless steel sieves. Full details of the analytical methods used are reported in Appendix A. QA/QC practices are reported in Appendix B.

3.6.2 Deionised water leach ICP-MS

Deionised water leach extracts the most labile, exogenic components in the soil, typically within soluble salts and adsorbed to clay mineral surfaces, soluble organic matter, and amorphous Mn- and Fe-(hydr)oxides (Chao, 1984; Hall et al., 1996a). Very weak leaches have been hypothesised as the most suitable application for soils developed on young glacial overburden, in which anomalies are interpreted to accumulate over time (Cameron et al., 2004). A deionised water leach would therefore be appropriate to extract exogenic elements that may have migrated from bedrock mineralisation over the short period of time since deglaciation (Cameron et al., 2004).

Aliquots of the <180 micron prepared soil material were submitted for deionised water extraction (method LH101) at BV followed by ICP-MS multi-element analysis. A pH measurement for each sample was conducted on the leachate at the end of the deionised water extraction by BV.

3.6.3 Aqua regia digest ICP-MS

Aqua regia digest is a non-selective acid digest which will extract water-soluble elements and those associated with carbonates, amorphous Mn- and Fe-oxides, crystalline Fe-oxides, organic matter, sulphides, and leach those contained in the lattice of clay minerals (Dalrymple, 2007). Aqua regia will not digest many major rock-forming minerals such as silicates (e.g. feldspars, quartz, muscovite) or stable oxides (e.g. rutile, zircon) (Dalrymple, 2007). The digestion method is applied to extract pathfinder elements related to underlying deposits, while leaving the sediment or substrate itself undigested. Aqua regia digest is commonly used in mineral exploration for the digestion of soils sampled over shallow, transported cover (Seneshen, 1997).

Aliquots of the <180 micron prepared sample material were submitted for a modified 1:1:1 HNO_3 : HCl : H_2O aqua regia digestion with ultratrace add-on (method AQ250+ext) at BV followed by ICP-MS multi-element analysis.

3.6.4 Organic carbon

Organic carbon (C_{org}) in soil influences the mobility of various elements and influences the pH of the soil which itself determines element mobility (Reimann et al., 2014). The dissociation of organic acids from the breakdown of organic matter in the soil increases a soil's cation exchange capacity (CEC). Metal cations in the soil strongly bind to the negatively charged humic and fulvic acids (Ketterings et al., 2007).

Organic carbon (method TC007) was measured at BV by determining the total carbon and subtracting inorganic (CO_2) carbon and graphite carbon. Total carbon is analysed by combustion in an infrared spectrometric cell (Carbon-Sulphur Analyser). Inorganic carbon is determined by measuring the CO_2 gas released in the analyzer when a sample is leached with perchloric acid. Graphite carbon is measured by leaching samples with dilute HCl followed by ignition at 500°C and analysis of residue.

3.6.5 Field-portable XRF analysis

Field-portable x-ray fluorescence spectroscopy (pXRF) instruments have potential to provide in-field, real-time multi-element analysis of soils (Schneider et al., 2016). When proven applicable to in-field geochemical surveys following orientation analysis, pXRF instruments can be a time- and cost-effective, non-destructive alternative to sample analysis at commercial geochemical laboratories which can often be costly and time consuming (Simandl et al., 2014). There are

typical limitations to current pXRF instruments which may deem the method not fit for purpose (Natural Resources Canada, 2013), particularly with low-concentration materials. Minimum detection limits are in the parts per million range, and the instruments are not usually able to detect elements equal to or lighter than magnesium (atomic number Z=12) (Natural Resources Canada, 2013).

Pulps from the upper B horizon soil samples were analysed at UBC for total element concentrations using an Olympus Innov-X field-portable x-ray fluorescence analyser. Two different operating modes were tested to determine their accuracy in the detection of elements of interest in upper B horizon soil samples: 'soil' mode and 'geochem' mode. Soil mode is most effective for analysis of trace elements at low detection limits in a light matrix (e.g. Si-Al dilution in soil), whilst being less effective at detecting iron or lighter elements (Natural Resources Canada, 2013). Geochem mode is more appropriate to measure Fe and lighter elements but with higher detection limits (Piercey and Devine, 2014).

3.6.6 Cu isotopes

Copper has two naturally occurring stable isotopes: ^{63}Cu with an abundance of 69.17% and ^{65}Cu with an abundance of 30.83% (Shields et al., 1965). Ratios for primary magmatic Cu isotopes (e.g. in porphyry systems) have a narrow range between $\delta^{65}Cu$ -1‰ to +1‰ (Mathur, 2009). Isotopic fractionation of Cu in soil occurs via redox reactions (Mathur et al., 2005), organic complexation (Bigalke et al., 2010b), sorption onto metal oxides and clays (Balistrieri et al., 2008), sorption by microbes (Navarette et al., 2011), precipitation from solution (Ehrlich et al., 2004), and different forms of biological uptake and recycling (Weinstein et al., 2011). Groundwater and supergene enriched zones containing Cu derived from primary magmatic

sulphides are isotopically heavier (positive δ^{65}Cu values) and the Cu that remains in leached zones is isotopically lighter (negative δ^{65}Cu values) (Figure 3-1) (Mathur and Fantle, 2015).

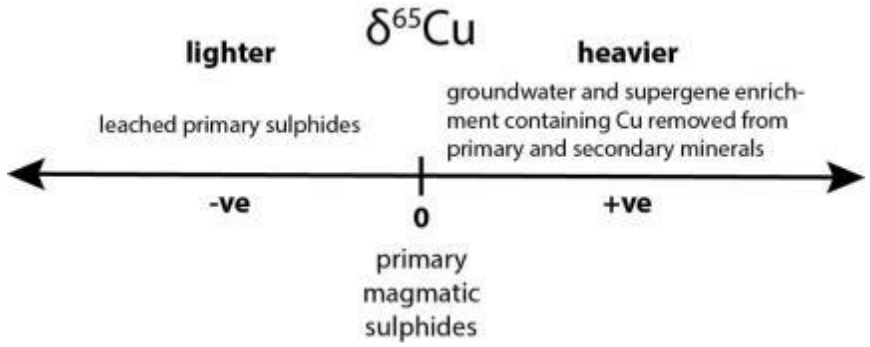

Figure 3-1. Values for δ^{65}Cu will fractionate if leached (lighter δ^{65}Cu values) or enriched (heavier δ^{65}Cu values) (Mathur and Fantle, 2015).

Copper ions in the soil samples may be fractionated from their original ratio by any of the processes in Table 3-1 and still potentially remain within the primary magmatic range.

Process	Reported fractionation of ΔCu^{65}	Source(s)
Adsorption on Fe- and Al-oxides and hydroxides	0.34‰ to 1.26‰	Clayton et al., 2005; Balistrieri et al., 2008; Pokrovsky et al., 2008
Complexation with insolubilised humic acid	0.15‰ to 0.37‰	Bigalke et al., 2010b
Binding on microbial surfaces	-1.8‰ to 0.6‰	Borrok et al., 2008; Pokrovsky et al., 2008
Reduction of Cu^{2+} to Cu^{+}	-4.1‰ to -2.8‰	Zhu et al., 2002; Ehrlich et al., 2004
Oxidation of Cu^{+} to Cu^{2+}	0.94‰ to 3‰	Asael et al, 2005; Mathur et al, 2005
Uptake from soil by plants and internal translocation	0.41‰	Jouvin et al., 2008; Zhu et al., 2010

Table 3-1. Various processes contributing to the fractionation of stable Cu isotopes in soil. Compiled based on Bigalke et al. (2011).

It is hypothesised that if Cu has migrated from bedrock mineralisation to surface soils above mineralisation, Cu isotope results for the loosely bound portion of Cu in the soil matrix will be heavier than the primary magmatic range.

Nine selected anomalous and local background soil samples from each buried target, for a total of 18 samples, were submitted to the Pacific Centre for Isotopic and Geochemical Research (PCIGR) at UBC for Cu-isotope studies.

3.6.7 Sequential extractions

Sequential extraction employs an ordered sequence of selective extraction and digestion methods increasing in strength and each meant to target in turn a specific soil phase(s) in the sample. The objective is to determine the residence of elements of interest in the soil matrix.

Selected anomalous and local background soil samples were submitted to ALS laboratories, North Vancouver, Canada for sequential extraction. Nine soil samples total (4 from Highmont South, 5 from J.A.) were sequentially subjected to deionised water leach (method ME-MS03), ammonium acetate leach (method ME-MS04), cold hydroxylamine-hydrochloride leach (method ME-MS05), hot hydroxylamine-hydrochloride leach (method ME-MS06), sodium pyrophosphate leach (method ME-MS07), aqua regia digest (method ME-MS41L), and four acid digest (method ME-MS61L) with analysis of the leachate by ICP-MS after each stage and continuation of the residue to the next stage. A fresh portion of each sample was run through four acid digest (method ME-MS61L) with ICP-MS finish to obtain total element concentrations for comparison.

Table 3-2 lists the steps in the sequential extraction performed on select upper B horizon soil samples from Highmont South, in order of the sequence. Each step is followed by ICP-MS analysis of the leachate.

Sequential extraction/digestion	Symbol	ALS analysis code	Target phase
Deionised water leach	DW_s	ME-MS03	Labile, water-soluble components, e.g. salts
Ammonium acetate-acetic acid	AmA_s	ME-MS04	Carbonates and exchangeable ions
Cold hydroxylamine-hydrochloride	CHH_s	ME-MS05	Amorphous Mn-oxides
Hot hydroxylamine-hydrochloride	HHH_s	ME-MS06	Amorphous Fe-oxides
Sodium pyrophosphate	NaP_s	ME-MS07	Organic matter, and humic and fulvic acids
Aqua regia (HNO_3-HCl)	AR_s	ME-MS41L	All remaining phases except silicates and stable oxides
Four acid (HF-$HClO_4$-HNO_3-HCl)	$4A_s$	ME-MS61L	Soil phases/components not attacked by previous digestions

Table 3-2. Steps of sequential extraction in order of sequence and the phases within the soil that are targeted (Dalrymple, 2007).

3.7 Soil hydrocarbon collection

Sulphide mineral degradation and associated microbial activity releases a variety of free ions which can then migrate to the surficial environment (Townley et al., 2007). The measurement of these hydrocarbon and organo-sulphur compounds in surficial materials has been evaluated as a method for detecting zones of buried sulphide mineralisation (Hamilton, 2007).

A soil hydrocarbon collector module from Amplified Geochemical Imaging LLC (AGI) – AGI Sampler – was inserted at the bottom of each hole from the 2015 upper B horizon soil sampling campaigns on Highmont South and J.A. AGI Samplers consist of activated charcoal enclosed in a Gore-Tex® membrane (see Appendix F, page 6 of AGI report) which allows the passive

collection of volatile and semi-volatile compounds without the entry of water (Anderson, 2006). The Samplers were inserted at a minimum depth of 50 centimetres from surface and left buried in soil for 50 days at Highmont South and 44 days at J.A. before retrieval. Ninety-two AGI Samplers from Highmont South and 95 from J.A. were analysed for 86 hydrocarbon and organo-sulphur compounds (Table 3-3) by AGI Laboratories using custom thermal desorption gas chromatography-mass spectrometry (TD-GC/MS). Full details of the installation and retrieval process and the analysis method are reported in Appendix A. QA/QC practices are reported in Appendix B.

Normal alkanes	Iso-alkanes	Cyclic alkanes	Aromatics
Ethane, C_2H_6	2-Methylbutane, C5H12	Cyclopentane, C_5H_{10}	Benzene, C_6H_6
Propane, C_3H_8	2-Methylpentane, C_6H_{14}	Methylcyclopentane, C_6H_{12}	Toluene, C_7H_8
Butane, C_4H_{10}	3-Methylpentane, C_6H_{14}	Cyclohexane, C_6H_{12}	Ethylbenzene, C_8H_{10}
Pentane, C_5H_{12}	2,4-Dimethylpentane, C_7H_{16}	cis-1,3-Dimethylcyclopentane, C_7H_{14}	m,p-Xylene, C_8H_{10}
Hexane, C_6H_{14}	2-Methylhexane, C_7H_{16}	trans-1,3- Dimethylcyclopentane, C_7H_{14}	o-Xylene, C_8H_{10}
Heptane, C_7H_{16}	3-Methylhexane, C_7H_{16}	trans-1,2- Dimethylcyclopentane, C_7H_{14}	Propylbenzene, C_9H_{12}
Octane, C_8H_{18}	2,5-Dimethylhexane, C_8H_{18}	Methylcyclohexane, C_7H_{14}	1-Ethyl-2/3-methylbenzene, C_9H_{12}
Nonane, C_9H_{20}	3-Methylheptane, C_8H_{18}	Cycloheptane, C_7H_{14}	1,3,5-Trimethylbenzene, C_9H_{12}
Decane, $C_{10}H_{22}$	2,6-Dimethylheptane, C_9H_{20}	cis-1,3/1,4-Dimethylcyclohexane, C_8H_{16}	1-Ethyl-4-methylbenzene, C_9H_{12}
Undecane, $C_{11}H_{24}$	Pristane, $C_{19}H_{40}$	cis-1,2- Dimethylcyclohexane, C_8H_{16}	1,2,4-Trimethylbenzene, C_9H_{12}
Dodecane, $C_{12}H_{26}$	Phytane, $C_{20}H_{42}$	trans-1,3/1,4- Dimethylcyclohexane, C_8H_{16}	Indane, C_9H_{10}
Tridecane, $C_{13}H_{28}$		trans-1,2- Dimethylcyclohexane, C_8H_{16}	Indene, C_9H_8
Tetradecane, $C_{14}H_{30}$		Ethylcyclohexane, C_8H_{16}	Butylbenzene, $C_{10}H_{14}$
Pentadecane, $C_{15}H_{32}$		Cyclooctane, C_8H_{16}	1,2,4,5-Tetramethylbenzene, $C_{10}H_{14}$
Hexadecane, $C_{16}H_{34}$		Propylcyclohexane, C_9H_{18}	Napthalene, $C_{10}H_8$
Heptadecane, $C_{17}H_{36}$			2-Methylnapthalene, $C_{11}H_{10}$
Octadecane, $C_{18}H_{38}$			Acenapthylene, $C_{12}H_8$
Alkenes	**Aldehydes**	**Biogenic**	**Nitrogen/sulphur/oxygen/other**
Ethene, C_2H_4	Octanal, $C_8H_{16}O$	alpha-Pinene, $C_{10}H_{16}$	Carbon dioxide, CO_2
Propene, C_3H_8	Nonanal, $C_9H_{18}O$	beta-Pinene, $C_{10}H_{16}$	Carbonyl sulphide, COS
1-Butene, C_4H_8	Decanal, $C_{10}H_{20}O$	Camphor, $C_{10}H_{16}O$	Dimethyl sulphide, C_2H_6S
1-Pentene, C_5H_{10}		Caryophyllene, $C_{15}H_{24}$	Dimethyl disulphide, $C_2H_6S_2$
1-Hexene, C_6H_{12}			Furan, C_4H_4O
1-Heptene, C_7H_{14}			Carbon disulphide, CS_2
1-Octene, C_8H_{16}			2-Methylfuran, C_5H_6O
1-Nonene, C_9H_{18}			Benzofuran, C_8H_6O
1-Decene, $C_{10}H_{20}$			Benzothiazole, C_7H_5NS
1-Undecene, $C_{11}H_{22}$			

Table 3-3. The 86 hydrocarbon and hydrogen sulphide compounds analysed from AGI Samplers.

3.8 Biogeochemical sampling

Biogeochemical exploration has been successfully used in locating mineral deposits in glaciated terrain (e.g. Dunn et al., 1996; van Geffen et al., 2012; Bluemel et al., 2015). Plants uptake elements from the material in which they grow and may have deep-penetrating root systems which tap into soil and groundwater containing metals from buried mineralisation (Dunn, 1995). This makes biogeochemical exploration advantageous in areas with transported cover (e.g.

glaciolacustrine or glaciofluvial sediments) where surficial geochemistry is detached from the underlying bedrock (Cohen et al., 1987).

Elements taken up by plants that are in excess of metabolic requirements are typically accumulated in extremities such as roots, outer bark, and the ends of twigs and foliage. This is especially common in conifers which lack more evolved barrier mechanisms to prevent the uptake of unwanted elements (Dunn, 1995). Biogeochemical cycling has been shown to result in the accumulation of elements in upper soil profiles which can, in areas with mineralised bedrock, produce surficial geochemical anomalies (Dunn, 2007).

Dunn et al. (2007) sampled western redcedar (*Thuja plicata*) foliage and subalpine fir (*Abies lasiocarpa*) foliage as well as B horizon soil over the buried Boundary and Pond Zones of alkalic porphyry Cu-Au mineralisation at the Mount Polley deposit in central BC. Cedar foliage is enriched in Au, Cu, and Mo (aqua regia, ICP-MS) over the Boundary Zone, where B horizon soil is enriched in Ag, As, Au, Cu, Hg, and V (aqua regia, ICP-MS). The biogeochemical anomalies were more spatially coincident with the buried mineralisation, while the multielement enrichment in the soil was displaced downslope up to 100 metres (Dunn et al., 2007). Fir foliage is enriched in Au, Cu, Mo, Zn, and Re (aqua regia, ICP-MS) over the Pond Zone, where B horizon soil is enriched in As, Au, Cu, and Re (aqua regia, ICP-MS). The glacial cover over the Pond and Boundary Zones is classified as till blanket indicating the till is over 2 metres in thickness (Hashmi et al., 2015) however no additional information was found regarding cover thickness. Table 3-4 summarises the results for surficial geochemical sampling at the Pond and Boundary Zones at Mount Polley.

Buried target	Veg. sample type	Soil pH	Enrichments in vegetation	Enrichments in B horizon soil
Boundary Zone	Western redcedar foliage	4.4–6.7	• up to 6 ppb Ag • up to 5 ppb Au • up to 11 ppm Cu	• up to 1,545 ppb Ag • up to 40 ppb Au • up to 1,106 ppm Cu

			• up to 10 ppm Mo	• up to 4 ppm Mo
Pond Zone	Subalpine fir foliage	4.3–6.4	• up to 36 ppb Ag • up to 6 ppb Au • up to 34 ppm Cu	• up to 17 ppb Ag • up to 149 ppb Au • up to 652 ppm Cu

Table 3-4. Highlights of results for soil (<180 microns) and biogeochemical sampling (both by aqua regia, ICP-MS) over till-covered porphyry Cu-Au targets at Mount Polley in central BC. Data compiled from Dunn et al. (2007).

Distribution and concentration of elements in tissues varies by species. Studies have concentrated on determining which species and which tissue(s) of that species are ideal to sample when exploring for a defined type of mineralisation. It is common in British Columbia to sample coniferous tree tissues in biogeochemical surveys for various types of mineralisation buried by transported glacial material (Dunn, 1995). Conifers have a more primitive nature that allows for a broader tolerance of the uptake of many trace elements for which more evolved species have developed barrier mechanisms (Dunn and Hastings, 2000). Limitations to exploration biogeochemistry exist depending on the distribution and health of targeted plant species. This is governed by a number of factors including geology, altitude, moisture conditions, pests/disease, and anthropogenic activities (e.g. silviculture) (Dunn, 1995).

Lodgepole pine (*Pinus contorta* var. *Latifolia*) is the most widely distributed, mature species from which to sample vegetation at HVC. Metals are most enriched in the outer bark of lodgepole pine trees (Dunn, 2007). The outer bark is the desired sample medium because there is no seasonal variation in the storage of elements through the course of a year, unlike tissues such as twigs and needles (Dunn et al., 1996). The outer bark is however the most susceptible to entrapment and accumulation of atmospheric particles (van Geffen et al., 2012). Due to the proximity to active open pit mining, needles were sampled in preference to bark from lodgepole pine trees and rinsed with deionised water prior to analysis.

Conifer needle samples were collected from lodgepole pine (*Pinus contorta* var. *Latifolia*) trees at each site, where available, following the B horizon soil sampling transects at both field sites. Samples were taken from trees with a target circumference of 30 centimetres ± 5 centimetres. Due to extensive logging as well as tree death from the mountain pine beetle (MPB) infestation, younger lodgepole pines were sampled to maximise sample coverage. A twig with healthy needles was cut from a branch growing from the same height on each tree. Special care was taken to not touch any tree recognised as a culturally modified tree (CMT).

A total of 69 pine needle samples were collected from 65 sites at Highmont South, and 65 samples from 62 sites at J.A. At UBC needles were removed from the twigs, rinsed with deionised water and sent to Bureau Veritas Laboratories, Vancouver, for analysis. The needles were macerated to 1 millimetre, dissolved with nitric acid, followed by aqua regia digestion and instrumental finish by ICP-MS (method VG101). Twigs were archived at UBC for potential future analyses. Full details of sampling and analysis methods are reported in Appendix A. QA/QC practices are reported in Appendix B.

3.9 Dendrochemical sampling

Dendrochemistry, the science that involves the chemical analysis of tree rings, is used as a biological monitor of changes in soil and atmospheric trace element contents over time. The technique has multiple applications within the geosciences and has mainly been used in environmental studies to define anthropogenic inputs to natural systems (e.g. Savard et al., 2006; Witte et al., 2004; Padilla and Anderson, 2002; Watmough, 1999).

Recently dendrochemistry has been applied in geochemical exploration as a tool to decouple anthropogenic inputs from natural geochemical signals over buried mineralisation (e.g. Kyser et

al., 2015; van Geffen et al., 2012; Kozuskanich et al., 2009). Biogeochemistry typically involves the sampling and analysis of various plant tissues such as foliage, twigs, and bark. The advantage of dendrochemistry is that despite lower metal concentrations expressed in the heartwood of a tree compared to other tissues, chronology of the tree rings provides a temporal dimension to the geochemical data (Watmough, 1997).

Due to extensive logging and tree death from mountain pine beetle (MPB) (*Dendroctonus ponderosae*) infestation (Figure 3-2a), beetle-killed lodgepole pines were sampled with the assumption that the tree died in approximately 2005, at the height of the MPB epidemic in the Merritt region (Carroll et al., 2006; BC Ministry of Forests, Lands and Natural Resource Operations, 2015). Beetle-killed lodgepole pine trees were identified by pitch tubes (Figure 3-2b). These are sites where a mountain pine beetle has bored into the wood and pitch is released by the tree as a defence mechanism (Safranyik and Carroll, 2006). The outer rings of the beetle-killed trees' trunks are stained grey-blue by blue stain fungi (Figure 3-2c) which inoculates the tree as the beetle bores inward (Safranyik and Carroll, 2006). The tree core samples collected from the study area were analysed to define a pre-mining geochemical signature from mineralisation and decouple it from anthropogenic inputs after the start of large-scale open pit mining on site.

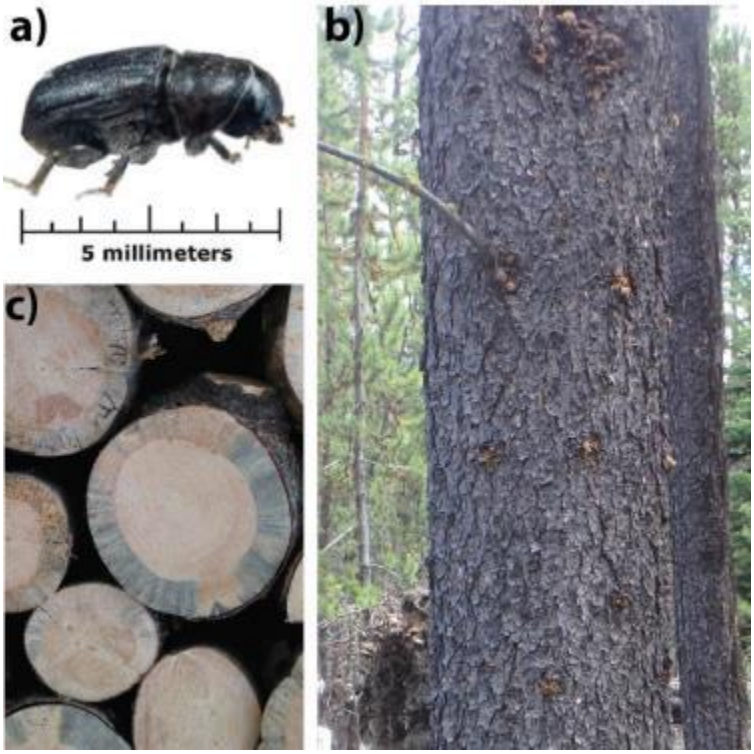

Figure 3-2. a) The mountain pine beetle (MPB), a species native to western pine forests which has exploded in numbers causing an epidemic infestation due to anthropogenic climate change, forest fire prevention, and single-species reforestation (image in public domain courtesy of the United States Forest Service); b) Pitch tubes in a lodgepole pine tree on Highmont South, where MPBs bored into the tree and pitch was released in self-defence; c) Blue stains from blue stain fungus in the outer rings of a tree associated with MPB attack (image from the Government of Alberta, URL: http://www1.agric.gov.ab.ca/$department/deptdocs.nsf/all/formain15837/$file/blue_stain.jpg).

The availability of trees to collect core samples from was severely limited by silvicultural practices. There remain few areas of forest on Highmont South. These are interpreted to be an older generation of regrowth after harvesting, dominated by single-species (lodgepole pine) reforestation. Tree core samples from Highmont South were predominantly collected from the margins of water features. This is an artefact of silvicultural harvesting practices as trees within a set distance from a water body cannot be removed according to BC's Riparian Areas Protection Act (Government of British Columbia, 1997). The water features on Highmont South are both

natural (streams and areas of waterlogged soil/till) and anthropogenic (exploration trenches and drilling sumps).

Tree core samples were collected in July 2016 from lodgepole pine (*Pinus contorta* var. *Latifolia*) trees where available along upper B horizon soil sampling transects on both field sites. Sampled trees were required to be old enough to pre-date large scale open pit mining at HVC, which began in 1962 (Carr, 1966). Tree cores were collected using a 16 inch long, 5.15 millimetre steel Haglöf increment borer. This instrument was hand-drilled through to the centre of the tree at chest-height in a consistent south-north orientation. Core samples were extracted and promptly inserted in a plastic drinking straw, which was sealed at both ends with tape and labelled. Special care was taken to not touch any tree recognised as a culturally modified tree (CMT).

A total of 50 tree cores were collected from 47 sites over Highmont South and 32 tree cores from 31 sites over J.A. Fifteen of the best quality tree core samples (9 from Highmont South, 6 from J.A.) were prepared and analysed at the Queens Facility for Isotope Research (QFIR) in Kingston, Ontario. Full details of sampling and analysis methods are reported in Appendix A. QA/QC practices are reported in Appendix B.

Chapter 4: Surficial geochemistry of the buried Highmont South target at HVC

4.1 Surficial environment and climate

The Highmont South field area sits at an average elevation of 1,640 metres above mean sea level (AMSL), with a range of approximately 1,600 to 1,660 metres AMSL. The rolling uplands of Highmont South are a function of ice retreating northward at the end of the last glaciation, approximately 10 ka (Fulton, 1975; Plouffe and Ferbey, 2015a). Ground moisture is a direct function of climate, where wetter, colder years result in widespread waterlogged depressions, swamps, and actively running streams. The Highmont South field area is in the Montaine Spruce Zone biogeoclimatic zone of British Columbia, with mean annual precipitation of 648 millimetres and a mean annual temperature of 1.9°C (BC Ministry of Forests and Range, 2008).

4.2 Geomorphology

Highmont South consists of small, gently rolling hills of till often streamlined parallel to the south-southeast ice-flow direction (Plouffe and Ferbey, 2015a) (Figure 4-1). Till surface topography generally follows that of bedrock topography. Low-lying areas occur where streams and drainage channels have cut through the surface of the till. There are numerous scattered waterlogged depressions in the till as well as a small number of swamps. The only naturally occurring outcrop is exposed at the bottom of an approximately 15 metres deep incised stream valley in the northwest of the field area. This valley is an example of the clear surficial evidence

of structural features with several major drainage pathways/streams lying along the projection of bedrock faults. The water table is close to surface due to the thin cover at Highmont South.

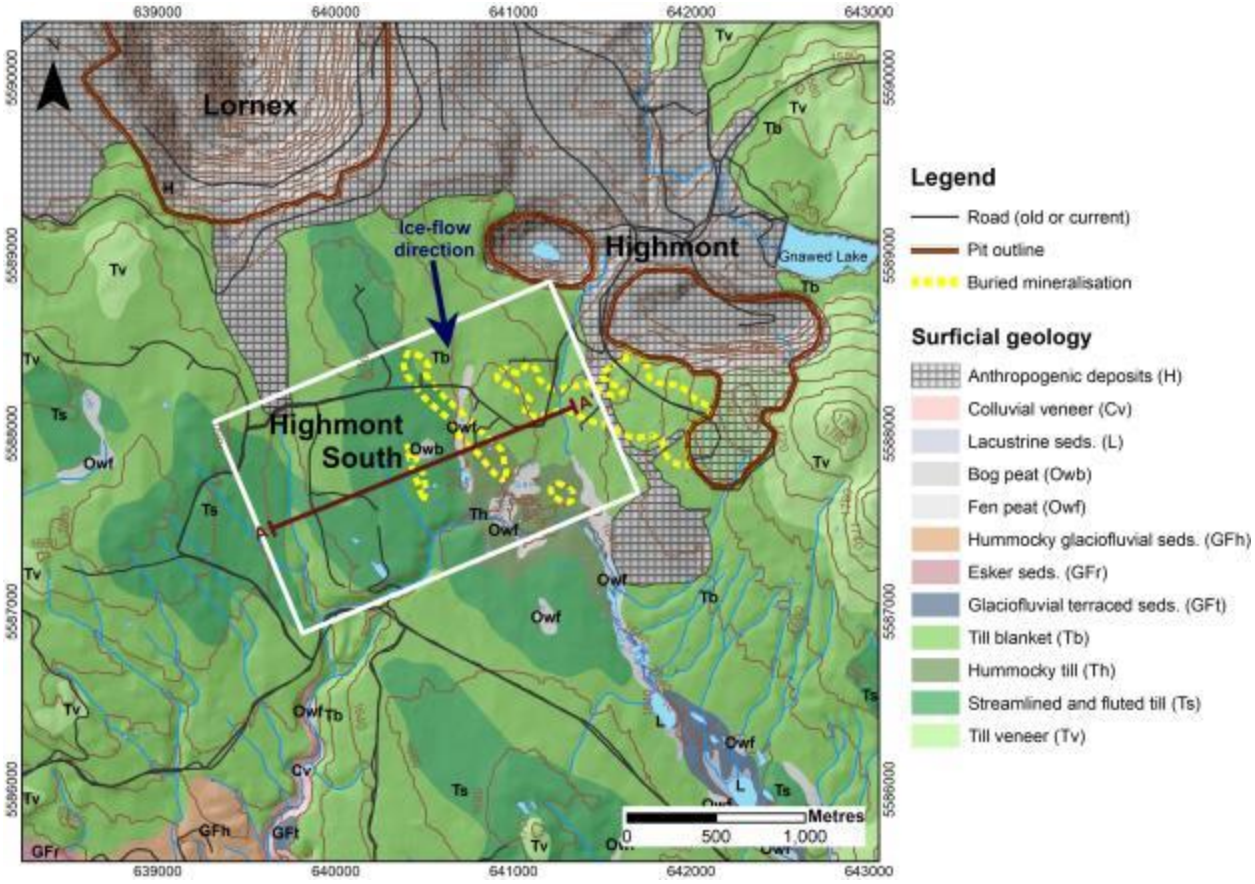

Figure 4-1. Geomorphology of Highmont South and the surrounding area. White box indicates surficial mapping area for this study. Approximate location of cross section (Fig. 4-2) shown by A–A' line. Contours are plotted at 20 metre interval spacing. Adapted from Plouffe and Ferbey (2015b); pit and buried mineralisation outlines from Teck (pers. comm., Teck, 2018).

4.3 Surficial geology

The main cover material type at Highmont South is till blanket (Tb). The till blanket ranges in thickness from approximately 2 to 10 metres (Figure 4-2) (based on historic drilling, pers. comm., Teck, 2016). The till facies in this area (Section 1.5.5.2) is recognised as a subglacial till (Ferbey et al., 2016). Surficial mapping produced a detailed record of areas where sediments are water saturated during wet seasons, as well as main surficial drainage pathways (Figure 4-3). To

reduce sample variability the program is designed to sample from within Tb surficial units where possible.

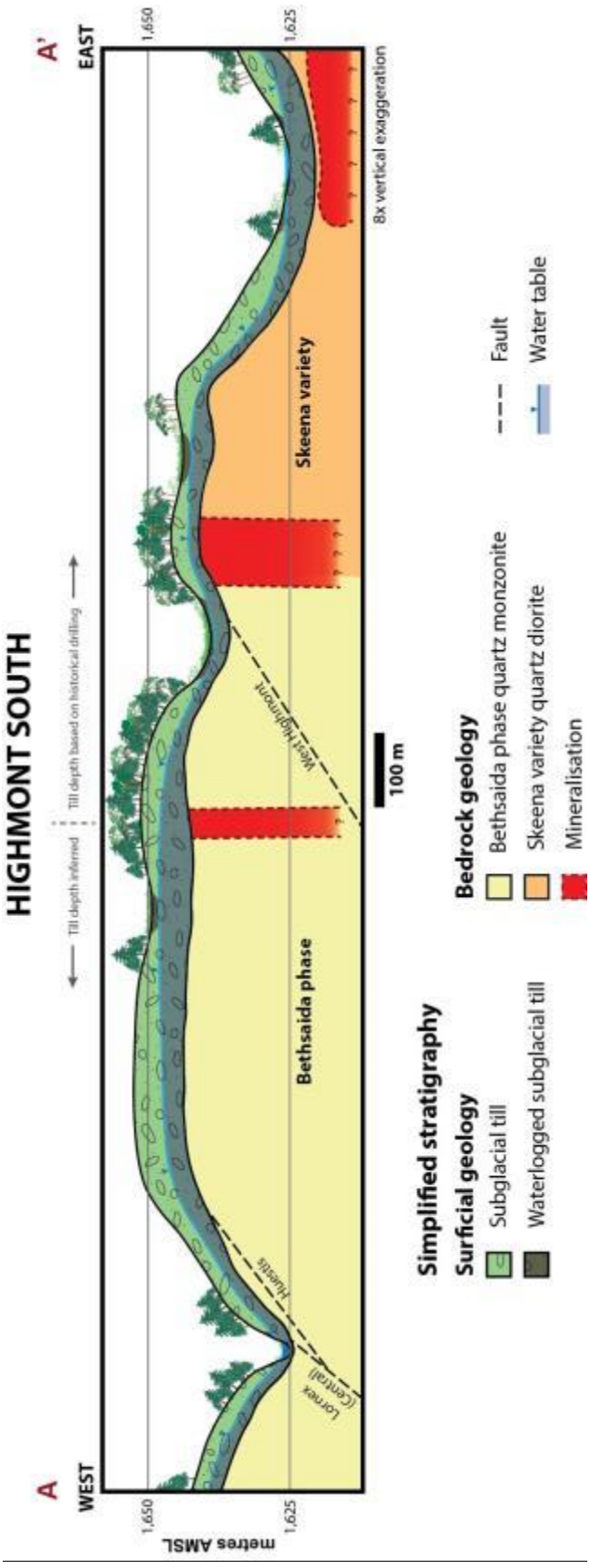

Figure 4-2. A cross section through the Highmont South field area indicates the depth of burial of bedrock mineralisation. Till thickness and bedrock topography estimated based on historical drilling results from Teck (pers. comm., Teck, 2016). Mineralisation and faults are estimated and purely diagrammatical. Trace of section indicated on Fig. 4-1. Bedrock geology and surface trace of faults based on work completed in August 2016 by Teck and CMIC, modified from McMillan et al. (2009). Surface trace of mineralisation provided by Teck (pers. comm., Teck, 2017).

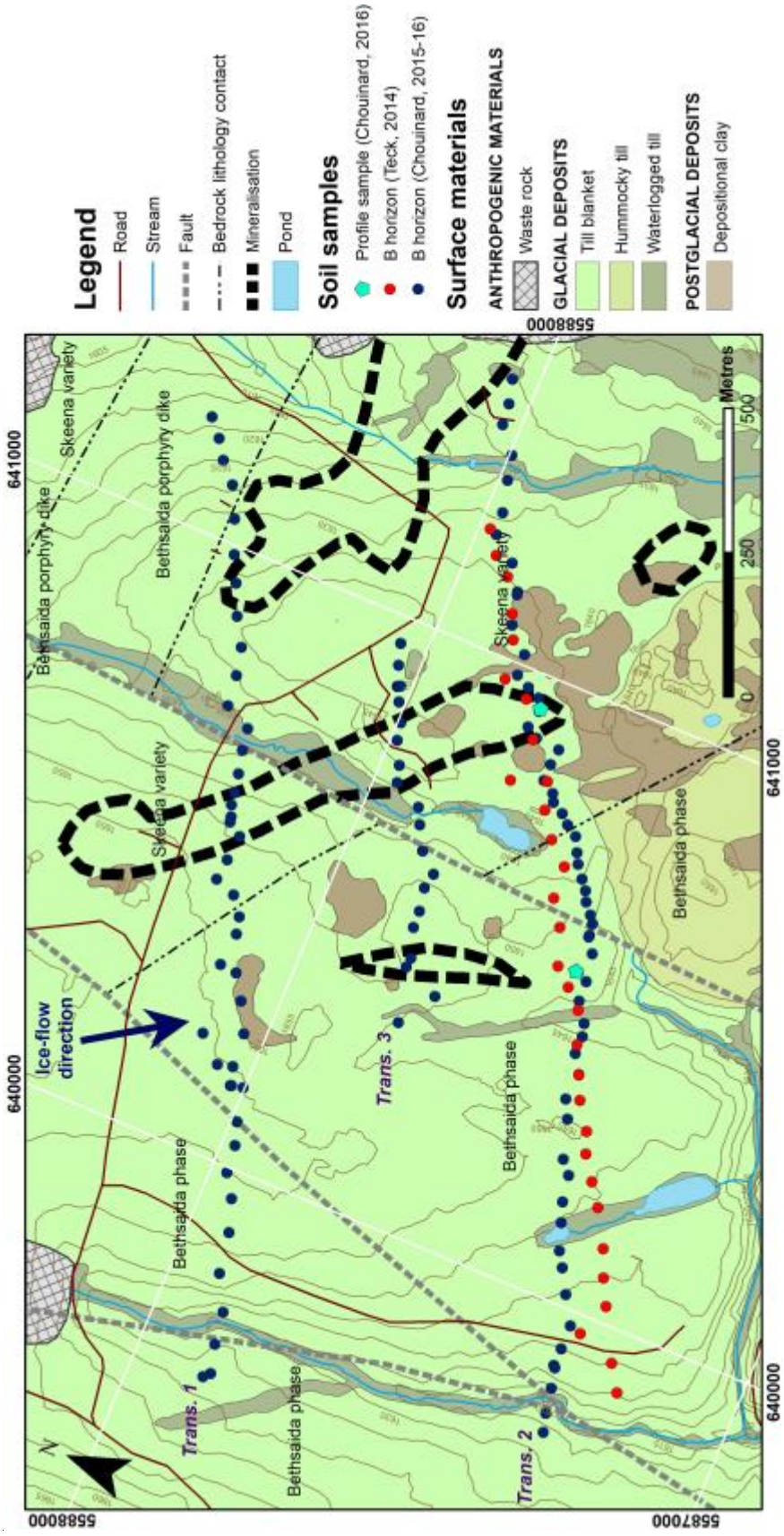

Figure 4-3. Surficial geology of the Highmont South study area at Highland Valley Copper. Contours plotted at 5 metre interval spacing. Surficial geology is modified from Plouffe and Ferbey (2015b), using the Geological Survey of Canada's (GSC) data model for surficial geology, version 1.2 (Deblonde et al., 2012); ice-flow direction from Plouffe and Ferbey (2015b); locations of buried mineralisation from Teck (pers. comm., Teck, 2018); bedrock geology and structure modified based on work completed in August 2016 by Teck and the Canadian Mining Innovation Council (CMIC), and modified from McMillan et al. (2009).

A thin (approximately 30–50 centimetres) layer of soil is developed over the till blanket. Undisturbed soils are typically identified as brunisols (Figure 4-4) with a very thin organic top (LFH) horizon, rarely a discernable eluviated mineral (Ae) horizon, and a relatively thin illuviated mineral (B) horizon over the unoxidised mineral (C) horizon. These brunisols have low visible organic matter content and have an increase in sand and clast content down profile. Soils in waterlogged depressions are typically more reduced (grey-green in colour) and clay-rich, with the same clast content as surrounding non-waterlogged soil. Infrequent, small swamps exist where clay-rich gleysols are present with little to no clast content (Figure 4-4c).

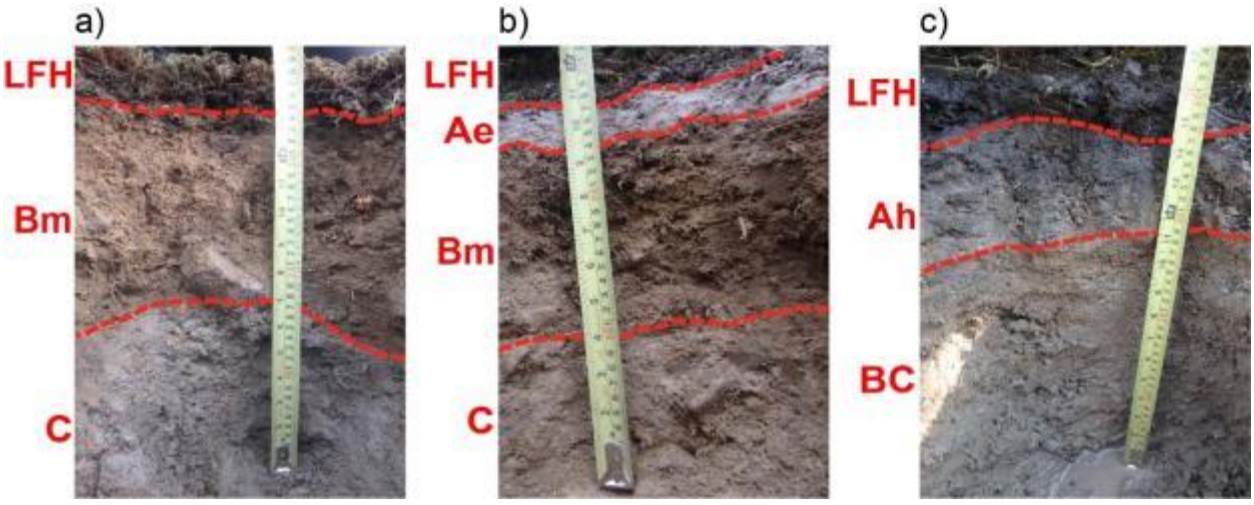

Figure 4-4. Typical soil profiles encountered during sampling at Highmont South, showing a) a brunisol developed over till blanket material (RC-16-HVC-013: 640578 m E, 5587847 m N); b) a more well-developed profile with an eluviated (Ae) horizon, likely a podsol, developed over till blanket material (RC-15-HVC-075: 640714 m E, 5587616 m N); c) a depositional clay-rich, waterlogged soil (gleysol) (RC-15-HVC-013: 640225 m E, 5588038 m N). Soil horizon nomenclature follows the Canadian system of soil classification (Agriculture Canada, 1998).

4.4 Vegetation

Overstory vegetation currently growing at Highmont South is dominated by cultivated lodgepole pine, with lesser spruce and rare fir. In areas that remain forested, there is significant pine tree

death due to the mountain pine beetle infestation. Open cut blocks are dominated by scattered wildflower, grasses, and ground berries. Water-logged depressions contain longer grasses and sedges, mosses, and dwarf birch. Areas that remain forested and relatively undisturbed host a variety of moss, lichen, fungi, wildflower, ground berries, and shrubs.

4.5 Anthropogenic influences

Silviculture has had an impact on the Highmont South field area (Figure 4-4), as it has in much of the surrounding area. Trees have been harvested in most of the field area, with cut blocks in varying stages of preparation (e.g. plowed, aerated) and reforestation. The large scale industrialisation of the logging industry has potential to limit an exploration geochemical soil survey due to soil disturbance and potential inputs of fertilisers, pesticides, fungicides, and herbicides. Machines are used to till and aerate land in various ways before tree saplings are planted. The forestation map (Figure 4-5) records new areas of silviculture which were not predicted based on satellite imagery, as well as cut blocks that have been recently replanted. The anthropogenic map (Figure 4-6) records all other evidence of activities that have potential to disturb and rework surficial material and influence results of surficial geochemical sampling, including current roads, old overgrown roads, landings, drill pads, trenches, ditches, and forestry burn piles. Considerable care was taken during sampling to minimise the potential effects of anthropogenic influences.

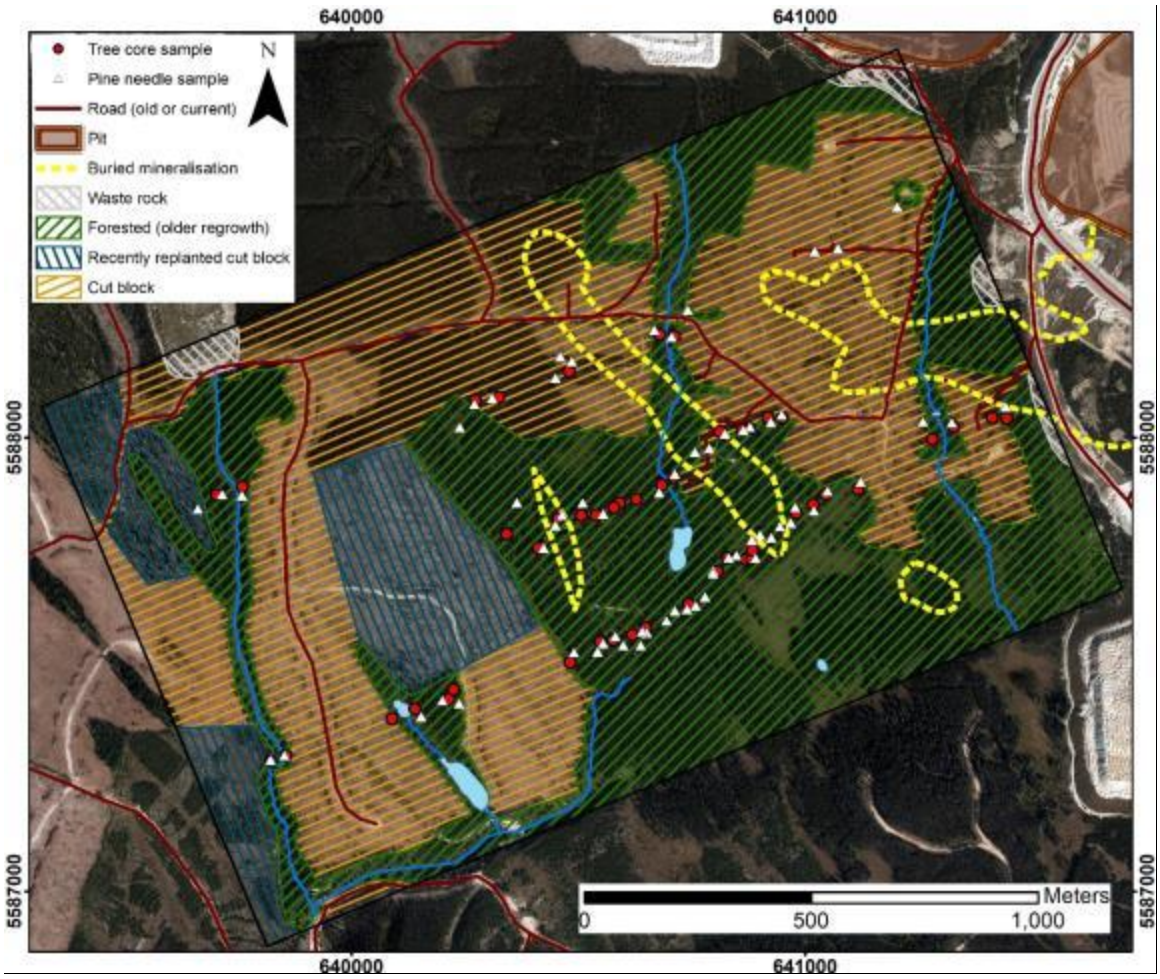

Figure 4-5. Zones in varying states of silvicultural harvesting and regrowth within the surficial mapping area at Highmont South (as of 2016). Tree core samples (from deceased lodgepole pine) and needle samples (from younger, living lodgepole pine) are marked on map to indicate biogeochemical sample coverage. Pit and buried mineralisation outlines from Teck (pers. comm., Teck, 2018).

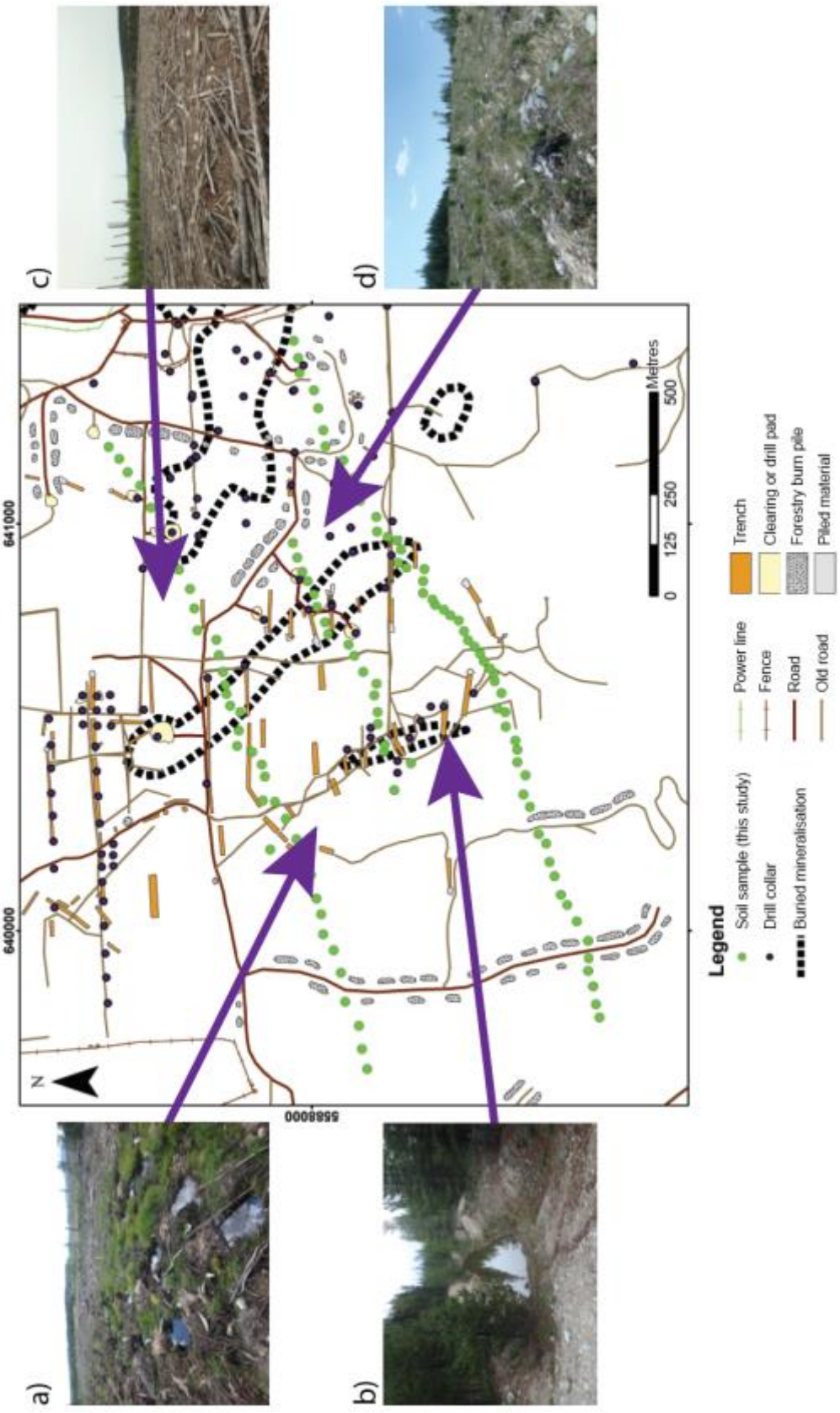

Figure 4-6. A map of observed anthropogenic features in the Highmont South field area shows the complexity of care required to attain a surficial geochemical sample (e.g. soil) from undisturbed material. Accompanying photos show various anthropogenic features encountered while mapping and sampling in 2015 and 2016: a) mechanical aeration in a cut block; b) exploration trench; c) recent cut block with waste wood present; d) plow marks in cut block with waste wood removed and recently planted pine saplings. Buried mineralisation outline and drill collar locations from Teck (pers. comm., Teck, 2017).

4.6 Upper B horizon soil analysis

4.6.1 Physicochemical properties

Physicochemical measurements (pH, acidified pH, electrical conductivity, oxidation reduction potential, and moisture) were conducted at each soil sample site in order to interpret geochemical data in terms of soil conditions as well as to identify potential physicochemical anomalies related to bedrock mineralisation. QA/QC practices and results are detailed in Appendix B. The data was deemed acceptable and fit for purpose following evaluation of QC results.

All three soil transects on Highmont South show a correlation between moisture and electrical conductivity (EC) for in situ measurements (Figure 4-7). Values for both of these types of measurements generally correspond to the grain size of the sediment into which the probes are inserted and therefore reflect the water-bearing capacity of the soil. Typical soil profiles on Highmont South coarsen downwards toward the C horizon. As a result, EC and moisture measurements are generally lower in the coarser and more clast-rich C horizon, in comparison to the B horizon. The highest EC and moisture values occur in the waterlogged, depositional clay units. In situ pH is generally mildly acidic (median pH = 5.3) except in waterlogged soils which are more circumneutral (median pH = 6.3). There is no correlation between areas of known bedrock mineralisation and patterns of in situ EC or pH in the overlying soils.

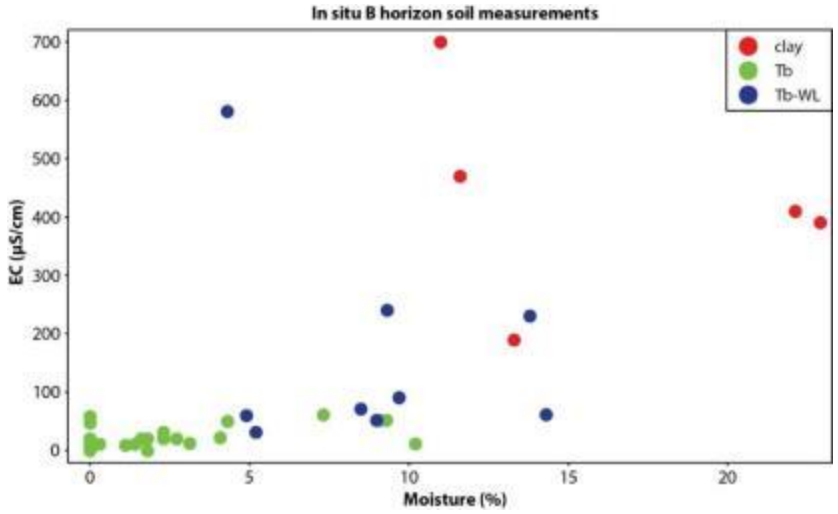

Figure 4-7. A plot of in situ moisture measurement data versus that of in situ electrical conductivity (EC) indicates a general positive trend. Outlier samples are from within waterlogged till blanket and depositional clay units, where soils have higher cation contents due to the lack of drainage. Abbreviations: clay = waterlogged depositional clay; Tb = till blanket; Tb-WL = waterlogged till blanket.

pH values from measurement of 1:1 by volume soil-deionised water slurry follow the same general trends as in situ pH values. The clay units have more circumneutral pHs and higher EC (Figure 4-8). Similar to the in situ measurement values, there is no correlation between areas of known bedrock mineralisation and patterns of slurry measurement values in overlying soils. Oxidation reduction potential (ORP) values have a narrow range (244–333 mV; calculated Eh of 466–555 mV) and indicate dominantly oxidising conditions (Figure 4-9).

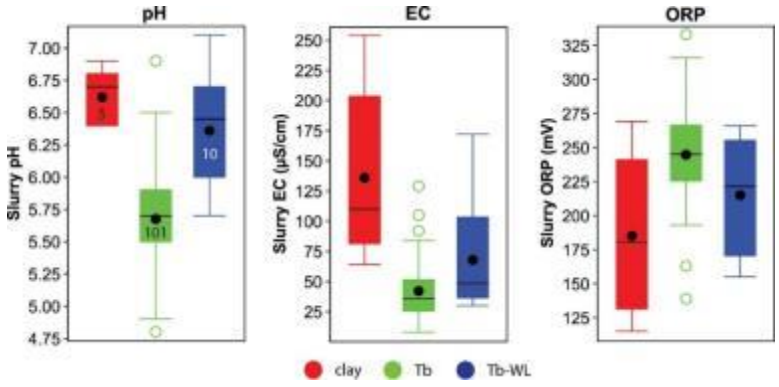

Figure 4-8. Slurry pH, EC, and ORP measurements for upper B horizon soil developed on waterlogged depositional clay, till blanket, and waterlogged till blanket materials at Highmont South. Numbers on boxes on pH plot indicate the number of sample results.

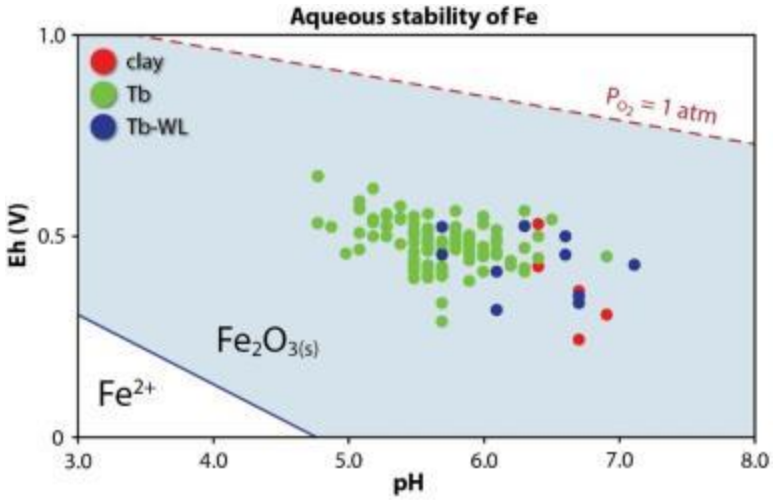

Figure 4-9. Upper B horizon soil samples plotted on a Pourbaix diagram for Fe (0.001 mol/kg) indicating proportion of samples in which Fe likely is oxidised or reduced. All samples plot within the $Fe_2O_{3(s)}$ field, indicating Fe within the soil is oxidised. pH values from soil slurry measurements; Eh values calculated from soil slurry measurements for ORP (Section 3.4). Diagram modified from plot generated on materialsproject.org.

In the clay units the concentrations of elements Mn, Co, As, and Bi (<180 microns, aqua regia, ICP-MS) increase as Eh becomes more oxidising (Figure 4-10). The majority of samples from the clay units plot within the mobile Mn^{2+} stability field of a Mn Pourbaix diagram, close to Mn-oxide stability fields (Figure 4-11). An increase in Eh would result in the precipitation of Mn-oxides which would limit the mobility of Mn in the soil. Slurry EC values increase with increasing Ca and Li concentrations in soils sampled from both till blanket and clay units (Figure 4-12).

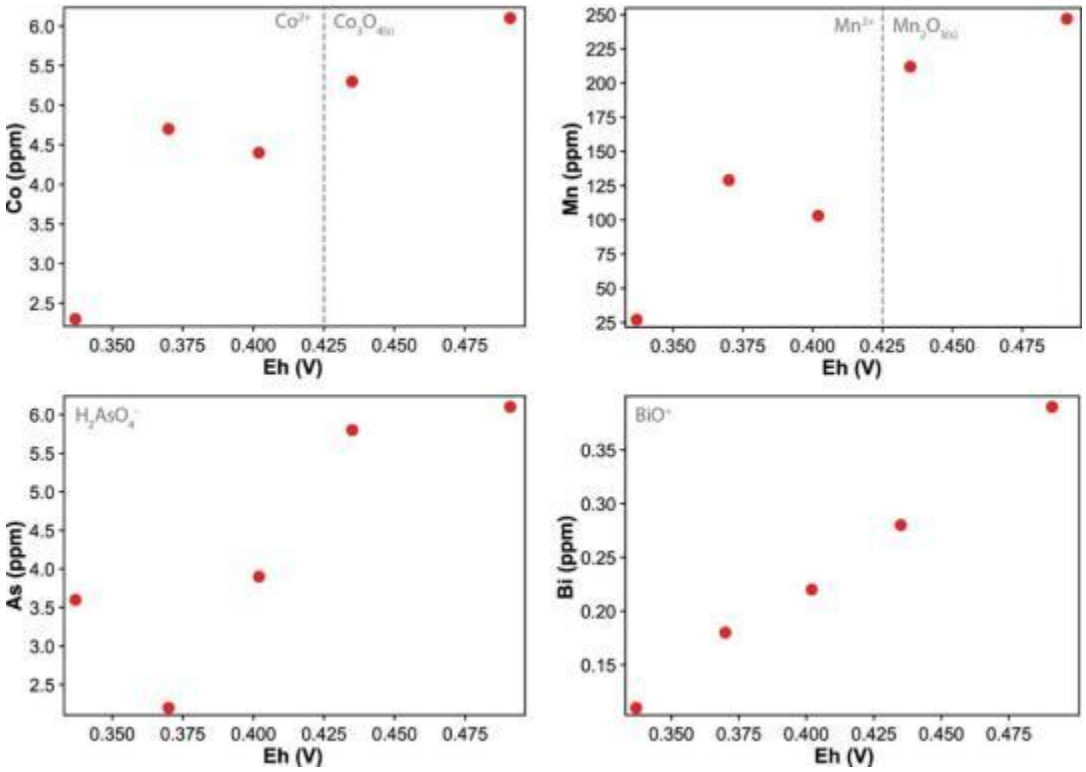

Figure 4-10. Concentrations of Mn, Co, As, and Bi in waterlogged depositional clay units (upper B horizon, <180 microns, aqua regia, ICP-MS) increase with increasing Eh. Stability lines indicate a change in speciation of the element in soil based Pourbaix diagrams (generated on materialsproject.org) using median concentrations of the element and median slurry pH (pH = 6.7) for the clay unit material. ORP measured on upper B horizon soil-deionised water 1:1 by volume soil-deionised water slurry and converted to Eh (Section 3.4).

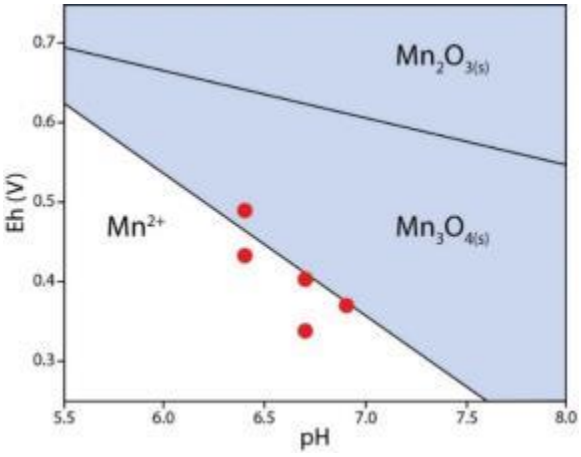

Figure 4-11. Slurry pH and Eh from waterlogged depositional clay material plotted on a Pourbaix diagram for Mn (0.001 mol/kg) indicate that Mn is dominantly stable as the mobile Mn^{2+} ion. An increase in Eh can result in precipitation of a Mn-oxide species which would limit the mobility of Mn in the soil. Diagram modified from plot generated on materialsproject.org.

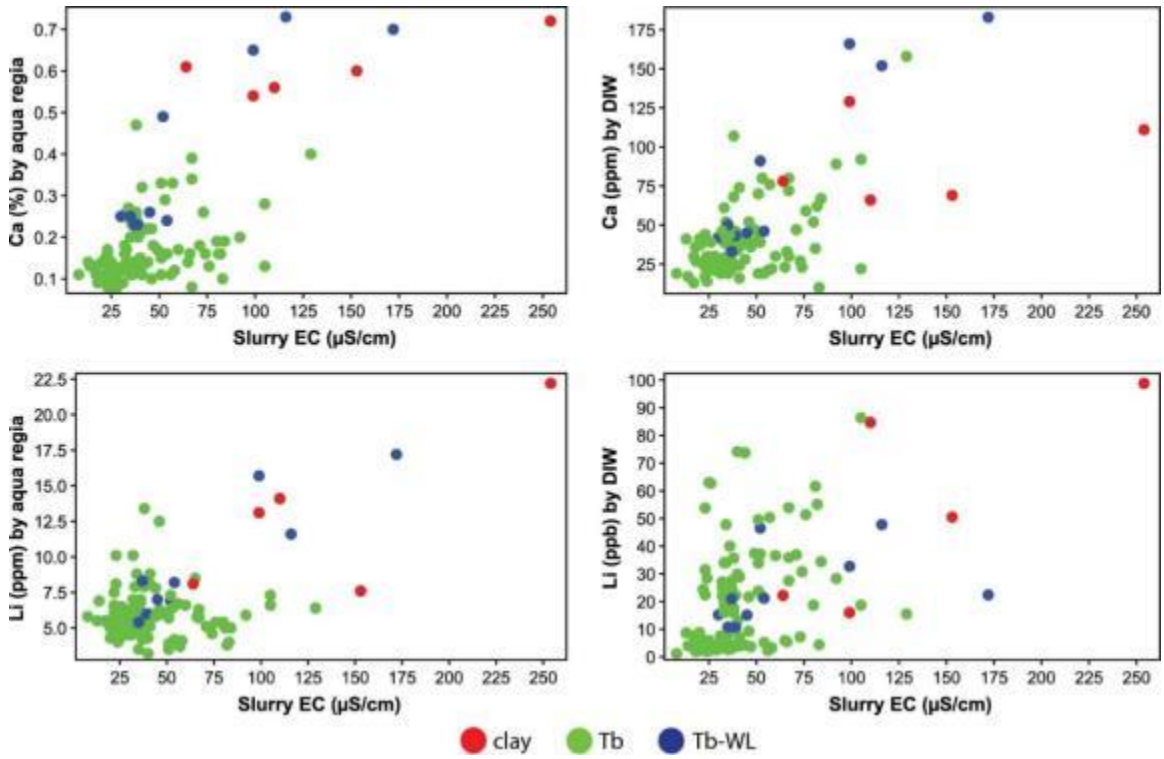

Figure 4-12. Slurry EC values increase with increasing Ca and Li (upper B horizon, <180 microns, separate aqua regia digest and deionised water leach, ICP-MS finish on both) concentrations in soils sampled from both till blanket and depositional clay units. DIW = deionised water leach.

4.6.2 Inverse Difference Hydrogen

Upper B horizon soil samples from Highmont South have high Inverse Difference Hydrogen (IDH; Section 3.5) values where soil was sampled from areas of waterlogged depositional clay and waterlogged till blanket compared to dry till blanket (Figure 4-13), reflecting higher clay contents and physicochemical conditions in which $CaCO_3$ is stable (Figure 4-14).

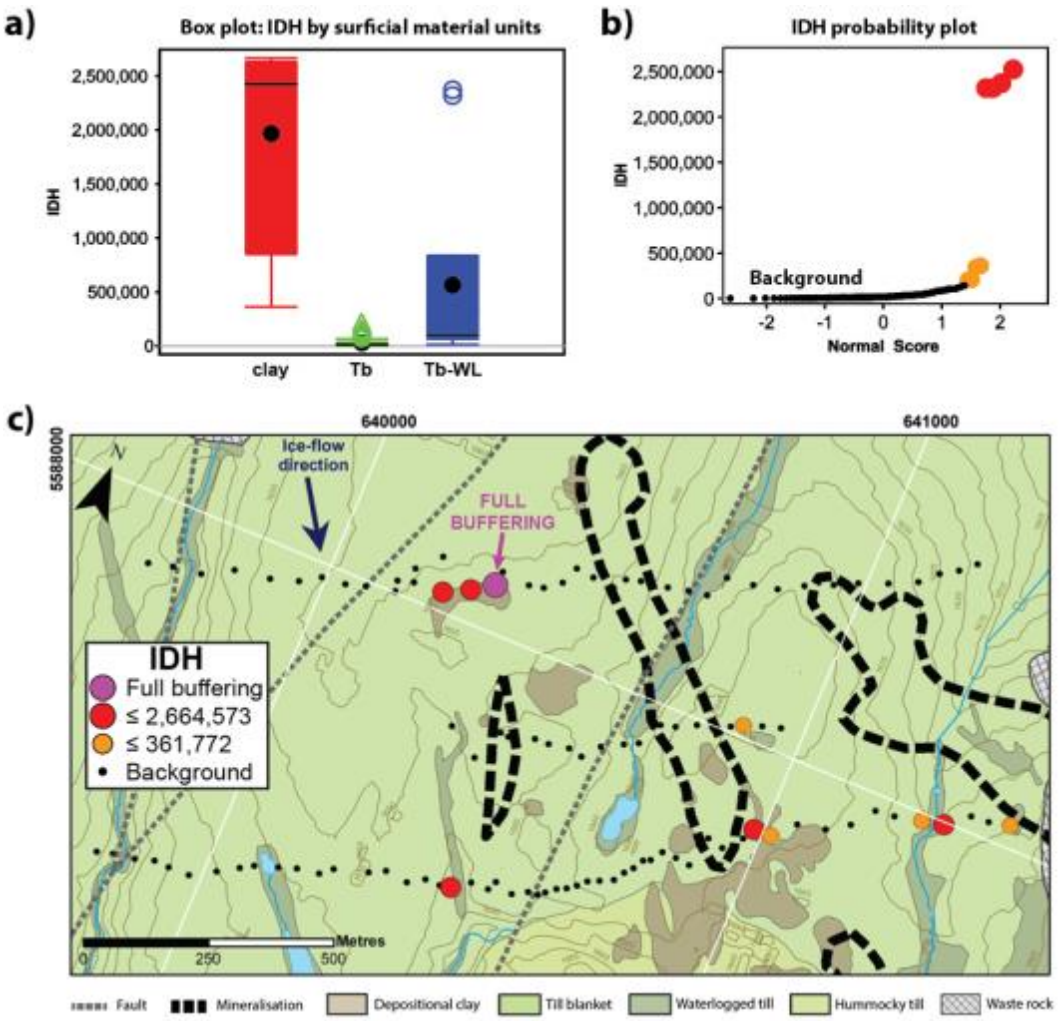

Figure 4-13. a) Inverse difference hydrogen (IDH) values for soils at Highmont South. Buffering capacity of the soil, represented by the calculated IDH value, is highest in the waterlogged depositional clay material. b) Anomalous populations of IDH values determined by visual estimation of population breaks on a probability plot. c) Anomalous populations of IDH values occur within soils sampled from within waterlogged units of both depositional clay and till blanket. Sample RC-15-HVC-016 achieved full buffering. Contours plotted at 5 metre interval spacing. Surficial geology is modified from Plouffe and Ferbey (2015b), using the GSC data model for surficial geology, version 1.2 (Deblonde et al., 2012); ice-flow direction from Plouffe and Ferbey (2015b); buried mineralisation outlines from Teck (pers. comm., Teck, 2017); faults modified from McMillan et al. (2009).

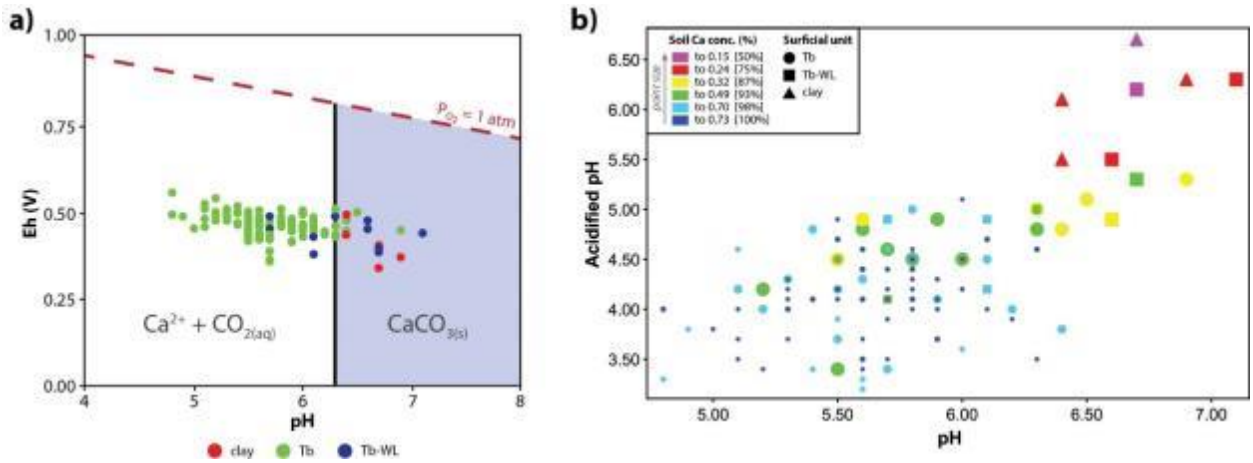

Figure 4-14. a) Upper B horizon soil samples plotted on a Pourbaix diagram for $CaCO_3$ (0.001 mol/kg Ca, 0.001 mol/kg C). pH values from soil slurry measurements; Eh values calculated from soil slurry measurements for ORP (Section 3.4). Modified from diagram generated on materialsproject.org. b) Plot of slurry pH vs. slurry pH with one drop of 10% HCl added for 1:1 by volume soil-deionised water slurries using upper B horizon soils from Highmont South. Data points follow a size and colour scale determined by simple percentile intervals for soil Ca concentrations (<180 microns, aqua regia, ICP-MS).

Clays have a mild ability to buffer acidity by cation exchange (e.g. H^+ in soil exchanges for K^+ on clay surface) (Yong and Phadungchewit, 1993). Sample RC-15-HVC-016 (640317 m E, 5588091 m N) from within a clay unit achieved full buffering with a soil slurry pH of 6.7 both before and after the addition of one drop of 10% HCl.

4.6.3 Aqua regia digest ICP-MS results

The aqua regia digest applied is a relatively weak mix of equal parts concentrated HNO_3, HCl, and deionised H_2O (Bureau Veritas, method AQ250) compared to standard aqua regia. Analytical results are reported in Appendix C and QA/QC practises and results in Appendix B. Selected elements were compared to certified and indicated values of OREAS25a certified reference material (CRM) to assess precision. Mean percentage difference (MPD) for field duplicate results was used to assess natural variability. Data quality is summarized as follows:

- Elements for which all values were reported below ten times stated analytical detection limits and are not discussed further are: B, K, Tl, S, Se, Te, Ge, Sn, Ta, In, Re, Pd, and Pt;
- Elements for which the median of values was below ten times stated analytical detection limits and are interpreted with caution are: U, Au, Th, Cd, Sb, Bi, La, Na, W, Hg, Hf, and Be;
- Elements which are of acceptable accuracy and precision are: Mo, Cu, Pb, Zn, Ag, Ni, Co, Mn, Fe, As, Sr, V, Ca, P, Cr, Mg, Ba, Ti, Al, Sc, Ga, Cs, Nb, Rb, Zr, Y, Ce, and Li.

Geochemical differences occur between dry and waterlogged sediments within the till blanket unit. Soil samples from areas of waterlogged till generally have higher Mo, Cu, Ag, Ni, Co, Mn, As, Sr, Bi, Ca, La, Mg, Ba, Na, Sc, Cs, Rb, Y, Ce, and Li concentrations compared to dry till blanket (Figure 4-18). Waterlogged areas of depositional clay have higher Cu, Ag, Ni, Co, Fe, As, Sr, Ca, Cr, Mg, Ba, Al, Na, Sc, Hg, Be, Li, and REE (La, Ce, Y, U, Th) concentrations than both dry and waterlogged till blanket material (Figure 4-15).

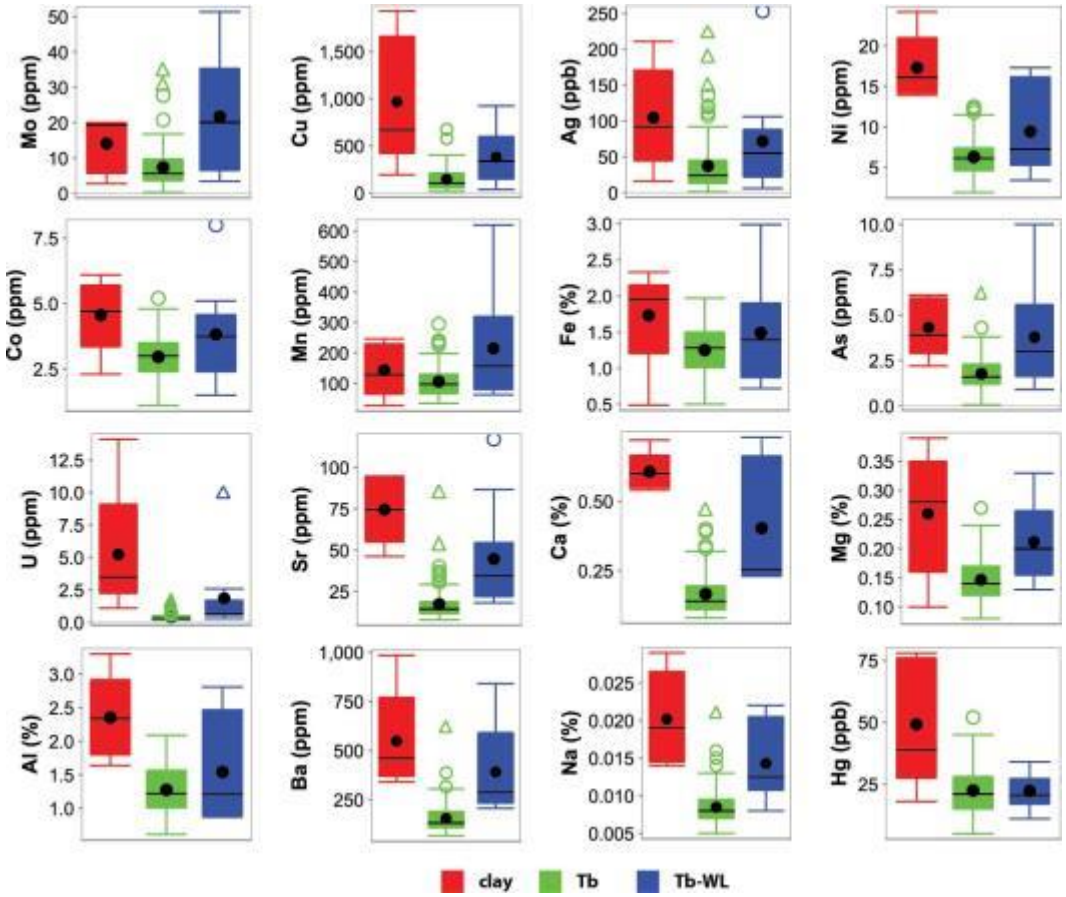

Figure 4-15. Geochemical differences between soils (<180 microns, aqua regia, ICP-MS) sampled from different surficial material units at Highmont South.

A sample of water-saturated soil includes the pore water and its dissolved constituents in addition to the mineral and organic components of the soil matrix. Elements released from weathering processes are better retained in a water-saturated surface environment compared to a dry environment in which elements are more likely to be eluviated by the percolation of rain water through open pore space. Flooding of soil increases its cation exchange capacity over time through the reductive dissolution of Fe-oxyhydroxide coatings (Favre et al., 2002). Additionally, the high clay content of the depositional clay units adds to the potential to sorb higher concentrations of elements compared to samples from more coarse-grained till blanket. To avoid the generation of false anomalies, data investigation for anomalous responses focuses on samples

from the till blanket surficial unit and exclude those from depositional clay units. Data from waterlogged till blanket units is interpreted with caution.

Probability plots (Figure 4-16) were produced from aqua regia ICP-MS results for upper B horizon soils sampled above till blanket to identify anomalous populations. Anomalous populations identified were spatially plotted for interpretation in context of the Highmont South surficial map (Figure 4-17). Elements with populations considered anomalous based on probability plot distribution and which spatially coincide with mineralised bedrock are Cu, Mo, Bi, and Ag. The elements Sb, As, and W indicate weak anomalous responses above mineralisation, but are subject to low values near detection limits (Figure 4-17).

Elements that indicate an anomalous response both in soil overlying bedrock mineralisation and in soil overlying the West Highmont fault, which crosscuts mineralisation, are Cu and Ag (Figure 4-17). The elements Sb and W indicate weak anomalous responses both above mineralisation and the West Highmont fault, but are subject to low values near detection limits (Figure 4-17). Elements Pb, Cd, and Zn indicate anomalous responses above both the West Highmont fault and the westernmost body of mineralisation (Figure 4-18). Manganese indicates an anomalous response over the West Highmont fault but not over mineralised bedrock (Figure 4-18).

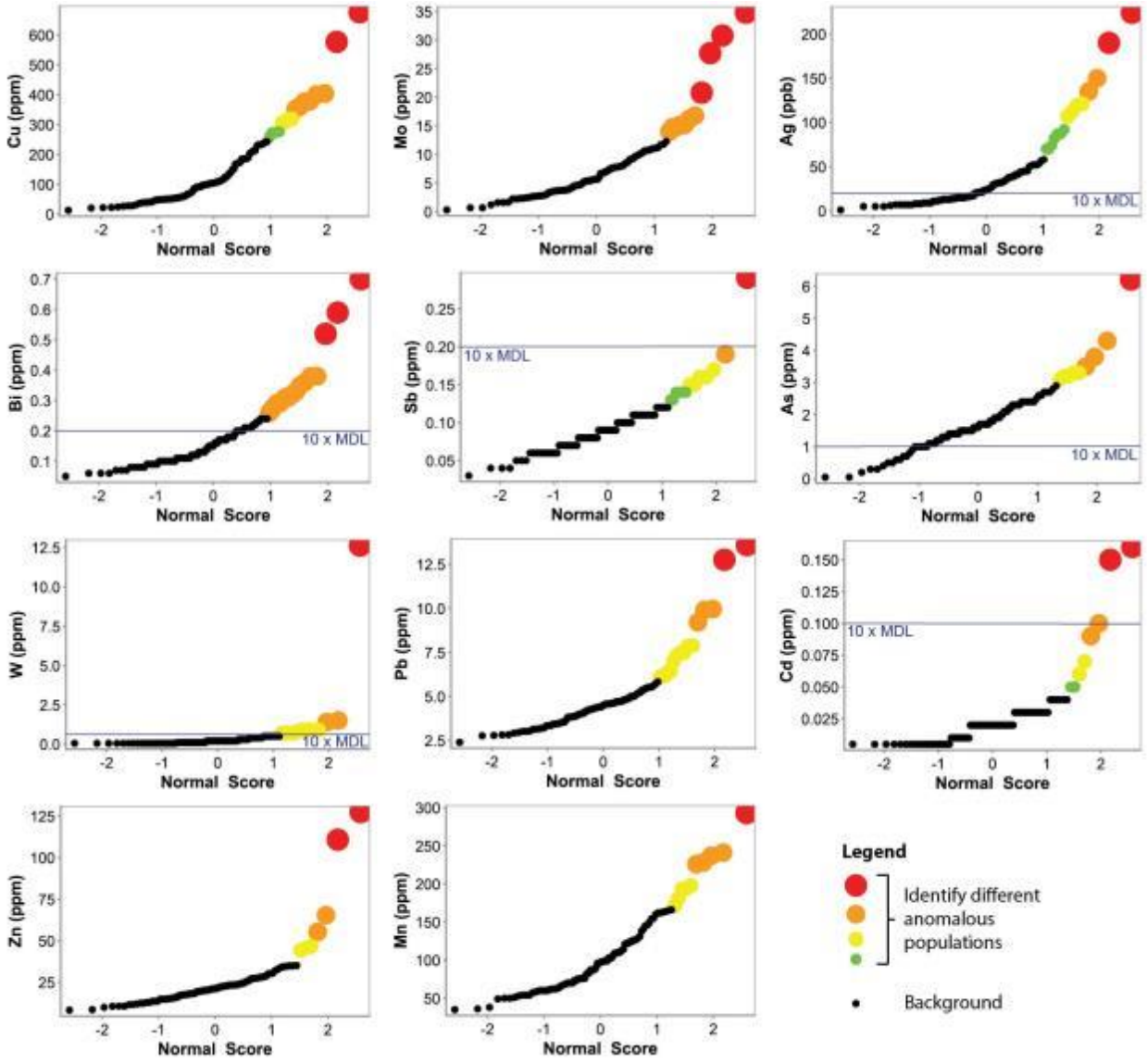

Figure 4-16. Probability plots showing distribution of element results in upper B horizon soil (<180 microns, aqua regia, ICP-MS) sampled from till blanket surficial units at Highmont South. Anomalous population intervals were selected based on visual estimation of population breaks on these plots. Anomalous intervals are determined separately for each individual plot and symbols of the same size and colour are not related between plots for different elements. MDL = minimum detection limit.

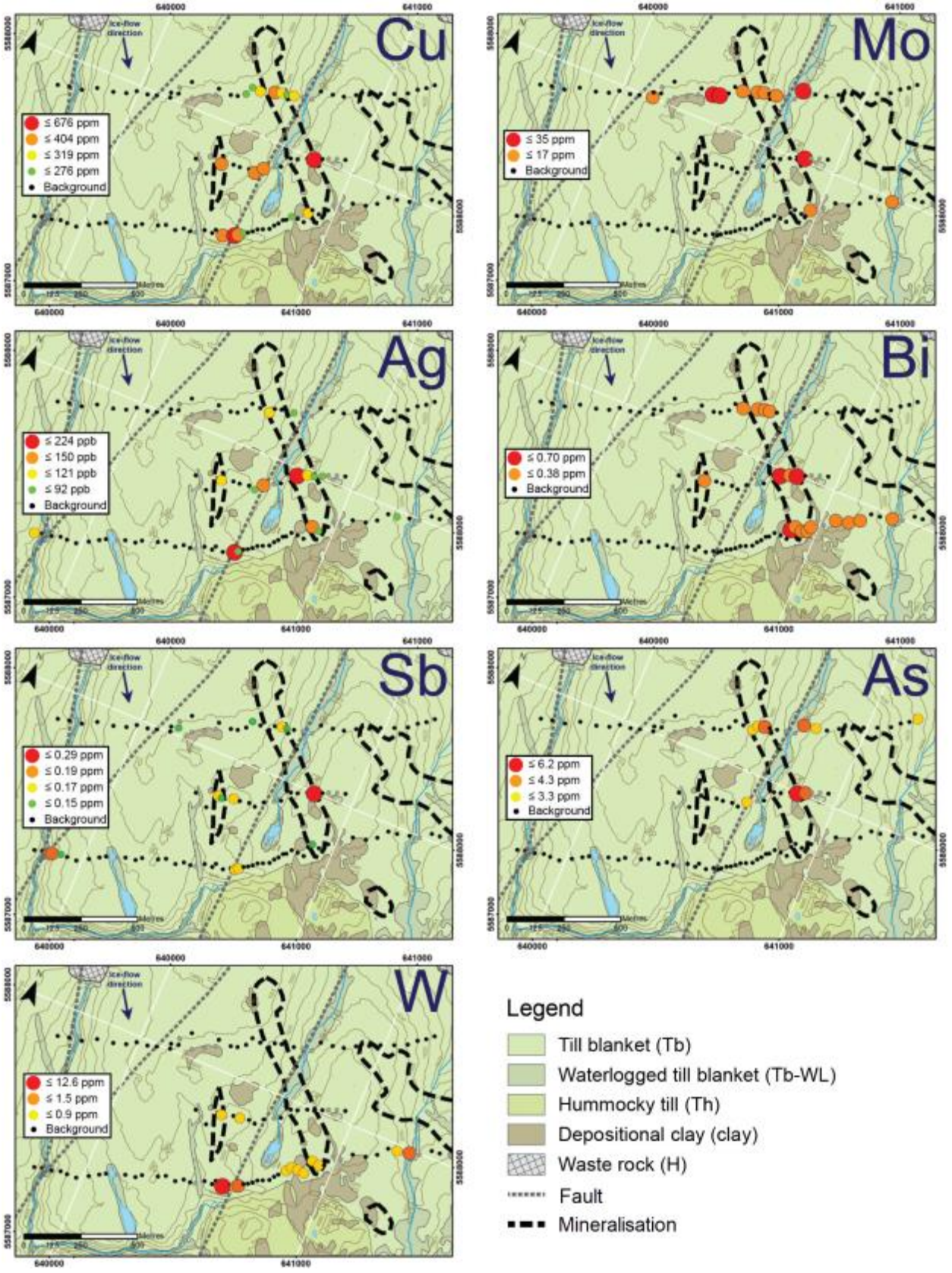
Cu
≤ 676 ppm
≤ 404 ppm
≤ 319 ppm
≤ 276 ppm
Background
Mo
≤ 35 ppm
≤ 17 ppm
Background
Ag
≤ 224 ppb
≤ 150 ppb
≤ 121 ppb
≤ 92 ppb
Background
Bi
≤ 0.70 ppm
≤ 0.38 ppm
Background
Sb
≤ 0.29 ppm
≤ 0.19 ppm
≤ 0.17 ppm
≤ 0.15 ppm
Background
As
≤ 6.2 ppm
≤ 4.3 ppm
≤ 3.3 ppm
Background
W
≤ 12.6 ppm
≤ 1.5 ppm
≤ 0.9 ppm
Background
Ice-flow direction
Metres
640000
641000
Legend
Till blanket (Tb)
Waterlogged till blanket (Tb-WL)
Hummocky till (Th)
Depositional clay (clay)
Waste rock (H)
Fault
Mineralisation

Figure 4-17 (*overleaf*). Elements with anomalous concentration populations in soil (upper B horizon, <180 microns, aqua regia, ICP-MS) overlying bedrock mineralisation are Cu, Mo, Ag, Bi, Sb, As, and W. Elements with anomalous concentration populations overlying both the mineralised bedrock and the West Highmont fault which crosscuts mineralisation are Cu, Ag, Sb, and W. Contours plotted at 5 metre interval spacing. Surficial geology is modified from Plouffe and Ferbey (2015b), using the GSC data model for surficial geology, version 1.2 (Deblonde et al., 2012); ice-flow direction from Plouffe and Ferbey (2015b); buried mineralisation outlines from Teck (pers. comm., Teck, 2017); faults modified from McMillan et al. (2009).

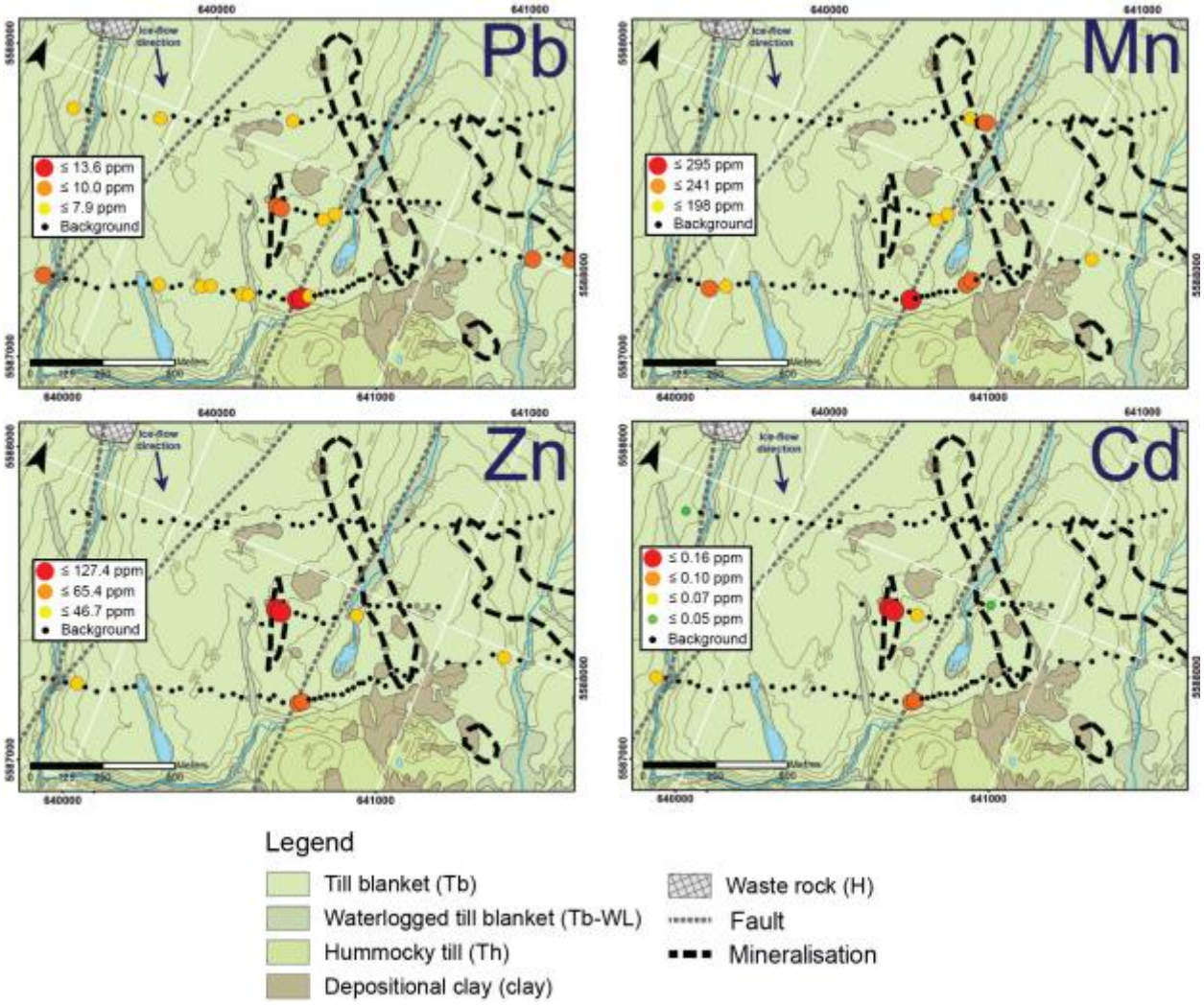

Figure 4-18. Additional elements which have anomalous concentration populations in soil (upper B horizon, <180 microns, aqua regia, ICP-MS) overlying both the westernmost body of mineralisation (with the exception of Mn) and the West Highmont fault which crosscuts mineralisation. Contours plotted at 5 metre interval spacing. Surficial geology is modified from Plouffe and Ferbey (2015b), using the GSC data model for surficial geology, version 1.2 (Deblonde et al., 2012); ice-flow direction from Plouffe and Ferbey (2015b); buried mineralisation outlines from Teck (pers. comm., Teck, 2017); faults modified from McMillan et al. (2009).

Silver, Bi, As, and Sb are known to exhibit strong chalcophile properties (Kabata-Pendias, 2010) and are likely present in Cu-bearing sulphide ore minerals such as chalcopyrite and bornite, indicated by strong positive relationships with Cu in the soil data (Figure 4-19).

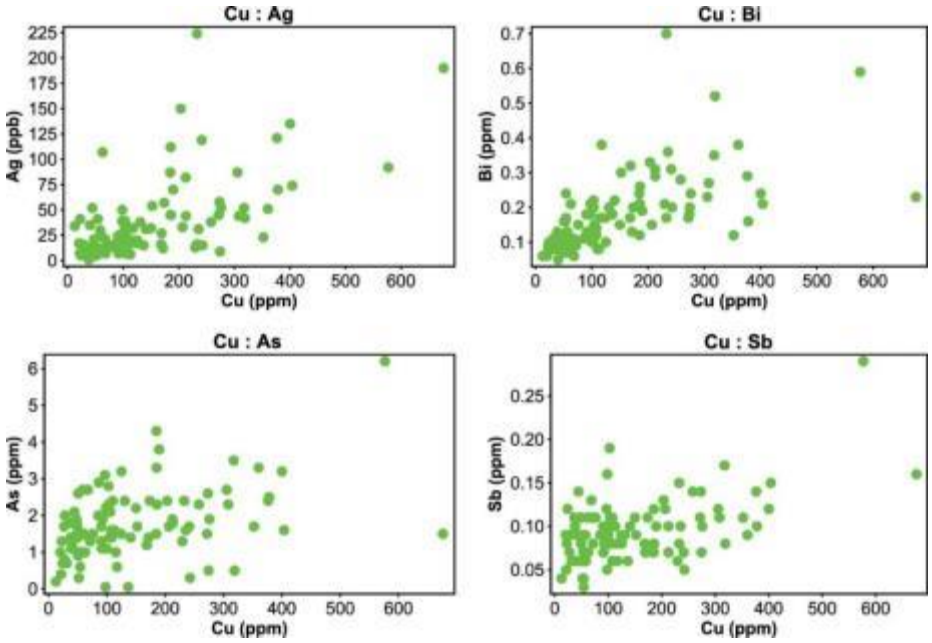

Figure 4-19. Plots of Cu vs. Ag, Bi, As, and Sb (<180 microns, aqua regia, ICP-MS) for upper B horizon soils developed over till blanket at Highmont South show positive trends. This indicates that Ag, Bi, As, and Sb, which have strong chalcophile character (Kabata-Pendias, 2010), are likely present within Cu-bearing sulphide ore minerals such as chalcopyrite and bornite.

Element	Units	Local background median concentration	Median concentration over West Highmont fault (transects #2 and #3)	Median concentration over bedrock mineralisation (transects #2 and #3)
Cu	ppm	124.11	402.04	212.45
Mo	ppm	7.34	8.14	10.31
Ag	ppb	30.5	104.5	82.0
Bi	ppm	0.15	0.22	0.31
Sb	ppm	0.09	0.14	0.10
As	ppm	1.85	2.05	2.20
W	ppm	0.20	0.65	0.40
Pb	ppm	4.04	9.46	4.59
Cd	ppm	0.030	0.065	0.020
Zn	ppm	23.95	44.95	22.80
Mn	ppm	100.0	187.5	110.0

Table 4-1. Median element concentrations in upper B horizon soils (<180 microns, aqua regia, ICP-MS) in transects two and three comparing samples from local background, overlying bedrock mineralisation, and overlying the West Highmont fault which crosscuts mineralisation.

4.6.4 Deionised water leach ICP-MS results

Analytical results are reported in Appendix C and QA/QC practises and results in Appendix B. Selected elements were compared to certified and indicated values of OREAS25a CRM to assess precision. Mean percentage difference for field duplicate results was used to assess natural variability. Data quality is summarized as follows:

- Elements for which all values were reported below ten times stated analytical detection limits and are not discussed further are: Pb, Ag, Au, Th, Cd, Bi, V, W, Sc, Tl, S, Hg, Se, Te, Sn, Ta, In, and Be;
- Elements for which the median of values was below ten times stated analytical detection limits and are interpreted with caution are: Zn, Ni, Co, Mn, As, Cl, Sb, Ca, La, Na, K, Cs, Ge, Nb, Re, Pr, Sm, Eu, Ho, Tb, Tm, Yb, and Lu;
- Elements which are of acceptable accuracy and precision are: Mo, Cu, Fe, U, Sr, P, Mg, Ba, Ti, Al, Br, Ga, Hf, Rb, Zr, Y, Ce, Nd, Gd, Dy, Er, and Li.

Copper concentrations from deionised water leach ICP-MS indicate an anomalous response in soil developed on till overlying mineralisation at Highmont South. Anomalous Cu values in soil overlie bedrock mineralisation as well as the trace of the West Highmont fault (Figure 4-20). Deionised water-extractable Mo responses appear at slurry pH values more alkaline than 6.0 and slurry ORP values lower than 250 mV, which occur almost exclusively within waterlogged till blanket and waterlogged depositional clay units. Molybdenum is known to be most mobile within alkaline and oxidising soils (Schwedt, 2001). With Cu as the only successfully detectable anomalous element in the labile portion of soil samples at Highmont South, it is clear that despite the young glacial material overlying bedrock mineralisation, aqua regia is a much more appropriate digestion method for multi-element anomaly detection in this setting.

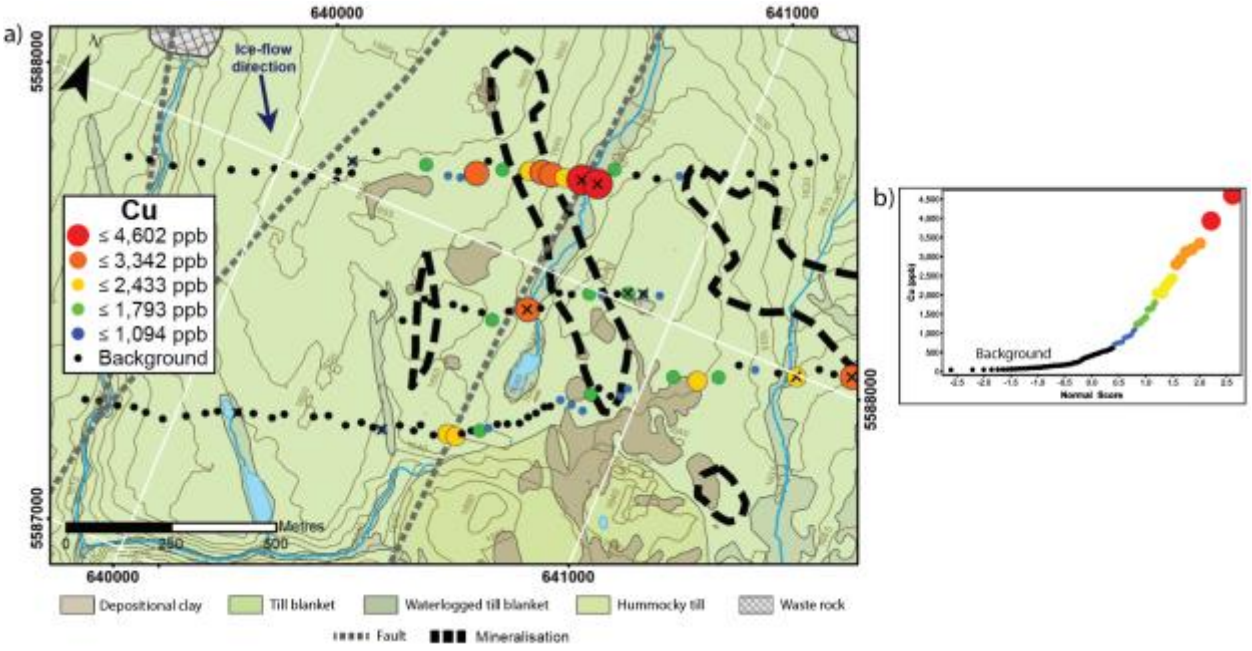

Figure 4-20. a) Copper results for deionised water leach ICP-MS of upper B horizon (<180 microns) soils at Highmont South indicate an anomalous response overlying bedrock mineralisation and the West Highmont fault which crosscuts mineralisation. Samples from depositional clay units are excluded; samples marked with an 'x' are from waterlogged till blanket units. Contours plotted at 5 metre interval spacing. Surficial geology is modified from Plouffe and Ferbey (2015b), using the GSC data model for surficial geology, version 1.2 (Deblonde et al., 2012); ice-flow direction from Plouffe and Ferbey (2015b); buried mineralisation outlines from Teck (pers. comm., Teck, 2017); faults modified from McMillan et al. (2009). b) Anomalous intervals were selected based on visual estimation of population breaks on a probability plot.

4.6.5 Organic carbon results

Analytical results are reported in Appendix C and QA/QC practises and results in Appendix B. Selected elements were compared to certified and indicated values of OREAS25a CRM to assess precision. Mean percentage difference for field duplicate results was used to assess natural variability.

The C_{org} content in Highmont South upper B horizon soil samples has a median concentration of 1.18%. The median C_{org} contents of waterlogged till blanket material, depositional clay, and till blanket are 1.71%, 1.19%, and 1.09%, respectively (Figure 4-21a). The only element which C_{org}

trends with is Hg (aqua regia, ICP-MS) (Figure 4-21b) known to bind strongly to organic material (Kabata-Pendias, 2010).

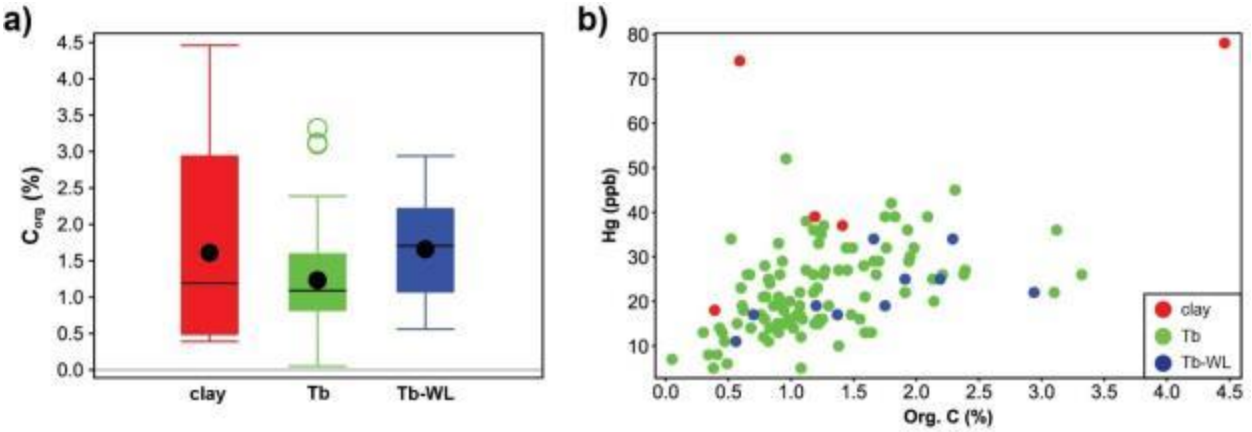

Figure 4-21. a) Organic carbon concentrations in upper B horizon soils developed on different surficial materials at Highmont South. b) Mercury concentrations (<180 microns, aqua regia, ICP-MS) have an overall positive trend with C_{org} concentrations in upper B horizon soils developed on different surficial materials at Highmont South.

Although organic matter is generally low in all surficial material at Highmont South, the CEC associated with soil organic matter is pH dependant (Ketterings et al., 2007). A soil with a pH of ~7 will have a higher CEC than a soil with a more acidic pH (e.g. pH 5), given the same organic matter content (Ketterings et al., 2007). Table 4-2 summarises the median pH C_{org} values for soils from the different surficial units at Highmont South.

Surficial unit	Median pH	Median C_{org}
Waterlogged depositional clay	6.7	1.19%
Waterlogged till blanket	6.5	1.71%
Till blanket	5.7	1.09%

Table 4-2. Summary table of 1:1 soil-deionised water by volume slurry pH values and organic carbon content for upper B horizon soils sampled from the different surficial material units at Highmont South.

4.6.6 Field-portable XRF results

Analysis of <180 microns upper B horizon soil samples using a pXRF analyser was conducted using both 'soil' and 'geochem' modes. Selected elements were compared to certified and indicated values of OREAS25a CRM to assess precision. Mean percentage difference (MPD) for field duplicate results was used to assess natural variability. Results for Cu, Mo, Pb, Zn, and Mn by soil mode are deemed acceptable following evaluation of QC results. Detailed QA/QC results are reported in Appendix B.

The pXRF mode most fit for purpose is soil mode, as trace elements report less than 1% in the sample medium. Using this mode the bench-top pXRF analysis was relatively successful at analysing concentrations of Cu, Mo, Pb, Zn, and Mn (Figure 4-23). Anomalous element populations were determined visually based on population plots and histograms. pXRF analyses for Ag and Bi are below ten times detection limits.

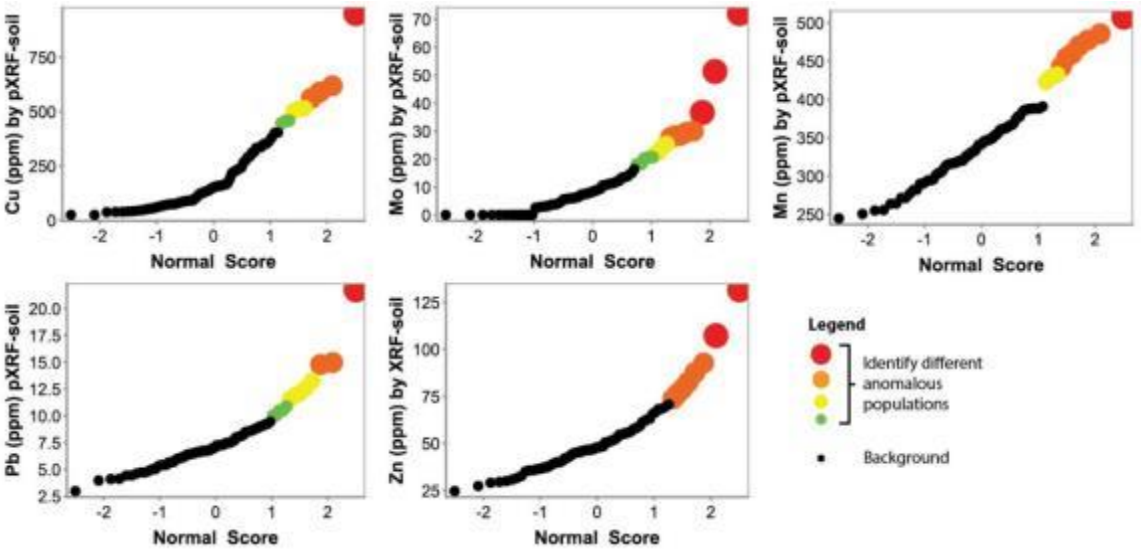

Figure 4-22. Probability plots showing distribution of element results in upper B horizon soil (<180 microns, pXRF soil mode) sampled from Highmont South. Samples from clay units are excluded. Anomalous population intervals were selected based on visual estimation of population breaks on these plots. Anomalous intervals are determined separately for each individual plot and symbols of the same size and colour are not related between plots for different elements.

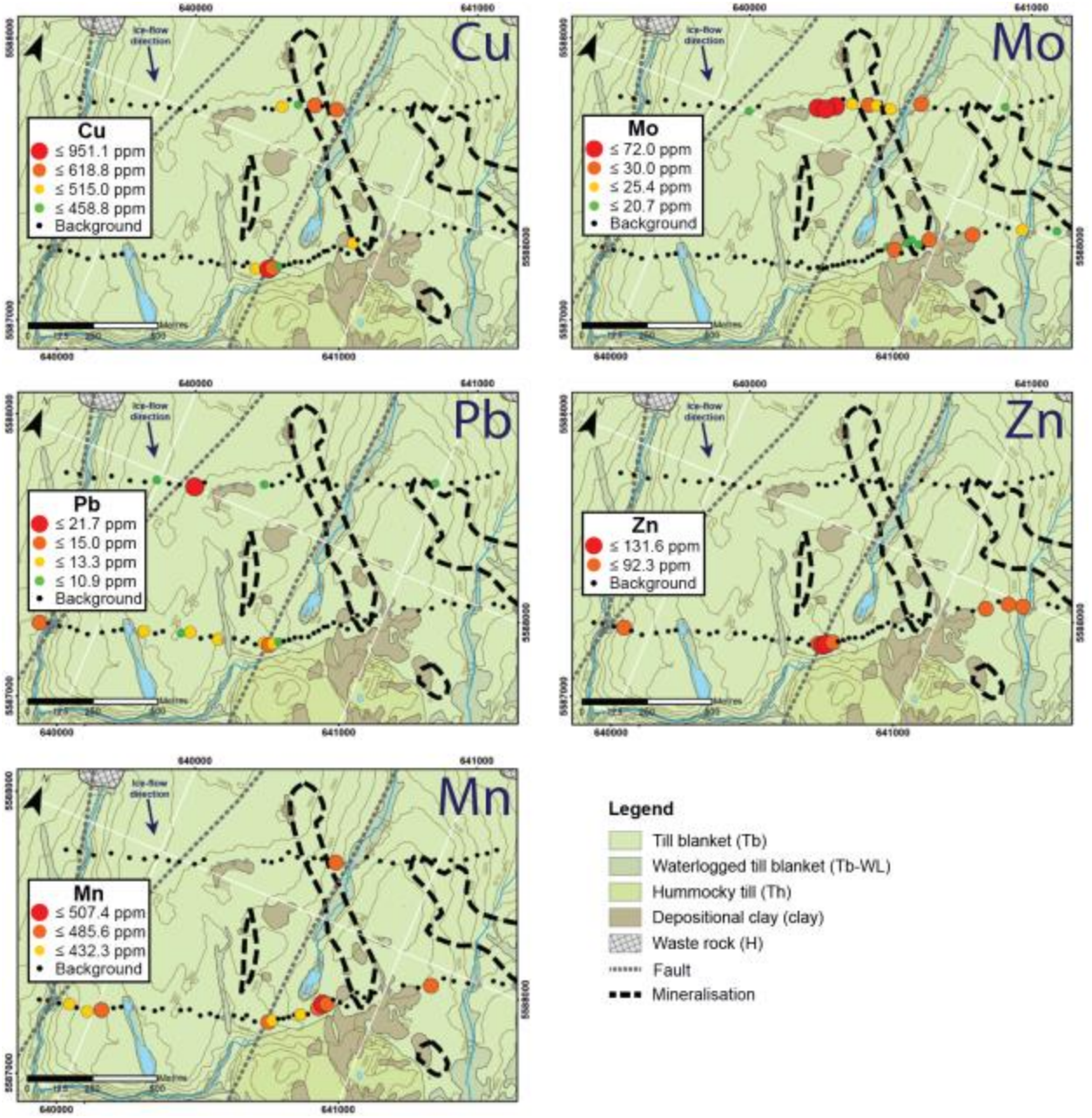

Figure 4-23. Elements with anomalous concentration populations in soil (till blanket surficial units, upper B horizon, <180 microns, pXRF soil mode) overlying bedrock mineralisation are Cu and Mo. Elements with anomalous concentration populations overlying the West Highmont fault which crosscuts mineralisation are Pb, Zn, and Mn. Grey points indicate excluded soil samples from waterlogged sediments. Contours plotted at 5 metre interval spacing. Surficial geology is modified from Plouffe and Ferbey (2015b), using the GSC data model for surficial geology, version 1.2 (Deblonde et al., 2012); ice-flow direction from Plouffe and Ferbey (2015b); buried mineralisation outlines from Teck (pers. comm., Teck, 2017); faults modified from McMillan et al. (2009).

4.7 Soil profile sample analysis

4.7.1 Physicochemical properties

Two complete soil profiles were sampled on Highmont South: profile site RC-16-HVC-028 (640941 m E, 5587781 m N) overlying mineralisation, and profile site RC-16-HVC-029 (640545 m E, 5587549 m N) in the down-ice direction from mineralisation. Both profiles have similar downhole patterns for slurry pH (Figure 4-24a) as well as in situ pH measurements (Figure 4-13b), which are overall acidic. pH (slurry and in situ) values are more acidic at the top of each profile (pH ~ 4.6), where organic matter is present, than in the lowest horizons sampled in or closer to the C horizon (pH ~ 5.5). Slurry EC (Figure 4-24a) and in situ EC values (Figure 4-24b) are low for both soil profiles. Slurry ORP and pH for RC-16-HVC-028 indicate reducing conditions in the surface LFH and B horizons, and oxidising conditions downhole in the C horizon. Slurry ORP (Figure 4-24a) for RC-16-HVC-029 is more oxidising in the surface (LFH) horizon, is most reducing in the eluviated (Ae) horizon, and borders between oxidising and reducing in the B horizon.

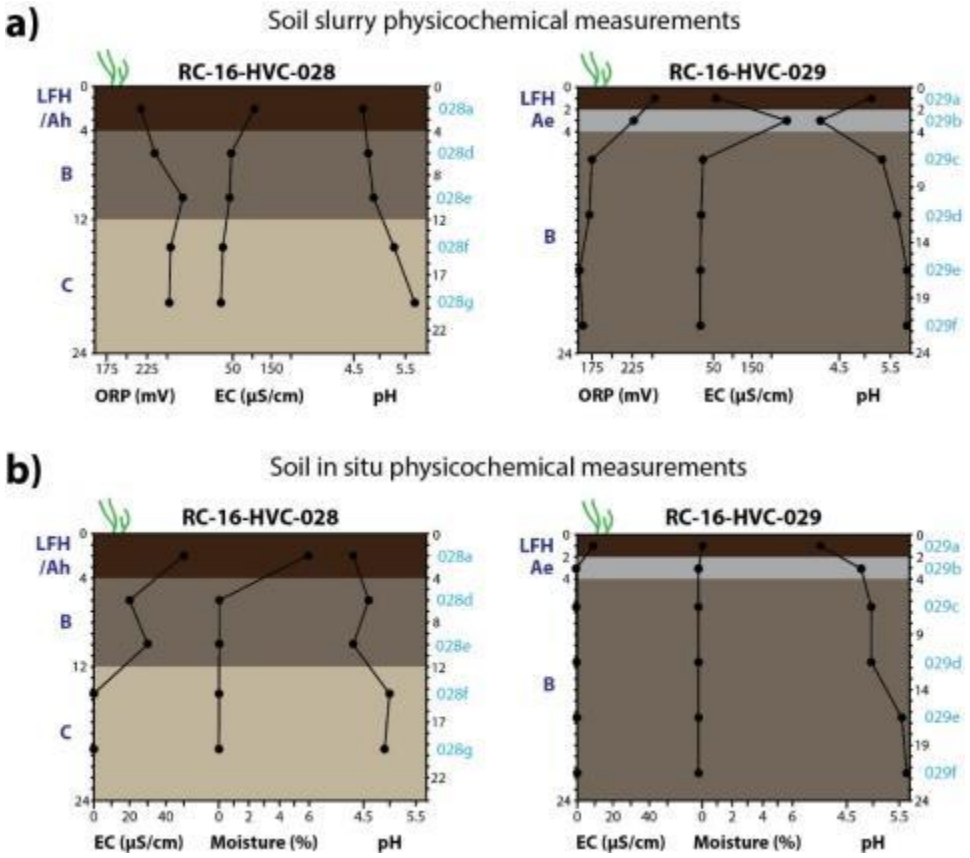

Figure 4-24. a) Soil slurry measurements for ORP, EC, and pH in each sampling interval (sample intervals marked in light blue on right axis) in soil profiles at Highmont South. b) In situ measurements for EC, moisture, and pH in each sampling interval in soil profiles at Highmont South. Depth measurements are in centimetres. Nomenclature of soil horizons, marked in dark blue (left axis), follows the Canadian system of soil classification (Agriculture Canada, 1998).

4.7.2 Aqua regia digest ICP-MS results

Analytical results are reported in Appendix C and QA/QC practises and results in Appendix B. Selected elements were compared to certified and indicated values of OREAS25a CRM to assess precision. Mean percentage difference for field duplicate results was used to assess natural variability. Elements analysed by aqua regia ICP-MS which are all below ten times stated analytical detection limits for both profiles and are not discussed further are: U, Au, Th, Sb, B, Na, W, Tl, S, Se, Te, Ge, Hf, Sn, Ta, In, Re, Be, Pd, and Pt. The remaining data was deemed acceptable following evaluation of QC results.

Profile RC-16-HVC-028, sampled over mineralisation, has higher median concentrations of Cu, Mo, Ag, and Bi compared to RC-16-HVC-029, sampled down-ice from mineralisation (Figure 4-25).

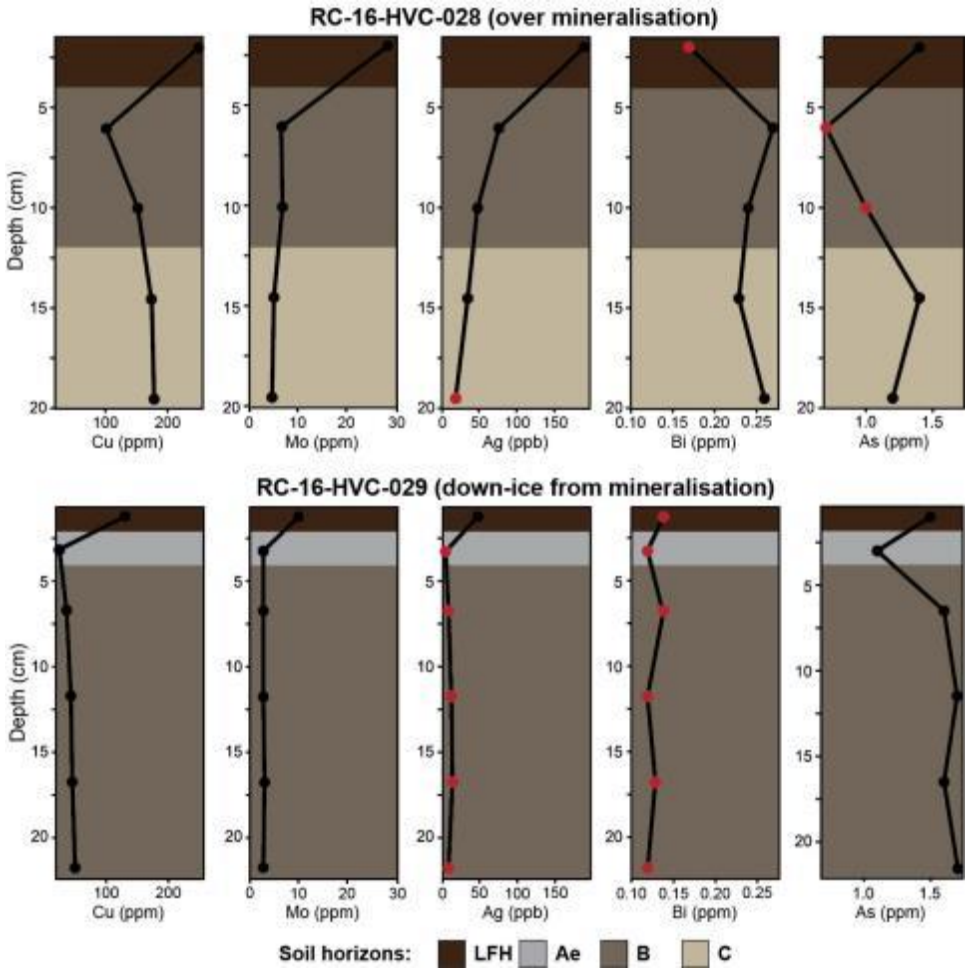

Figure 4-25. Downhole concentrations of Cu, Mo, Ag, Bi, and As in soil profiles at Highmont South (<180 microns, aqua regia, ICP-MS). The elements Cu, Mo, Ag, and Bi have higher median concentrations in profile RC-16-HVC-028, sampled overlying mineralisation, compared to profile RC-16-HVC-029, sampled down-ice from mineralisation. Red points represent values below ten times stated analytical detection limits.

The distribution of arsenic in profile RC-16-HVC-029 is a good example of the eluviation process in soil which forms the Ae horizon (Figure 4-25). Organic acids from the organic-rich surface (LFH or O) horizon leach clays, ions, and/or organic matter from the A horizon directly

below, leaving an Ae horizon which is light coloured and more coarse-grained. The leached clays and ions are deposited below, typically in the upper 10 centimetres of the B horizon (Agriculture Canada, 1998). This, the zone of illuviation, is the ideal target for soil sampling in environments with anthropogenic inputs which may affect the more organic-rich surface horizons (Blaser et al., 2000). When present in brunisolic soil profiles over Highmont South, Ae horizons are weakly developed and therefore classified as juvenile 'Aej' horizons.

4.7.3 Deionised water leach ICP-MS results

Analytical results are reported in Appendix C and QA/QC practises and results in Appendix B. Selected elements were compared to certified and indicated values of OREAS25a CRM to assess precision. Mean percentage difference for field duplicate results was used to assess natural variability. Elements analysed by deionised water leach ICP-MS which are all below ten times stated analytical detection limits for both profiles and are not discussed further are: Pb, Ag, Ni, Au, Th, Cd, Sb, Bi, V, Na, W, Sc, Tl, S, Hg, Se, Te, Cs, Nb, Tm, Yb, Lu, Ta, In, Re, and Be. The remaining data was deemed acceptable following evaluation of QC results.

Profile RC-16-HVC-028, sampled over mineralisation, has higher median Cu, Mo, and As compared to that of RC-16-HVC-029, sampled down-ice from mineralisation. These elements follow a trend of high concentrations in the surface (LFH) horizon, decreasing down profile (Figure 4-26).

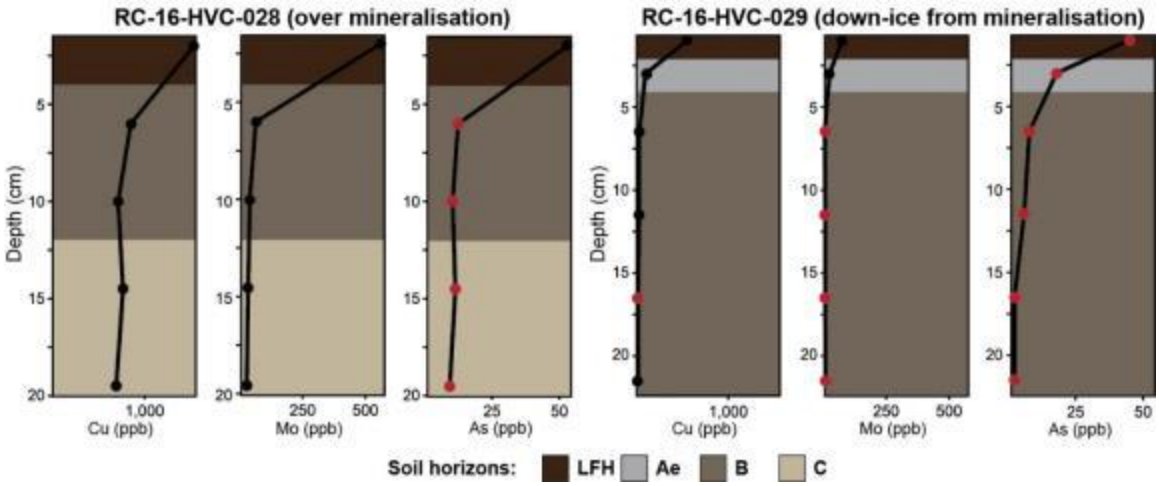

Figure 4-26. Copper, Mo, and As concentrations in Highmont South soil profiles (<180 microns, deionised water leach, ICP-MS). Red points represent values below ten times stated analytical detection limits.

4.7.4 Organic carbon results

Analytical results are reported in Appendix C and QA/QC practises and results in Appendix B. Selected elements were compared to certified and indicated values of OREAS25a CRM to assess precision. Mean percentage difference for field duplicate results was used to assess natural variability.

For profile RC-16-HVC-028 the highest C_{org} concentration of 34.77% is in the surface organic litter (LFH) horizon. The remainder of the sample intervals down profile show a downwards decrease from 1.27% C_{org} in the top of the B horizon to 0.31% C_{org} in the last interval sampled in the C horizon (Figure 4-27).

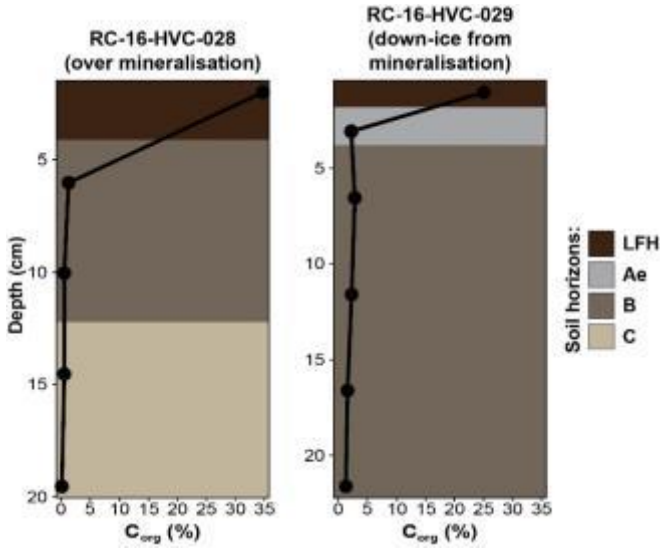

Figure 4-27. Organic carbon concentrations in Highmont South soil profiles. The highest concentrations of C_{org} in both profiles occur within the surface (LFH) horizon.

For profile RC-16-HVC-029 the highest C_{org} concentration of 25.12% is in the surface (LFH) horizon. The LFH horizon is thinner and less well developed than that of RC-16-HVC-028. Profile RC-16-HVC-029 contains an eluviated (Ae) horizon which, as expected, has a lower C_{org} concentration (2.31%) than the illuviated (B horizon) interval below (2.87%). The remainder of the intervals in RC-16-HVC-029 follow the same pattern of downhole decrease in C_{org} concentration as RC-16-HVC-028. The lowest sample interval in RC-16-HVC-029, within the B horizon, has 1.44% C_{org} (Figure 4-27).

The approximate amount of soil organic matter (SOM) can be calculated by multiplying the analysed concentration of C_{org} by the "Van Bemmelen factor" 1.724 (Bemmelen, 1890), using the following equation:

$$SOM\ (\%) = C_{org}\ (\%) \times 1.724 \qquad (3)$$

This equation assumes organic matter contains 58% organic carbon. The Van Bemmelen factor is a universal factor that can only approximate SOM from C_{org}, which can be highly variable in

different soils and even between soil horizons (USDA, 2014). Using this equation, the LFH horizon in soil profile RC-15-HVC-028 contains approximately 60% organic matter, and that of RC-15-HVC-029 contains approximately 44% organic matter.

4.8 Sequential extractions

4.8.1 Sample selection

Four samples were selected for sequential extraction from the 2015 upper B horizon soil samples from Highmont South to identify the deportment of trace elements in the soil (Figure 4-28). Geochemical data from previous analyses was considered in the selection of samples for sequential extraction.

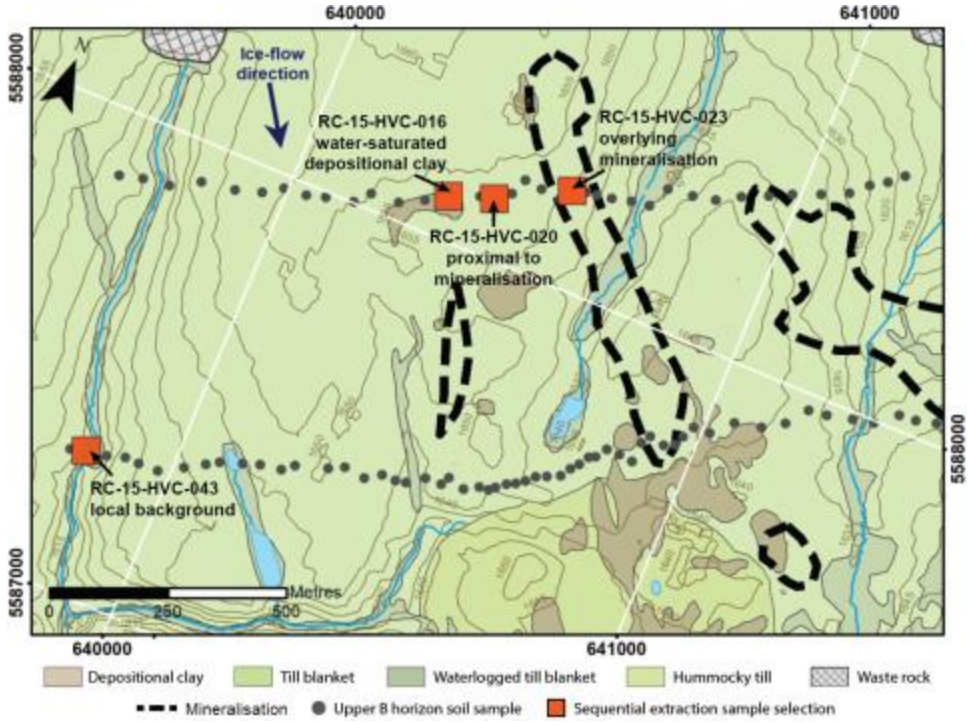

Figure 4-28. Upper B horizon (<180 microns) soil sample sites selected for sequential extractions. Contours plotted at 5 metre interval spacing. Surficial geology is modified from Plouffe and Ferbey (2015b), using the GSC data model for surficial geology, version 1.2 (Deblonde et al., 2012); ice-flow direction from Plouffe and Ferbey (2015b); buried mineralisation outlines from Teck (pers. comm., Teck, 2017).

4.8.2 Results

Analytical results are reported in Appendix C and QA/QC practises and results in Appendix B. The data was deemed acceptable and fit for purpose following evaluation of QC results. The sum of sequential extractions was typically 100% ±20% of separate total chemical analysis. Consistency of final pH values (Table 4-3) for the leachate at the end of each extraction indicate whether or not the buffering of each extraction was successful and the elements associated with each target phase were effectively extracted.

	Final pH of leachate				
Sample	**DW_s**	**AmA_s**	**CHH_s**	**HHH_s**	**NaP_s**
RC-15-HVC-016	7.6	5.0	2.6	1.2	9.4
RC-15-HVC-020	5.3	5.0	2.2	1.1	9.9
RC-15-HVC-023	5.2	5.0	2.3	1.1	9.6
RC-15-HVC-043	5.1	5.0	2.3	1.1	10.0
Median:	**-**	**5.0**	**2.3**	**1.1**	**9.8**
Target:	**-**	**5.0**	**1.5**	**1.5**	**10.0**

Table 4-3. Final leachate pH values for DW_s, AmA_s, CHH_s, HHH_s, and NaP_s extractions in sequence. Target pHs are provided by Katerina Paley, ALS Minerals Division.

Sample RC-15-HVC-016 has high buffering capacity (Section 4.7.2) and it is likely that the sample is able to buffer some of the reactions in the sequenction extraction, resulting in off-target final leachate pH values. The AmA_s leach results on this sample show that it contains 5,070 ppm Ca in the carbonate ($CaCO_3$) soil phase. Samples RC-15-HVC-020, -023 and -043 contain 900 ppm, 2,260 ppm and 240 ppm Ca as the $CaCO_3$ phase, respectively. The high buffering capacity of sample -016 is attributed to its $CaCO_3$ content as well as its high clay content.

Total Cu, Mo, Ag and Bi in the four samples is dominantly recovered from the aqua regia and four acid extractions indicating the principal source phase in the soil is clastic (Figure 4-29). The majority of silver in all four samples is reported from $4A_s$ (Figure 4-29). Silver can have poor

solubility in aqua regia (HNO_3, HCl) due to the formation of an insoluble coating of AgCl which prevents further dissolution (Park and Fray, 2009).

Compared to other samples, sample RC-15-HVC-016, from a depositional clay unit, contains a significant portion of:

- Cu reported from the weaker leaches (HHH_s, AmA_s, and CHH_s) which indicates a higher proportion of amorphous Fe-oxide, carbonate, and amorphous Mn-oxide components controlling the distribution of Cu in the sample; and
- Mo (approximately 20% of the total) extracted by DW_s, representing the most labile, loosely-bound portion of Mo within the sample which is likely present in the porewater of this waterlogged sample.

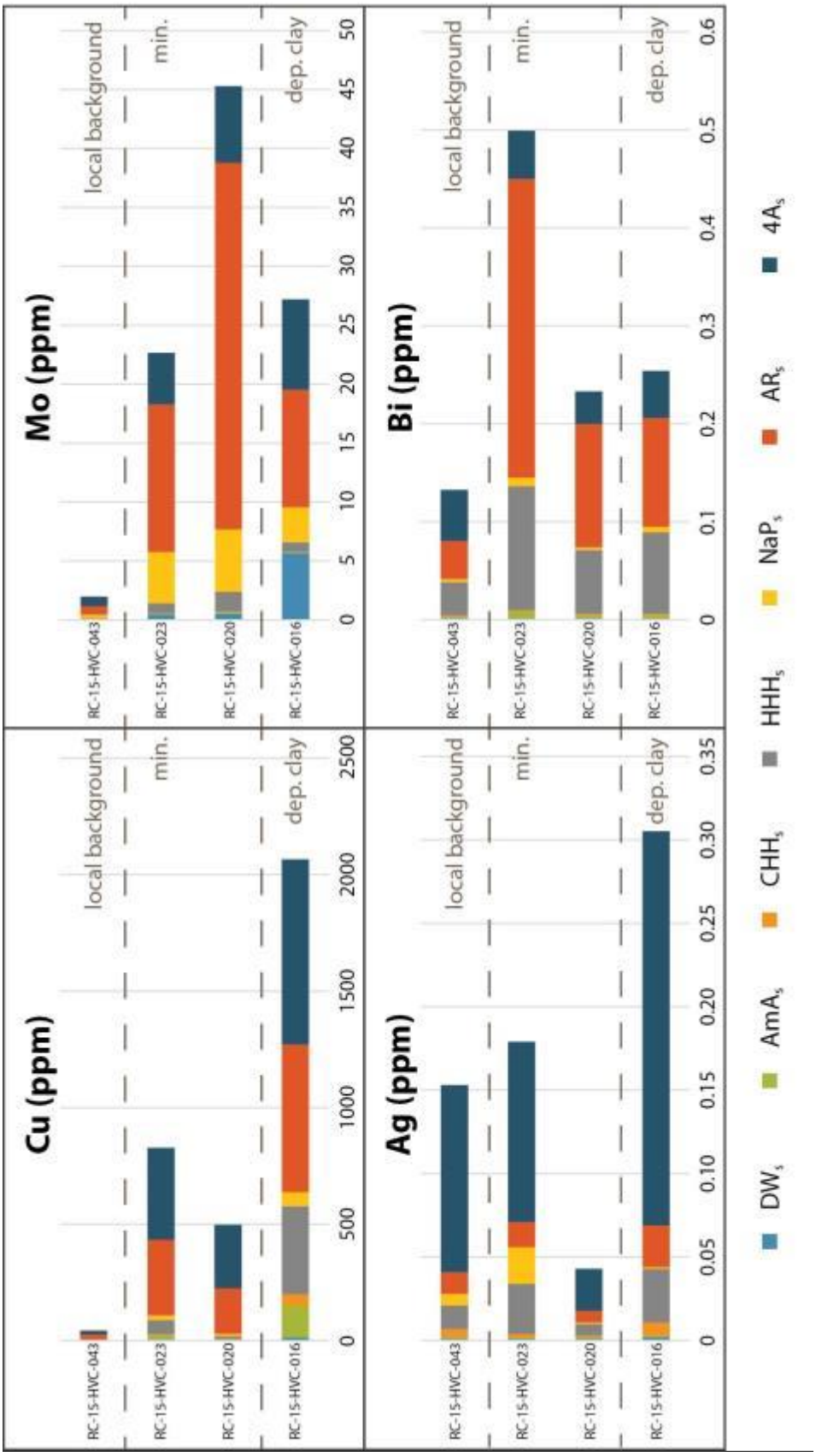

Figure 4-29. Sequential extraction results for all four upper B horizon soil samples (<180 microns portion) selected for Highmont South. The top sample (RC-15-HVC-043) represents local background. The bottom sample (-016) is from water-saturated depositional clay materials determined to produce false anomalies. The two middle samples (-023 and -020) are from till blanket material overlying mineralisation and proximal to mineralisation, respectively. For reference to extraction symbols see Table 3-2 in Section 3.6.7.

Figure 4-32 displays the concentrations of Ca as carbonates, Mn as amorphous Mn-oxides, Fe as amorphous Fe-oxides, and C_{org} in the four analysed soil samples. Sample RC-15-HVC-016 has the highest amount of Cu associated with carbonates (Figure 4-29) as well as the highest concentration of Ca extracted in AmA_s (Figure 4-30). Calcium carbonate appears to be a controlling phase on Cu in the soil (Figure 4-31). This is the only instance in which the amount of the controlling phase in the soil may be the reason for the higher sorbed concentration of the metal of interest. For example, samples -023 (overlying mineralisation) and -043 (local background) contain the same concentration of C_{org}, however the concentration of Ag extracted by NaP_s is significantly higher in the sample overlying mineralisation.

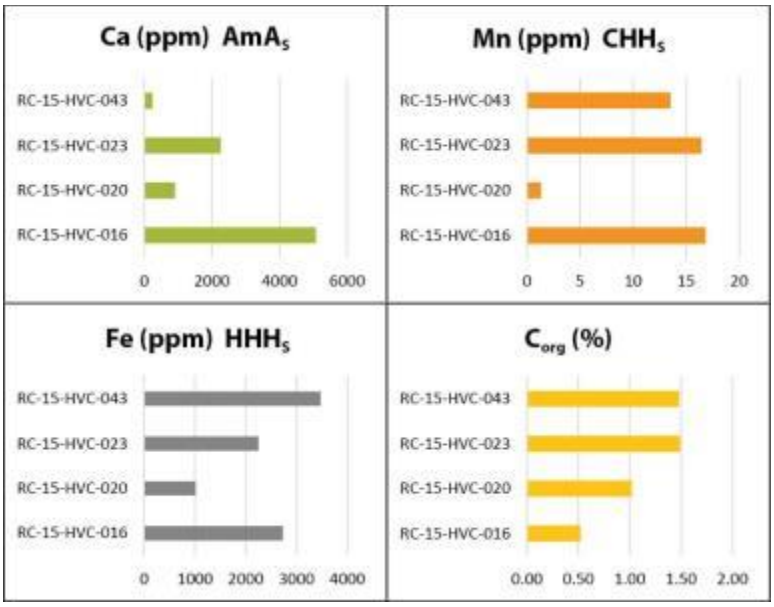

Figure 4-30. Selective extraction results for all four upper B horizon (<180 microns) soil samples selected for Highmont South. Concentrations of different target phases in each sample are presented corresponding to the step in the sequential extraction which targets that specific phase. Calcium is a proxy for relative $CaCOF_3$ content extracted in AmA_s. Manganese and Fe are proxies for amorphous Mn- and Fe-oxides extracted by CHH_s and HHH_s, respectively. Organic C (determined by previous separate analysis at Bureau Veritas) is a proxy for organic matter extracted by NaP_s. For reference to extraction symbols see Table 3-2.

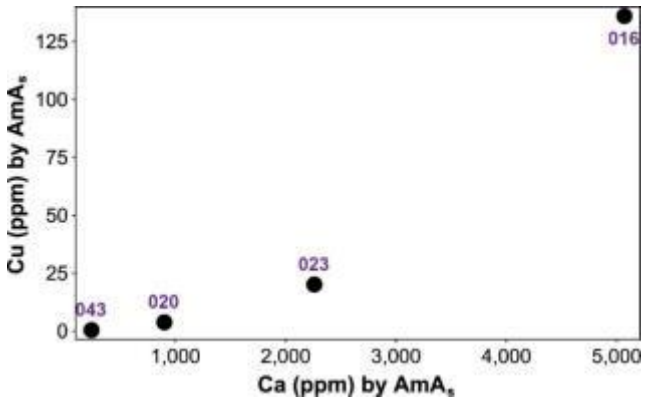

Figure 4-31. AmA$_s$ results for Cu plotted against those for Ca in the sequential extraction process (<180 microns, upper B horizon soil). A positive trend between the two elements indicates that soil Ca is probably a controlling phase for Cu speciation in the soil at Highmont South.

With the removal of sample -016 as a falsely anomalous sample, there exists a high anomaly-background contrast between samples overlying and next to mineralisation (samples -023 and -020, respectively), and the sample representing local background (sample -043). Focusing on the weaker extractions before AR$_s$ and 4A$_s$ shows that the next most significant phase controlling the distribution of Cu, Ag, and Bi in the soil is adsorption by amorphous Fe-oxides, reported from HHH$_s$ (Figure 4-32). There is a more significant proportion of Mo associated with organic matter compared to Cu, Ag, and Bi, shown by NaP$_s$ results. Molybdenum is easily taken up by plants and can become substantially enriched in plant tissues (Dunn, 2007). It is determined in Section 4.12 with biogeochemical sampling results that there exists vegetation cycling of Mo from bedrock mineralisation to the surface environment in mineralised areas. Additionally Mo has a strong tendency to sorb to organic matter (Kabata-Pendias, 2010).

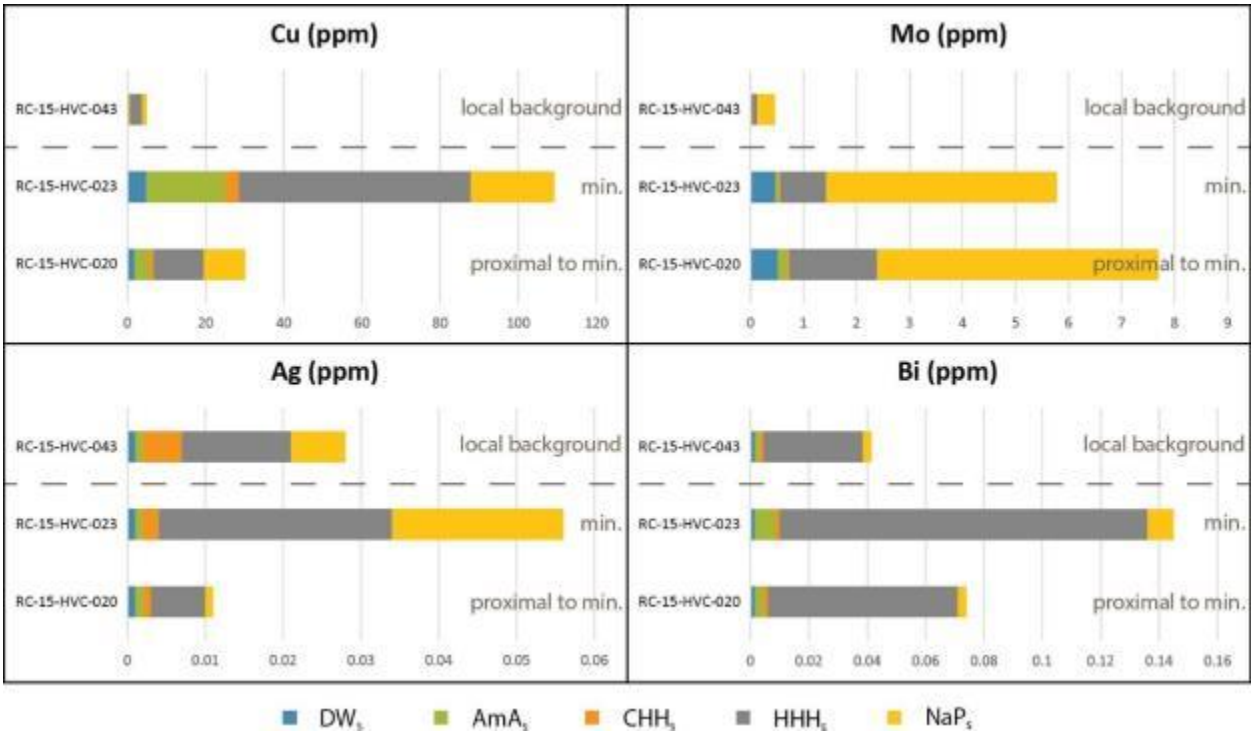

Figure 4-32. Results for the weaker leaches in the sequential extraction before AR_s and $4A_s$, with the removal of sample RC-15-HVC-016, from a depositional clay unit, for better mineralisation-background contrast.

4.9 Soil hydrocarbon results

A total of 86 hydrocarbon and organo-sulphur compounds (Table 3-3, Section 3.7) were analysed by thermal desorption and gas chromatography-mass spectrometry at Amplified Geochemical Imaging (AGI) laboratories in Newark, Delaware. Compounds removed from interpretation by AGI during signal-to-noise filtering are: ethane, propane, tetradecane, heptadecane, ethane, pristane, phytane, decanal, cis-1,3/1,4-dimethylcyclohexane, alpha-pinene, beta-pinene, camphor, caryophyllene, acenapthylene, and benzothiazole. Outlier samples RC-15-HVC-013, -054, and -063 were identified and removed from interpretation by AGI. The report compiled by AGI is available in Appendix F. QA/QC practices and results are detailed in Appendix B. The data was deemed acceptable on the basis of the AGI evaluation of QC results.

Compounds which have elevated concentrations in transect two soils overlying known bedrock mineralisation and the trace of the West Highmont fault are normal alkanes in the C_{12}–C_{15} range: dodecane, tridecane, and pentadecane (Figure 4-33). The difference between a signal displaying on transect two and not on transect one could be a function of relative soil disturbance. Transect one is sampled in cut blocks, where soil was recently disturbed by logging, while most of transect two is sampled in forest.

Comparison of soil physicochemical measurements to the analysed hydrocarbon and organo-sulphur compounds indicate that there are no clear relationships between any of these compounds and pH, Eh, EC, or moisture.

Interpretation by AGI (Appendix F) failed to determine any meaningful anomalous signatures overlying mineralisation at Highmont South. Interpretation was completed by AGI in the context of bedrock geology and did not include consideration of surficial materials and processes. This lead to the identification by AGI of anomalies which, when plotted with surficial geology, are clearly a result of waterlogged depositional clay units.

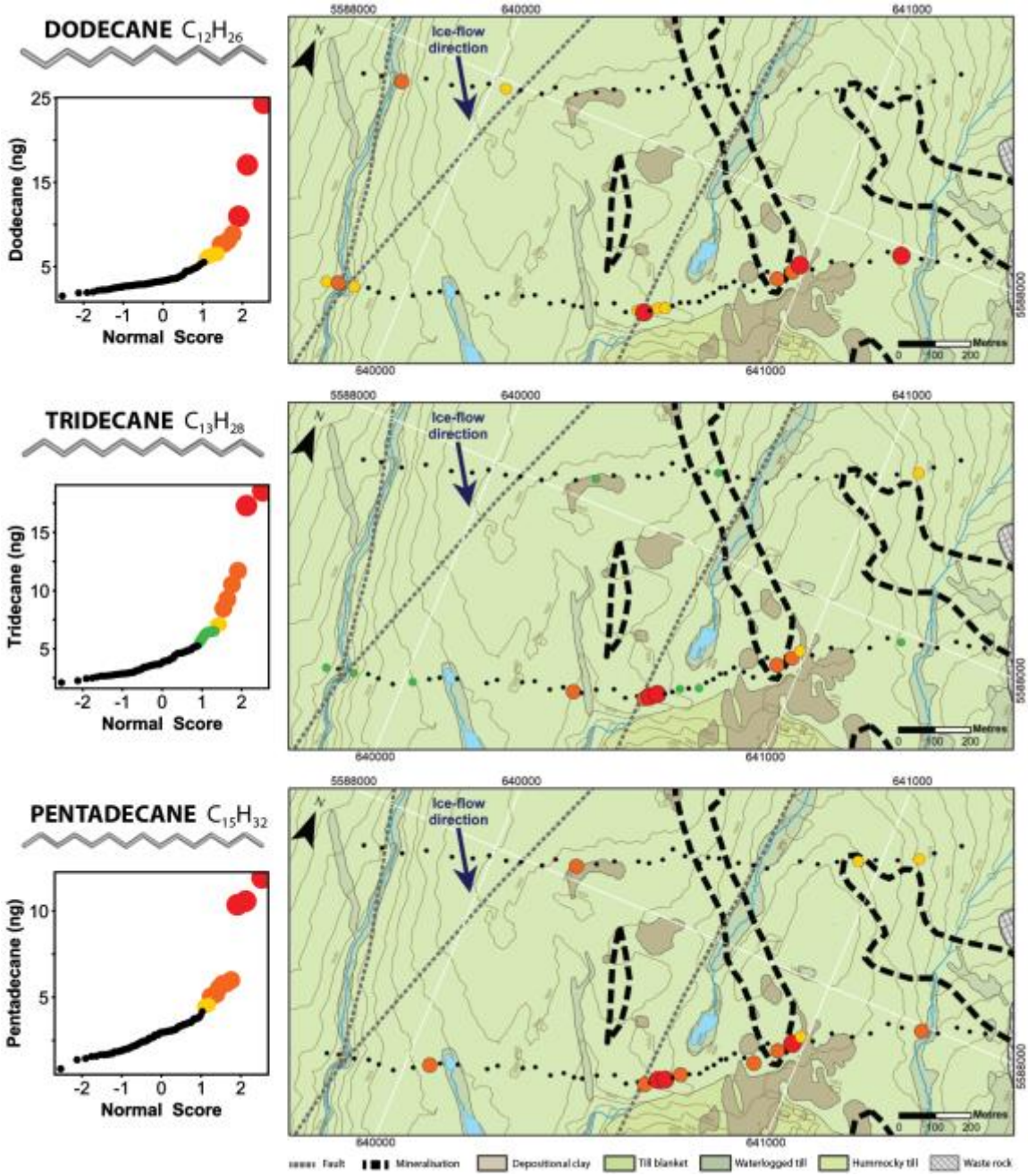

Figure 4-33. C_{12}-C_{15} range normal alkanes which are anomalous in soil overlying mineralisation and the West Highmont fault in transect two at Highmont South. Different anomalous population intervals, represented on a colour and size scale, were selected based on visual estimation of population breaks on population plots shown. Contours plotted at 5 metre interval spacing. Surficial geology is modified from Plouffe and Ferbey (2015b), using the GSC data model for surficial geology, version 1.2 (Deblonde et al., 2012); ice-flow direction from Plouffe and Ferbey (2015b); buried mineralisation outlines from Teck (pers. comm., Teck, 2017); faults modified from McMillan et al. (2009). Compound image source: PubChem (URL: https://pubchem.ncbi.nlm.nih.gov).

4.10 Copper isotopes

4.10.1 Sample selection

The nine samples selected from the 2015 upper B horizon soil samples are all from within transect one in till blanket surficial units, spanning from soils overlying bedrock mineralisation out towards local background (Figure 4-34).

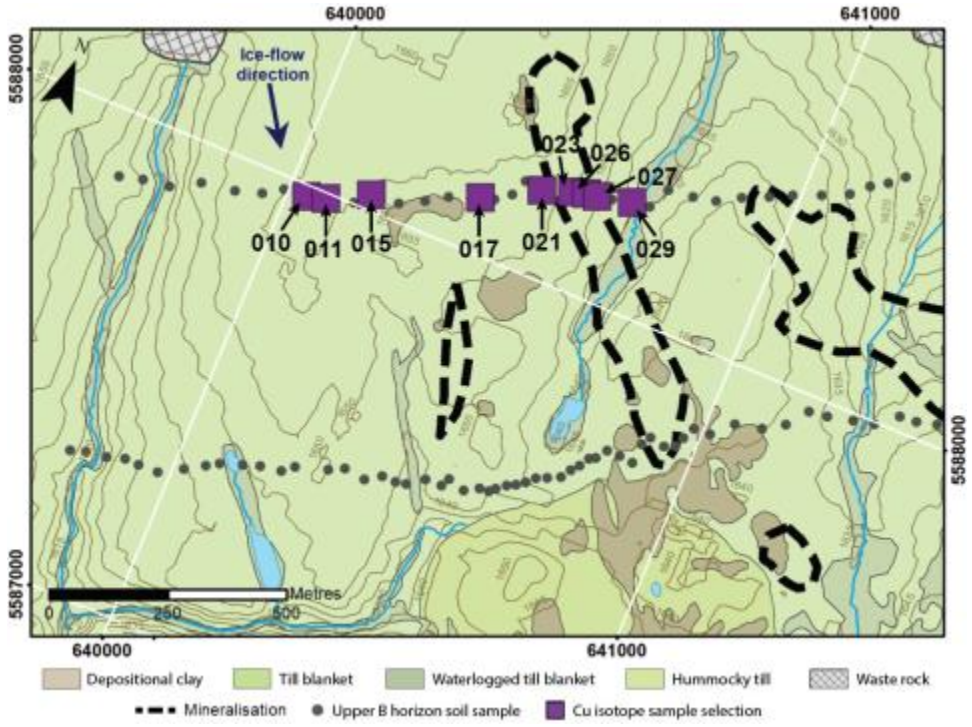

Figure 4-34. Locations of nine upper B horizon soil sample sites selected for Cu isotope analysis. Geochemical data from previous analyses was considered in the selection process. Contours plotted at 5 metre interval spacing. Surficial geology is modified from Plouffe and Ferbey (2015b), using the GSC data model for surficial geology, version 1.2 (Deblonde et al., 2012); ice-flow direction from Plouffe and Ferbey (2015b); buried mineralisation outlines from Teck (pers. comm., Teck, 2017).

4.10.2 Results

The isotopic signature for the Cu extracted in the total digest of each sample lies within the expected range for primary magmatic Cu ($\delta^{65}Cu = 0 \pm 1‰$). Copper isotope values measured

from the total digestion show no significant difference between samples from background and those overlying mineralisation (Table 4-4).

Sample	Location	Total digest		Partial leach		
		Cu (ppm)	δ^{65}Cu (‰)	Cu (ppm)	% Cu extracted	δ^{65}Cu (‰)
RC-15-HVC-010	Background	57.38	-0.49	0.51	0.89	-0.21
RC-15-HVC-011	Background	112.70	-0.20	0.79	0.70	No result
RC-15-HVC-015	Background	71.62	-0.30	0.41	0.57	-0.51
RC-15-HVC-017	Background	193.66	-0.44	1.43	0.74	-0.61
RC-15-HVC-021	Mineralisation	668.87	-0.39	2.86	0.43	-0.28
RC-15-HVC-023	Mineralisation	68.54	-0.24	4.87	7.10	-0.27
RC-15-HVC-026	Mineralisation	1,392.47	-0.29	6.16	0.44	-0.43
RC-15-HVC-027	Mineralisation	229.33	-0.22	5.85	2.55	-0.36
RC-15-HVC-029	Mineralisation	273.23	-0.30	11.23	4.11	-0.29

Table 4-4. Analytical Cu isotope results for selected upper B horizon (<180 microns) soils at Highmont South. 'Total digest' refers to HCl-HNO_3-HF digest and 'partial leach' refers to a 2% HNO_3 leach. The separate digest and leach were both analysed by Q-ICP-MS. Isotope ratios with reference to NIST976. Full methodology is reported in Appendix A.

A partial leach (2% nitric acid) was analysed to determine the isotopic signature for the loosely bound portion of Cu in the soil samples. It is hypothesised that if the Cu isotope results for the partial leach were outside of the primary magmatic range, this would indicate fractionation as the labile component of Cu in the soil matrix migrated from mineralisation at depth. The partial leach extracted a small portion (0.57–0.89%) of the total Cu content in the background samples (Table 4-4). An overall larger portion (up to 7.10%) of the total Cu content was extracted by the partial leach of the samples overlying mineralisation. Isotopic results for Cu extracted by the partial leach of all samples cluster closely together within the primary range of δ^{65}Cu indicating that the Cu has not migrated from bedrock mineralisation at depth (Figure 4-35). Results indicate that Cu in the soil samples analysed is locally derived from the till.

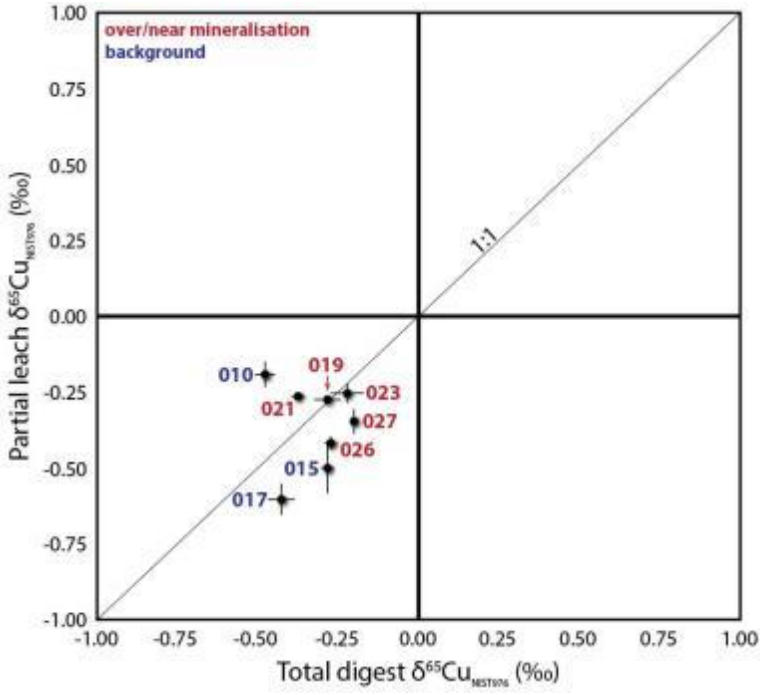

Figure 4-35. Soil (<180 microns, upper B horizon) Cu isotope results are tightly clustered within the primary magmatic range of -1‰ to +1‰ (represented by the entire plot area). Point labels refer to sample ID numbers. Error bars represent 2σ.

4.11 Biogeochemistry results

Analytical results are reported in Appendix C and QA/QC practises and results in Appendix B. Selected elements were compared to indicated values of 'P6' spruce needle internal reference material (IRM) provided by Colin Dunn to assess precision. Mean percentage difference for field duplicate results was used to assess natural variability. Data quality is summarized in Table 4-5, below.

All values below 10x detection limit:	As, Au, Bi, La, Ti, W, Sc, Tl, Se, Cs, Ge, Ce, Pd, Pt
Median of values below 10x detection limit:	Ni, Fe, Cd, B, Al, Na, S, Hf, Zr, Re, Li
Median of values above 10x detection limit:	**Ag, Co, Sb, Ba, Hg, Rb, Sn, Y**
All values above 10x detection limit:	**Mo, Cu, Pb, Zn, Mn, Sr, Ca, P, Cr, Mg, Ba, K**

Table 4-5. Data quality for elements analysed from lodgepole pine needles (aqua regia digest, ICP-MS). As a general rule of thumb, values within ten times the stated analytical detection limit are to be interpreted with caution and considered more as more "qualitative" data due to lower precision.

The circumferences of lodgepole pine trees sampled range from 24 to 36 centimetres (median: 29 centimetres). There are no discernable relations between tree circumference and chemistry of the needles sampled. There are relationships between element concentrations and the surficial unit in which the tree was sampled (Figure 4-36). Needles from lodgepole pine sampled in waterlogged depositional clay units are elevated in Cr, Mo, Na, S, Sr, and depleted in Ag, Al, B, Hg, K, Mn, P, and Zn relative to those in both waterlogged and dry till blanket units.

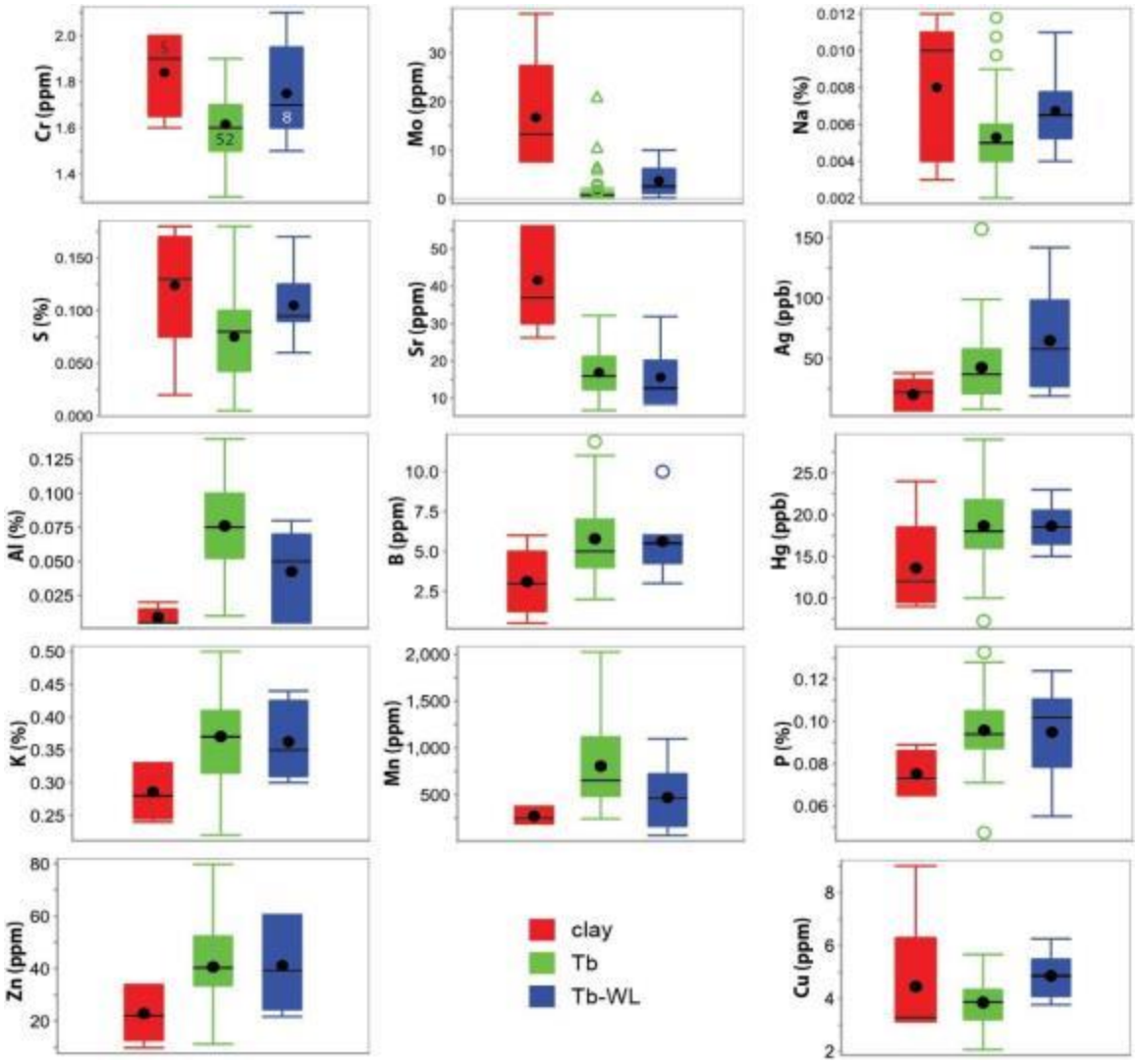

Figure 4-36. Lodgepole pine needle chemistry (aqua regia, ICP-MS) differs with the surficial material unit present at the site.

Elements related to porphyry mineralisation which indicate a fair mineralisation-background contrast in pine needle samples from Highmont South in dry till blanket material, based on visual estimations of population breaks from probability plots and histograms, are Mo, Ag, Sb, and Mn (Figure 4-38). Anomalous populations of Cu concentrations do not show a clear relationship with buried mineralisation (Figure 4-38).

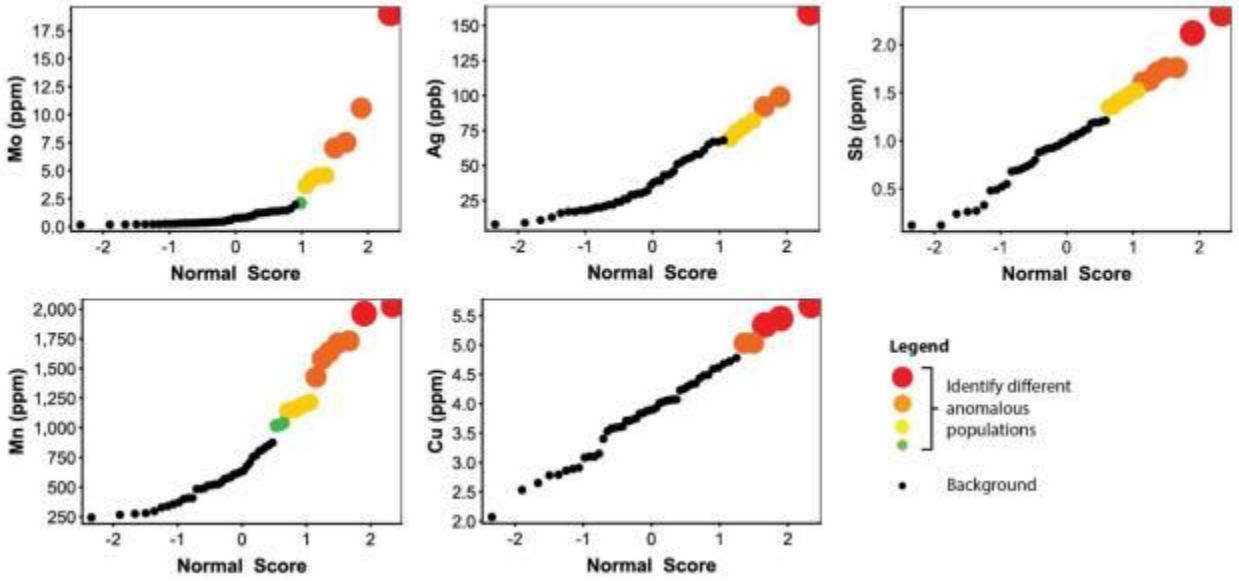

Figure 4-37. Probability plots showing distribution of element results in lodgepole pine needles (aqua regia, ICP-MS) sampled from Tb units on Highmont South. Anomalous population intervals were selected based on visual estimation of population breaks on these plots. Population intervals are determined separately for each individual plot and symbols of the same size and colour are not related between plots for different elements.

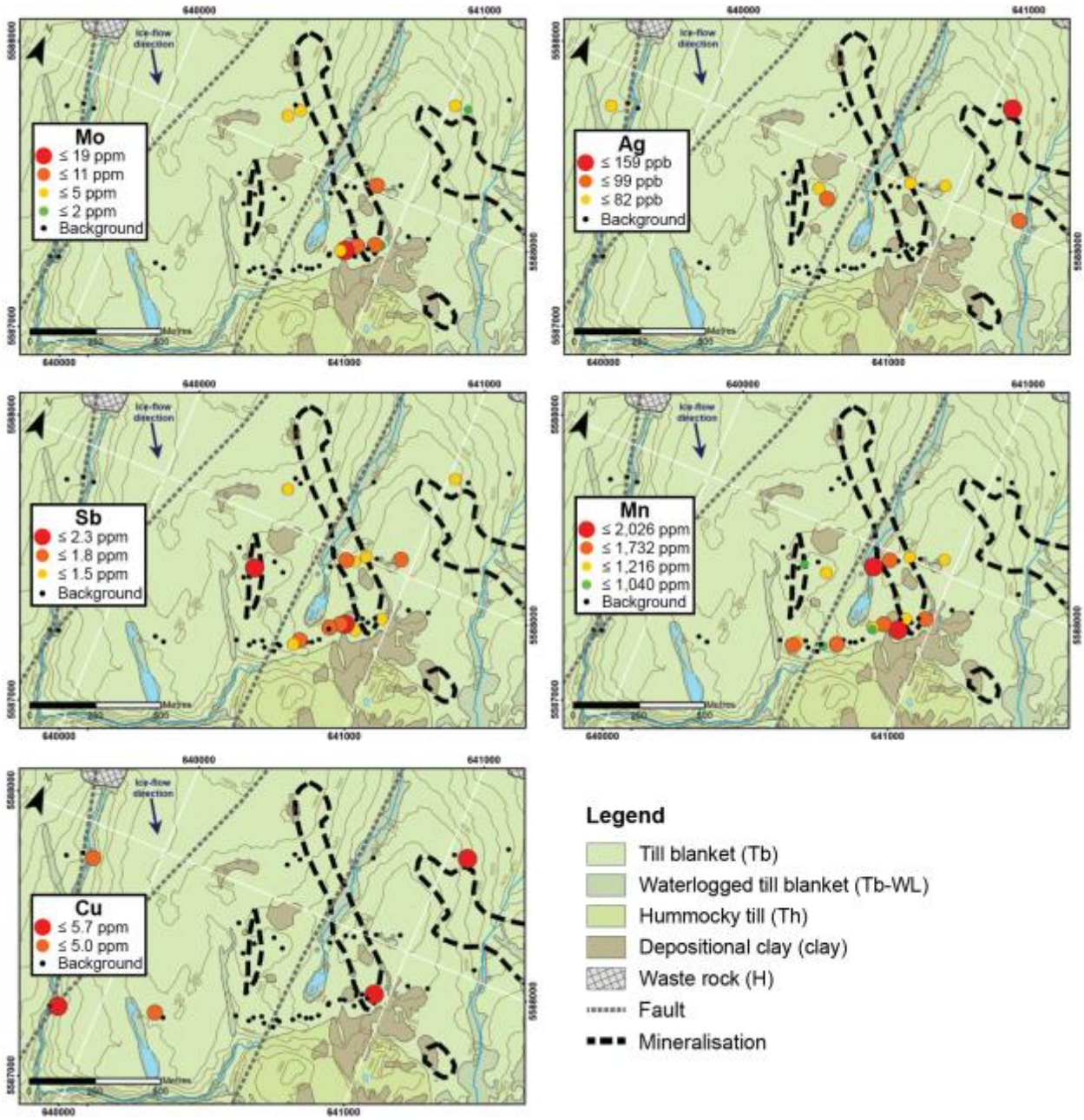

Figure 4-38. Lodgepole pine needle element concentrations (aqua regia, ICP-MS) for Mo, Ag, Sb, Mn, and Cu. Grey points are excluded samples from waterlogged areas. Contours plotted at 5 metre interval spacing. Surficial geology is modified from Plouffe and Ferbey (2015b), using the GSC data model for surficial geology, version 1.2 (Deblonde et al., 2012); ice-flow direction from Plouffe and Ferbey (2015b); buried mineralisation outlines from Teck (pers. comm., Teck, 2017); faults modified from McMillan et al. (2009).

Molybdenum exhibits the best anomaly-background contrast with the least amount of 'noise'. Copper-Mo porphyries are usually better defined by the Mo content in vegetation rather than that

of Cu because Mo is one of the most mobile, bioavailable elements in plants (Dunn, 2007). Additionally, Mo-Cu antagonism can occur in which the uptake of an excess of one of these elements will decrease the uptake of the other (Kabata-Pendias, 2010) which may explain the lack of significant Cu response in the pine needle data.

The bioavailability of trace elements to plants depends not only on their concentration in soil but a number of physical, chemical, and biological interactions which are influenced by factors such as pH and the presence and quantity of organic and inorganic ligands (Violante et al., 2010). After Mo is released by weathering from its host mineral molybdenite, the Eh-pH conditions of soils at Highmont South indicate that Mo is present in soil as molybdate oxyanions (MoO_4^{2-}) (Figure 4-39) which is a soluble form readily available to uptake by plants (Kabata-Pendias, 2010). Molybdenum is an essential micronutrient in plant enzymes and its most important function is nitrate reduction (Dunn, 2007).

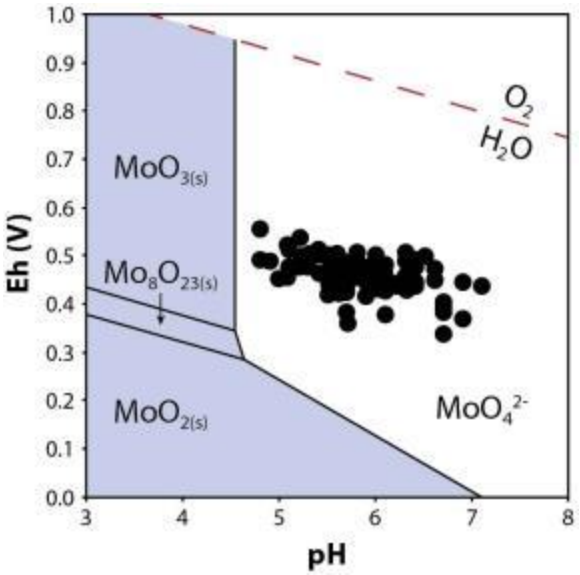

Figure 4-39. Upper B horizon soil samples plotted on a Pourbaix diagram for Mo (0.001 mol/kg) indicating its speciation in the Mo-H_2O system. pH values from soil slurry measurements; Eh values calculated from soil slurry measurements for oxidation reduction potential. Modified from diagram generated on materialsproject.org.

4.12 Dendrochemistry

4.12.1 Sample selection

The availability of trees to collect core samples from was severely limited by silvicultural practices. In order to maximise the age of lodgepole pine tree sampled from, core samples were collected from trees killed by the mountain pine beetle (MPB) outbreak. The circumference of trees sampled ranges from 70 to 165 centimetres (median: 98 centimetres). Nine of the total 47 tree core samples collected from deceased lodgepole pine trees in the Highmont South field area were selected for analysis based primarily on core quality and age of the tree (Figure 4-40). A tree core was not selected for analysis if it did not have enough tree rings (i.e. not old enough) to obtain the 1935–1945 sample interval or which had blue stain fungus (e.g. Figure 4-41) staining the 1965–1975 sample interval.

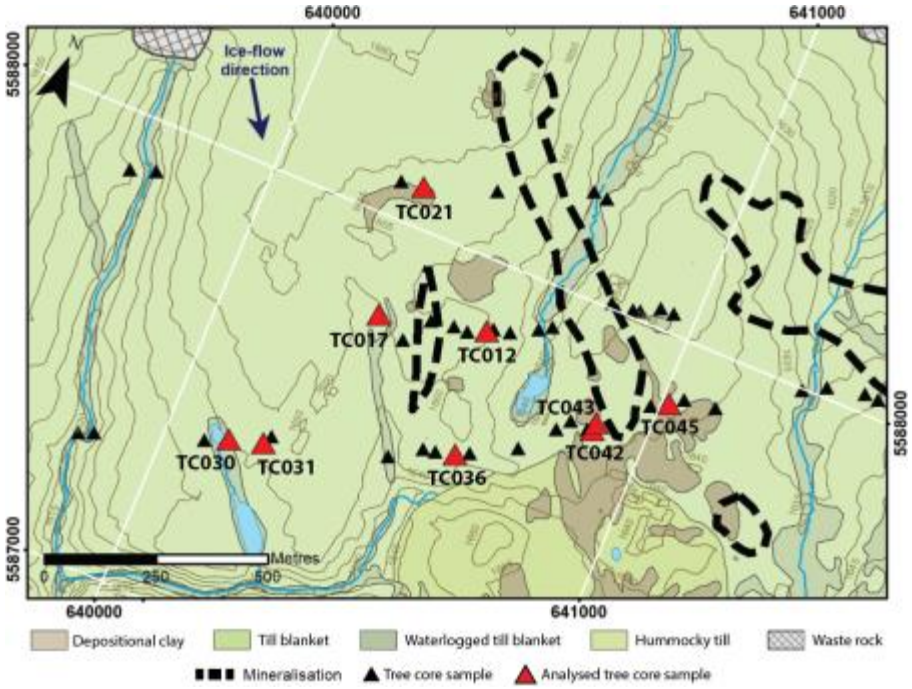

Figure 4-40. A location map of lodgepole pine tree core samples indicating the 9 samples selected for analysis. Contours plotted at 5 metre interval spacing. Surficial geology is modified from Plouffe and Ferbey (2015b), using the GSC data model for surficial geology, version 1.2 (Deblonde et al., 2012); ice-flow direction from Plouffe and Ferbey (2015b); buried mineralisation outlines from Teck (pers. comm., Teck, 2017); faults modified from McMillan et al. (2009).

Figure 4-41. An example of a beetle-killed lodgepole pine tree core sample with blue stain fungus staining the outer tree rings.

4.12.2 Results

Metadata

Plots of ring width over time show each sampled tree's growth curve and, where any irregularities in the curve appear, the presence of stress to the tree (Figure 4-42). The growth curve for tree core sample TC012 is a good example of healthy tree growth over time with no significant irregularities. Tree core samples TC030 and TC031 generally follow an ideal growth curve; samples TC017, TC021, TC036, TC043, and TC045 display slightly irregular periods of growth; and those of sample TC042 are very irregular.

Sources of stress which cause irregularity in growth profiles include outbreaks of insects or fungi, climate change, and forest fire (Watmough, 1997). In ideal tree core analyses, samples are not selected from intervals which show irregular growth due to stress because this may affect how the tree uptakes and stores trace elements (Watmough, 1999). Due to limited selection of quality tree core samples, however, not all sample intervals could avoid irregular growth periods.

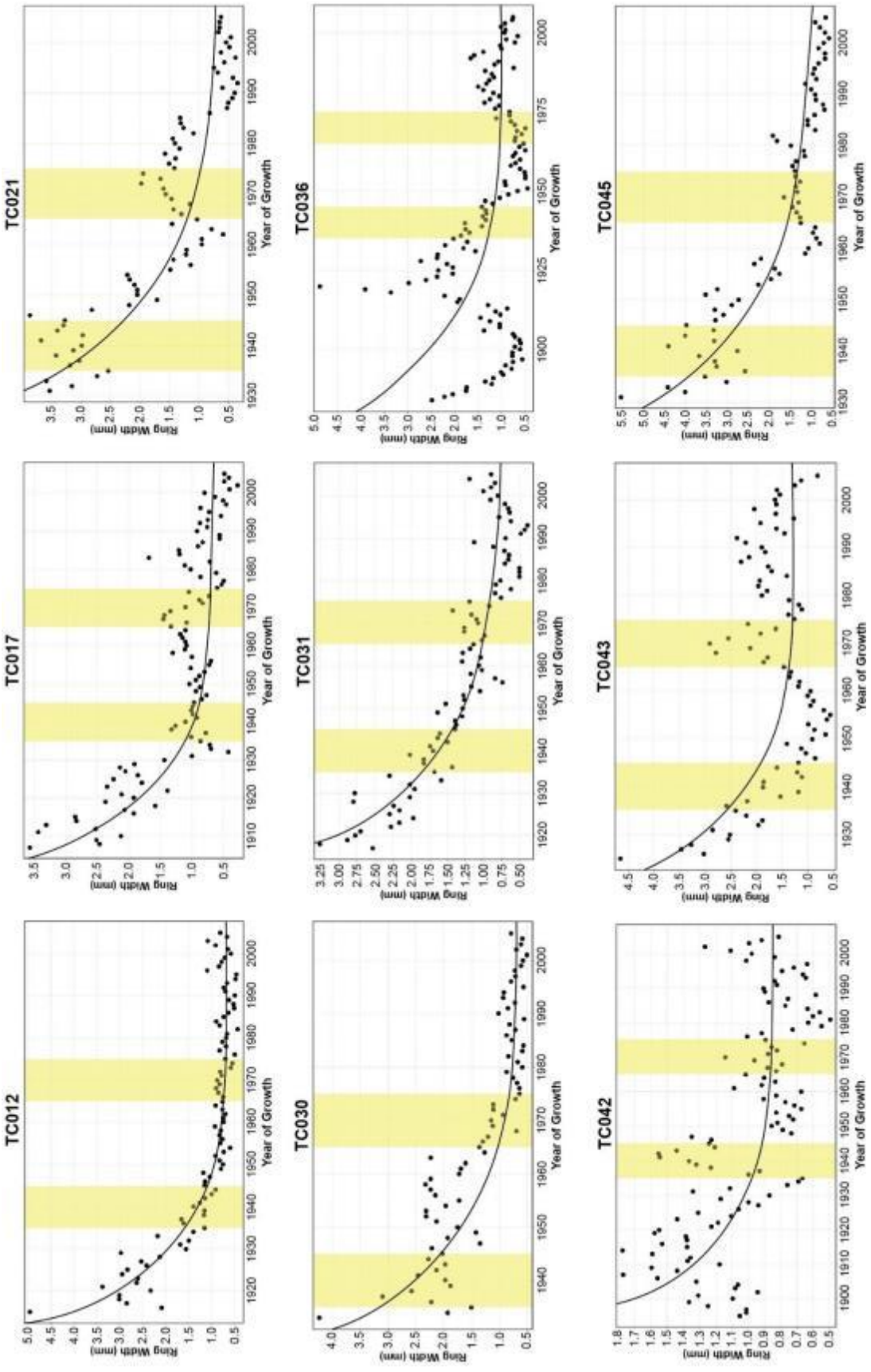

Figure 4-42. Plots of tree ring width over time for tree core samples selected for analysis from Highmont South. Each point represents one tree ring (i.e. one year of growth). Highlighted intervals indicate the two chosen sampling intervals from each tree core: 1935–1945 and 1965–1975. Black curves on each plot represent the ideal 'healthy' growth curve (pers. comm., Kurt Kyser, 2016).

Dendrochemistry

Analytical results are reported in Appendix C and QA/QC practises and results in Appendix B. Selected elements were compared to certified and indicated values of NIST1547 peach leaf CRM to assess precision. Elements from the analysis of tree cores collected from lodgepole pine trees at Highmont South under ten times the stated analytical detection limits and not discussed further are: As, Au, Be, Bi, Ce, Cs, Dy, Er, Eu, Ga, Gd, Ge, Hf, Hg, Ho, La, Li, Lu, Nb, Nd, Pd, Pr, Pt, Re, Sb, Sc, Se, Sm, Sn, Tb, Te, Th, Ti, Tm, V, W, Y, Yb, and Zr. The remaining data was deemed acceptable following evaluation of QC results.

There is no apparent relationship between tree diameter and chemistry of the heartwood, however there are relationships between heartwood chemistry and surficial material in which the tree grew. Compared to core sampled from lodgepole pine trees growing within dry till units, those sampled in waterlogged surficial units (clay and till) have higher Mg, Ca, and Sr concentrations and lower Cu, Pb, Zn, Ni, Mn and Al concentrations (Figure 4-43).

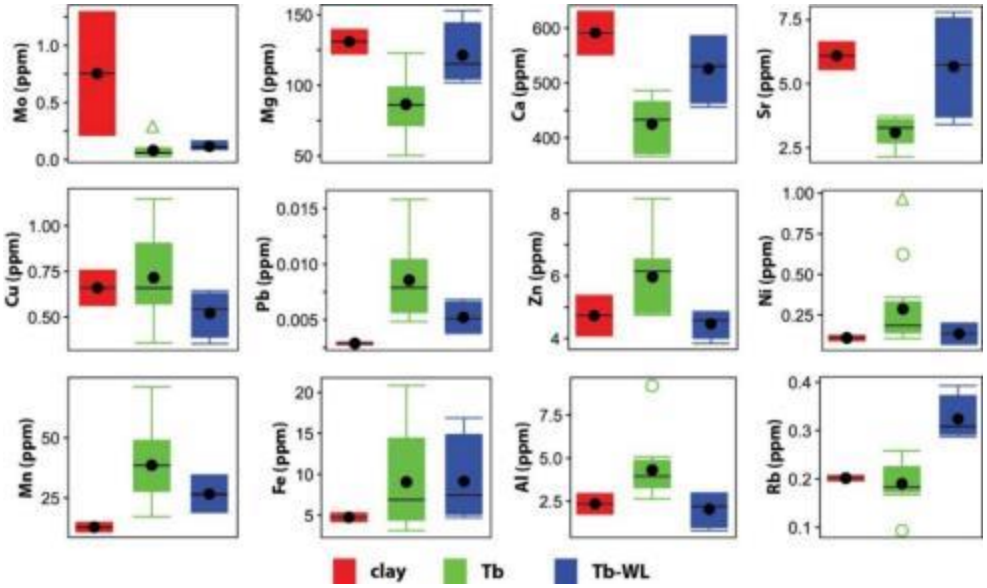

Figure 4-43. Box plots of lodgepole pine tree core chemistry (HNO_3 digest, HR-ICP-MS) based on the surficial material unit from in the tree was sampled. Sample counts: clay = 2, Tb = 14, Tb-WL = 2.

The elements Ca, Mg, and Zn in tree cores sampled from Highmont South increase with a corresponding increase in upper B horizon soil (<180 microns, aqua regia, ICP-MS) (Figure 4-44).

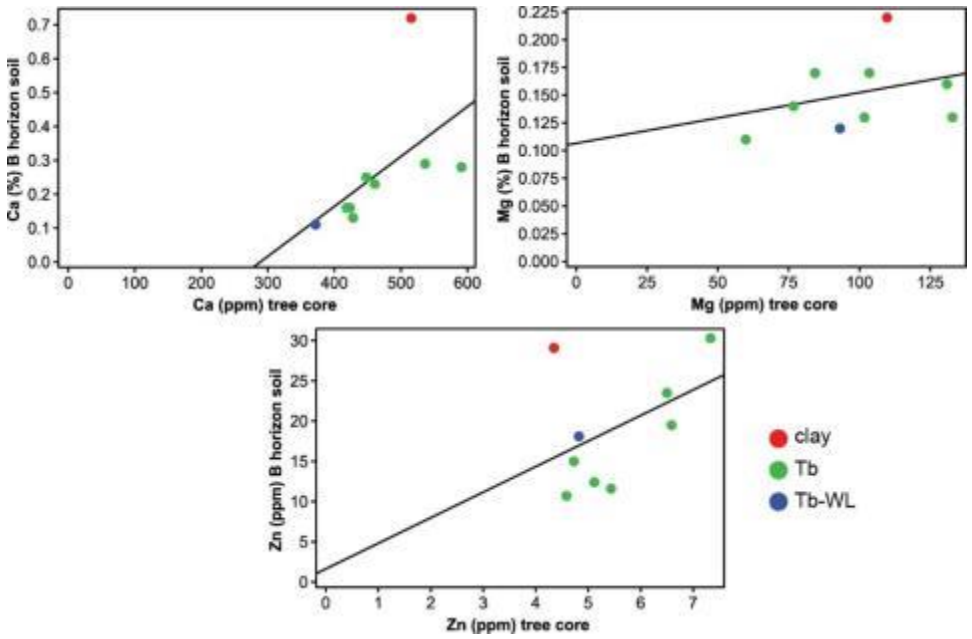

Figure 4-44. Calcium, Mg and Zn concentrations (HNO_3 digest, HR-ICP-MS) increase in lodgepole pine tree cores as they increase in upper B horizon soils (<180 microns, aqua regia, ICP-MS). Tree core data is represented by the averaging results from the two different tree ring intervals sampled per core. Black lines are lines of best fit.

Median Cu concentrations stay relatively the same from the 1935–1945 sample interval to the 1965–1975 sample interval, only increasing from 0.604 ppm to 0.633 ppm (Figure 4-45). Median relative standard deviation (RSD) on Cu values is 1.7% which deems the 4.8% increase insignificant. Median Mo concentrations slightly increase from the 1935–1945 sample interval to the 1965–1975 sample interval, from 0.067 ppm to 0.093 ppm. Median RSD on Mo values is 6.6% which deems the 38.8% increase significant. The tree with the highest increase in Mo concentration (498.6% increase) is sample TC021 from within a waterlogged depositional clay unit.

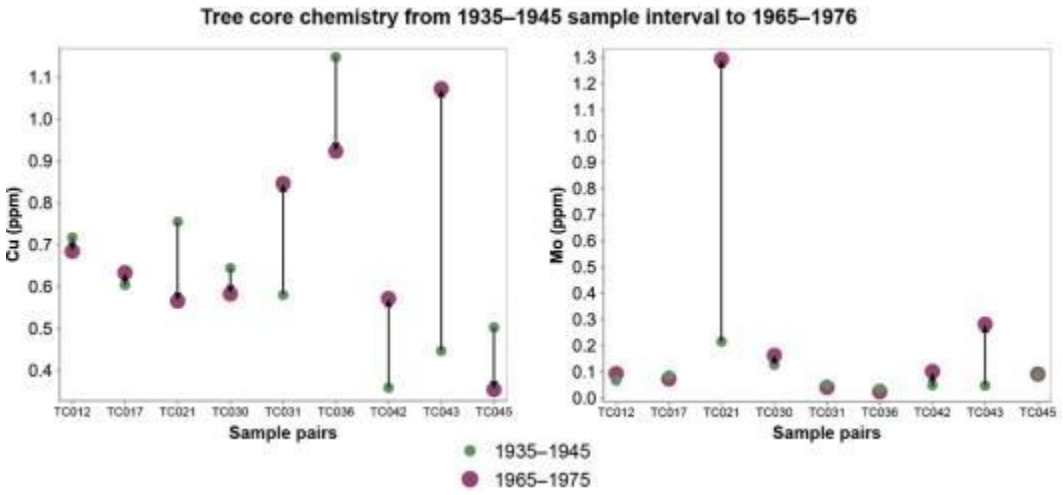

Figure 4-45. Copper and Mo concentrations (HNO_3 digest, HR-ICP-MS) for analysed lodgepole pine tree core sample intervals from 1935–1945 and 1965–1975. Median Cu slightly increases from 0.604 ppm in the 1935–1945 interval to 0.633 ppm in the 1965–1975 interval. Median Mo slightly increases from 0.067 ppm to 0.093 ppm.

The BC forestry industry has a long silvicultural history of applying fertiliser as well as herbicides, fungicides, insecticides, and/or pesticides to forests intended for future harvesting. The most common fertiliser applied to lodgepole pine stands in interior BC is an N-P-K fertiliser, commonly with the addition of S and B (Brockley, 2001). Other types of fertiliser include Cu sulphate, ferrous sulphate, ammonia sulphate and urea (Brockley, 2001). Common herbicides authorised through a BC Regional Pest Management Plan include aminopyralid ($C_6H_4Cl_2N_2O_2$), picloram ($C_6H_3Cl_3N_2O_2$), and glyphosate ($C_3H_8NO_5P$) (pers. comm., Tracy Coombes, 2017). Although N was not analysed in the tree core samples, the increases in the elements in Table 4-6 indicate a dendrochemical signature of industrially applied fertiliser and potentially herbicide in the lodgepole pine trees sampled.

Element commonly used in silvicultural fertiliser	Increase from 1935–1945 population to 1965–1975 population			
	Median increase		Highest increase	
P	2.4 ppm	278%	23.0 ppm	1164%
K	40.9 ppm	121%	126.5 ppm	144%
B	17.0 ppm	402%	38.8 ppm	911%
S	11.7 ppm	148%	24.2 ppm	186%

Table 4-6. Elements commonly used in silvicultural fertiliser increase in concentration in lodgepole pine heartwood over time.

Pesticides commonly used in forestry include forms of sodium borate (i.e. borax, $Na_2B_4O_7 \cdot H_2O$) and Cu sulphate. Figure 4-46 shows a strong relationship between Na and B in Highmont South samples which closely matches the Na:B ratio in borax.

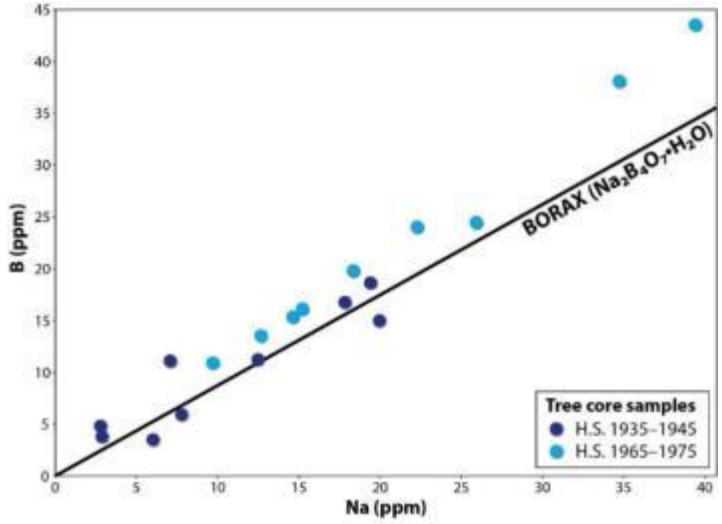

Figure 4-46. Sodium and boron concentrations in tree core samples from Highmont South closely match the trend line for Na:B in borax insecticide ($Na_2B_4O_7 \cdot H_2O$). There is an overall shift along the trend line towards higher attenuated concentrations of borax over time when comparing the two sampled time intervals.

4.13 Summary

Brunisolic soils are weakly developed at Highmont South on young till blanket. Small depressions of waterlogged depositional clay have been determined to cause false anomalies in surficial geochemical sampling due to water-saturation and retention of weathered elements, high

CEC of clay, pH and Eh conditions which allow the stability of $CaCO_3$, and aqueous transport and deposition of soluble ions from surficial drainage.

Those elements elevated in concentration in upper B horizon soils developed on till blanket, determined by aqua regia ICP-MS, overlying bedrock porphyry Cu-Mo mineralisation are Cu, Mo, Ag, and Bi, and, to a lesser extent Sb, As, and W. Copper, Ag, Sb, and W are also anomalous above the trace of the West Highmont fault which crosscuts mineralisation. Other elements which are elevated above the West Highmont fault are Pb, Mn, Zn and, to a lesser extent, Cd (aqua regia, ICP-MS). Analysis of the same soils by deionised water leach and ICP-MS finish resulted solely in anomalous concentrations of Cu above mineralisation and the West Highmont fault.

Aqua regia digest provided the best background-mineralisation contrast for Cu, Mo, Bi, As, Sb, and W compared to other extractions in the sequential extractions of select upper B horizon soil samples. This indicates that a large fraction of the total concentration of these elements in the soil are associated with phases such as crystalline Fe-oxides and residual sulphides. From the weaker leach results, Mo is most significantly associated with organic matter (as determined by sodium pyrophosphate leach), while Cu, Ag, and Bi are most significantly associated with amorphous Fe-oxides (determined by hot hydroxylamine-hydrochloride leach).

Results of Cu isotope analysis of select upper B horizon soil samples are within the expected δ^{65}Cu -1‰ to +1‰ range for primary magmatic Cu. There is no evidence in the partial leach data for significant isotopic fractionation of Cu as a result of migration of Cu ions from bedrock mineralisation to the surface. Results indicate that the Cu in the soil matrix is locally derived from the till.

Results from the analysis of hydrocarbon sequestration modules installed in soils across Highmont South indicate anomalous C_{12}-C_{15} normal alkane concentrations, particularly dodecane, tridecane, and pentadecane, over mineralisation and the West Highmont fault.

Lodgepole pine needles from trees growing over mineralisation are anomalous in Mo, Ag, Sb, and Mn (aqua regia, ICP-MS). Molybdenum results from pine needle analysis indicate the best background-anomaly contrast. There is no elevation of Cu in lodgepole pine needles sampled from trees growing over bedrock mineralisation. This is attributed to Cu-Mo antagonism, where the excess uptake of Mo, which is readily available to vegetation, limits the uptake of Cu (Kabata-Pendias, 2010). The analysis of two different time intervals selected from beetle-killed lodgepole pine tree core samples shows an increase in Cu, P, K, B, and S concentrations in the heartwood of these trees from interval 1935–1945 to interval 1965–1975.

Chapter 5: Surficial geochemistry of the deeply buried J.A. target at HVC

5.1 Surficial environment and climate

The J.A. field area consists of a relatively steep-walled, flat-floored valley, a result of the damming of the valley by retreating ice during the last deglaciation (Plouffe and Ferbey, 2015). The valley is 2.5 to 3 kilometres wide and open to the northwest and southeast. The floor of the valley sits at an average elevation of 1,190 metres AMSL. Ground moisture is mostly a function of climate, where wetter, colder years result in increased surface water. J.A. is typically much drier than Highmont South and has experienced anthropogenic influences on its natural drainage systems (Section 5.6). The J.A. field area is in the Interior Douglas Fir Zone biogeoclimatic zone of British Columbia, with mean annual precipitation of 493 millimetres and a mean annual temperature of 4.0°C (BC Ministry of Forests and Range, 2008).

5.2 Geomorphology

The J.A. field area spans across a partially buried bedrock valley (Figure 5-1). The centre of the field area is generally quite flat, with a central anastomosing dried-up stream bed (Witches Brook) which flowed out of Quiltanton Lake in the northwest, where the Valley pit exists today (Clague, 1988). In the middle of the field area is a mound of glaciofluvial sediments giving a small area of positive relief to the otherwise slightly incised glacial lake bed. Both valley bedrock walls are blanketed by sediments which are incised by narrow and steep drainage channels. The difference in slope of the north and south valley walls (Figure 5-1) is interpreted to be due to differential glacial erosion. The south valley wall (north-facing slope) represents an adverse slope relative to the south-southeast ice-flow and was thus abraded and polished (Plouffe

and Ferbey, 2015) into a gentler slope compared to the north valley wall (south-facing slope). A seasonal stream runs down part of the south valley wall, draining into Witches Brook and has deposited a small alluvial fan at the base of the slope. The north valley wall has a steeper slope with cliffs of outcropping rock along parts of its upper edge.

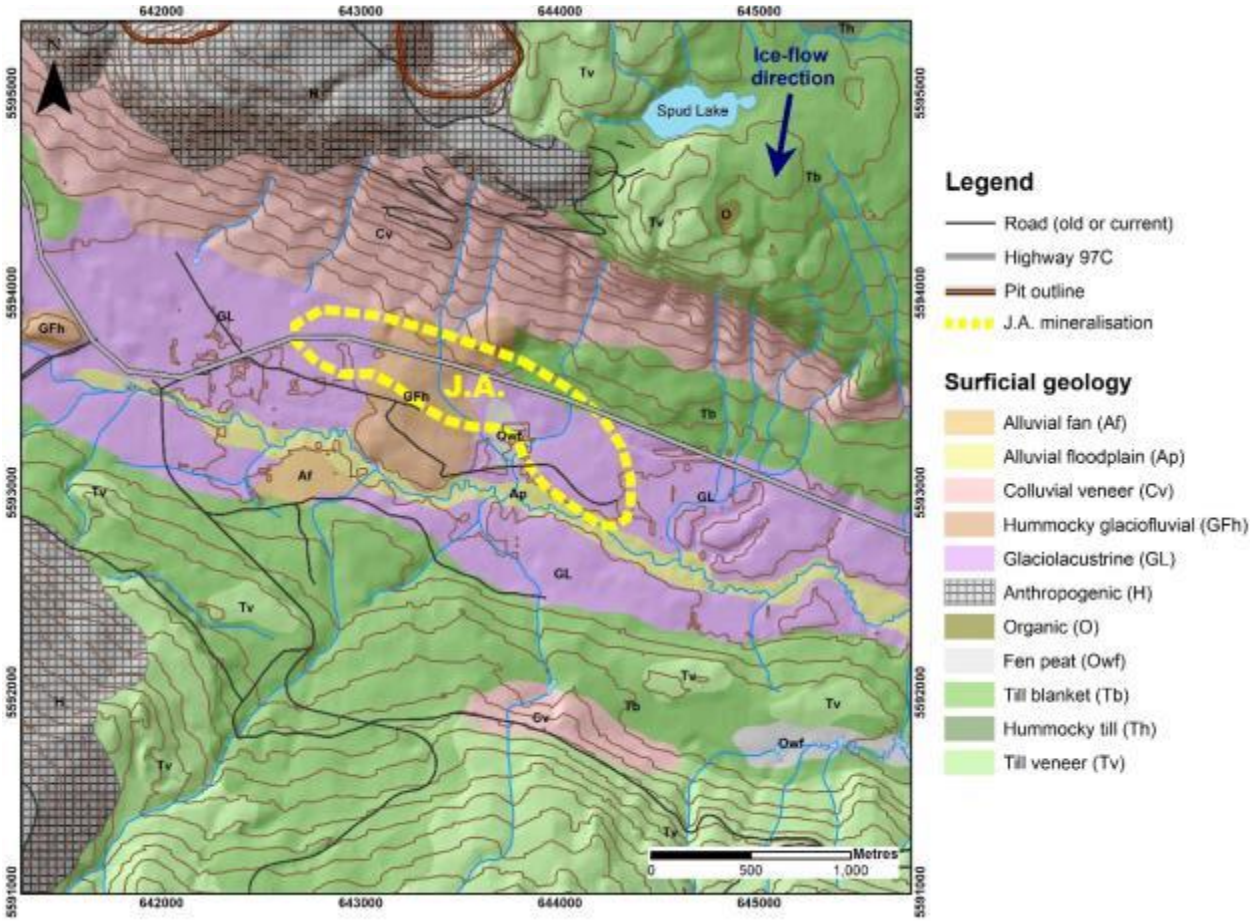

Figure 5-1. Geomorphology of J.A. and the surrounding area. Regional surficial geology and ice-flow direction from Plouffe and Ferbey (2015b); mineralisation outline from McMillan (1985).

5.3 Surficial geology

The J.A. mineralised target sits beneath significantly thicker sediment cover than does Highmont South, averaging 170 metres and up to 300 metres in thickness (Figure 5-2) (based on historic

drilling, pers. comm., Teck, 2016). The valley-fill sequence starts at the base with pre-Quaternary sediments which include poorly consolidated conglomerates, bedded sand units and coal seams, and glacial lake sediments that pre-date the most recent glaciation. Stratigraphically overlying the pre-Quaternary sequences are Quaternary sediments deposited during the most recent glaciation, including till, glaciolacustrine sediments and glaciofluvial sediments (Bobrowsky et al., 1993). The glacial materials in this area are young, deposited during the Late Wisconsinan (Clague and Ward, 2013). The last deglaciation played a significant role in the distribution and grain size of the surficial materials in this valley (Bobrowsky et al., 1993). Holocene alluvial deposits stratigraphically overlie Quaternary sediments in the centre of the field area, associated with Witches Brook (Figure 5-3).

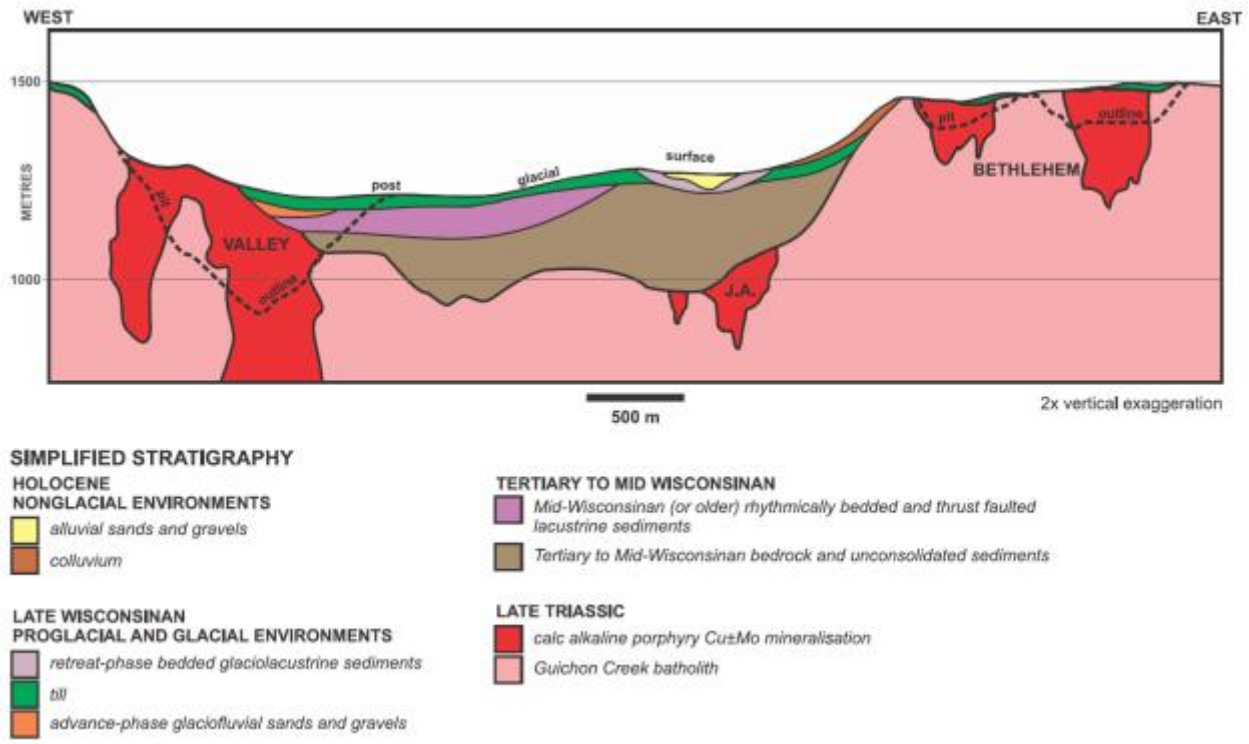

Figure 5-2. Cross section through the Valley, J.A., and Bethlehem porphyry centres indicating the depth of burial of the J.A. target. Cross section from Ferbey et al. (2016), which uses simplified stratigraphy modified after Bobrowsky et al. (1993), and Plouffe and Ferbey (2015b).

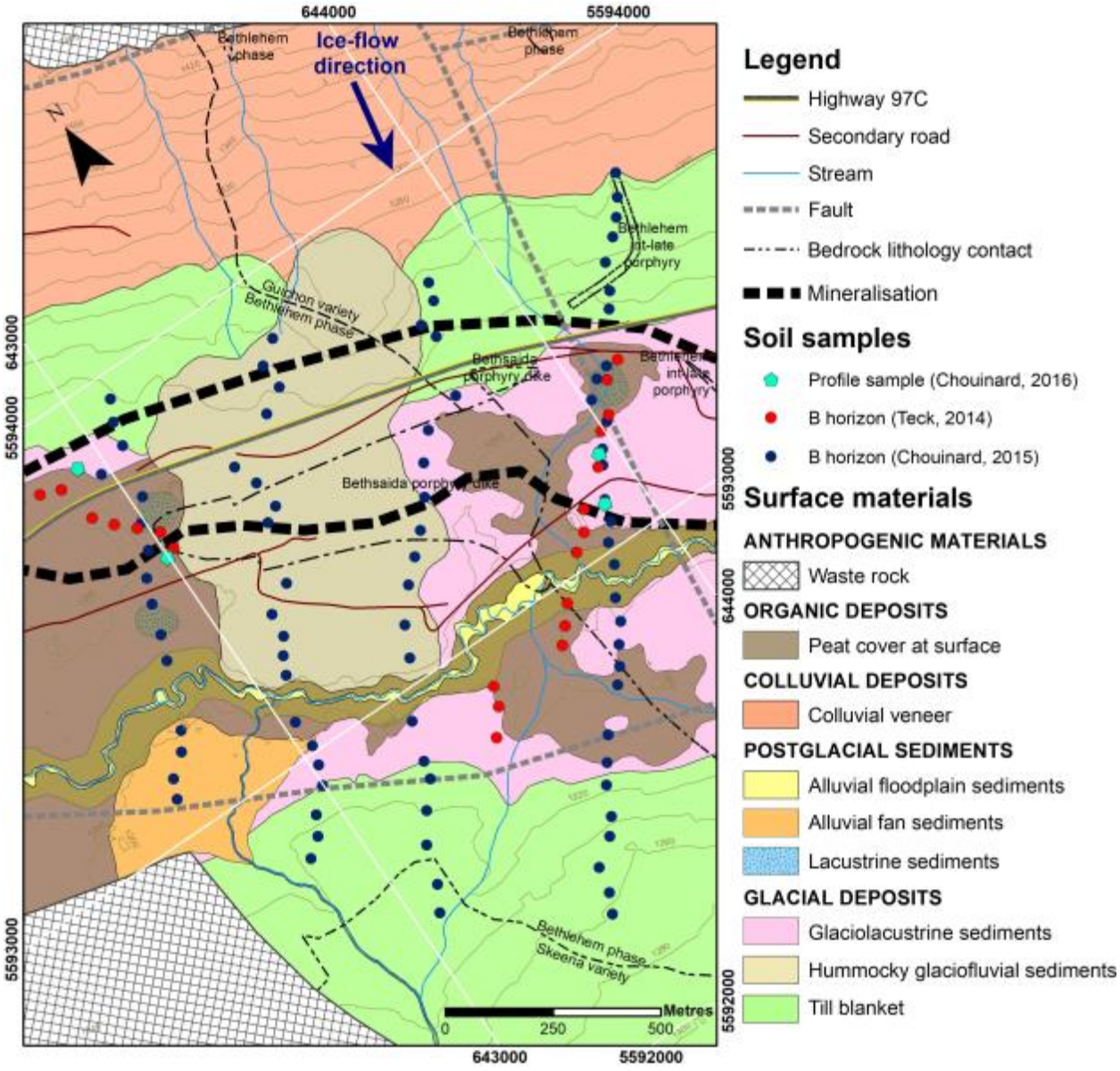

Figure 5-3. Surficial geology of the J.A. study area at the Highland Valley Copper mine operations. Contours plotted at 20 metre interval spacing. Surficial geology is modified from Plouffe and Ferbey (2015b), using the Geological Survey of Canada's data model for surficial geology, version 1.2 (Deblonde et al., 2012); ice-flow direction from Plouffe and Ferbey (2015b); mineralisation outline from McMillan (1985); bedrock geology and structure based on work completed in August 2016 by Teck and CMIC, and modified from McMillan et al. (2009).

Key units to the surficial geology map include:

- postglacial alluvial sediments – potential for the presence of transported porphyry material from other porphyry centres;

- peat cover – ability of organic matter to strongly adsorb metals (Ketterings et al., 2007);
- colluvial veneer from waste rock piles on the north valley wall – potential to generate false porphyry-related anomalies.

Glaciolacustrine sediments deposited during the last glaciation are clay-silt-rich and clast-poor. These sediments dominate the valley floor and are centrally overlain by postglacial alluvial sediments deposited by Witches Brook. These modern alluvial sediments are typically oxidised, very coarse, and sand- and clast-rich, with rounded clasts of local intrusive origin. Postglacial lacustrine sediments, encountered in small local depressions, are identified by the presence of recent freshwater snail and bivalve shells (Figure 5-4). A relatively thick (in some places >2 metres) organic peat deposit derived from a recent wetland, covers portions of the glaciolacustrine, lacustrine, and alluvial material. Both valley walls are blanketed by massive, well-compacted, and relatively clay-rich subglacial till. Erosion of the outcropping bedrock coupled with anthropogenic waste rock from the Bethlehem deposits has resulted in colluvial veneer along the upper portion of the north valley wall.

Typical undisturbed soils developed over till blanket and hummocky glaciofluvial sediments at J.A. consist of a very thin organic (LFH) horizon with a silty, downward-coarsening, poorly-horizonated mineral (BC) horizon, interpreted as brunisols (Figure 5-5a). These profiles have low organic matter content and show a downward increase in sand and clast content. Clasts are typically subangular to subrounded and are of local intrusive and extrusive origin. Iron oxide staining on igneous clasts is common however no Cu oxide staining was observed. There is a much greater diversity of soil types at J.A. relative to Highmont South (e.g. Figures 5-5b and 5-5c), owing to a wider array of surficial deposit types.

Figure 5-4. Examples of at least two different species of freshwater snail shells within postglacial lacustrine sediments in small local depressions in the J.A. field area. Sample number RC-15-HVC-115 (642991 m E, 5593665 m N).

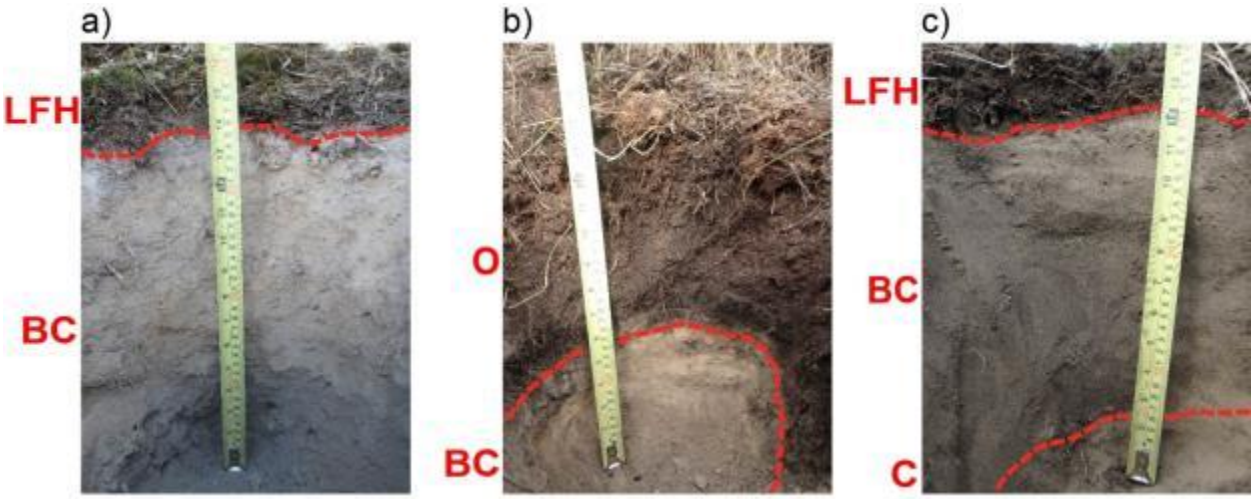

Figure 5-5. Typical soil profiles encountered during sampling at J.A., showing a) a poorly differentiated brunisol developed over sandy glaciofluvial sediments (RC-15-HVC-171: 643542 m E, 5592558 m N); b) an organic soil (peat) developed over glaciolacustrine sediments (RC-15-HVC-165: 643694 m E, 5592735 m N); c) a sand-rich soil profile with no real B horizon (regosol) (RC-15-HVC-172: 643573 m E, 5592600 m N). Soil horizon nomenclature follows the Canadian system of soil classification (Agriculture Canada, 1998).

5.4 Vegetation

Tree species other than the dominant cultivated lodgepole pine include ponderosa pine (only on the north valley slope), with lesser spruce, fir, birch, and aspen. In areas that remain forested (Figure 5-6), there has been extensive lodgepole pine tree death due to the mountain pine beetle. Cut blocks are dominated by scattered wildflower, grasses, and ground berries. Areas that remain

forested and relatively undisturbed host a variety of lichen, wildflower, ground berries, juniper shrub, stonecrop, and Labrador tea. The flat valley centre is dominated by tall grasses and sedges, dwarf birch, and sagebrush growing over an organic peat deposit. The overall vegetation zonation at J.A. follows the distribution of surficial material types.

5.5 Anthropogenic influences

Silviculture has had an impact on the J.A. field area, as it has in much of the surrounding area (Figure 5-6). Cut blocks at J.A. are in varying stages of regrowth, dominated by replanted lodgepole pine. Highway 97C runs through the centre of the field area, contributing automobile emissions, litter and, in the winter, road salt. Waste rock piles at the top of both valley walls contribute colluvium as well as chemical inputs through drainage. Before the mine added dome structures over its three stockpiles, in 2011 (pers. comm., Teck, 2015), the stockpiles were open to the air and had the potential to generate windblown dust. Other anthropogenic features include drill pads, trenches, roads, water wells and pumping stations, an underground water line, an underground natural gas line, power lines, old farming and exploration camp ruins, and fences (Figure 5-7). Considerable care was taken during sampling to minimise the potential effects of anthropogenic influences.

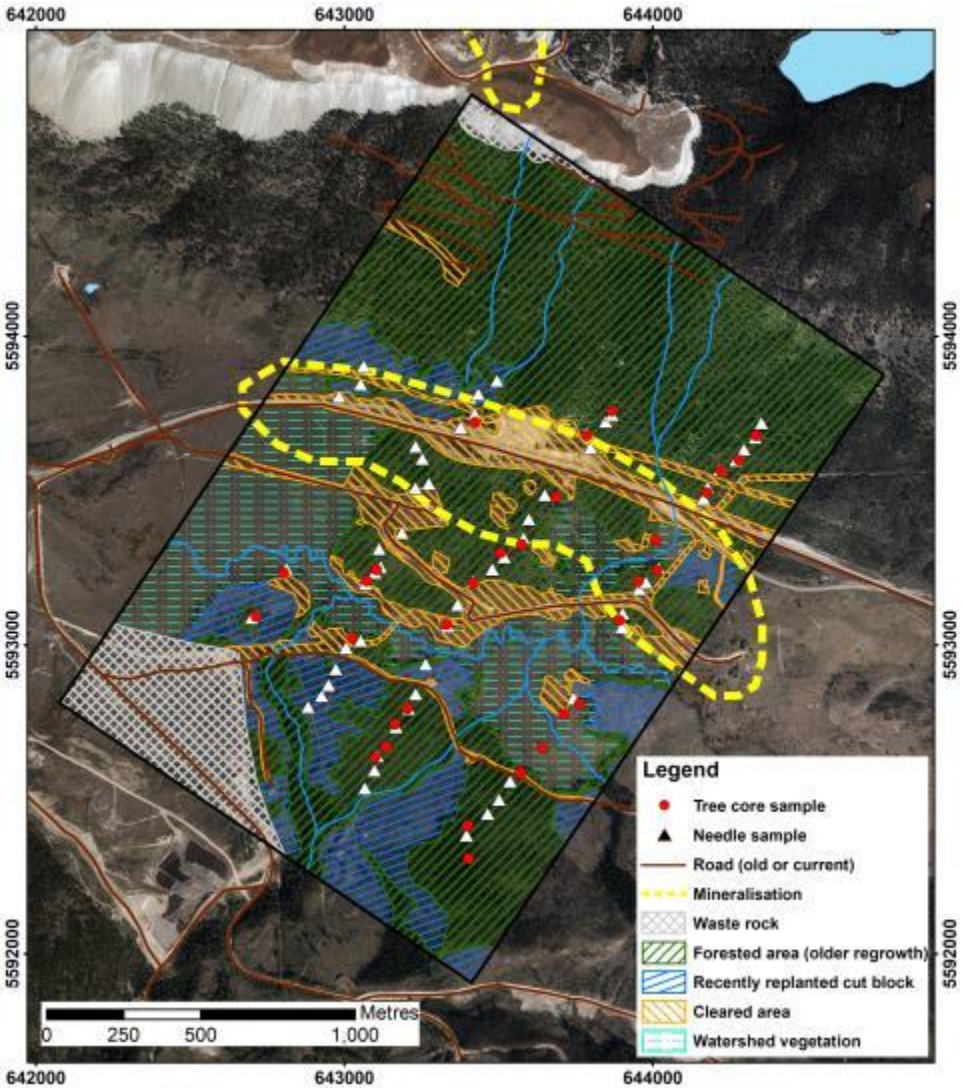

Figure 5-6. Zones in varying states of silvicultural harvesting and regrowth within the surficial mapping area at J.A. (as of 2016). An additional vegetation zone consists of watershed vegetation which is mostly devoid of trees. Tree core samples (from deceased lodgepole pine) and needle samples (from younger, living lodgepole pine) are marked on map to indicate biogeochemical sample coverage. Mineralisation outline from McMillan (1985).

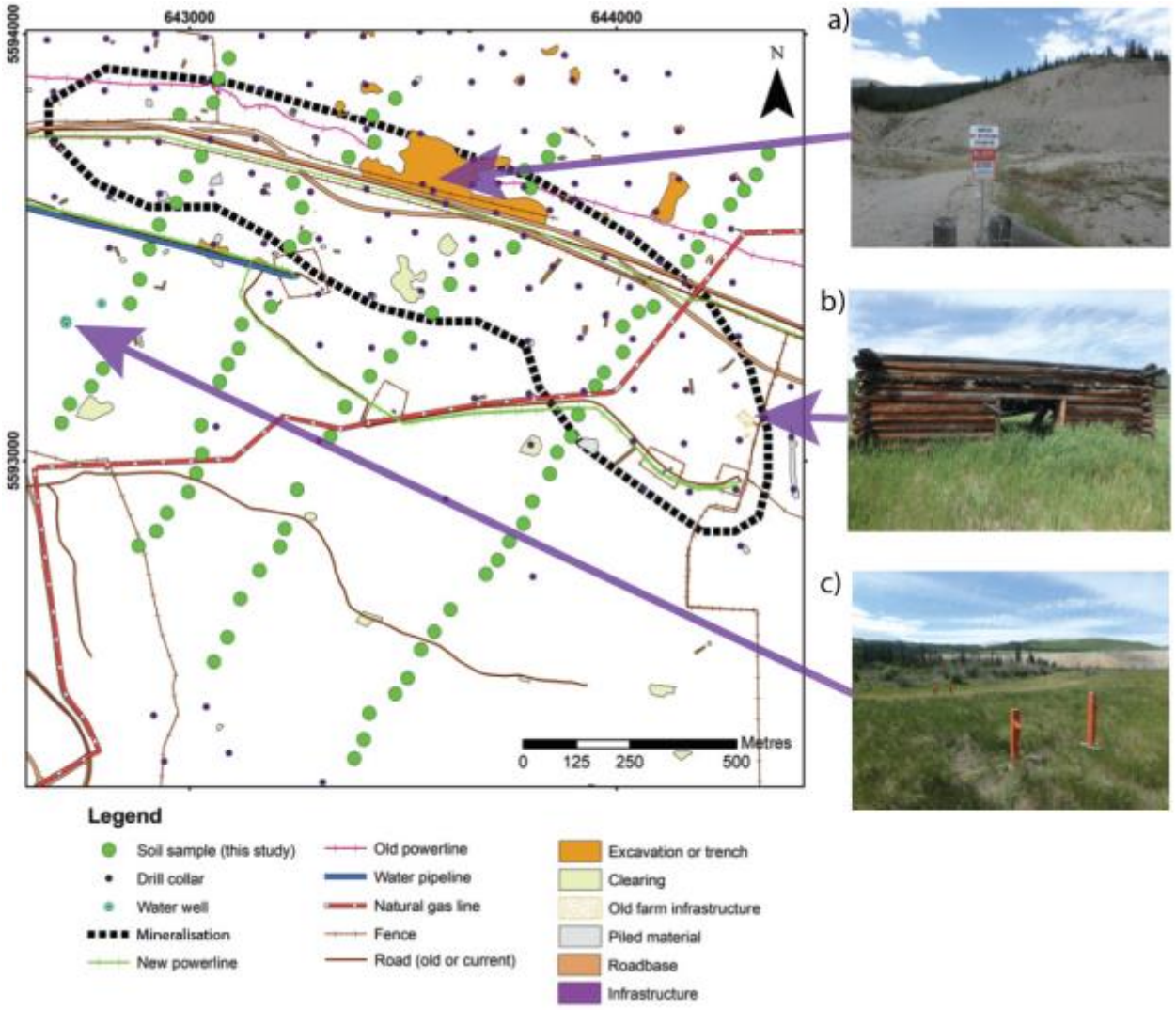

Figure 5-7. A map of observed anthropogenic features in the J.A. field area shows the complexity of care required in attaining a surficial geochemical sample (e.g. soil) from undisturbed material. Accompanying photos show various anthropogenic features encountered while mapping and sampling in 2015: a) discontinued Ministry of Transportation aggregate pit; b) historic agricultural infrastructure; and c) groundwater monitoring wells. Mineralisation outline from McMillan et al. (2009); drill hole locations provided by Teck (pers. comm., Teck, 2017).

5.6 Upper B horizon soil analysis

5.6.1 Physicochemical properties

Physicochemical measurements (pH, acidified pH, electrical conductivity, oxidation reduction potential, and moisture) were conducted at each soil sample site in order to interpret geochemical

data in terms of soil conditions as well as to identify potential physicochemical anomalies related to bedrock mineralisation. QA/QC practices and results are detailed in Appendix B. The data was deemed acceptable and fit for purpose following evaluation of QC results.

Physicochemical measurement values at J.A. typically correspond to the surficial material type and show no change over projected bedrock mineralisation. In situ and slurry pH values are mildly acidic for alluvial floodplain sediments underlying organic peat cover (Ap-O slurry pH median = 5.0), and mildly alkaline in areas where postglacial lacustrine sediments exist between glaciolacustrine material and peat cover (L-O slurry pH median = 8.0) (Figure 5-8). Moisture values correspond with the presence of peat and material grain size. Higher moisture percentages occur in clay-rich glaciolacustrine (GL-O median 10% moisture) and alluvial floodplain (Ap-O median 9.3% moisture) sediments under cover of peat. Clay-rich GL and L-O sediments are also elevated in moisture compared to coarser Af, Tb, and GFh sediments (Figure 5-8). Occasional highly compacted material was encountered preventing proper insertion of the moisture probe and measurements were not collected. In situ and slurry EC measurements are highest in clay-rich L-O and GL-O material (slurry EC medians 347 µS/cm and 276.5 µS/cm, respectively) (Figure 5-8).

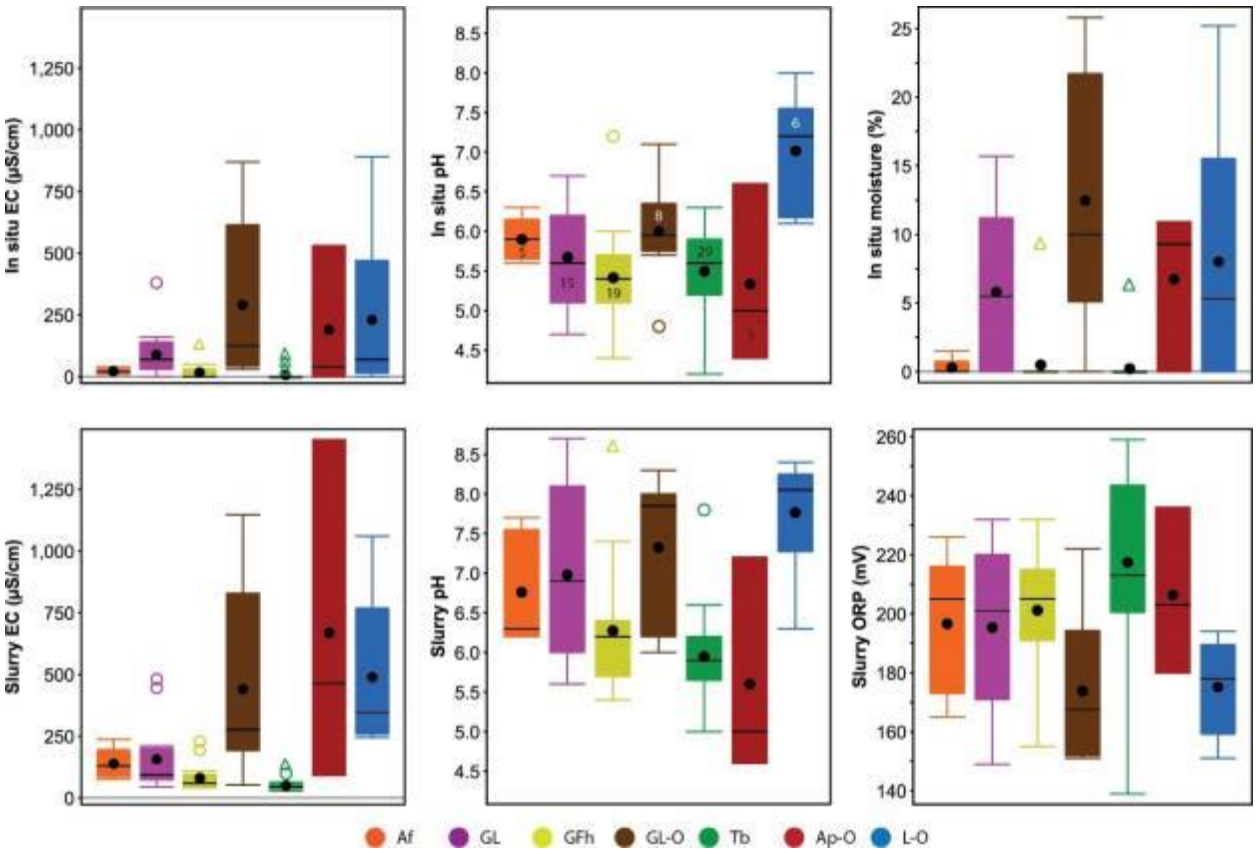

Figure 5-8. In situ measurements for EC, pH, and moisture, and measurements of 1:1 by volume soil-deionised water slurry for EC, pH, and ORP. Physicochemical properties of sampled upper B horizon soils in the J.A. field area differ between surficial material types, controlled grain size and the presence of organic peat cover. Numbers on boxes on in situ pH plot indicate number of sample results. Abbreviations: Af = alluvial fan sediments; GL = glaciolacustrine sediments; GFh = hummocky glaciofluvial sediments; GL-O = glaciolacustrine sediments with peat cover; Tb = till blanket; Ap-O = alluvial floodplain sediments with peat cover; L-O = postglacial lacustrine sediments with peat cover.

Slurry ORP values have a very narrow range (203–259 mV; calculated Eh of 425–481 mV) and indicate dominantly oxidising conditions (Figure 5-9).

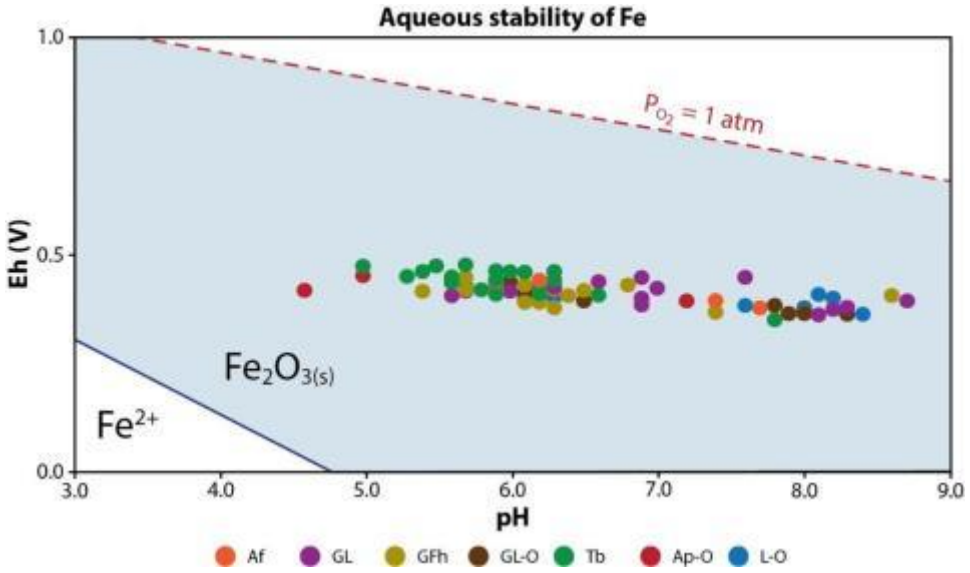

Figure 5-9. Upper B horizon soil samples plotted on a Pourbaix diagram for Fe (0.001 mol/kg) indicating proportion of samples in which Fe likely is oxidised or reduced. All samples plot within the $Fe_2O_{3(s)}$ field, indicating Fe within the soil is likely oxidised. pH values from soil slurry measurements; Eh values calculated from soil slurry measurements for ORP (Section 3.4). Diagram modified from plot generated on materialsproject.org.

At pH values more alkaline than 7.5, there is a significant increase in concentrations of Ca, Sr, Mg, and Na in the soils (<180 microns, aqua regia, ICP-MS) (Figure 5-10).

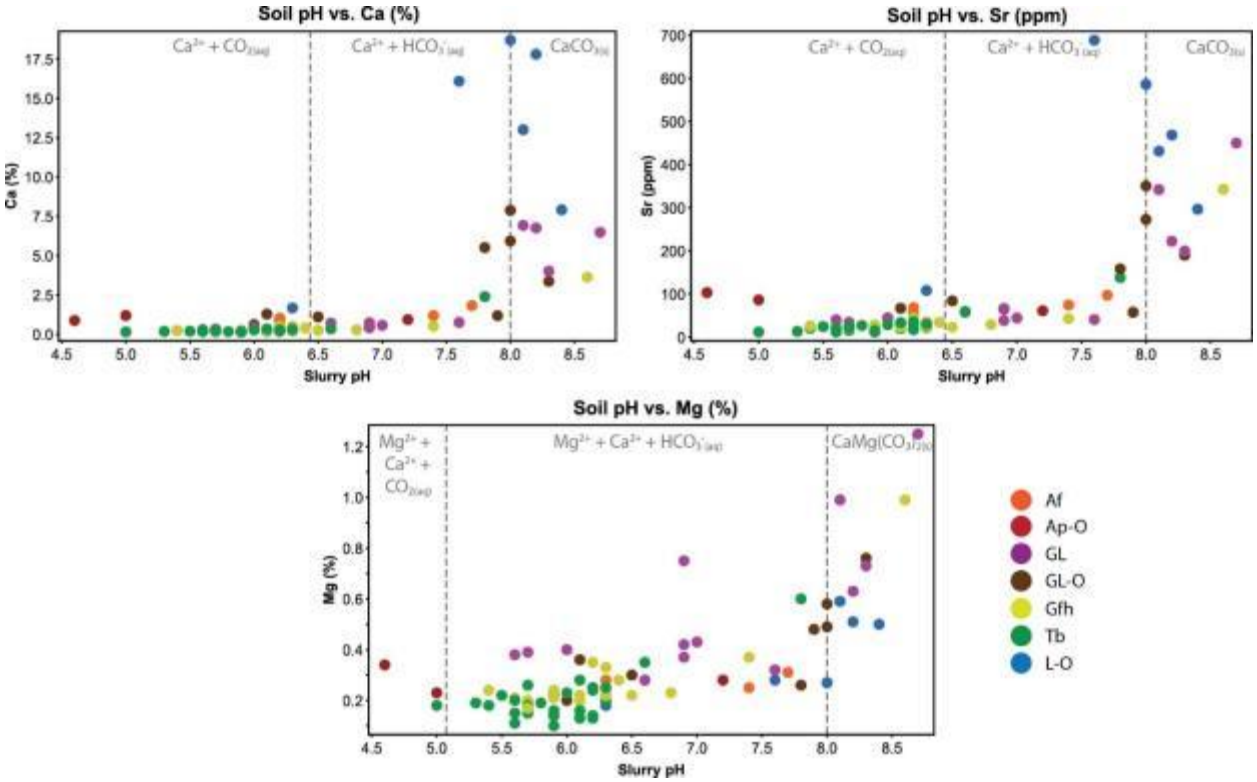

Figure 5-10. Concentrations of Ca, Sr, and Mg in upper B horizon soil samples (<180 microns, aqua regia, ICP-MS) increase at soil pH values more alkaline than 7.5. Soil pH measured by 1:1 by volume soil-deionised water slurry. Mineral stabilities (using 0.0001 mol/kg element concentrations) determined from materialsproject.org.

In soils sampled from glacially derived units (GFh, Tb, GL), rare earth elements (La, Ce) and those that act similar to the REEs (Sc, Y) accumulate in higher concentrations (<180 microns, aqua regia, ICP-MS) at pHs of greater than 6.25–6.5 (Figure 5-11). This is potentially explained by:

- the mobility of La and Ce in soil decreases with decreasing soil acidity (Vodyaniskii and Savichec, 2012; Reimann et al., 2014);
- Y tends to sorb to clay particles (Vodyaniskii and Savichec, 2012) which are more abundant in the glacially-derived materials at J.A.; and

- Y, La, and Ce concentrations in soil can be connected to the presence of ferrous oxides (Vodyaniskii and Savichec, 2012), e.g. Fe_2O_3 which is the dominant phase of Fe in the soil at J.A. (Figure 5-9).

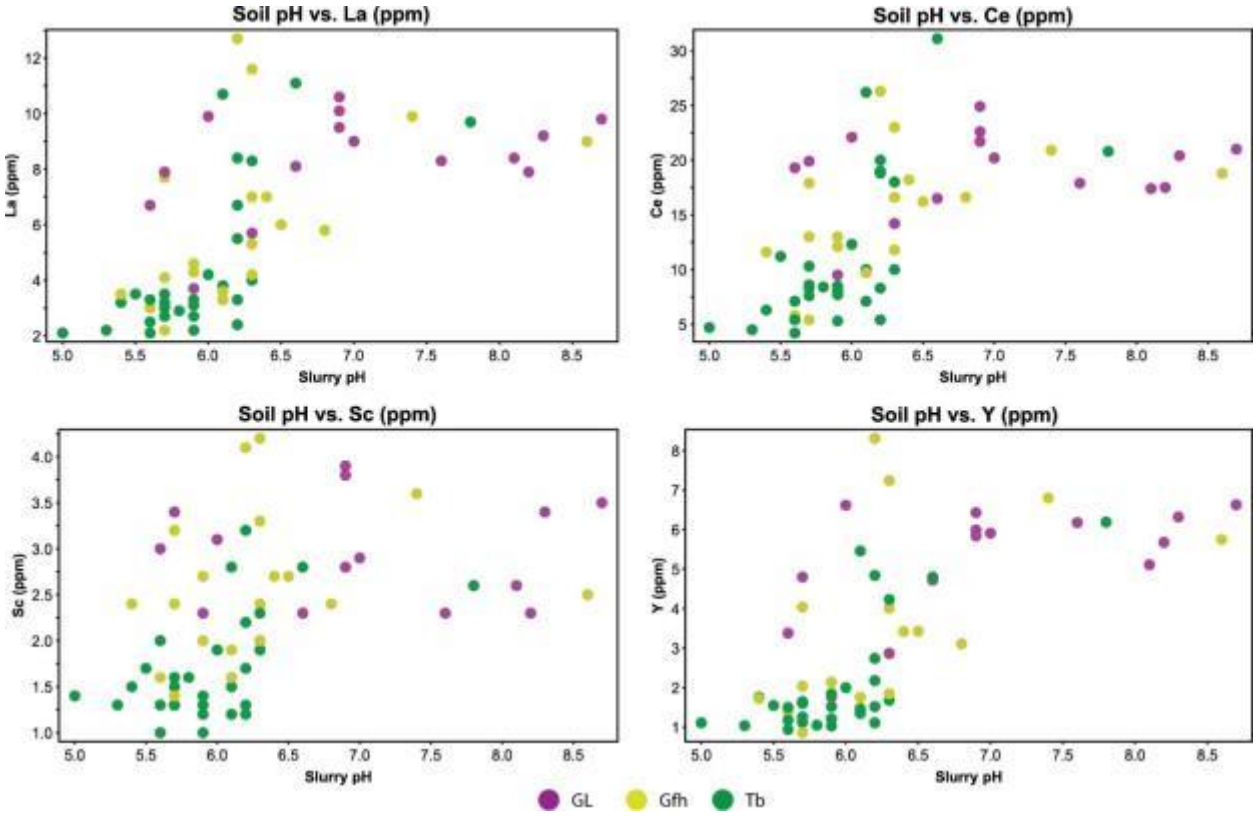

Figure 5-11. Rare earth elements (La, Ce) and those that act as REEs (Sc, Y) accumulate in higher concentrations (<180 microns, aqua regia, ICP-MS) soil pHs of greater than 6.25–6.5 in clay-rich glacially-derived sediments.

5.6.2 Inverse Difference Hydrogen

Inverse Difference Hydrogen (IDH) (detailed in Section 3.5) values for soil samples from J.A. reflect the different surficial materials (Figure 5-13). Buffering capacity is highest in soil sampled on postglacial lacustrine sediments (L-O) which contain preserved freshwater shells (composed of $CaCO_3$) (Figure 5-3), and high in glaciolacustrine sediments whether or not

underneath peat cover (GL and GL-O), and which frequently contain carbonate nodules (Figure 5-12).

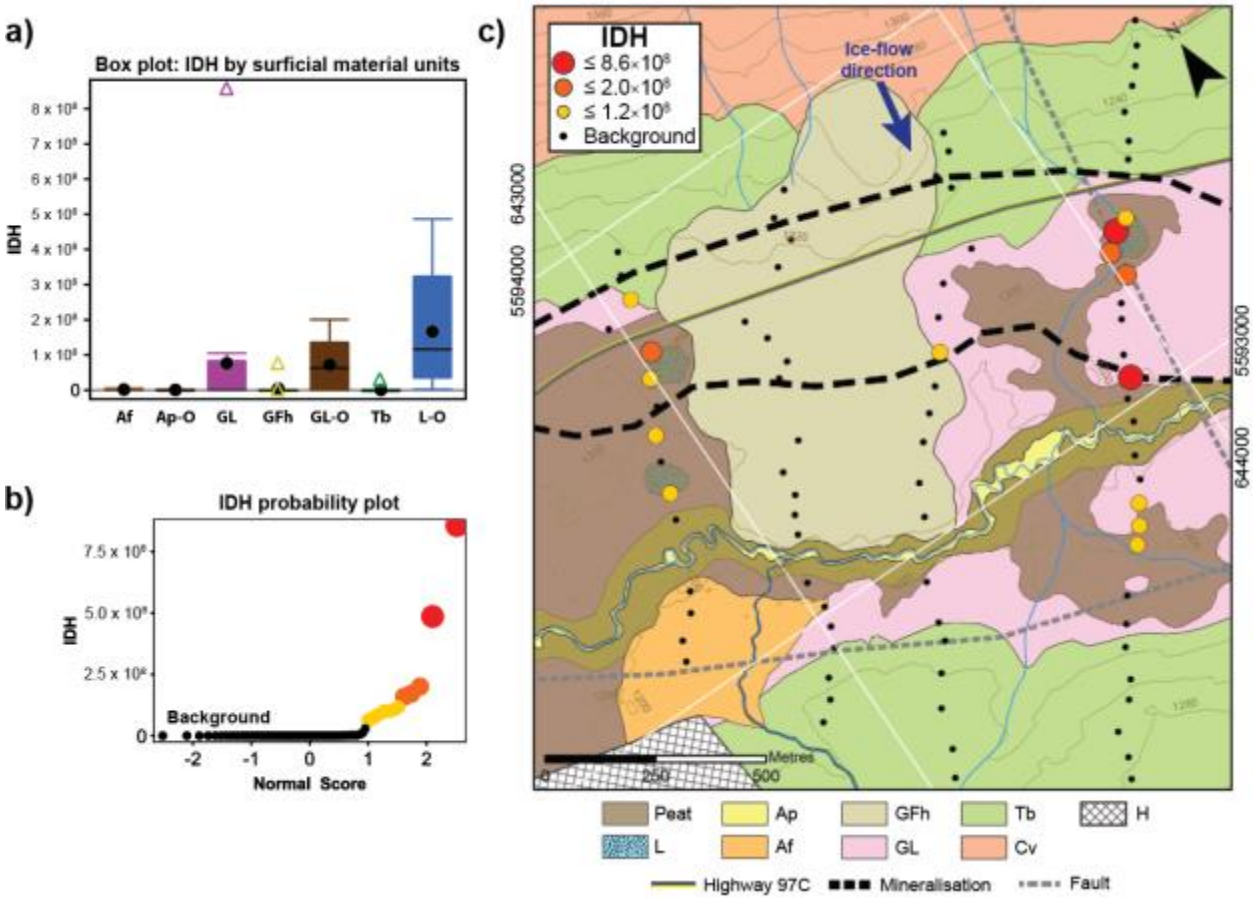

Figure 5-12. a) Inverse difference hydrogen (IDH) values for surficial materials at J.A. Buffering capacity of the soil, represented by the calculated IDH value, is highest in soils sampled from L-O, GL-O, and GL surficial units. b) Anomalous populations of IDH values determined by visual estimation of population breaks on a probability plot. c) Anomalous populations of IDH values are within clay-rich soils sampled from L-O, GL-O, and GL surficial units. Contours plotted at 20 metre interval spacing. Surficial geology is modified from Plouffe and Ferbey (2015b), using the Geological Survey of Canada's data model for surficial geology, version 1.2 (Deblonde et al., 2012); ice-flow direction from Plouffe and Ferbey (2015b); mineralisation outline from McMillan (1985); faults modified from McMillan et al. (2009).

pH and Eh conditions indicate $CaCO_3$ is stable in some soil samples (Figure 5-13a). The majority of soil samples from within Tb units do not allow for the stability of $CaCO_3$, whereas all samples from L-O units fall within the $CaCO_3$ stability field. Samples in which $CaCO_3$ is stable are

generally spatially correlated to Witches Brook and major drainage channels and areas of recent ponding (delineated by peat cover) (Figure 5-13b).

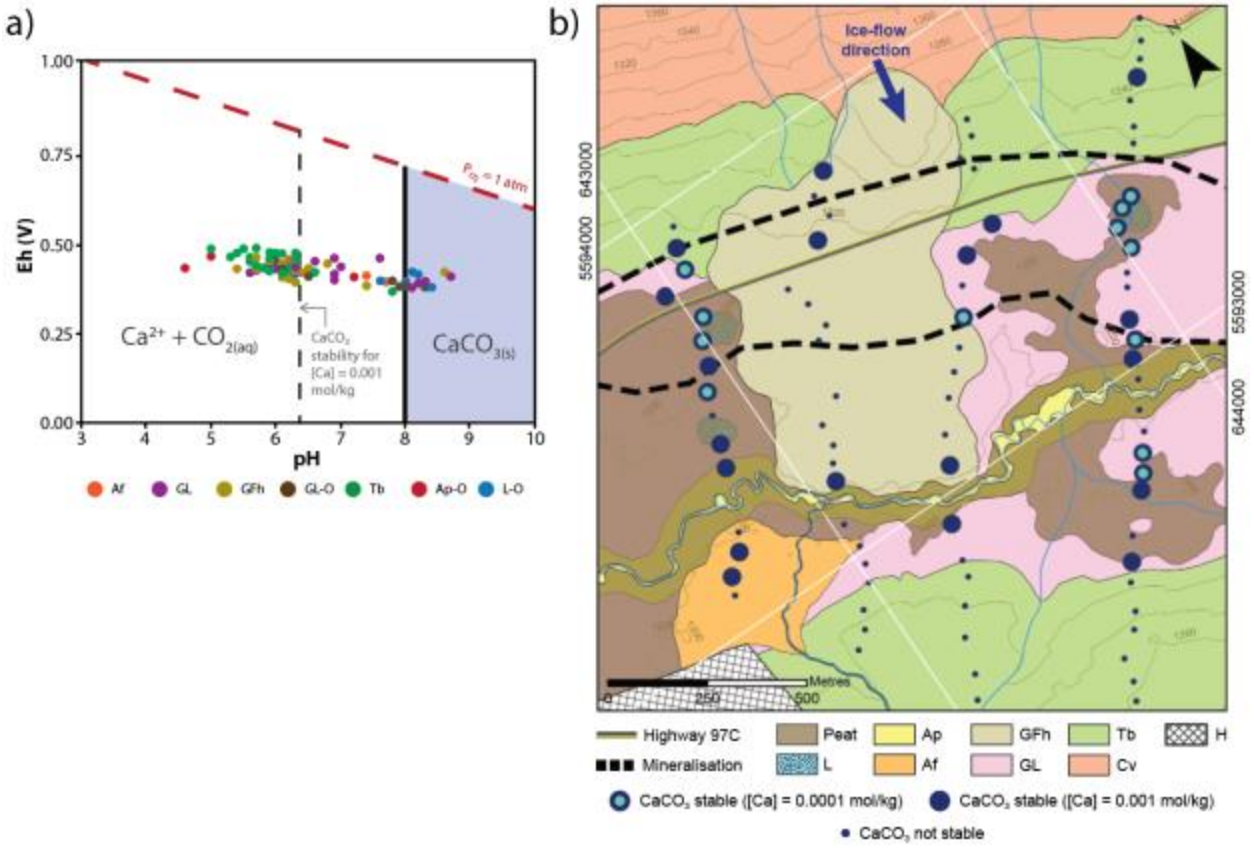

Figure 5-13. a) Upper B horizon soil samples plotted on a Pourbaix diagram for $CaCO_3$ (Ca = 0.0001 mol/kg, C = 0.0001 mol/kg). pH values from soil slurry measurements; Eh values calculated from soil slurry measurements for ORP (Section 3.4). Modified from diagram generated on materialsproject.org. b) Spatial distribution of soil samples for which pH and Eh conditions allow $CaCO_3$ stability generally corresponds to Witches Brook, main drainage channels, and areas of recent ponding (delineated by peat cover). Contours plotted at 20 metre interval spacing. Surficial geology is modified from Plouffe and Ferbey (2015b), using the GSC data model for surficial geology, version 1.2 (Deblonde et al., 2012); ice-flow direction from Plouffe and Ferbey (2015b); mineralisation outline from McMillan (1985).

5.6.3 Aqua regia digest ICP-MS results

The aqua regia digest applied is a relatively weak mix of equal parts concentrated HNO_3, HCl, and deionised H_2O (Bureau Veritas, method AQ250) compared to standard aqua regia. Analytical results are reported in Appendix C and QA/QC practises and results in Appendix B.

Selected elements were compared to certified and indicated values of OREAS25a CRM to assess precision. Mean percentage difference (MPD) for field duplicate results was used to assess natural variability. Data quality is summarized as follows:

- Elements for which all values were reported below ten times stated analytical detection limits and are not discussed further are: B, Tl, Te, Ge, Sn, Ta, In, Be, Pd, and Pt;
- Elements for which the median value was below ten times stated analytical detection limits and are interpreted with caution are: U, Au, Cd, Sb, Bi, K, S, Hg, Se, Hf, and Re;
- Elements which are of acceptable accuracy and precision are: Mo, Cu, Pb, Zn, Ag, Ni, Co, Mn, Fe, As, Th, Sr, V, Ca, P, La, Cr, Mg, Ba, Ti, Al, Na, W, Sc, Ga, Cs, Nb, Rb, Zr, Y, Ce, and Li.

Geochemical trends in soils from J.A. reflect differences among surficial material types and show no clear changes over projected bedrock mineralisation. Soils sampled overlying alluvial fan (Af) sediments contain high concentrations of Cu (median 1,212 ppm) and Ag (median 276 ppb) (Figure 5-14). The soils are also elevated in Cd, Sb, Bi, La, Ba, and Y compared to those from other surficial material units. The stream which formed the alluvial fan can be traced south to the main Highmont deposits. Although the area is increasingly obscured by anthropogenic activity and the stream is now ephemeral, it is likely that weathered porphyry material and associated trace elements were transported downstream and deposited with other sediments in the alluvial fan. The alluvial fan is interpreted as post-glacial as it overlies glacial sediments in the valley at J.A.

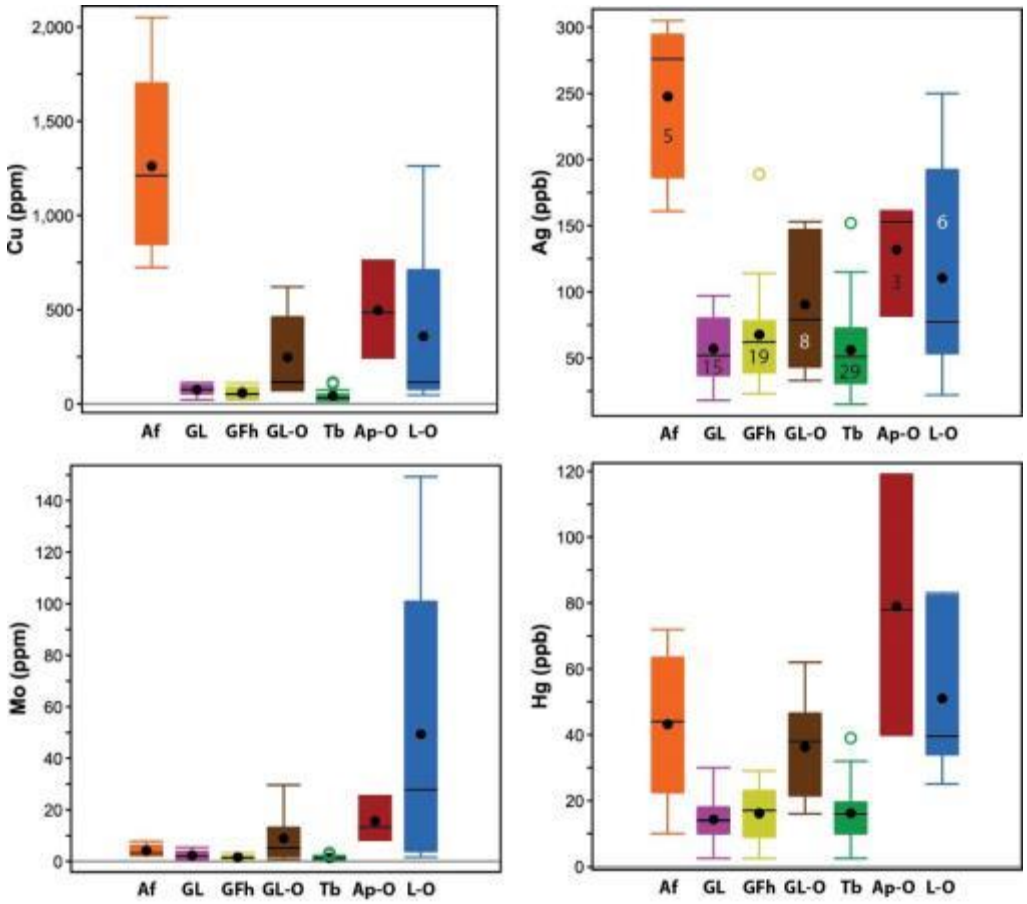

Figure 5-14. Copper, Ag, Mo, and Hg concentrations (<180 microns, aqua regia, ICP-MS) in upper B horizon soil samples for all surficial material units at J.A. Copper and Ag concentrations are enriched in soils sampled overlying alluvial fan (Af) material. Soils sampled beneath organic peat (GL-O, Ap-O, and L-O units) are elevated in Cu, Ag, Mo, and Hg.

Soils sampled from upper B horizon soil below peat cover (L-O, GL-O, and Ap-O units) are elevated in Cu, Ag, Mo, and Hg (Figure 5-14). Molybdenum concentrations are significantly high within the L-O surficial material (Figures 5-14 and 5-15), reaching up to 149.27 ppm (sample RC-15-HVC-115) compared to a local background value range of 0.36–7.80 ppm.

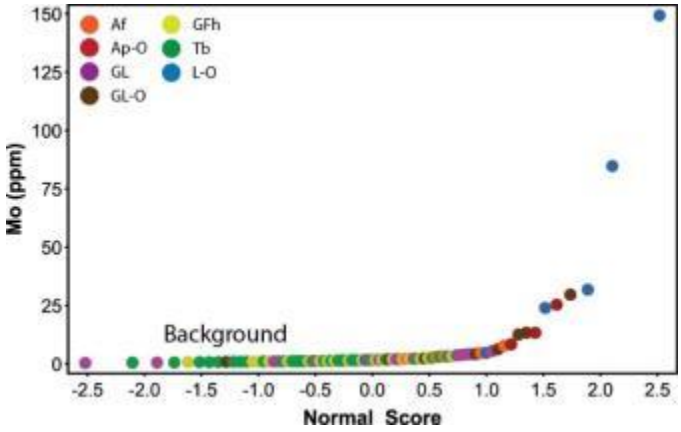

Figure 5-15. Probability plot for soil Mo (<180 microns, aqua regia, ICP-MS) shows concentrations in select peat-covered postglacial lacustrine material unit samples are significantly above background.

Copper versus S concentrations show certain samples to plot either on the chalcopyrite ($CuFeS_2$) or bornite (Cu_2FeS_4) Cu:S line (Figure 5-16). All samples from the Af unit contain very high Cu:S ratios indicating S has been weathered from the original sulphide mineral source and Cu is likely associated with an oxide and/or carbonate phase. Samples from L-O units, excluding those which plot on the chalcopyrite and bornite trend lines for Cu:S have high S, however contain very low Cu:S ratios indicating the presence of sulphur-bearing compounds such as pyrite or gypsum. The samples plotting on the chalcopyrite and bornite Cu:S lines are from Ap-O, L-O, and GL-O surficial units, and spatially plot very close to Witches Brook and a main drainage channel to the northeast (Figure 5-17).

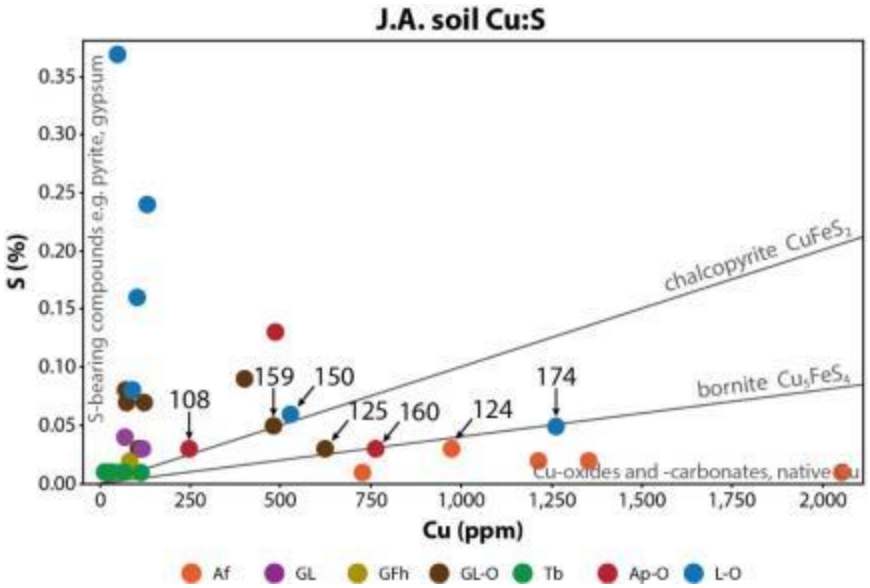

Figure 5-16. Some upper B horizon soil samples have similar ratios of Cu:S (<180 microns, aqua regia, ICP-MS) as ore minerals chalcopyrite or bornite. Soils from alluvial fan units contain high Cu:S ratios indicating S is lost from the oxidation of a sulphide mineral source and Cu is likely associated with an oxide and/or carbonate phase. Three samples from postglacial lake units with high S but low Cu:S ratios indicate the presence of other S-bearing compounds such as pyrite or gypsum.

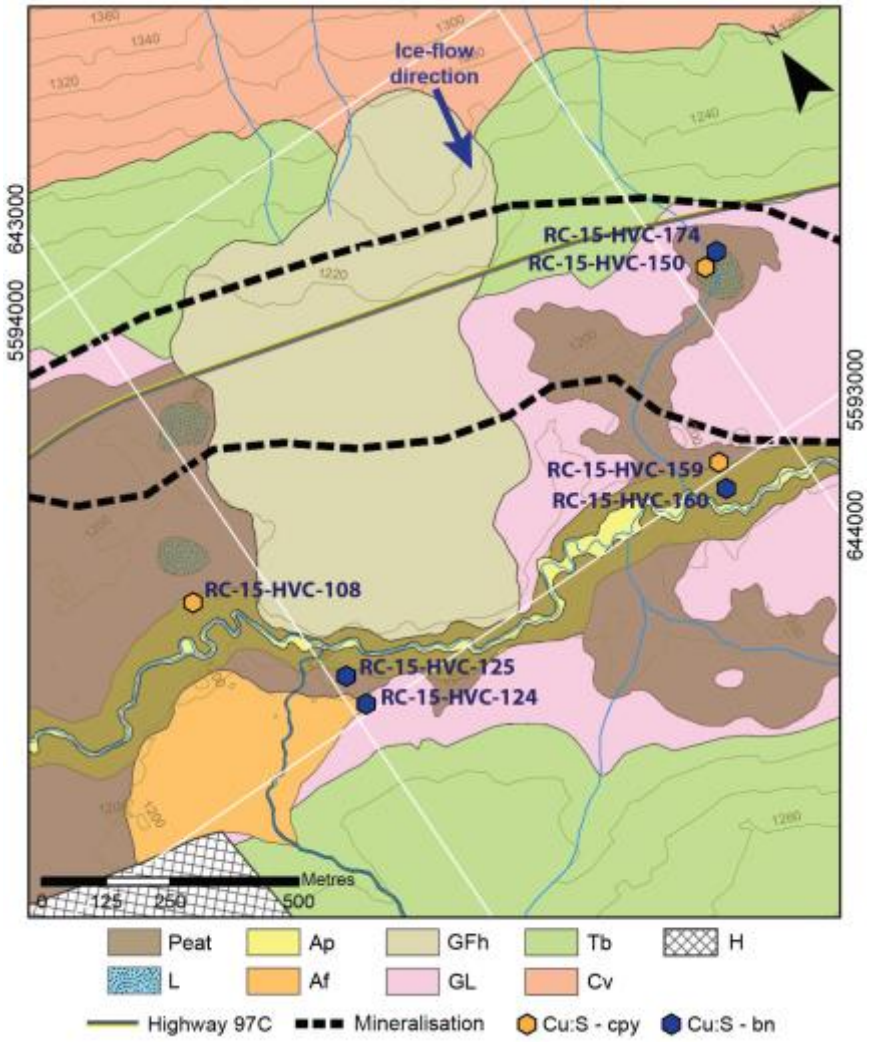

Figure 5-17. Upper B horizon soil samples in which the Cu:S ratio (<180 microns, aqua regia, ICP-MS) is similar to ore minerals chalcopyrite or bornite are spatially associated with Witches Brook and a main drainage channel which ponded surface water postglacially. Contours plotted at 20 metre interval spacing. Surficial geology is modified from Plouffe and Ferbey (2015b), using the GSC data model for surficial geology, version 1.2 (Deblonde et al., 2012); ice-flow direction from Plouffe and Ferbey (2015b); mineralisation outline from McMillan (1985).

The spatial distributions of anomalous populations of the principal elements of interest Cu, Mo, Ag and Bi (identified in Section 4.7.3) do not display a relationship with the projected outline of the deeply buried mineralisation at J.A. (Figure 5-19). With such high concentrations (Cu up to 2,432 ppm; Mo up to 205 ppm) these populations are very unlikely to be associated with ion migration from deeply buried bedrock mineralisation at J.A., which is expected to result in a

much more subtle response (e.g. Heberlein, 2010). In comparison, the maximum Mo response for aqua regia ICP-MS of upper B horizon soil over Tb material at Highmont South is 35 ppm, and that of Cu is 676 ppm. Both of these responses are attributed to local glacial clastic transport rather than ion migration from mineralisation.

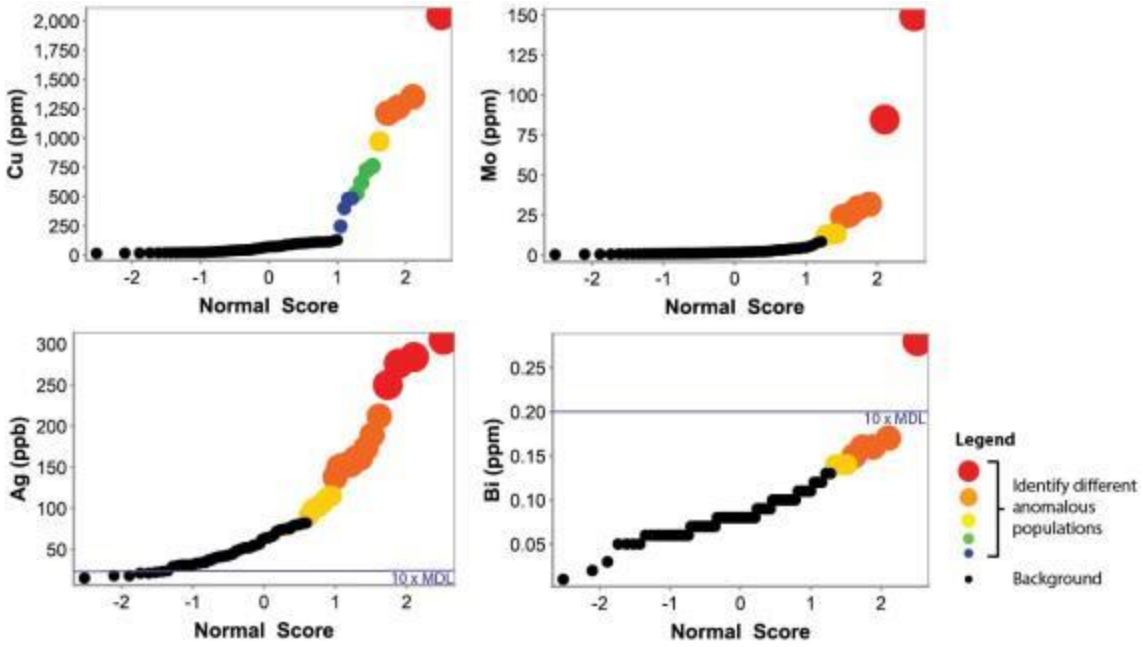

Figure 5-18. Probability plots showing distribution of element results in upper B horizon soil (<180 microns, aqua regia, ICP-MS) sampled on J.A. Anomalous population intervals were selected based on visual estimation of population breaks on these plots. Anomalous intervals are determined separately for each individual plot and symbols of the same size and colour are not related between plots for different elements. MDL = minimum detection limit.

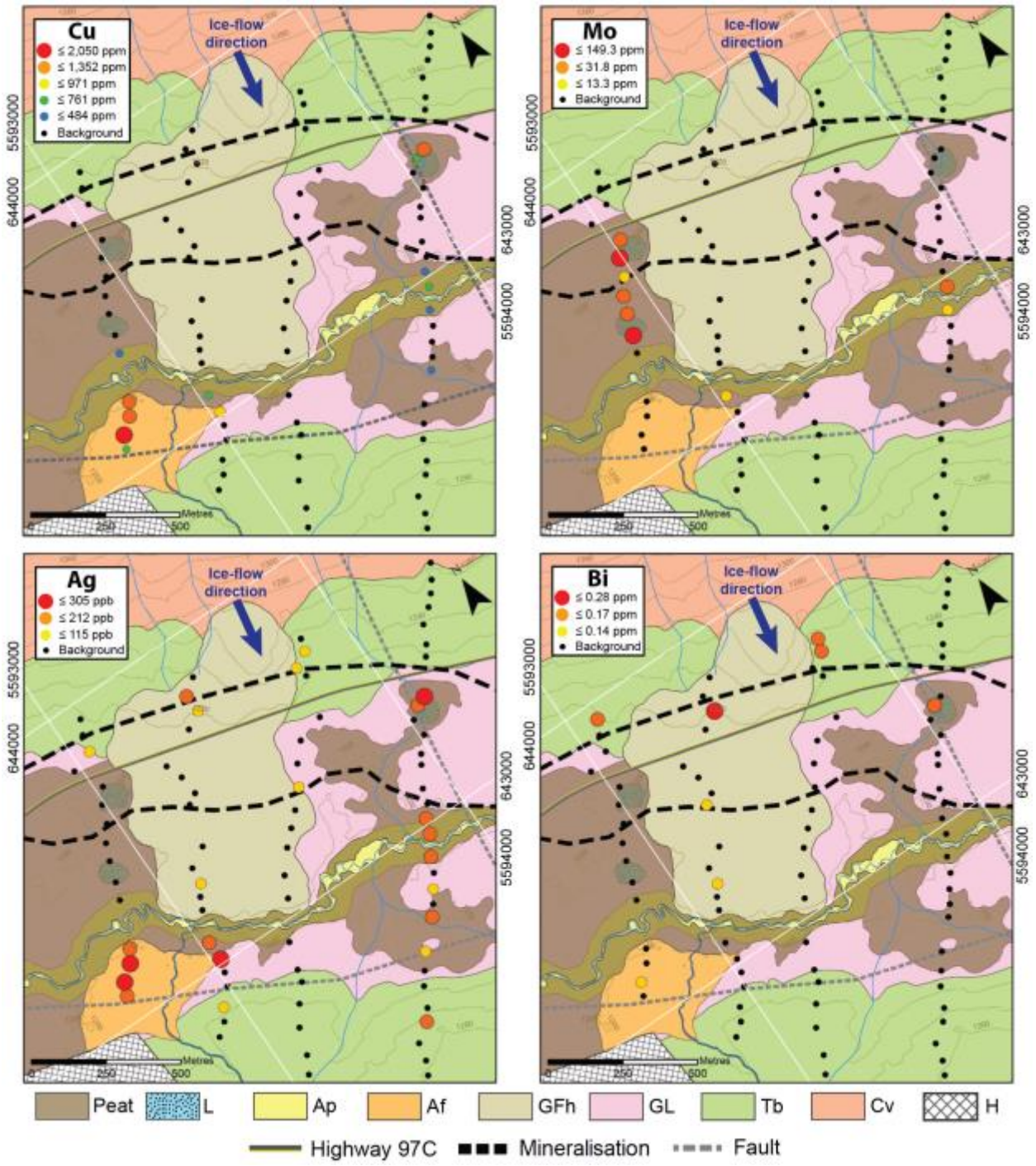

Figure 5-19. The spatial distributions of anomalous populations of Cu, Mo, Ag, and Bi (<180 microns, aqua regia, ICP-MS) have no clear relationship to deeply buried mineralisation at J.A. Contours plotted at 20 metre interval spacing. Surficial geology is modified from Plouffe and Ferbey (2015b), using the GSC data model for surficial geology, version 1.2 (Deblonde et al., 2012); ice-flow direction from Plouffe and Ferbey (2015b); mineralisation outline from McMillan (1985); faults modified from McMillan et al. (2009).

5.6.4 Deionised water leach ICP-MS results

Analytical results are reported in Appendix C and QA/QC practises and results in Appendix B. Selected elements were compared to certified and indicated values of OREAS25a CRM to assess precision. Mean percentage difference for field duplicate results was used to assess natural variability. Data quality is summarized as follows:

- Elements for which all values were reported below ten times stated analytical detection limits and are not discussed further are: Pb, Ag, Au, Cd, Bi, Sc, Tl, Hg, Te, Cs, Ta, Nb, In, and Be;
- Elements for which the median value was below ten times stated analytical detection limits and are interpreted with caution are: Zn, Ni, Co, As, Br, Cl, Th, Sb, V, Ca, La, Na, W, S, Se, Ga, Ge, Rb, Sn, Re, Pr, Sm, Eu, Tb, Tm, Yb, and Lu;
- Elements which are of acceptable accuracy and precision are: Mo, Cu, Mn, Fe, U, Sr, P, Mg, Ba, Ti, Al, K, Hf, Zr, Y, Ce, Nd, Gd, Dy, Ho, Er, and Li.

There is no clear indication of anomalous responses from vertical ion migration in the principal identified elements of interest (Cu, Mo, Ag, Bi) in soils overlying mineralisation at J.A. Sample RC-15-HVC-115 from an L-O surficial unit contains the highest concentration of soluble molybdenum at 16,917 ppb Mo (Figure 5-21). This concentration is more than five times the highest concentration of soluble Mo in upper B horizon soil from Tb units at Highmont South: 2,980 ppb. This response at Highmont South is attributed to local glacial clastic transport and vegetation cycling rather than ion migration from mineralisation. In soil samples from J.A. there is an organic control of soluble Mo concentrations (Section 5.7.5).

It remains unclear what is controlling the distribution of the deionised water-soluble Cu in the soils sampled at J.A. (Figure 5-21). There is no indication of control by pH, Eh, moisture, or

elements representative typical controlling soil phases such as Fe, Mn, Al, or C_{org}. Sample RC-15-HVC-168 from a till blanket surficial unit contains the highest concentration of soluble Cu at 5,097 ppb. The highest soluble Cu concentrations in Highmont South soil samples from dry till blanket surficial units and spatially coincident with buried mineralisation are 3,121 ppb and 2,925 ppb Cu. These samples likely contain Cu from glacial erosion and transport of mineralised fragments at Highmont South where till is maximum 10 metres thick. No glacial erosion of J.A. mineralisation occurred during the last glaciation due thickness of overburden and shielding of mineralised bedrock by preglacial sequences (Plouffe and Ferbey, 2015a), therefore this scenario is not possible at J.A.

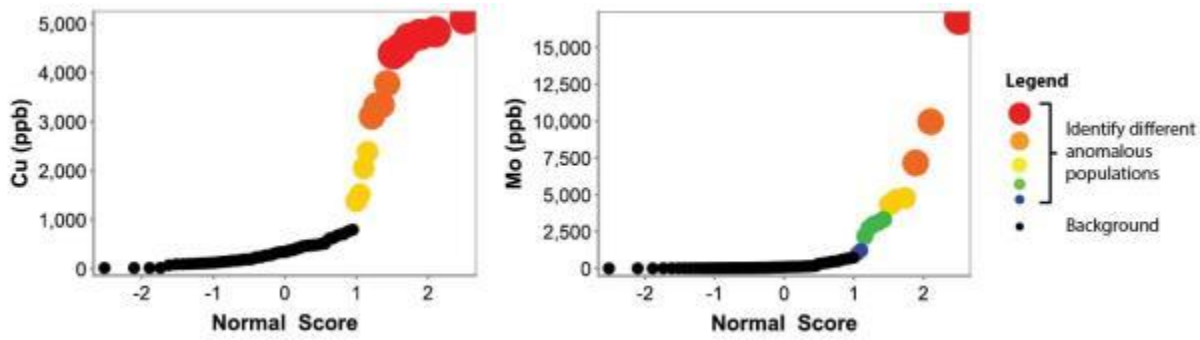

Figure 5-20. Probability plots showing distribution of element results in upper B horizon soil (<180 microns, deionised water leach, ICP-MS) sampled on J.A. Anomalous population intervals were selected based on visual estimation of population breaks on these plots. Anomalous intervals are determined separately for each individual plot and symbols of the same size and colour are not related between plots for different elements.

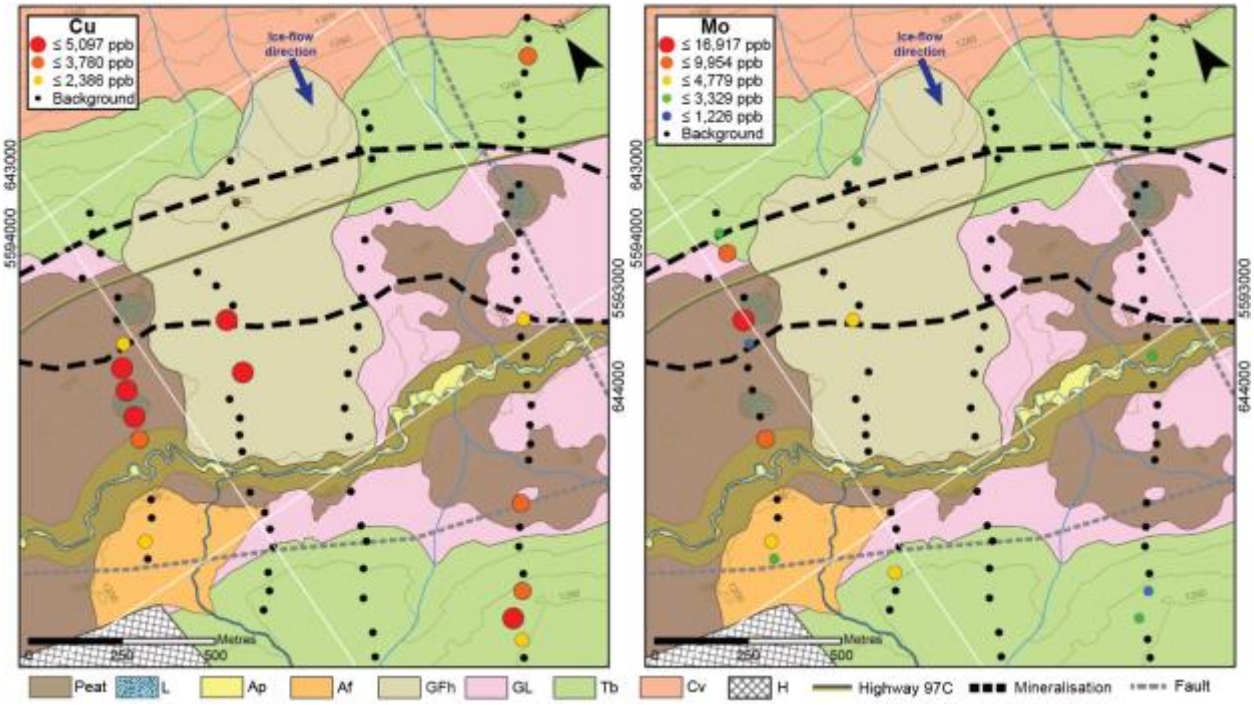

Figure 5-21. Concentrations of water-soluble Cu and Mo (<180 microns, deionised water leach, ICP-MS) in upper B horizon soil samples at J.A. Contours plotted at 20 metre interval spacing. Surficial geology is modified from Plouffe and Ferbey (2015b), using the GSC data model for surficial geology, version 1.2 (Deblonde et al., 2012); ice-flow direction from Plouffe and Ferbey (2015b); mineralisation outline from McMillan (1985); faults modified from McMillan et al. (2009).

5.6.5 Organic carbon results

Analytical results are reported in Appendix C and QA/QC practises and results in Appendix B. Selected elements were compared to certified and indicated values of OREAS25a CRM to assess precision. Mean percentage difference for field duplicate results was used to assess natural variability.

Median C_{org} content in upper B horizon soils from J.A. is 1.14% C_{org}. Three outlier samples exist with high C_{org} concentrations: RC-15-HVC-115 (24.18% C_{org}), RC-15-HVC-116 (10.73% C_{org}), and RC-15-HVC-169 (10.66% C_{org}) (Figure 5-22a). Organic C exhibits a control on deionised water-extractable Mo in soil samples from J.A. Samples RC-15-HVC-115 (642991 m E,

5593665 m N) and -116 (663055 m E, 5593838 m N) contain the highest concentrations of water-soluble Mo (deionised water leach ICP-MS) as well as C_{org} (Figure 5-22b). Molybdenum is known to bind strongly to organic material as well as to be readily available for uptake by vegetation (Kabatta-Pendias, 2010).

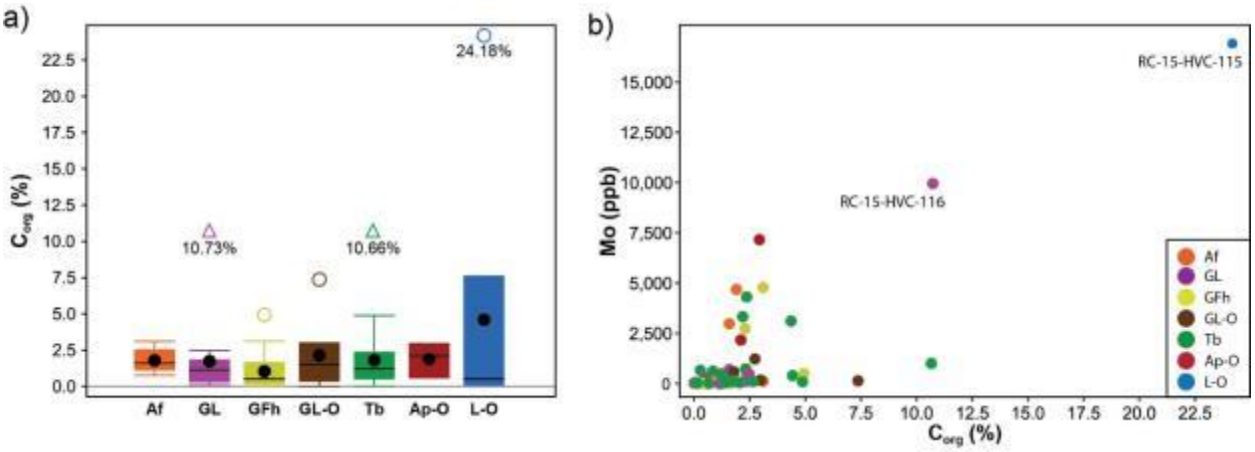

Figure 5-22. a) Organic C concentrations in surficial materials at J.A. are low with the exception of three outlier samples. Soil samples RC-15-HVC-115 (10.73% C_{org}) and -116 (24.18% C_{org}) contain the highest concentrations of soluble Mo (16,914 ppb and 9,954 ppb, respectively). b) Water-soluble Mo concentrations (<180 microns, deionised water leach, ICP-MS) and organic C concentrations in upper B horizon soil samples from J.A.

5.6.6 Field portable XRF results

Analysis of <180 microns upper B horizon soil samples using a pXRF analyser was conducted using both 'soil' and 'geochem' modes. Selected elements were referenced to certified and indicated values of OREAS25a CRM to assess precision. Mean percentage difference for field duplicate results was used to assess natural variability. Results for Cu and Mo by soil mode are deemed acceptable following evaluation of QC results. Detailed QA/QC results are reported in Appendix B.

pXRF results (soil mode) for upper B horizon soil samples from J.A. are similar in magnitude to aqua regia ICP-MS results. Anomalous populations of Cu and Mo, determined by visual estimation from probability plots, are effectively identical to those determined for aqua regia ICP-MS (Figure 5-23). Similar to aqua regia ICP-MS results, the magnitudes of the concentrations of Cu and Mo are very unlikely to be associated with ion migration from deeply buried mineralisation, which is expected to result in a much more subtle response (e.g. Heberlein, 2010). Results for Ag and Bi are below ten times detection limits of the pXRF. The pXRF reports marginally higher concentrations of Cu and Mo relative to the aqua regia ICP-MS. Assuming good calibration of the pXRF, this could reflect the difference between a 'total' technique (pXRF) and a partial digest (weak aqua regia).

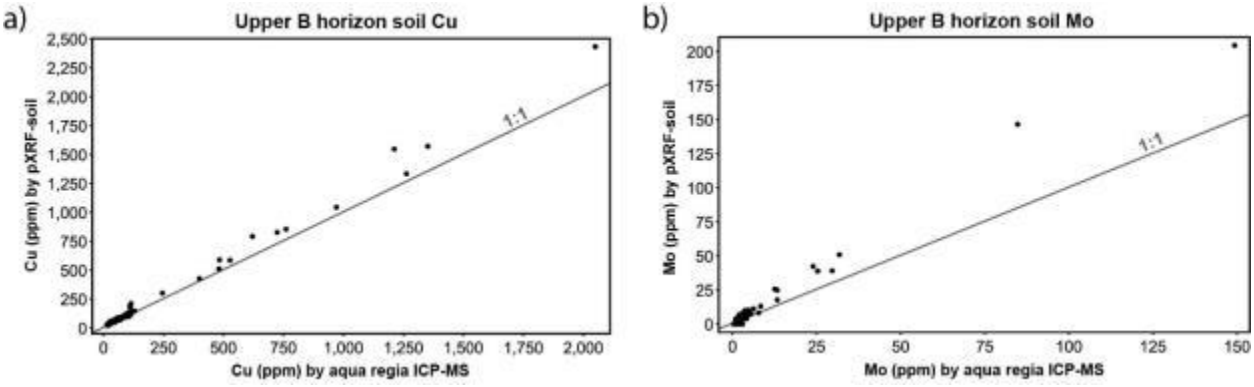

Figure 5-23. Comparison of Cu and Mo concentrations by pXRF in soil mode and by aqua regia ICP-MS for upper B horizon soil samples from J.A.

5.7 Soil profile sample analysis

5.7.1 Physicochemical properties

Soil profiles RC-16-HVC-030 (642940 m E, 5593853 m N), RC-16-HVC-032 (643905 m E, 5593099 m N), and RC-16-HVC-033 (643959 m E, 5593203 m N) sampled in GL material share similar trends in physicochemical measurements (Figure 5-24). Slurry EC (58–430 μS/cm) and in situ moisture (0–14.4%) generally increase downhole with decreasing grain size of the profile material. pH is more circumneutral in the surface (LFH) horizon (slurry pH median 6.6; in situ pH median 5.8) which contains the most organic matter, and gradually becomes more alkaline downhole (slurry pH median 8.4; in situ pH median 7.3). Eh (calculated from ORP) is low (0.246–0.394 V), with the highest measurements in the surface (LFH) horizon of each profile.

Profile RC-16-HVC-031 (642996 m E, 5593566 m N) was sampled in GL-O surficial material. pH values are circumneutral to mildly alkaline (slurry pH 7.8–8.1; in situ pH 6.4–7.2) in all horizons (Figure 5-24). Slurry Eh values are low in all horizons (0.318–0.326 V) except the top 4 centimetres of the Ah horizon below the O (peat) horizon (1.155 V).

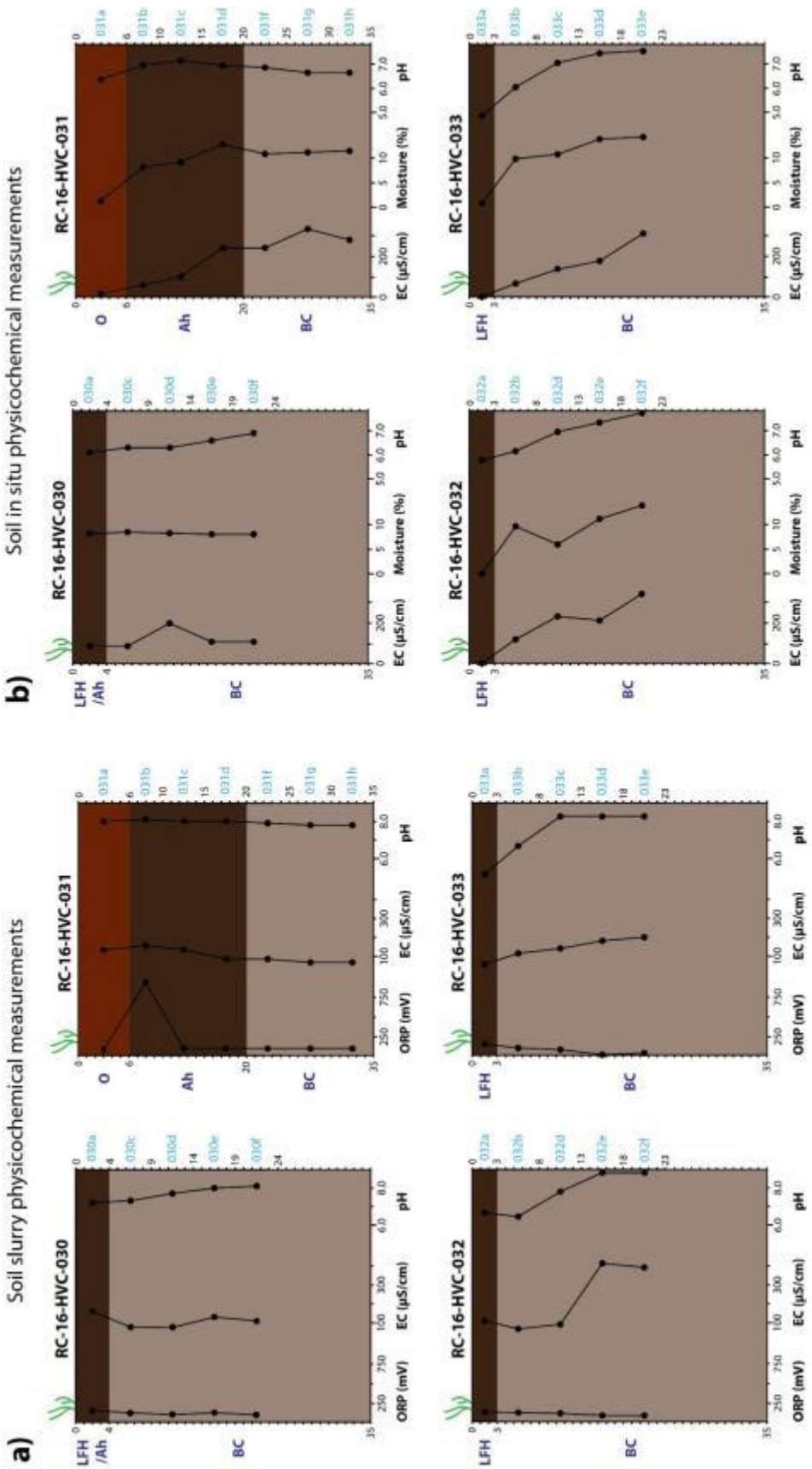

Figure 5-24. a) Soil slurry measurements for ORP, EC, and pH in each sampling interval (sample intervals marked in light blue on right axis) in soil profiles at J.A. b) In situ measurements for EC, moisture, and pH in each sampling interval in soil profiles at J.A. Depth measurements are in centimetres. Nomenclature of soil horizons, marked in dark blue (left axis), follows the Canadian system of soil classification (Agriculture Canada, 1998).

5.7.2 Aqua regia digest ICP-MS results

Analytical results are reported in Appendix C and QA/QC practises and results in Appendix B. Selected elements were compared to certified and indicated values of OREAS25a CRM to assess precision. Mean percentage difference for field duplicate results was used to assess natural variability. Elements analysed by aqua regia ICP-MS which are completely below ten times stated analytical detection limits for profile samples and are not discussed further are: B, W, Tl, Te, Ge, Sn, Ta, In, Be, Pd, and Pt. The remaining data was deemed acceptable following evaluation of QC results.

All soil profile samples were collected from the glaciolacustrine surficial unit (Figure 5-3), with one of the profiles sampled having organic peat cover (RC-16-HVC-031). Elements which have the highest concentrations in the surface (LFH or O) horizon, which contains the highest concentrations of organic matter (Section 5.7.5), for all four soil profile samples are Cu and Pb. The same is true for Mo in all profiles except -031, and for Ag in all profiles except -030 (Figure 5-25). The magnitudes of the surface (LFH or O) horizon concentrations of these elements are significantly higher than an expected response from deeply buried mineralisation (e.g. Heberlein, 2010). Lead has a tendency to be naturally enriched in organic-rich surface soil horizons (Reimann et al., 2014). Organic matter has a strong ability to bind the elements Cu, Mo, and Ag (Kabata-Pendias, 2010; Reimann et al., 2014).

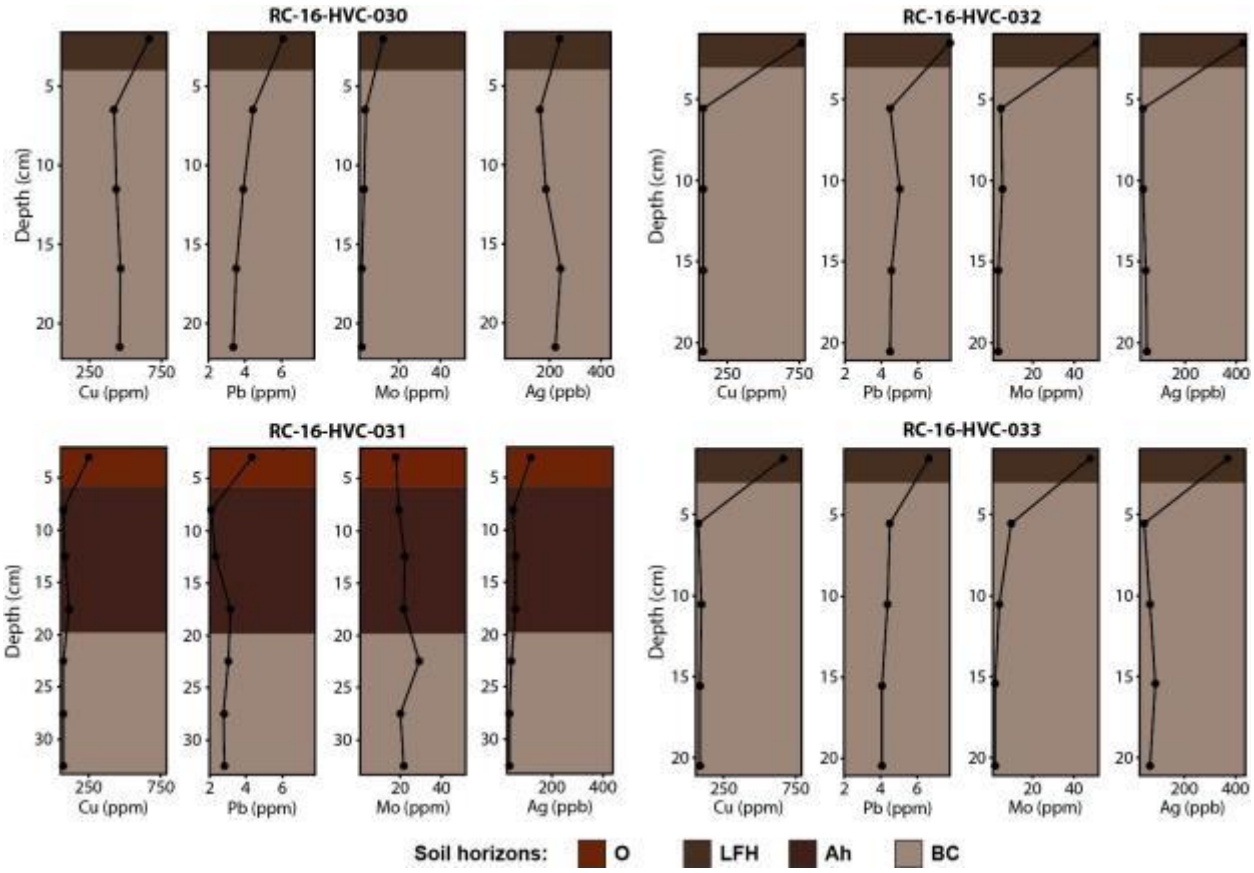

Figure 5-25. Concentrations of Cu, Pb, Mo, and Ag (aqua regia, ICP-MS) in soil profiles at J.A. are highest in the surface horizon which contains the most organic matter (with the exception of Mo in profile RC-16-HVC-031 and Ag in profile RC-15-HVC-030).

The concentration of Cu in all sample intervals of profile RC-16-HVC-030 ranges from 421 to 663 ppm. These concentrations are significantly higher than local background Cu for upper B horizon soil from Tb units at Highmont South which has a median value of approximately 124 ppm. Molybdenum concentrations in profile RC-16-HVC-031 range from 17.8 to 29.5 ppm, compared to Highmont South local background median value of 7.3 ppm.

5.7.3 Deionised water leach ICP-MS results

Analytical results are reported in Appendix C and QA/QC practises and results in Appendix B. Selected elements were compared to certified and indicated values of OREAS25a CRM to assess

precision. Mean percentage difference for field duplicate results was used to assess natural variability. Elements analysed by deionised water leach ICP-MS which are completely below ten times stated analytical detection limits for all profiles and are not discussed further are: Pb, Au, Cd, Bi, W, Sc, Tl, Hg, Te, Cs, Ge, Nb, Sn, Ta, In, and Be. The remaining data was deemed acceptable following evaluation of QC results.

Deionised water leach results for Mo compared to those from aqua regia digest give an indication of movement of the water-soluble portion of Mo in the soil column (Figure 5-26). In profiles RC-16-HVC-030, -032, and -033 results indicate that a minor portion of the Mo concentrated in the surface (LFH) horizon is being eluviated into the B horizon. The water-soluble portion of Mo decreases downwards from the top of the B horizon, indicating that it has not been carried far downwards. Water-soluble Mo concentrations in profile RC-16-HVC-031 are higher in the upper O (peat) and Ah horizons than the B horizon below. The highest concentrations for Mo are contained in the topmost horizons which contain the most organic carbon (LFH, O, and Ah horizons) reflecting the tendency of Mo to sorb to organic material (Kabata-Pendias, 2010).

In all profiles the highest concentrations of soluble Cu occur in the organic-rich surface horizon and decrease dramatically in sample intervals below. Similar to Mo, Cu has a strong affinity for organic matter (Kabata-Pendias, 2010).

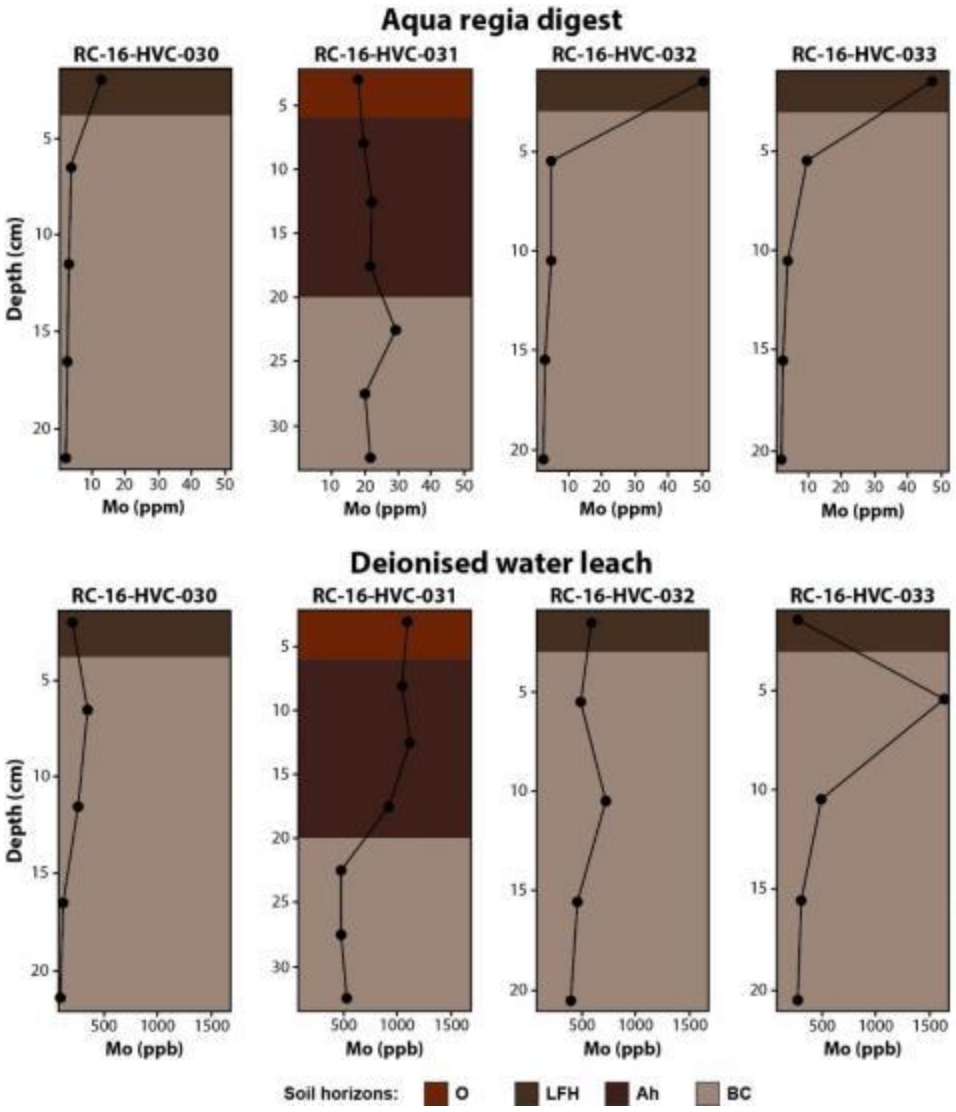

Figure 5-26. The comparison of soil profile Mo concentrations analysed by aqua regia digest to deionised water leach (both followed by ICP-MS) indicates a small portion of soluble Mo has been washed a short distance downhole from the organic-rich surface horizon.

5.7.4 Organic carbon results

Analytical results are reported in Appendix C and QA/QC practises and results in Appendix B. Selected elements were compared to certified and indicated values of OREAS25a CRM to assess precision. Mean percentage difference for field duplicate results was used to assess natural variability.

All four soil profiles have the highest C_{org} concentrations in the surface (LFH or O) horizon which receive the highest inputs of organic matter (Figure 5-27).

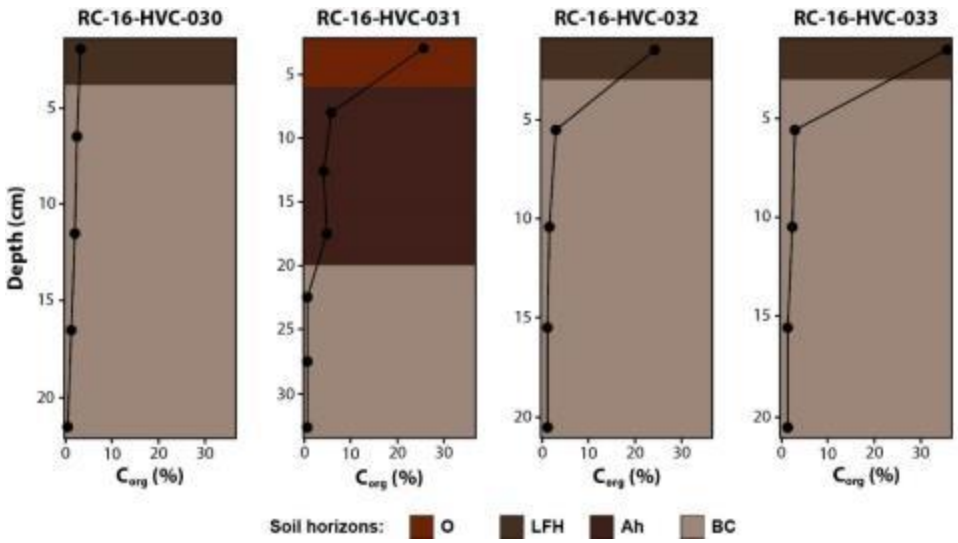

Figure 5-27. Organic C concentrations in J.A. soil profiles. The highest concentrations of C_{org} in all profiles occur within the surface (LFH or O) horizon.

Table 5-1 shows the approximate amount of soil organic matter (SOM) in the organic-rich horizons of the soil profiles, calculated from C_{org} concentrations using the Van Bemmelen factor (Section 4.8.4).

Profile ID	Horizon	C_{org} (%)	SOM (%)
RC-15-HVC-030	LFH	3.45	5.95
RC-15-HVC-031	O	25.71	44.32
RC-15-HVC-031	Ah	4.95	8.53
RC-15-HVC-032	LFH	24.39	42.05
RC-15-HVC-033	LFH	35.82	61.75

Table 5-1. Approximate percentage of soil organic matter (SOM) in the organic-rich horizons of soil profiles from J.A. calculated using the Van Bemmelin factor assuming organic matter contains 58% organic carbon.

5.8 Sequential extractions

5.8.1 Sample selection

Five samples were selected for sequential extraction from the 2015 upper B horizon soil samples from J.A. to identify the deportment of the trace elements in the soil (Figure 5-28). Geochemical data from previous analyses was considered in the selection of samples for sequential extraction.

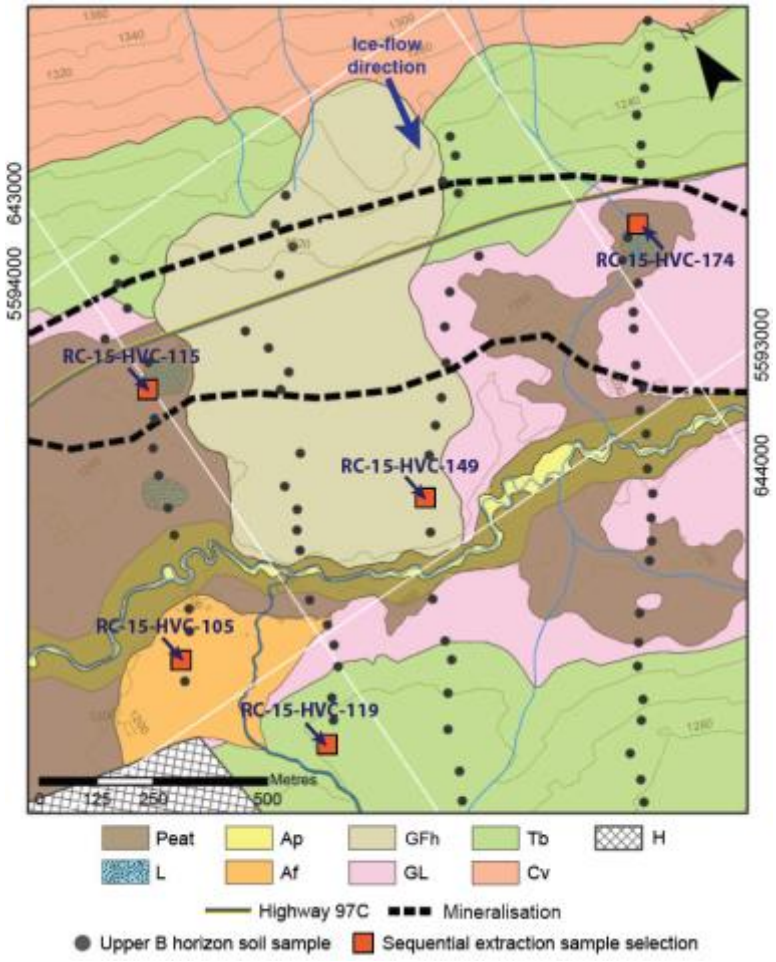

Figure 5-28. Upper B horizon (<180 microns) soil sample sites selected for sequential extractions. Samples RC-15-HVC-105, -115, and -174 were selected for their extremely high Cu and/or Mo concentrations. Sample RC-15-HVC-149 was selected as a representative sample for the GFh surficial unit, and -119 was selected as such for the Tb surficial unit. Contours plotted at 20 metre interval spacing. Surficial geology is modified from Plouffe and Ferbey (2015b), using the GSC data model for surficial geology, version 1.2 (Deblonde et al., 2012); ice-flow direction from Plouffe and Ferbey (2015b); mineralisation outline from McMillan (1985).

5.8.2 Results

Analytical results are reported in Appendix C and QA/QC practises and results in Appendix B. The data was deemed acceptable and fit for purpose following evaluation of QC results. The sum of sequential extractions was typically 100% ±20% of separate total chemical analysis. Consistency of final pH values (Table 5-2) for the leachate at the end of each extraction indicate whether or not the buffering of each extraction was successful and the elements associated with each target phase were effectively extracted.

	Final pH of leachate				
Sample	**DW_s**	**AmA_s**	**CHH_s**	**HHH_s**	**NaP_s**
RC-15-HVC-105	6.8	5.0	3.0	1.1	9.4
RC-15-HVC-115	8.0	5.2	3.3	1.2	9.5
RC-15-HVC-119	6.8	5.0	2.1	1.1	10.0
RC-15-HVC-149	6.3	5.0	2.2	1.2	9.9
RC-15-HVC-174	8.3	5.1	2.8	1.1	9.3
Median:	**-**	**5.0**	**2.8**	**1.1**	**9.5**
Target:	**-**	**5.0**	**1.5**	**1.5**	**10.0**

Table 5-2. Final leachate pH values for DW_s, AmA_s, CHH_s, HHH_s, and NaP_s extractions in sequence. Target pHs are provided by Katerina Paley, ALS Minerals Division.

Results for the AmA_s leach (which targets $CaCO_3$) for sample RC-15-HVC-105 report 14,700 ppm Ca in the carbonate ($CaCO_3$) soil phase. Samples RC-15-HVC-115, -119, -149 and -174 contain: >100,000 ppm (i.e. above detection limits), 830 ppm, 900 ppm, and 68,300 ppm Ca as the $CaCO_3$ phase, respectively. The extremely high carbonate contents of samples 115 and 174 are likely responsible for buffering reactions and generating alkaline pHs for DIW values of the leachate in the sequential extraction.

Samples RC-15-HVC-119 and -149, selected as local background samples, are low in total (separate four acid digest ICP-MS) Cu (27.9 and 32.5 ppm), Mo (1.6 and 1.8 ppm), Ag (both

0.07 ppm), and Bi (0.10 and 0.12 ppm) compared to the other sequential leach samples for J.A. (Figure 5-29).

Sample RC-15-HVC-105, from within the Af unit, is interpreted to contain weathered and transported porphyry material from other centres of the deposit upstream. This sample contains the highest total concentrations of Cu, Ag, and Bi. A significant portion of this sample's Cu and Bi are reported from HHH_s which indicates labile portions of these elements are scavenged by an amorphous Fe-oxide phase in the soil. Although this sample has a low C_{org} concentration (1.91%) (Figure 5-30), a significant portion (approximately 33% of total) of Mo is reported from NaP_s indicating an association with organic matter.

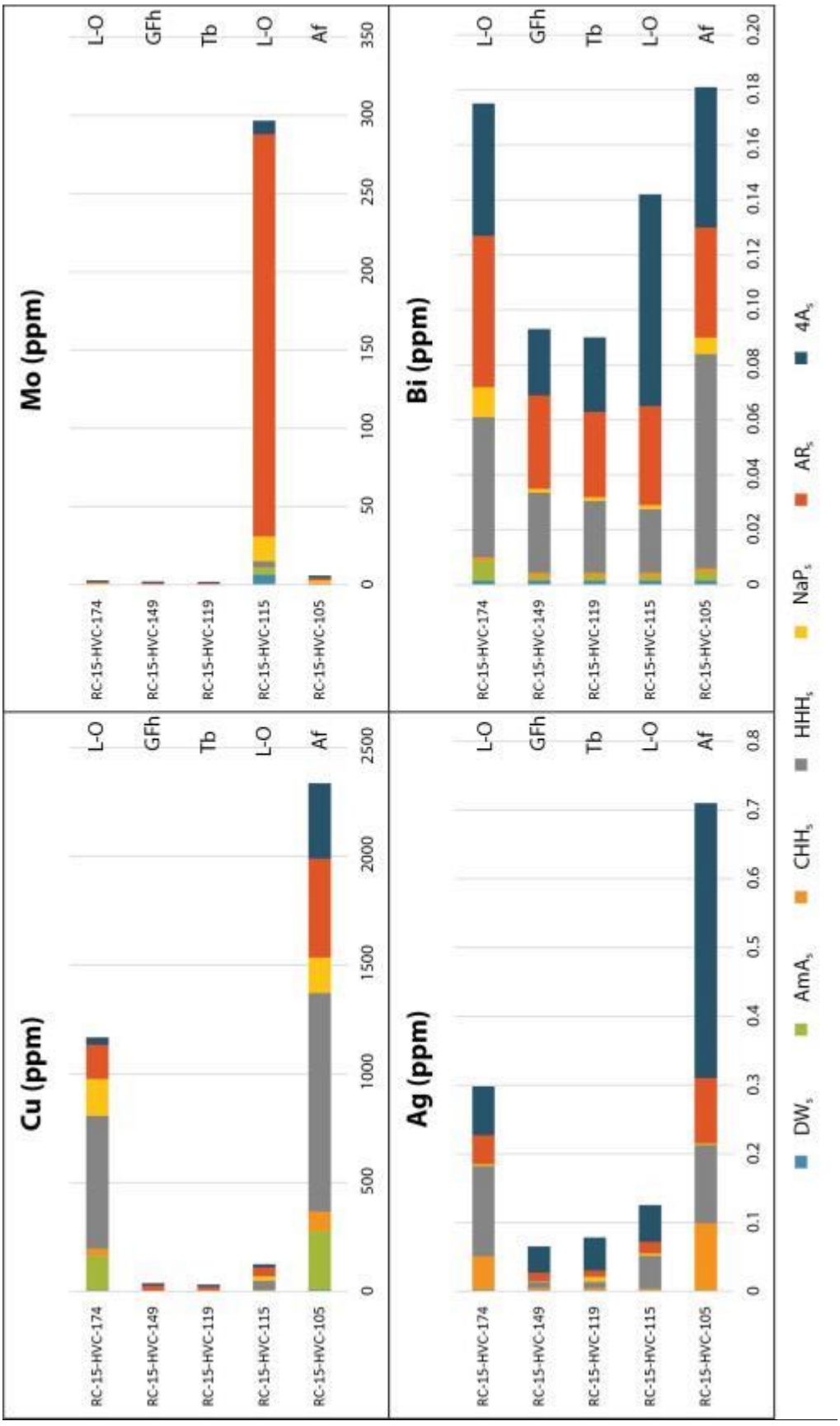

Figure 5-29. Sequential extraction results for all five upper B horizon soil samples (<180 microns portion) selected for J.A. Abbreviations along the right-hand side of each plot indicate the surficial material unit from which each sample was obtained. For reference to extraction symbols in legend see Table 3-2 in Section 3.6.7.

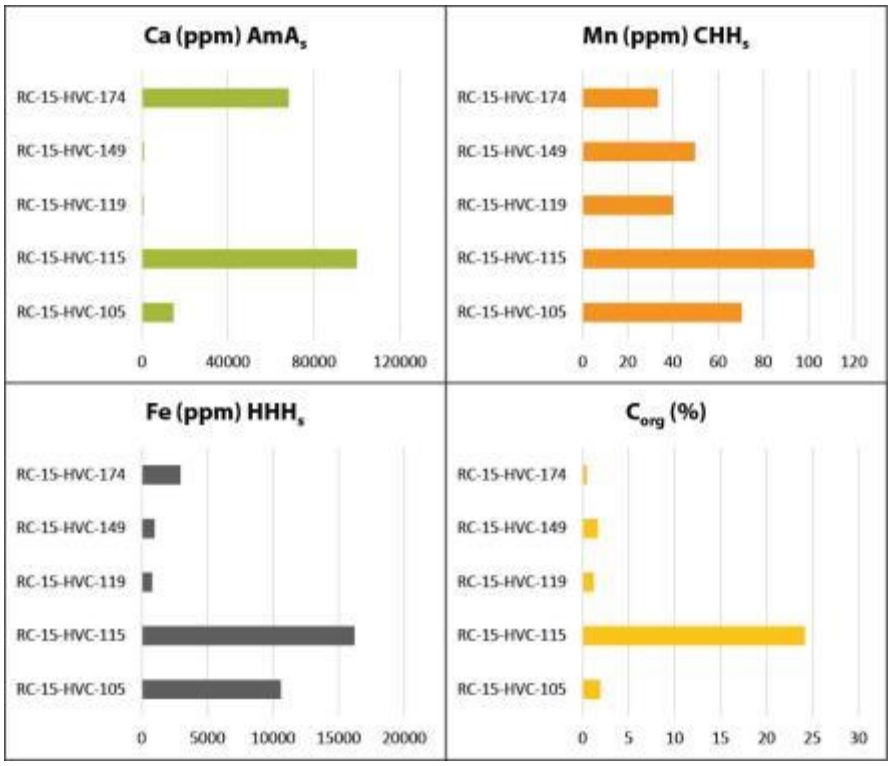

Figure 5-30. Selective extraction results for all five upper B horizon (<180 microns) soil samples selected for J.A. Concentrations of different target phases in each sample are presented corresponding to the step in the sequential extraction which targets that specific phase. Calcium is a proxy for relative $CaCO_3$ content extracted in AmA_s. Manganese and Fe are proxies for amorphous Mn- and Fe-oxides extracted by CHH_s and HHH_s, respectively. Organic C (determined by previous separate analysis at Bureau Veritas) is a proxy for organic matter extracted by NaP_s. For reference to extraction symbols see Table 3-2.

Samples RC-15-HVC-115 and -174 are from within two separate L-O surficial units. RC-15-HVC-174 contains high total concentrations of Cu (1,167 ppm), Ag (0.298 ppm), and Bi (0.175 ppm). The majority of Cu and Ag, and a significant portion of Bi, are reported from HHH_s which indicates amorphous Fe-oxide association. Sample RC-15-HVC-115 contains the highest total Mo concentration (296 ppm), the majority of which is reported from AR_s which suggests a clastic crystalline Fe-oxide (e.g. ferrimolybdenite) or residual sulphide phase source. Despite this sample containing the highest concentration of C_{org} (Figure 5-30), only approximately 5% of the total Mo is reported from the NaP_s leach. The Mo concentration in this sample is too high to be the surficial expression of vertical ion migration from deeply buried bedrock mineralisation.

5.9 Soil hydrocarbon results

A total of 86 hydrocarbon and organo-sulphur compounds (Table 3-3, Section 3.7) were analysed by thermal desorption and gas chromatography-mass spectrometry at the AGI laboratories in Newark, Delaware. Compounds removed from interpretation by AGI during signal-to-noise filtering are: ethane, propane, tetradecane, heptadecane, ethane, pristane, phytane, decanal, cis-1,3/1,4-dimethylcyclohexane, alpha-pinene, beta-pinene, camphor, caryophyllene, acenapthylene, and benzothiazole. Outlier sample RC-15-HVC-176 was identified and removed from interpretation by AGI. The report compiled by AGI is available in Appendix F. QA/QC practices and results are detailed in Appendix B. The data was deemed acceptable on the basis of the AGI evaluation of QC results.

None of the organic compounds analysed, including the normal alkanes in the C_{12}–C_{15} range which are anomalous over mineralisation at Highmont South, show an indication of a response to deeply buried mineralisation at J.A. (Figure 5-32).

Comparison of soil physicochemical measurements to the analysed hydrocarbon and organo-sulphur compounds indicated that clear no relationships occur between any of these compounds and pH, Eh, EC, or moisture.

Interpretation by AGI (Appendix F) did not identify coherent anomalous signatures overlying mineralisation at J.A. Interpretation was completed by AGI in the context of bedrock geology and did not include consideration of surficial materials and processes.

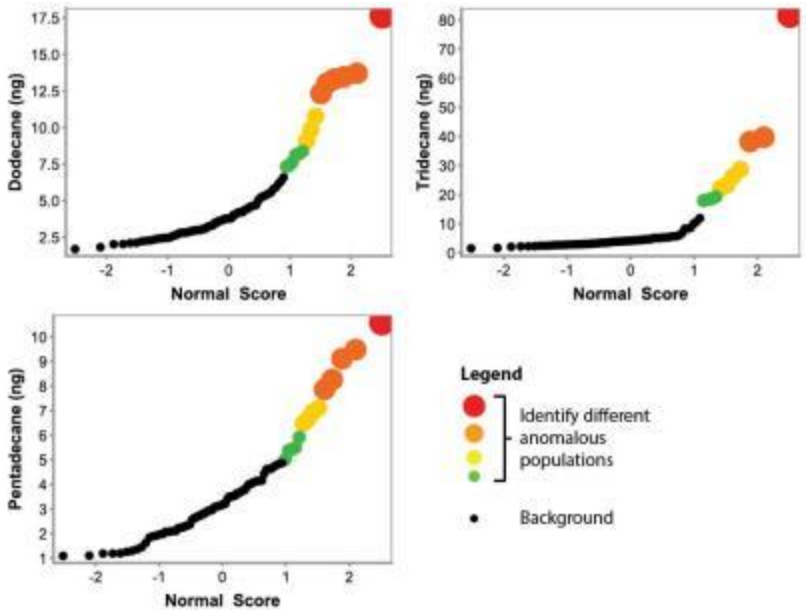

Figure 5-31. Probability plots showing distribution of dodecane, tridecane and pentadecane in soils at J.A. Anomalous population intervals were selected based on visual estimation of population breaks on these plots. Population intervals are determined separately for each individual plot and symbols of the same size and colour are not related between plots for different elements.

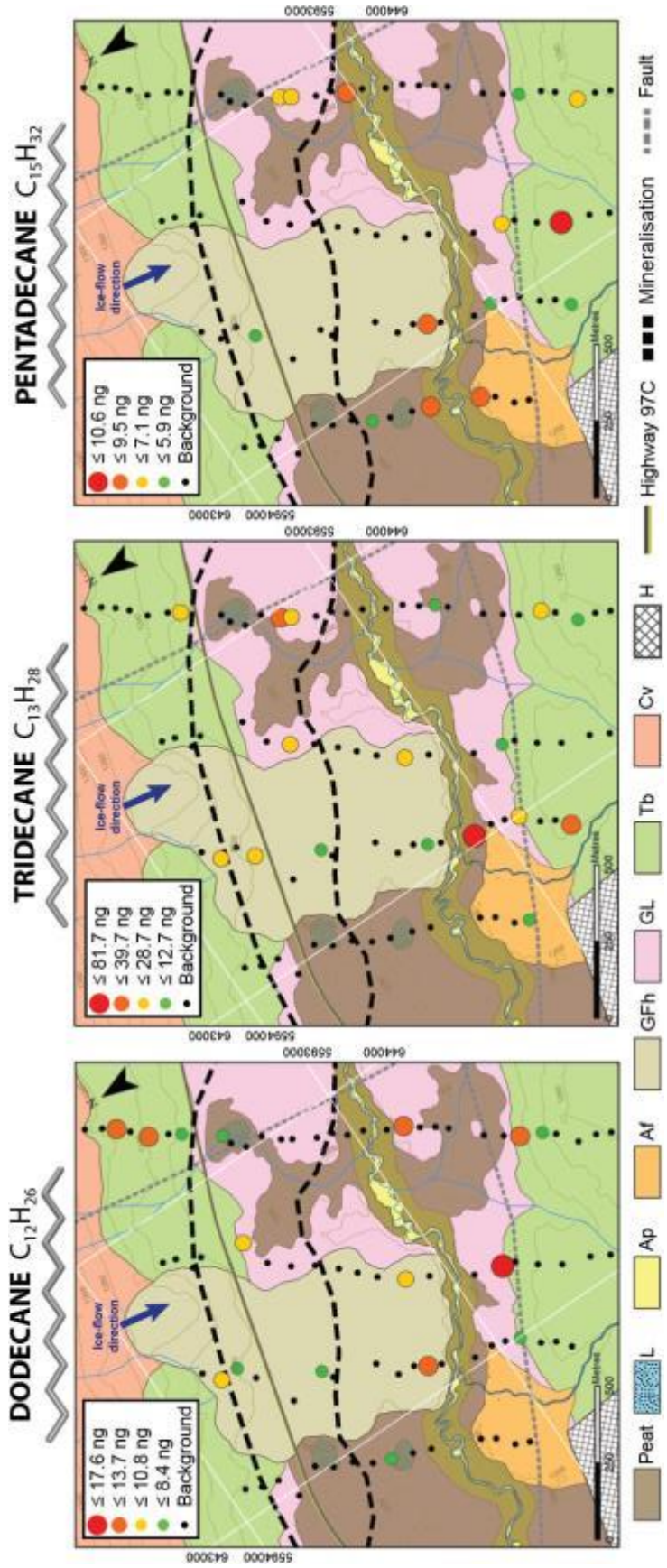

Figure 5-32. Normal alkanes in the C_{12} to C_{15} range, which proved anomalous in soils overlying bedrock mineralisation at Highmont South, show no discernable anomaly overlying bedrock mineralisation at J.A. Contours plotted at 20 metre interval spacing. Surficial geology is modified from Plouffe and Ferbey (2015b), using the GSC data model for surficial geology, version 1.2 (Deblonde et al., 2012); ice-flow direction from Plouffe and Ferbey (2015b); mineralisation outline from McMillan (1985); faults modified from McMillan et al. (2009).

5.10 Copper isotopes

5.10.1 Sample selection

Nine samples were selected for Cu isotope analysis from the 2015 upper B horizon soil samples (Table 5-3). The samples are from within the Tb, GFh, and GL surficial material units (Figure 5-33).

Sample	Unit	Overlying mineralisation	Additional rationale for selection	Cu concentration
RC-15-HVC-118	Tb	No	Potentially contains colluvial material	1,108 ppm
RC-15-HVC-129	GFh	No	Probable transported clastic material	43 ppm
RC-15-HVC-132	GFh	Yes	Probable transported clastic material	53 ppm
RC-15-HVC-148	GFh	No	Probable transported clastic material	30 ppm
RC-15-HVC-149	GFh	No	Probable transported clastic material	23 ppm
RC-15-HVC-153	GL	No	Clay-rich material	41 ppm
RC-15-HVC-163	GL	Yes	Clay-rich material	998 ppm
RC-15-HVC-176	GFh	Yes	Probable transported clastic material	25 ppm
RC-15-HVC-177	GFh	Yes	Probable transported clastic material	28 ppm

Table 5-3. Rationale for selection of upper B horizon (<180 microns) soil samples for Cu isotope analysis. Copper concentrations determined by previous aqua regia ICP-MS (AQ250) at Bureau Veritas.

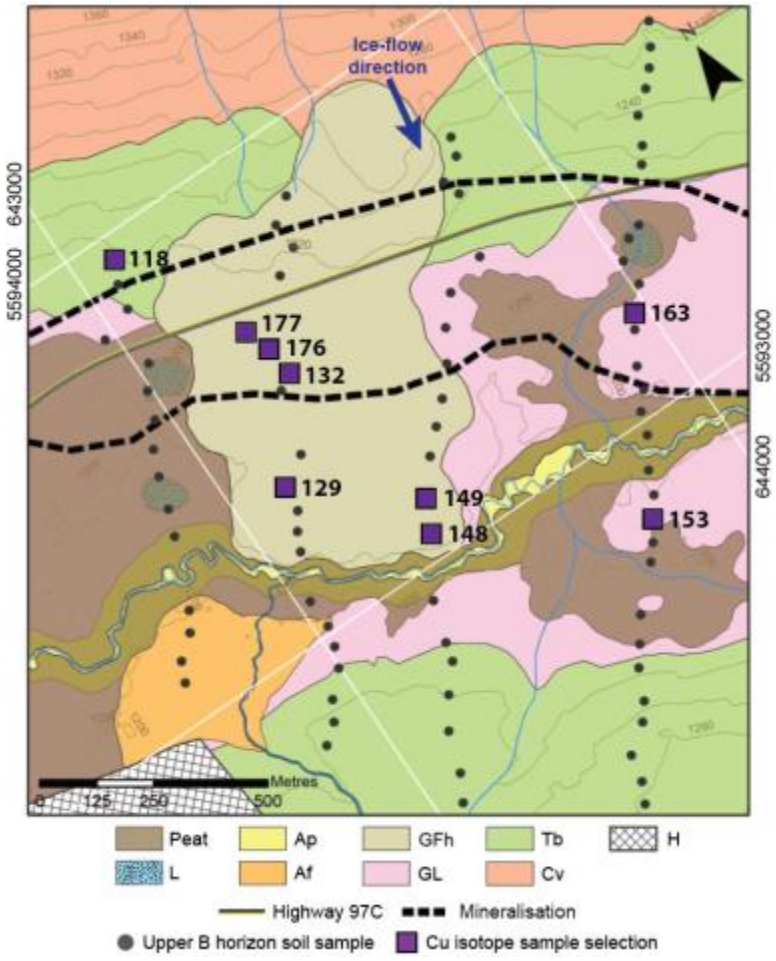

Figure 5-33. Locations of nine upper B horizon soil sample sites selected for Cu isotope analysis. Geochemical data from previous analyses was considered in the selection process. Contours plotted at 20 metre interval spacing. Surficial geology is modified from Plouffe and Ferbey (2015b), using the GSC data model for surficial geology, version 1.2 (Deblonde et al., 2012); ice-flow direction from Plouffe and Ferbey (2015b); mineralisation outline from McMillan (1985).

5.10.2 Results

The isotopic signature for the Cu extracted by the total digestion of each sample lies within the expected range for primary magmatic Cu ($\delta^{65}Cu = 0 \pm 1‰$) with the exception of sample RC-15-HVC-132 which is just outside the range at -1.12‰. Copper isotope values measured from the total digestion show no significant difference between samples from background and those overlying mineralisation (Table 5-4).

Sample	Location	Total digest		Partial leach		
		Cu (ppm)	δ^{65}Cu (‰)	Cu (ppm)	% Cu extracted	δ^{65}Cu (‰)
RC-15-HVC-118	Tb	1,108.40	-0.34	1.74	0.16	No result
RC-15-HVC-129	GFh	432.40	-0.49	0.45	0.10	No result
RC-15-HVC-132	GFh	532.00	-0.72	0.45	0.08	-1.12
RC-15-HVC-148	GFh	303.40	-0.49	0.44	0.15	-0.45
RC-15-HVC-149	GFh	228.10	-0.27	0.14	0.06	-0.56
RC-15-HVC-153	GL	406.20	-0.70	0.46	0.11	-0.19
RC-15-HVC-163	GL	998.00	0.05	1.31	0.13	0.28
RC-15-HVC-176	GFh	248.00	-0.33	0.45	0.18	-0.26
RC-15-HVC-177	GFh	284.30	-0.29	0.30	0.11	-0.14

Table 5-4. Analytical Cu isotope results for selected upper B horizon (<180 microns) soils at J.A. 'Total digest' refers to HCl-HNO_3-HF digest and 'partial leach' refers to a 2% HNO_3 leach. The separate digest and leach were both analysed by Q-ICP-MS. Isotope ratios with reference to NIST976. Full methodology is reported in Appendix A.

The partial leach extracted a very small portion (0.06–0.18%) of the total Cu content in all samples, compared to Highmont South where up to 7.10% (median 0.74%) of the total Cu was extracted. Isotopic results for Cu extracted by the partial leach of all samples cluster closely together within the primary range of δ^{65}Cu with the exception of sample RC-15-HVC-132 which just outside of the range with a negative value (-1.12‰) (Figure 5-34). The results do not support the hypothesis of migration of Cu ions from the buried porphyry which would be expected to be fractionated towards positive δ^{65}Cu values (Mathur and Fantle, 2015). Results support the contention that Cu in the soil samples analysed is locally derived from the till on which the soil developed.

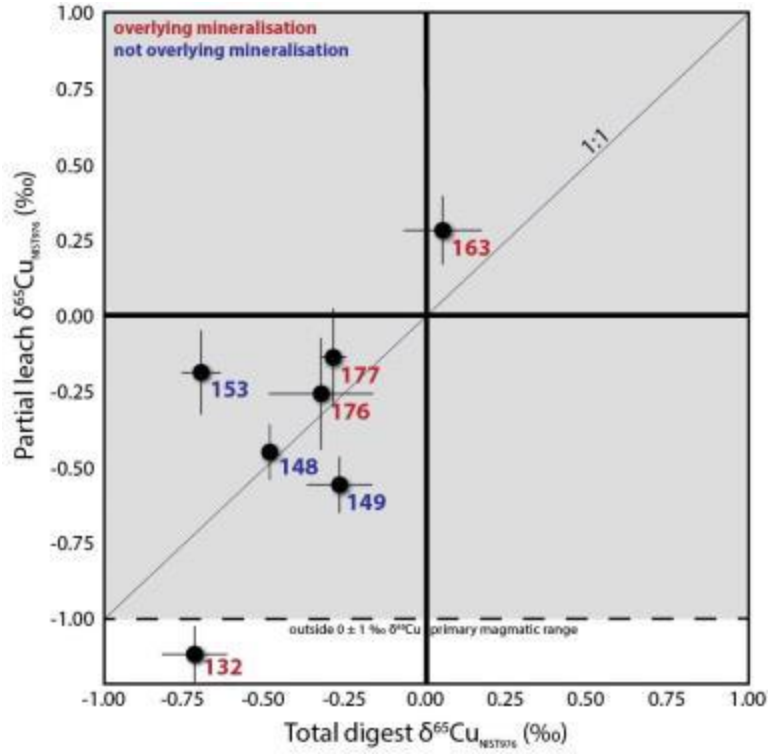

Figure 5-34. Soil (<180 microns, upper B horizon) Cu isotope results are tightly clustered within the primary magmatic range of 0 ± 1‰ (represented by the grey plot area). Error bars represent 2σ. Red sample numbers refer to samples overlying mineralisation and blue sample numbers refer to those not overlying mineralisation.

5.11 Biogeochemistry results

Analytical results are reported in Appendix C and QA/QC practises and results in Appendix B. Selected elements were compared to indicated values of 'P6' spruce needle IRM provided by Colin Dunn to assess precision. Mean percentage difference for field duplicate results was used to assess natural variability. Data quality is summarized in Table 5-5, below.

All values below 10x detection limit:	As, Au, Bi, La, Ti, Al, W, Sc, Tl, Se, Cs, Ge, Pd, Pt
Median of values below 10x detection limit:	Ni, Fe, Cd, B, Na, S, Hf, Zr, Ce, Re, Li
Median of values above 10x detection limit:	**Ag, Co, Sr, Sb, Ba, Hg, Rb, Sn, Y**
All values above 10x detection limit:	**Mo, Cu, Pb, Zn, Mn, Ca, P, Cr, Mg, K**

Table 5-5. Data quality for elements analysed from lodgepole pine needles (aqua regia digest, ICP-MS). Values within ten times detection limit are to be interpreted with caution and considered as more "qualitative" data due to lower precision.

The circumferences of lodgepole pine trees sampled range from 24 to 35 centimetres (median: 28 centimetres). There are no discernable relations between tree circumference and the chemistry of the needles sampled.

There exists a strong positive trend between Cu and Fe results from the pine needle analysis (Figure 5-35). Copper and Fe are both essential micronutrients to all plants and form components of enzymes involved in processes such as photosynthesis, respiration, oxidative stress protection, and multiple metabolic pathways (Waters and Armbrust, 2013).

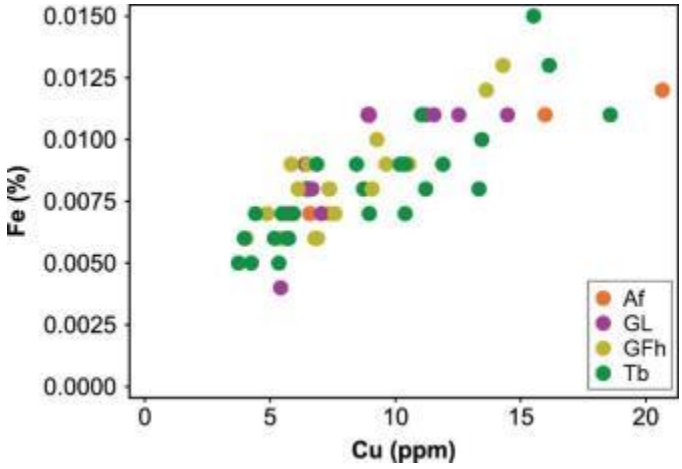

Figure 5-35. Copper and Fe reported from aqua regia ICP-MS of lodgepole pine needle samples at J.A. have a strong positive trend. These two elements are essential micronutrients for virtually all living organisms (Waters and Armbrust, 2013).

There is no indication of anomalous geochemical responses in the needles of lodgepole pine trees related to deeply buried bedrock mineralisation at J.A. Copper and Ag concentrations in the lodgepole pine needles sampled are highest in the trees sampled in the south of the field area, away from J.A. mineralisation (Figure 5-37).

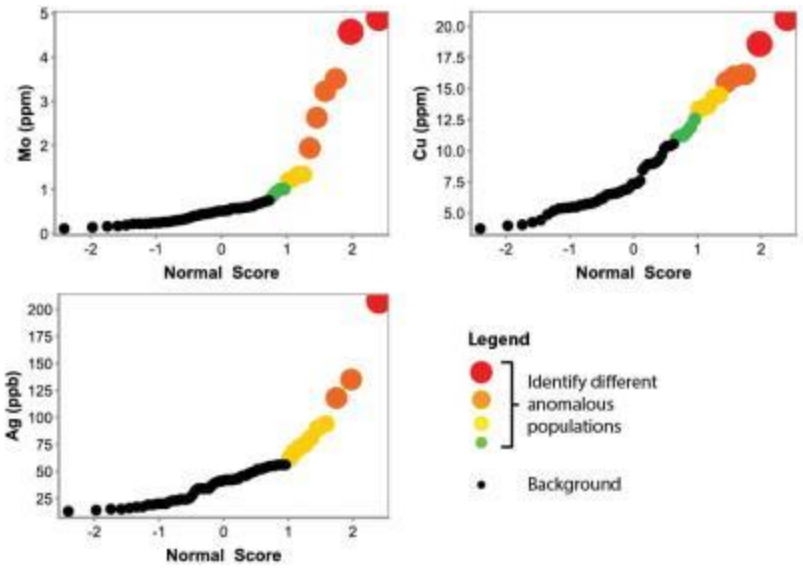

Figure 5-36. Probability plots showing distribution of element results in lodgepole pine needles (aqua regia, ICP-MS) sampled from J.A. Anomalous population intervals were selected based on visual estimation of population breaks on these plots. Population intervals are determined separately for each individual plot and symbols of the same size and colour are not related between plots for different elements.

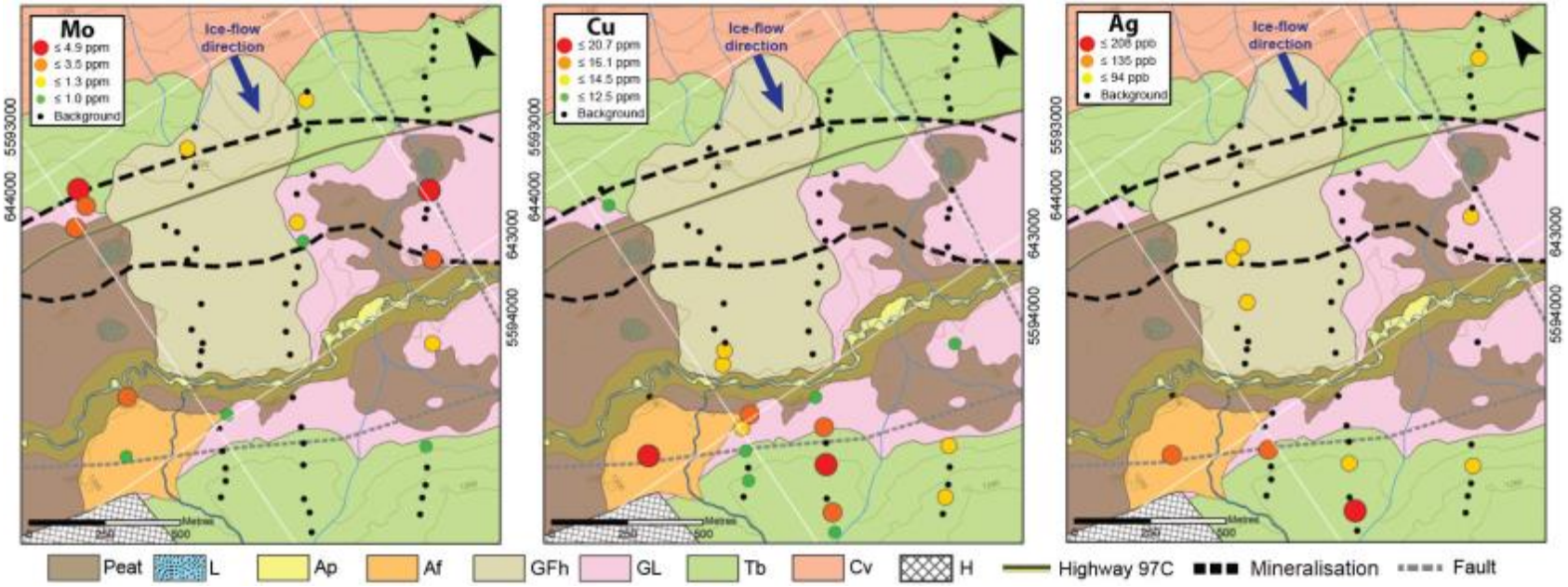

Figure 5-37. J.A. lodgepole pine needle element concentrations (aqua regia, ICP-MS) for elements of interest Mo, Cu, and Ag. Anomalous populations determined by visual estimation of population breaks from probability plots and histograms. Contours plotted at 20 metre interval spacing. Surficial geology is modified from Plouffe and Ferbey (2015b), using the GSC data model for surficial geology, version 1.2 (Deblonde et al., 2012); ice-flow direction from Plouffe and Ferbey (2015b); mineralisation outline from McMillan (1985); faults modified from McMillan et al. (2009).

Needles sampled from lodgepole pine trees growing within the Af surficial unit are elevated in a number of porphyry indicator elements including Cu, Mo, Ag, Sb, Hg, and Re (Figure 5-38). These elements are likely sourced from fragments of porphyry material or groundwater from other mineralised centres upstream at HVC that were eroded, transported and deposited as part of the alluvial fan sediments.

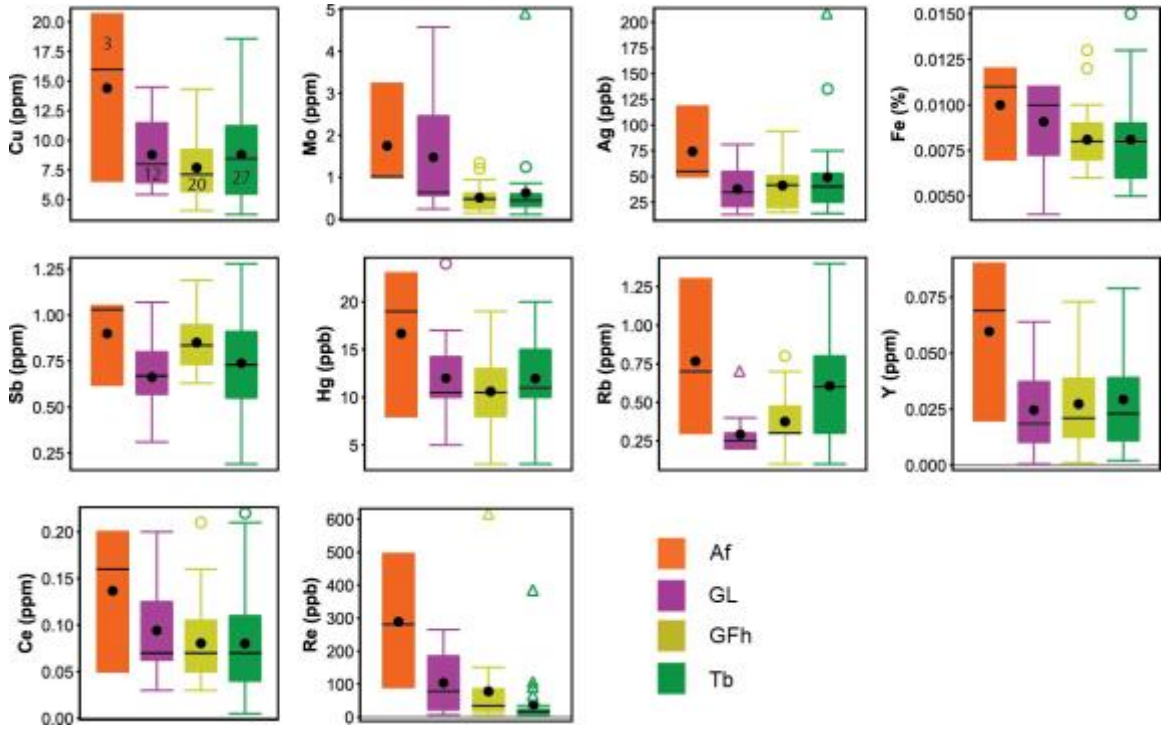

Figure 5-38. Needles sampled from lodgepole pine trees growing within the alluvial fan surficial unit are elevated in a number or porphyry-related elements (aqua regia, ICP-MS). This supports the interpretation that the alluvial fan contains weathered porphyry material transported from other centres of the deposit upstream.

5.12 Dendrochemistry

5.12.1 Sample selection

Similar to Highmont South, the availability of trees to collect core samples from on J.A. was severely limited by silvicultural practices. In order to maximise the age of lodgepole pine tree sampled from, core samples were collected from trees killed by the mountain pine beetle (MPB) outbreak. The circumferences of trees sampled range from 68 to 141 centimetres (median: 84 centimetres). Six of the total 31 tree core samples collected from deceased lodgepole pine trees in the J.A. field area were selected for analysis based primarily on core quality and age of the tree. A tree core was not selected for analysis if it did not have enough tree rings (i.e. not old enough) to obtain the 1935–1945 sample interval or which had blue stain fungus staining the 1965–1975 sample interval.

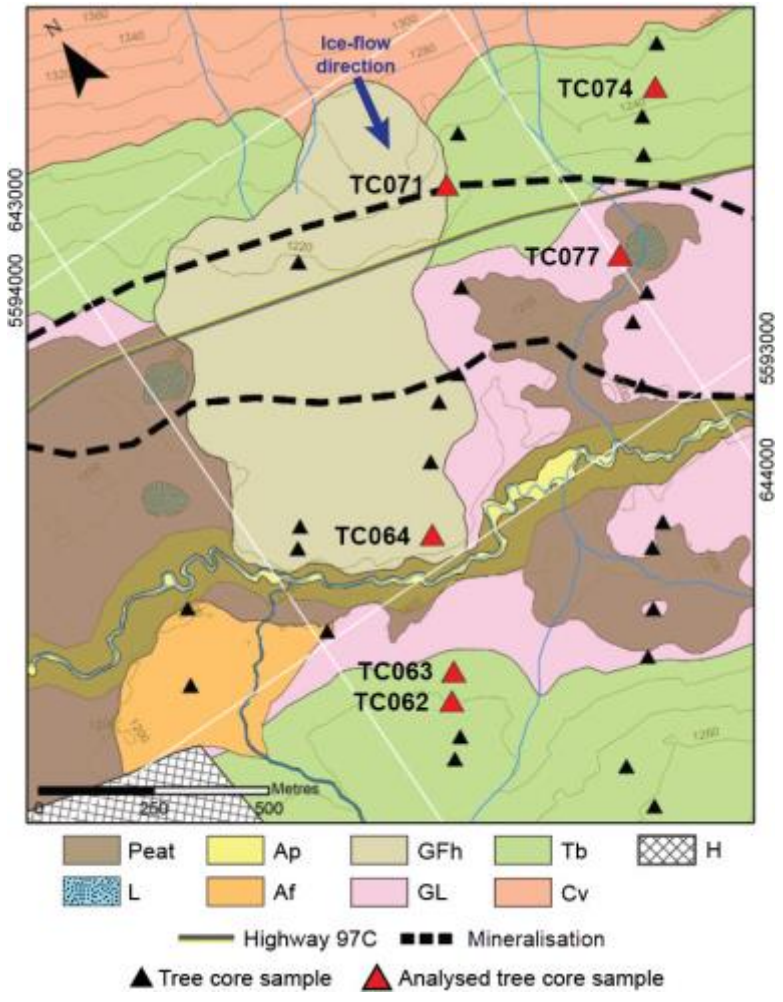

Figure 5-39. A location map of lodgepole pine tree core samples indicating the 6 samples selected for analysis. Contours plotted at 20 metre interval spacing. Surficial geology is modified from Plouffe and Ferbey (2015b), using the GSC data model for surficial geology, version 1.2 (Deblonde et al., 2012); ice-flow direction from Plouffe and Ferbey (2015b); mineralisation outline from McMillan (1985).

5.12.2 Results

Metadata

Plots of ring width over time show each sampled tree's growth curve and, where any irregularities in the curve appear, the presence of stress to the tree (Figure 5-40). Tree core samples TC062 and TC071 generally follow an ideal growth curve for a healthy tree with minimal disturbances. Samples TC074 and TC077 display slightly irregular periods of growth, and those of samples TC063 and TC064 are very irregular.

Sources of stress which cause irregularity in growth profiles include outbreaks of insects or fungi, climate change, and forest fire (Watmough, 1997). In ideal tree core analyses, samples are not selected from intervals which show irregular growth due to stress because this may affect how the tree uptakes and stores trace elements (Watmough, 1999). Due to limited selection of quality tree core samples, however, not all sample intervals could avoid irregular growth periods.

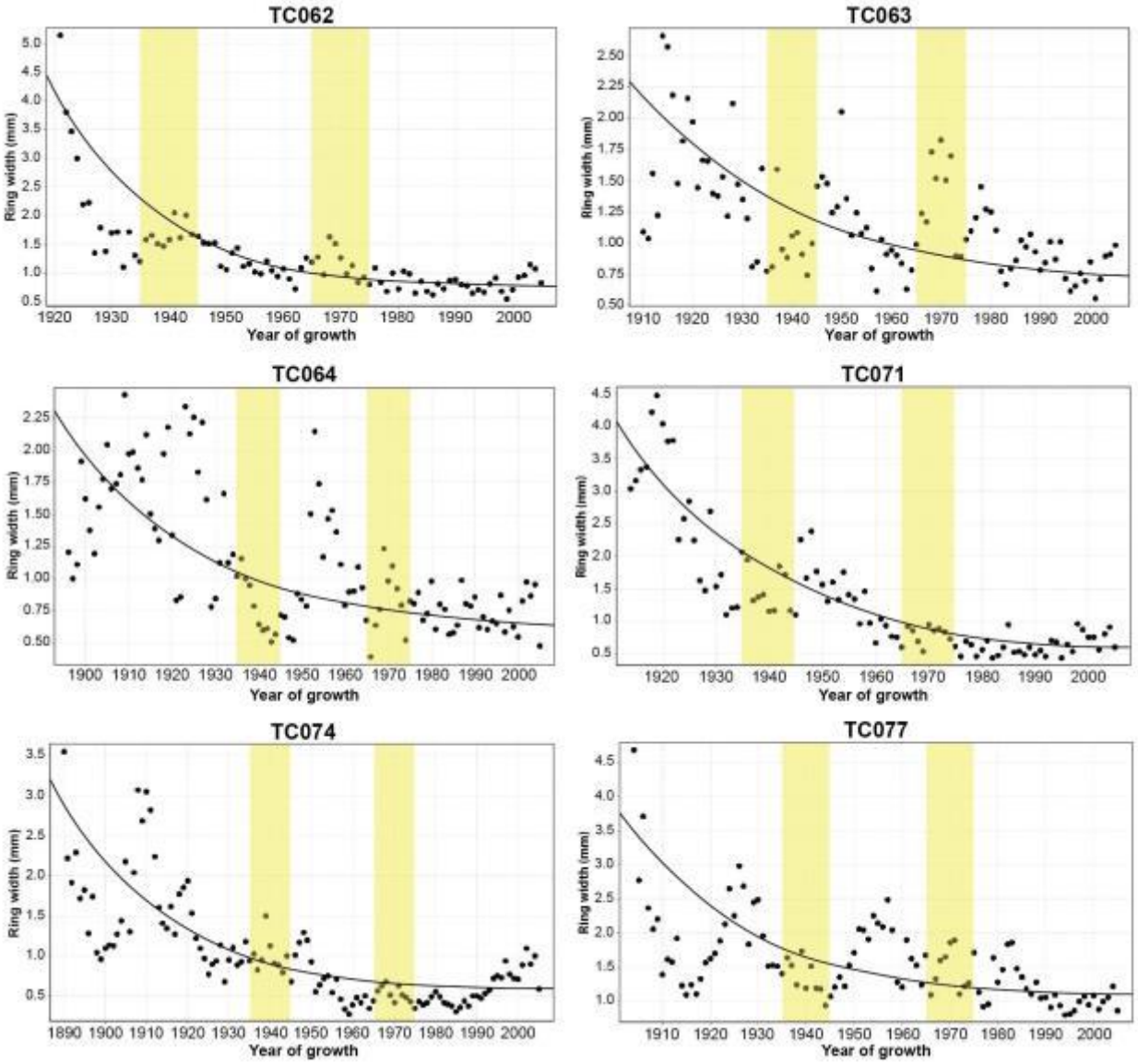

Figure 5-40. Plots of tree ring width over time for tree core samples selected for analysis from J.A. Each point represents one tree ring (i.e. one year of growth). Highlighted intervals indicate the two chosen sampling intervals from each tree core: 1935–1945 and 1965–1975. Black curves on each plot represent the ideal 'healthy' growth curve (pers. comm., Kurt Kyser, 2016).

Dendrochemistry

Analytical results are reported in Appendix C and QA/QC practises and results in Appendix B. Selected elements were compared to certified and indicated values of NIST1547 peach leaf CRM to assess precision. Elements from the analysis of tree cores collected from lodgepole pine trees at J.A which are under ten times stated analytical detection limits and are not discussed further

are: As, Au, Be, Bi, Cs, Dy, Er, Eu, Ga, Gd, Ge, Hf, Hg, Ho, La, Li, Lu, Nb, Nd, Pd, Pr, Pt, Re, Sb, Sc, Se, Sm, Sn, Tb, Te, Ti, Tm, W, Y, Yb, and Zr. The remaining data was deemed acceptable following evaluation of QC results.

There is no apparent relationship between tree diameter and chemistry of the heartwood, however there are relationships between heartwood chemistry and surficial material in which the tree grew. Cores sampled from lodgepole pine trees growing within GL surficial material contain higher concentrations of Cu (med. 0.50 ppm) and Ni (med. 0.19 ppm) (Figure 5-41). Cores sampled from lodgepole pine trees growing within GFh surficial material contain higher concentrations of Mo (med. 0.04 ppm) and Si (med. 3.10 ppm). Cores sampled from lodgepole pine trees growing within Tb surficial material contain higher concentrations of Ba (med. 4.47 ppm), Ca (med. 484.52 ppm), and Mn (med. 59.50 ppm).

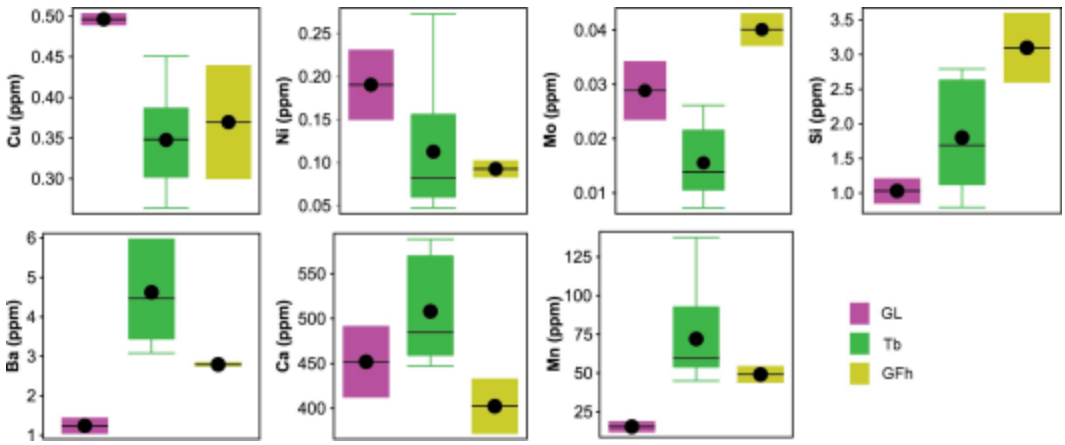

Figure 5-41. Element concentrations (HNO_3 digest, HR-ICP-MS) in lodgepole pine tree core samples from J.A. Sampled trees growing within GL surficial units have higher Cu concentrations, and lower Si, Ba, and Mn concentrations. Sampled trees growing within Tb surficial units have lower higher Ba, Ca, and Mn concentrations, and lower Mo concentrations. Sampled trees growing within GFh surficial units have higher Mo and Si concentrations, and lower Ca concentrations. Sample counts: GL = 2, Tb = 8, GFh = 2.

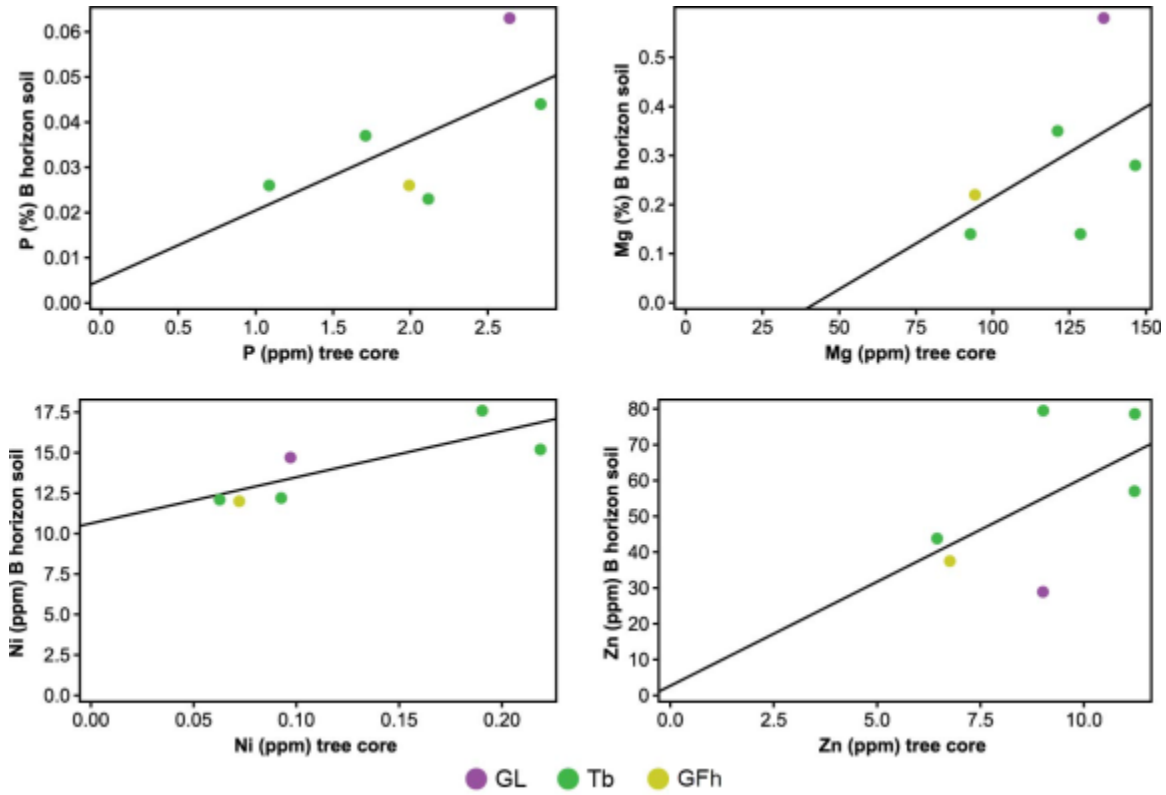

Figure 5-42. P, Mg, Ni and Zn concentrations (HNO_3 digest, HR-ICP-MS) increase in lodgepole pine tree cores as they increase in upper B horizon soils (<180 microns, aqua regia, ICP-MS). Tree core data is represented by the averaging results from the two different tree ring intervals sampled per core. Black lines represent lines of best fit.

Median Cu concentrations slightly increase from the 1935–1945 sample interval to the 1965–1975 sample interval, from 0.317 ppm to 0.380 ppm (Figure 5-43). Median relative standard deviation (RSD) reported on Cu values is 1.5%, which deems the 19.9% increase significant. Median Mo concentrations stay relatively the same from the 1935–1945 sample interval to the 1965–1975 sample interval, only increasing from 0.019 ppm to 0.021 ppm. Median RSD reported on Mo values is 6.4% which deems the 10.5% increase insignificant.

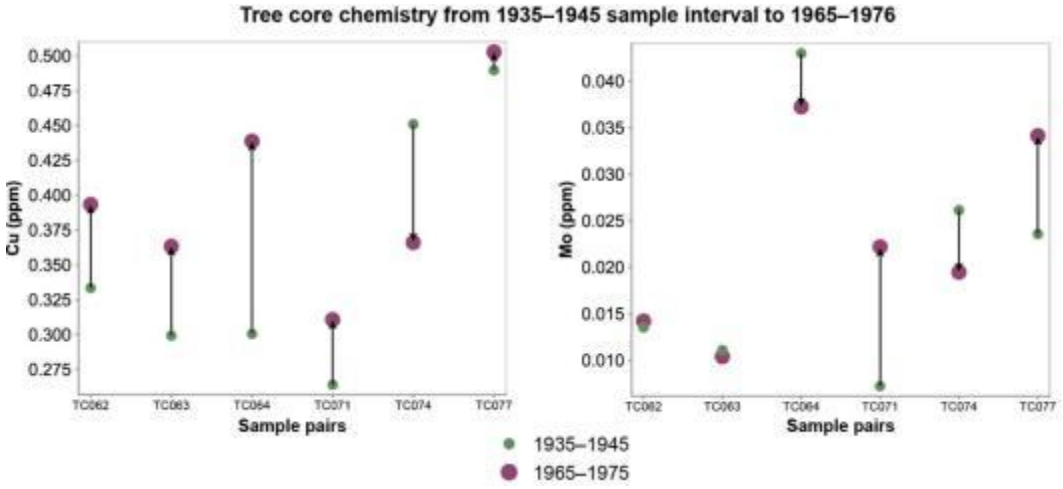

Figure 5-43. Copper and Mo concentrations (HNO_3 digest, HR-ICP-MS) for analysed lodgepole pine tree core sample intervals from 1935–1945 and 1965–1975. Median Cu slightly increases from 0.317 in the 1935–1945 interval to 0.633 ppm in the 1965–1975 interval. Median Mo slightly increases from 0.019 ppm to 0.021 ppm.

Lodgepole pine tree core samples from J.A. show a similar Na:B trend to those from Highmont South, which closely matches the Na:B trend for the industrial pesticide sodium borate (i.e. borax, $Na_2B_4O_7{\bullet}H_2O$) (Figure 5-44).

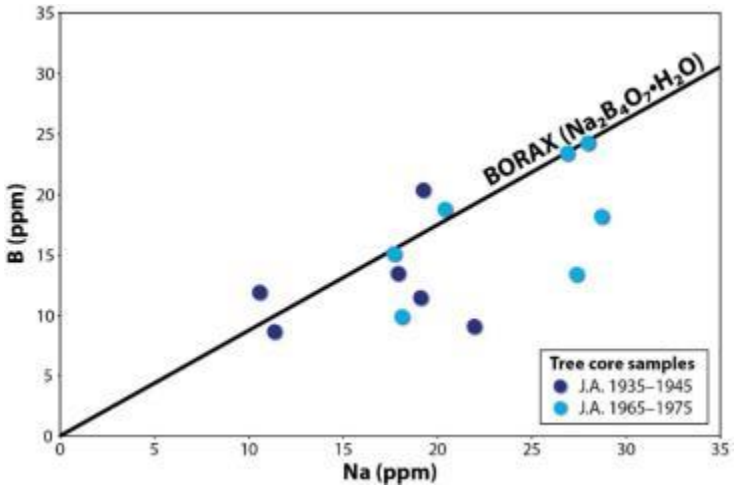

Figure 5-44. Sodium and boron concentrations in tree core sample from J.A. plot along the trend line for Na:B in borax insecticide ($Na_2B_4O_7{\bullet}H_2O$). There is an overall shift along the trend line towards higher attenuated concentrations of borax over time when comparing the two sampled time intervals.

Phosphorous, commonly used in silvicultural herbicide (e.g. glyphosate, $C_3H_8NO_5P$) (pers. comm., Tracy Coombes, 2017), increased in concentration from the 1935–1945 sample interval to the 1965–1975 sample interval. The median increase over time was 283%, while the highest increase was from tree core TC063 (643203 m E, 5592795 m N) by 573% (median RSD on P values is 4.9%).

5.13 Summary

Surficial materials at J.A. are much more variable than at Highmont South, with both glacial and post-glacial sediments. Glacial sediments consist of till blanket along the valley walls, and glaciolacustrine sediments covering the valley floor with occasional hummocky glaciofluvial sediment mounds. Postglacial streams deposited alluvial floodplain sediments along the valley centre and an alluvial fan located at the base of the south valley wall in the southwest portion of the field area. A recent wetland environment resulted in scattered areas of lacustrine sediments as well as widespread peat cover throughout the valley centre. Both natural and mine waste rock colluvium forms a veneer on the upper portion of the north valley wall. Soil development over surficial materials is poor and commonly disturbed by anthropogenic activities.

No evidence is present for a surficial geochemical anomaly from vertical ion migration from deeply buried bedrock mineralisation to the surficial environment. The following methods were unsuccessful at identifying a clear surficial footprint:

- physicochemical soil measurements (pH, acidified pH, EC, Eh)
- upper B horizon soil sampling
    - <180 microns, aqua regia, ICP-MS;
    - <180 microns, deionised water leach, ICP-MS;

- soil hydrocarbons (AGI Samplers); and
- lodgepole pine needle sampling (aqua regia, ICP-MS).

Results from these methods reflect differences among the various surficial materials and, potentially, from anthropogenic activities. Dendrochemical sampling was undertaken in order to characterise potential anthropogenic inputs over time. Increases in heartwood concentrations of Cu and P for beetle-killed lodgepole pine trees indicate potential inputs.

The alluvial fan surficial unit, deposited by a stream which can be traced back to the main Highmont deposits, is interpreted to contain weathered, transported porphyry material. Upper B horizon soil samples from soils developed above these sediments are elevated in Cu and Ag. The majority of the total Cu and Bi in the sequential extraction of a sample from this unit is reported from the hot hydroxylamine hydrochloride extraction which indicates the labile portions of these two elements are scavenged by amorphous Fe-oxides in the soil. Pine needle samples from lodgepole pine trees growing within this surficial unit are elevated in Cu, Mo, Ag, Fe, Sb, Hg, Rb, Y, Ce, and Re compared to those from other surficial units.

Ratios of Cu:S for aqua regia digest ICP-MS of all upper B horizon samples from the alluvial fan unit and some samples from peat-covered units (alluvial floodplain, glaciolacustrine, lacustrine) indicate a clastic Cu-sulphide soil phase. The mineralised bedrock at J.A. was shielded from erosion during the last glaciation (Plouffe and Ferbey, 2015a) which means that any clastic porphyry material present in the surficial materials over J.A. is from other mineralised centres (e.g. Bethlehem, directly up-ice from J.A.). Additionally, partial extraction Cu isotope results for upper B horizon soils, which cluster closely together within the expected range for primary magmatic Cu ($\delta^{65}Cu = 0 \pm 1‰$), indicate that Cu in the soil is locally, laterally derived.

Chapter 6: Discussion and conclusions

6.1 Definition of the local geochemical background

The study sites at Highland Valley Copper sit within a large natural surficial geochemical footprint of anomalous Cu and Mo around clusters of porphyry Cu-Mo mineralisation at the centre of the Guichon Creek batholith (Figure 6-1). Regional stream sediment sample results from Teck (pers. comm., Teck, 2015) and from the Geoscience BC QUEST-South program (Geoscience BC, 2010) show a broad envelope of anomalous Cu values as defined by population trends (406–8,102 ppm) around the mineralisation at HVC (Plouffe and Ferbey, 2015), and skewed in the dominant southern direction of water flow in this portion of the Thompson River basin (Johnsen and Brennand, 2004). A small area of stream sediment samples with anomalous Cu (650–2,300 ppm) is located to the northwest in the batholith. There are historic showings in this area, summarized in Table 6-1 below.

Showing name	UTM coordinates	Reported system	Reported evidence of mineralisation
HY 61	627,994 m E 5,613,334 m N	Skarn, disseminated	Disseminated pyrrhotite and pyrite, copper staining, high Pb-Zn
K	624,316 m E 5,605,211 m N	Fault-vein	*No data*
WREN	627,608 m E 5,603,524 m N	Fault-vein	*No data*

Table 6-1. Three historic showings are located in the vicinity of a small area of anomalous Cu concentrations in stream sediment samples in the Guichon Creek batholith, northwest of the main envelope of anomalous Cu concentrations. Data is compiled by Kevin Byrne (pers. comm., Kevin Byrne, 2018).

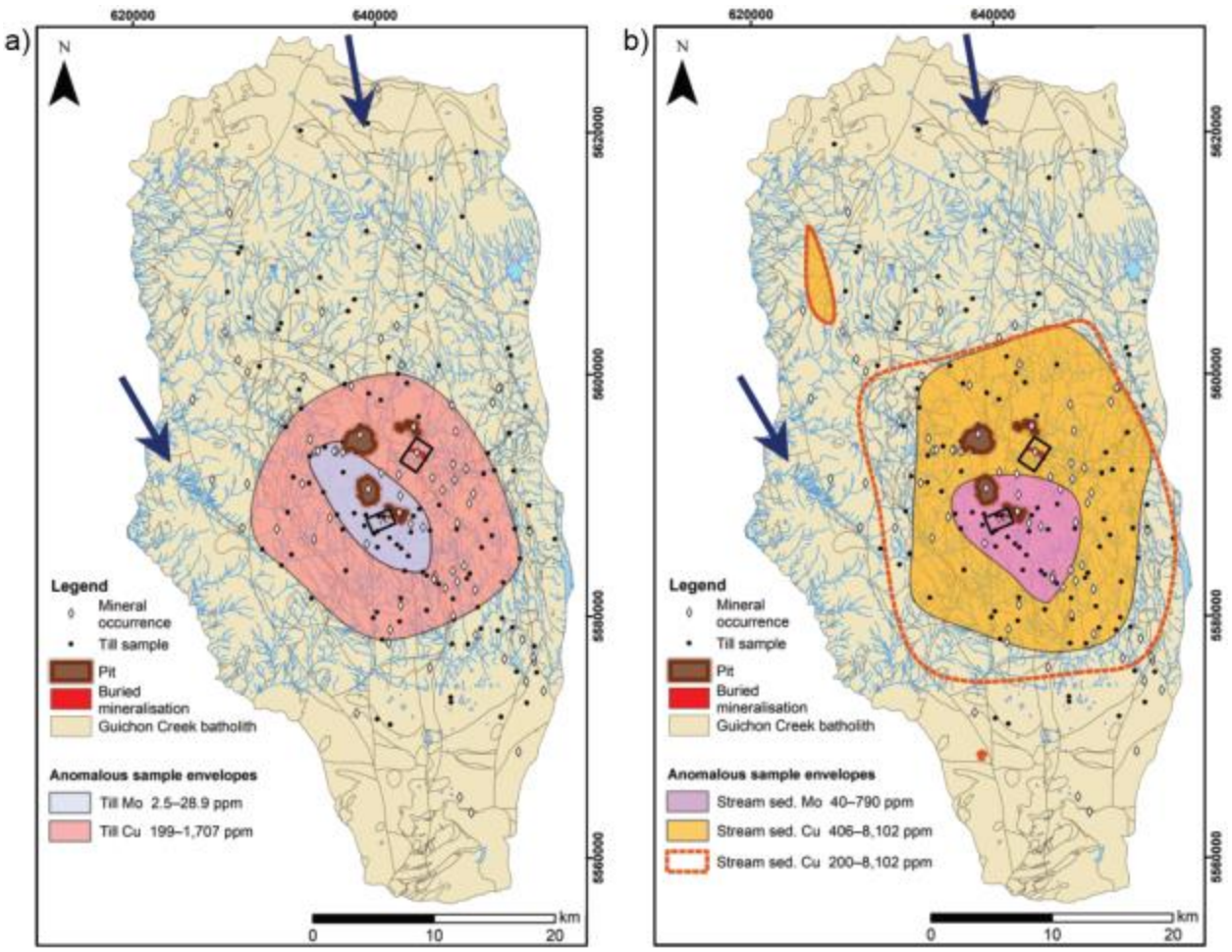

Figure 6-1. Surficial geochemical footprints within the Guichon Creek batholith for anomalous Cu and Mo concentrations in: a) till samples and b) stream sediment samples. Stream sediment samples are from a historical compilation by Teck and CMIC (pers. comm., Robert Lee, 2015) and from the QUEST-South program (Geoscience BC, 2010). Black boxes indicate this study's two field areas, Highmont South and J.A. Anomalous samples are determined by visual estimation of population breaks on probability plots. Till samples (<0.063 millimetre size fraction) are from QUEST-South and from GSC Open File 8038 (Plouffe and Ferbey, 2016). Ice-flow direction (blue arrows) from Plouffe and Ferbey (2015b). Buried mineralisation polygons and pit outlines from Teck (pers. comm., Teck, 2018). Guichon Creek batholith based on work completed in August 2016 by Teck and CMIC, and modified from McMillan et al., (2009).

The surficial geochemical footprint of anomalous Cu in till (<0.063 millimetre size fraction, i.e. clay and silt) from Geoscience BC QUEST-South and GSC sampling programs has lower anomalous values (199–1,707 ppm) compared to those of the stream sediment samples (406–8,102 ppm) which may have concentrated heavier minerals (e.g. Fe-oxides with adsorbed Cu) at the expense of fine silt/clay (Geoscience BC, 2010; Plouffe and Ferbey, 2016). The shape of the

anomalous Cu footprint in till is skewed more in the south down-ice direction than south-east (Plouffe and Ferbey, 2015), however it is also situated around the mineralised centres at HVC. The interpreted ice-flow history during the last glacial maximum is south-southeast, while later ice flow proceeding the maximum is interpreted to be southeast (Plouffe and Ferbey, 2015). The morphology of the anomalous till Cu envelope suggests it was mainly formed during the glacial maximum, with less influence afterwards when ice-flow shifted in the more southeast direction during glaciation.

The surficial footprints for anomalous Mo in both stream sediment and till samples is significantly more tightly constrained than those for Cu (Figure 6-1). Anomalous Mo concentrations in stream sediment samples (40–790 ppm) appear to originate from the Lornex and Highmont deposits area and are skewed in the south-southeast ice-flow direction. Anomalous Mo concentrations in till samples (<0.063 millimetre size fraction) appear closer to the Valley deposit at HVC and encompass the Lornex and Highmont deposits.

The GSC's Targeted Geoscience Initiative '4' (TGI-4) program reported enrichments of ore metal concentrations in till in the down-ice direction from porphyry mineralisation at Gibraltar (Cu-Mo), Mount Polley (Cu-Au), Woodjam (Cu-Au-Mo) and HVC (Cu-Mo) (Plouffe and Ferbey, 2015a) (Table 6-2). Of these four porphyry deposits, HVC has the most simple ice-flow history (Table 6-2). High counts for chalcopyrite grains (107–4,630 grains/10 kilograms compared to background counts of 1 grain/10 kilograms) in till samples collected up to 4 kilometres down-ice from the HVC deposits (Ferbey et al., 2016b) demonstrate the ability of chalcopyrite grains to be preserved following glacial transport and under post-glacial conditions (e.g. acidic pH) within the study area).

Deposit name	Porphyry type	Interpreted ice-flow vectors	Metal enrichments in down-ice till samples*	PIMs in down-ice till samples
Gibraltar	Calc-alkalic Cu-Mo	1. SE 2. SW 3. NW	• Cu over 380 ppm (3–6 km) • Mo up to 8 ppm	• Chalcopyrite • Green epidote (>10 km)
Mount Polley	Alkalic Cu-Au	1. SW 2. NW	• Cu over 380 ppm (c. 4 km) • Au up to 90 ppb (c. 8 km)	• Chalcopyrite (>6 km) • Green epidote (>3 km) • Gold (>5 km)
Woodjam	Alkalic and calc-alkalic Cu-Au-Mo	1. SW 2. NW	• Cu over 380 ppm (1–2 km) • Mo up to 8 ppm	• Chalcopyrite (<2 km) • Green epidote (<2 km)
Highland Valley Copper	Calc-alkalic Cu-Mo	1. S-SE	• Cu over 990 ppm • Mo up to 8 ppm	• Chalcopyrite • Green epidote

**aqua regia digest, ICP-MS*

Table 6-2. Glacial dispersal of mineralised material from Gibraltar, Mount Polley, Woodjam and HVC porphyries in British Columbia. Information is compiled from Plouffe and Ferbey (2015a).

The Galaxy alkalic Cu-Au porphyry deposit in the Iron Mask batholith southwest of Kamloops is a good example of a deposit in an area with a simple ice-flow history similar to HVC (Plouffe and Ferbey, 2015a; Lett, 2011). The Galaxy deposit has a simple ribbon-shaped surficial Cu dispersal train up to 1 kilometre in the down-ice direction from mineralisation which appears to be partly controlled by topography (Figure 6-2) (Kerr et al., 1993; Lett, 2011; Blaine and Hart, 2011). Copper concentrations in this dispersal train are greater than 200 ppm in till samples (-80 mesh, aqua regia, ICP-ES) and up to 599 ppm in B horizon soil samples (-80 mesh, aqua regia, ICP-ES) (Kerr et al., 1993; Blaine and Hart, 2011). There are also elevated Cu concentrations observed in stem, leaf and flower samples of rabbitbush (*Ericameria nauseosa*) (Kerr et al., 1993).

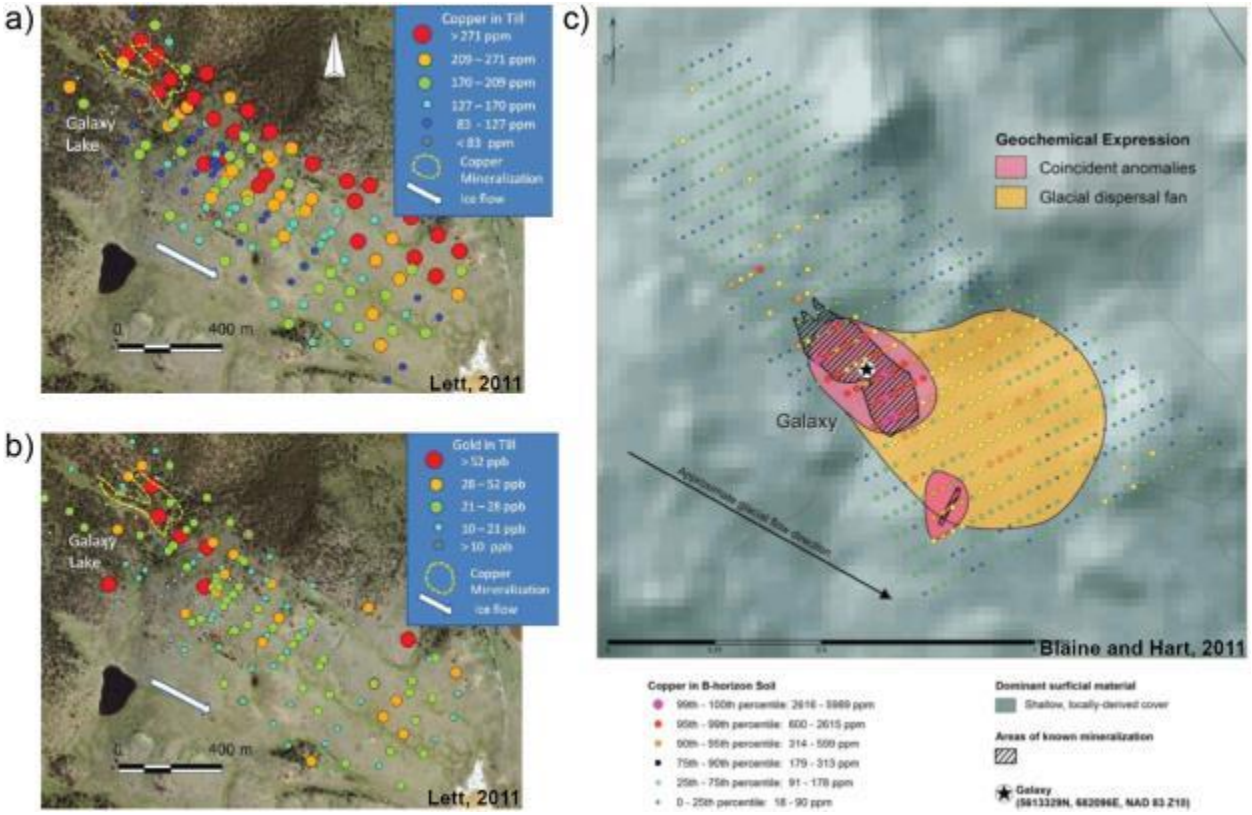

Figure 6-2. The Galaxy Cu-Au porphyry deposit has a simple ribbon-shaped Cu dispersal train in an area with a single vector for ice-flow history. a) Copper concentrations in till samples exceed 271 ppm up to 1 kilometre away from bedrock mineralisation (data from Kerr et al., 1993, figure from Lett, 2011); b) Gold concentrations in till samples exceed 52 ppb in till samples down-ice from mineralisation however the dispersal train is less defined than that of Cu (data from Kerr et al., 1993; figure from Lett, 2011); c) Copper concentrations in B horizon soil samples reach up to 599 ppm approximately 500 metres from mineralisation (data from Caron, 2007; figure from Blaine and Hart, 2011).

The J.A. field area sits within the broad anomalous surficial geochemical halo for Cu in both till and stream sediment samples. The Highmont South area also sits within these Cu envelopes, as well as the smaller surficial geochemical halos for Mo in both till and stream sediment samples. Surficial geochemical samples collected to represent 'background' conditions from within the field areas are termed 'local background' because these values would be considered anomalous when compared to more regional background values from outside of the broad anomalous envelopes in Figure 6-1.

Table 6-3 summarises the local background and anomalous value ranges of Cu and Mo for local upper B horizon soil (<180 microns, aqua regia, ICP-MS) at the two field study areas, and the regional background and anomalous value ranges for Cu and Mo for till (<0.063 millimetres, aqua regia, ICP-MS) and stream sediment (aqua regia, ICP-MS) samples from throughout the Guichon Creek batholith. Anomalous and background value ranges are determined by visual estimation of population breaks on probability plots and histograms.

	Local background value range		Local anomalous value range		Guichon Creek batholith background value range		Guichon Creek batholith anomalous value range	
Element	Highmont South soil	J.A. soil	Highmont South soil	J.A. soil	Till	Stream sed.	Till	Stream sed.
Cu (ppm)	12.7–275.8	14.5–129.7	275.8–1928.5	129.7–2050.0	17.4–188.3	0.5–400.0	188.3–1,707.0	400.0–8,102.0
Mo (ppm)	0.29–12.28	0.36–7.80	12.28–51.34	7.80–149.27	0.34–2.26	0.21–37.00	2.26–28.87	37.00–790.00

Table 6-3. Local background and anomalous value ranges for Cu and Mo from upper B horizon soil sampling (<180 microns, aqua regia, ICP-MS) at Highmont South and J.A. and regional background and anomalous value ranges for Cu and Mo from till (<0.063 millimetres, aqua regia, ICP-MS) and stream sediment (aqua regia, ICP-MS) sampling throughout the Guichon Creek batholith. Anomalous and background value ranges are determined by visual estimation of population breaks on probability plots and histograms.

Comparison of surficial geochemical values ranges for Cu and Mo to cut-off values of 0.1% Cu and 0.008% Mo (Teck, 2018) shows that surficial materials can become significantly enriched in elements related to mineralisation (Figure 6-3).

Figure 6-3. Compilation of background and anomalous values for Cu and Mo in bedrock at surficial materials of the Guichon Creek batholith, and comparison to Clarke values. Data sources: [1]Pohl (2011); [2]Teck (2018); [3]D'Angelo et al. (2017); [4]Ferbey et al. (2016); [5]this study.

6.2 Surficial geochemical anomalies at Highmont South

Surficial soil, vegetation, and soil hydrocarbon sample results above porphyry Cu-Mo mineralised bedrock at Highmont South beneath relatively thin (2–10 metres) till cover identify geochemical anomalies overlying mineralisation. Soil and soil hydrocarbon results also identify an additional anomalous geochemical signature over the West Highmont fault which crosscuts mineralisation. Anomalies within waterlogged depositional clay material units are considered false positives.

6.2.1 Anomaly above mineralisation

The surficial geochemical anomaly above mineralisation at Highmont South consists of:

- elevated concentrations of Cu, Mo, Ag, Bi and, to a lesser extent, Sb, As and W in soil (upper B horizon, <180 microns, aqua regia, ICP-MS);
- elevated Mo concentrations in lodgepole pine needles (aqua regia, ICP-MS); and
- elevated concentrations of dodecane ($C_{12}H_{26}$), tridecane ($C_{13}H_{28}$), and pentadecane ($C_{15}H_{32}$) in AGI hydrocarbon samplers.

6.2.1.1 Clastic transport of mineralised material

Anomalous Cu, Mo, Ag, Bi, Sb, As, and W in upper B horizon soils overlying mineralisation is attributed to glacial transport of weathered porphyry material. Copper and chalcophile elements Ag, Bi, Sb, and As in soil overlying mineralisation are likely from glacially transported fragments of mineralised rock containing sulphide ore minerals chalcopyrite and/or bornite (Figure 6-4). Glacially transported fragments of mineralised rock containing the ore mineral molybdenite likely contribute to the Mo anomaly in soil overlying mineralisation (Figure 6-4).

Tungsten and Mo have almost identical ionic radii and therefore very similar chemical behaviour (Bowen, 1982). Tungsten is sometimes used as a pathfinder element for porphyry Cu-Mo deposits (e.g. Heberlein and Samson, 2010; Lett et al., 2000). Silver enrichment associated with Cu mineralisation and W enrichment associated with Mo mineralisation is observed in the bedrock mineralisation at HVC (pers. comm., Teck, 2017).

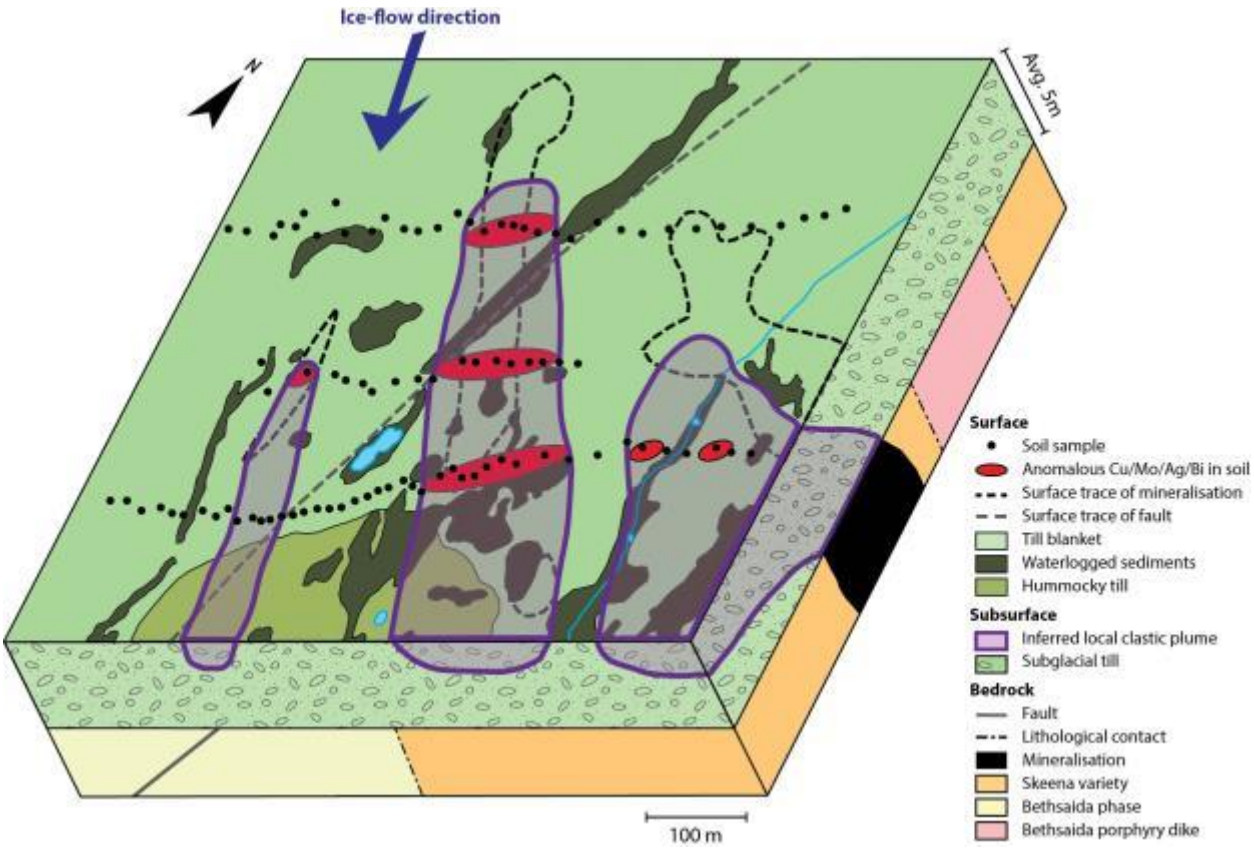

Figure 6-4. Schematic model of local clastic transport for fragments of bedrock mineralisation at Highmont South. Main anomalous elements in upper B horizon soil (<180 microns, aqua regia, ICP-MS) are Cu, Mo, Ag, and Bi, with lesser Sb, As, and W. Till blanket is thin at Highmont South (2–10 metres) and dispersal plumes are inferred to be close to their bedrock source. Features such as faults, lithological contacts, and morphology of mineralisation are purely diagrammatical. Bedrock and surface topography not shown. Surficial geology is modified from Plouffe and Ferbey (2015b), using the GSC's data model for surficial geology, version 1.2 (Deblonde et al., 2012); ice-flow direction from Plouffe and Ferbey (2015b); buried mineralisation outlines from Teck (pers. comm., Teck, 2017); bedrock geology and structure based on work completed in August 2016 by Teck and CMIC, modified from McMillan et al. (2009).

Evidence in support of a clastic model includes:

- The thin cover at Highmont South and the simple south-southeast ice-flow history (Plouffe and Ferbey, 2015) permits the formation of very simple, close-to-source dispersal plumes of locally eroded bedrock mineralisation (Hooke et al., 2013);
- Two subglacial till samples collected by the GSC/BCGS (Ferbey et al., 2016) within the Highmont South surficial mapping area (Figure 6-5) contain high chalcopyrite grain counts as well as high Cu and Mo concentrations by aqua regia ICP-MS (Table 6-4). Six other till samples collected just outside of the Highmont South mapping area contain 0–17 grains of chalcopyrite (Figure 6-5).

				<0.063 millimetre till	
Till sample	UTM coordinates	Till facies	Cpy grain counts	Cu (ppm)	Mo (ppm)
15PMA006A01	640,341 m E 5,588,246 m N	Subglacial	1,000	1,707.0	28.9
15PMA005A01	640,754 m E 5,588,253 m N	Subglacial	500	639.4	17.8
15PMA010A01	639,270 m E 5,588,375 m N	Subglacial	1	315.4	2.7
15PMA009A01	638,318 m E 5,588,505 m N	Subglacial	0	272.9	1.8
15PMA008A02	639,943 m E 5,586,514 m N	Subglacial	17	340.4	4.7
15PMA011A01	639,156 m E 5,587,485 m N	Ablation	0	75.2	0.7
15PMA008B01	639,943 m E 5,586,514 m N	Ablation	0	133.3	1.1
159MA112A01	641,226 m E 5,586,481 m N	Ablation	11	252.7	2.2

Table 6-4. Summary of chalcopyrite grain counts and geochemical results of subglacial till samples from the Highmont South field area collected by the GSC/BCGS (Ferbey et al., 2016). Element concentrations from <0.063 millimetres, aqua regia, ICP-MS. Abbreviation: cpy = chalcopyrite.

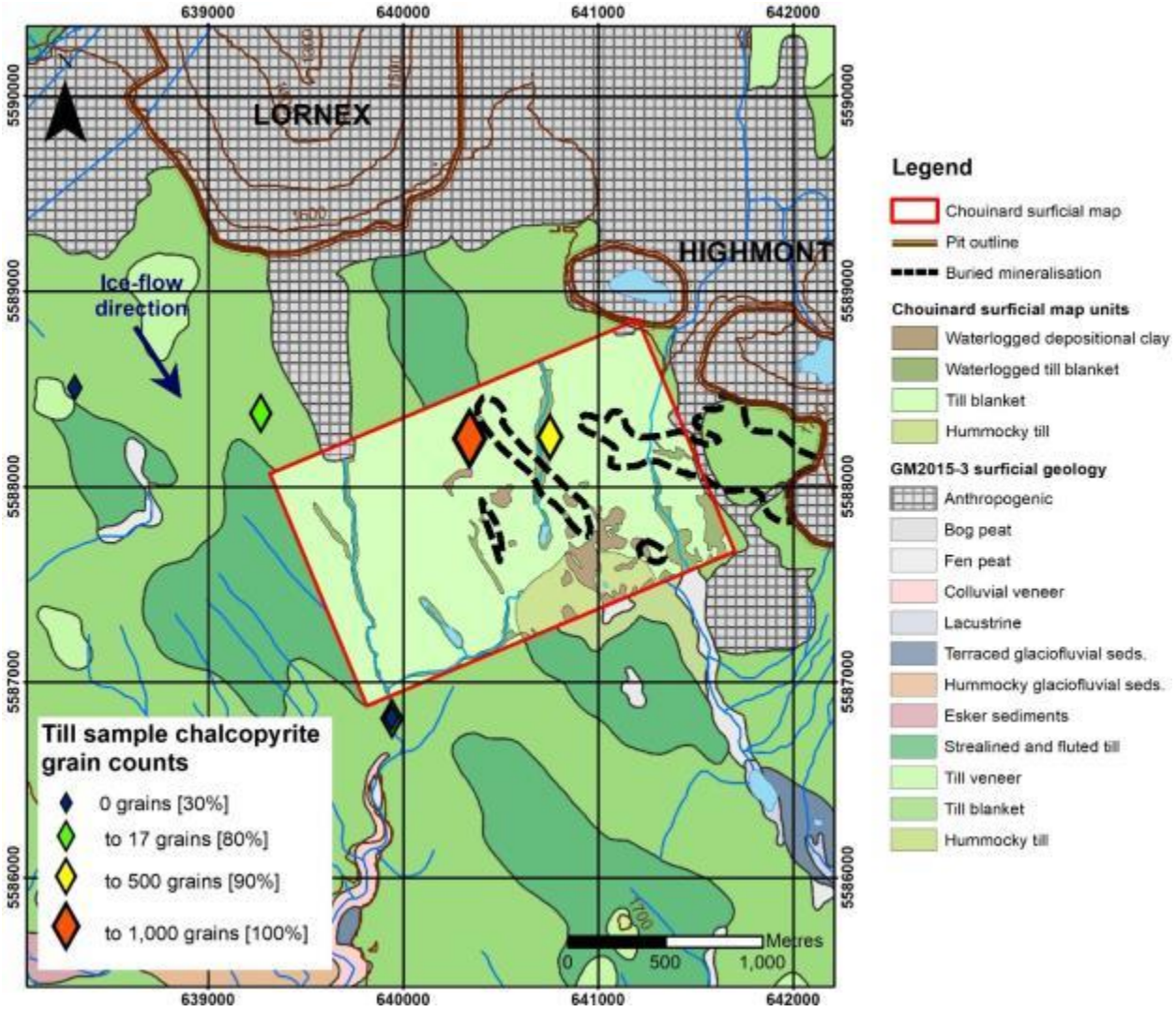

Figure 6-5. Till samples collected by the GSC/BCGS (Ferbey et al., 2016) near the Highmont South study area. Grain counts plotted by percentile intervals. Ice-flow direction and regional surficial geology from Plouffe and Ferbey (2015b). Pit and buried mineralisation outlines from Teck (pers. comm., Teck, 2018). Red box shows Highmont South field mapping area for this study; local surficial geology is modified from Plouffe and Ferbey (2015b), using the GSC data model for surficial geology, version 1.2 (Deblonde et al., 2012).

- Results from partial extraction Cu isotope analysis of select upper B horizon soil samples from Highmont South cluster tightly within the expected range for primary magmatic Cu ($\delta^{65}Cu = 0 \pm 1‰$), identical to results from total extraction. This lack of fractionation supports the contention that the Cu in the soil matrix is locally derived, likely from weathering of included fragments rather than transfer of ions from depth;

- Results from sequential extraction of select upper B horizon soil samples from Highmont South indicate that the major soil phases with which Cu, Mo, Ag, and Bi are associated in anomalous samples are the more physically robust mineral phases such as crystalline Fe-oxides and residual sulphides. These phases are indicative of glacially transported clastic porphyry material in the soil.

6.2.1.2 Vegetation uptake and cycling

Vegetation uptake and cycling contributes to the Mo anomaly in soil overlying and proximal to mineralisation at Highmont South (Figure 6-6). Molybdenum is readily available to vegetation in the form of the molybdate oxyanion (MoO_4^{2-}) (Kabata-Pendias, 2010) which is the proposed dominant speciation in Highmont South soils based on Eh and pH conditions following the release of Mo ions from oxidation of ore mineral molybdenite. Due to its bioavailability to plants in this form, Mo can become substantially enriched in plant tissues (Dunn, 2007). The cycling of Mo through vegetation and back into soil as decomposed organic matter has been occurring throughout the Holocene, allowing a 9000 year window for vegetation cycling to contribute Mo to the surficial environment.

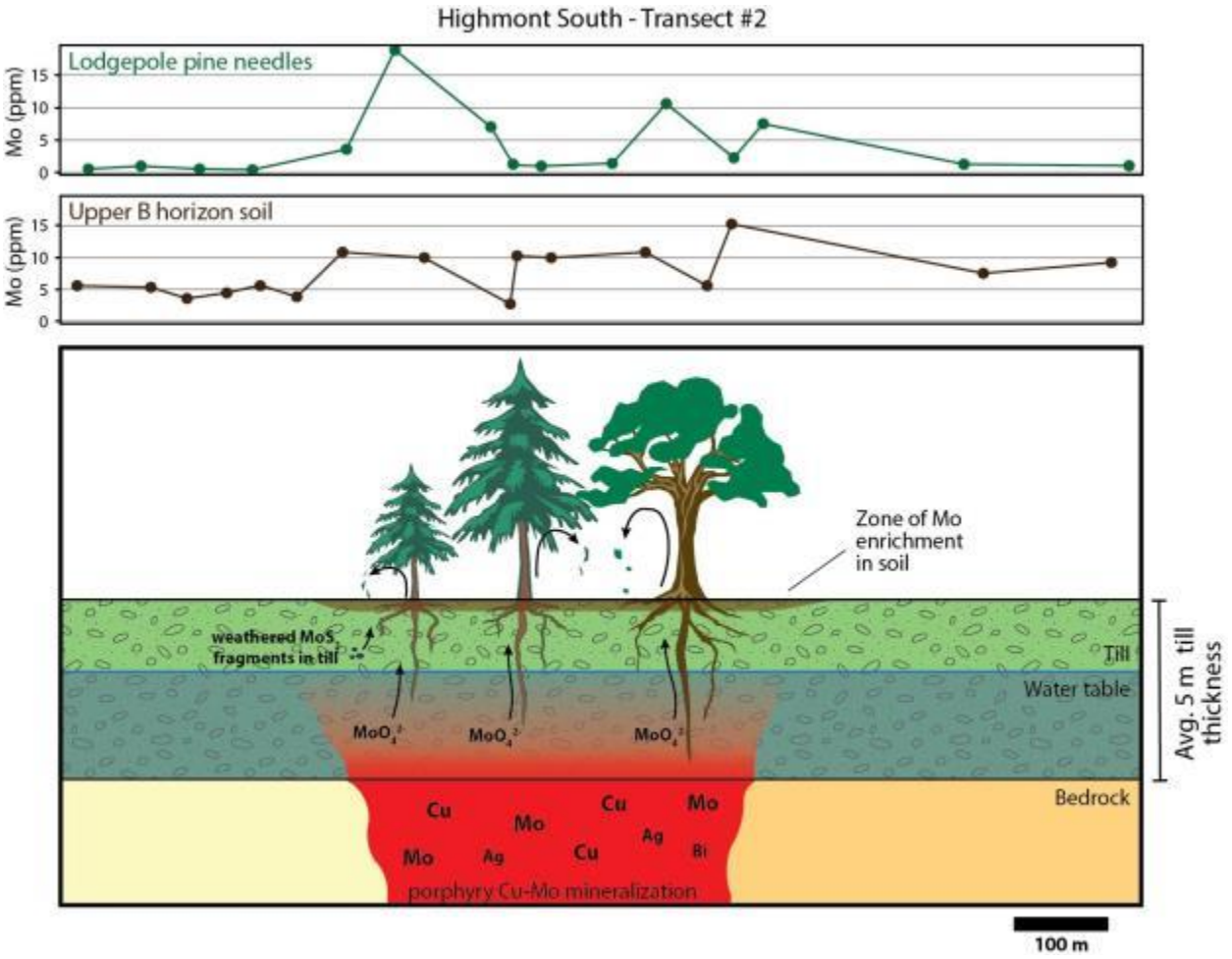

Figure 6-6. Model for vegetation uptake and recycling of Mo to the surficial environment at Highmont South. Measured soil Eh and pH conditions indicate that Mo is present in soil as the molybdate oxyanion (MoO_4^{2-}) which is highly soluble and readily bioavailable (Kabata-Pendias, 2010). Bedrock and surface topography not shown. Soil Mo by aqua regia ICP-MS; pine needle Mo by aqua regia ICP-MS. Morphology of mineralisation is purely diagrammatical.

Rooting depth of all trees depends on soil texture, however the average root depth reported for lodgepole pine trees is approximately 3.3 metres (Canadell et al., 1996). Till at Highmont South is relatively thin (2–10 metres) and the water table is observed to be close to surface in wet seasons. These conditions make it possible for the lodgepole pine trees to access groundwater which likely interacts with mineralised bedrock at Highmont South. Additionally the trees can take up Mo from mechanically transported material in the till on oxidation and release of the metal in a bioavailable form.

6.2.2 Anomaly above West Highmont fault

Anomalous Cu, Ag, Sb, W, Cd, Pb, Zn, and Mn is present in upper B horizon soil overlying the trace of the West Highmont fault, which crosscuts mineralisation (Figure 6-7). The Lornex fault zone to the west is characterised by its lithogeochemical enrichment in Zn, Mn, Pb, Cd, and Hg, elements that are not anomalous or abundant in the mineralised or altered zones at HVC (and Ag) (Olade and Fletcher, 1976). Zinc and Hg are particularly enriched in the north-trending structures at HVC (pers. comm., Teck, 2017). The enrichment of these elements may be the result of leaching from the alteration zones associated with mineralisation, followed by deposition along the fault zone (Olade and Fletcher, 1976). Soil sample coverage is inadequate to identify a similar element signature in the soils above the Lornex fault at Highmont South, however soils above the West Highmont fault contain elevated Zn, Mn, Ag, Pb, and Cd. The distribution of Hg in soils at Highmont South is controlled by the presence of organic matter, resulting in noisy data and inconclusive interpretations over the West Highmont fault.

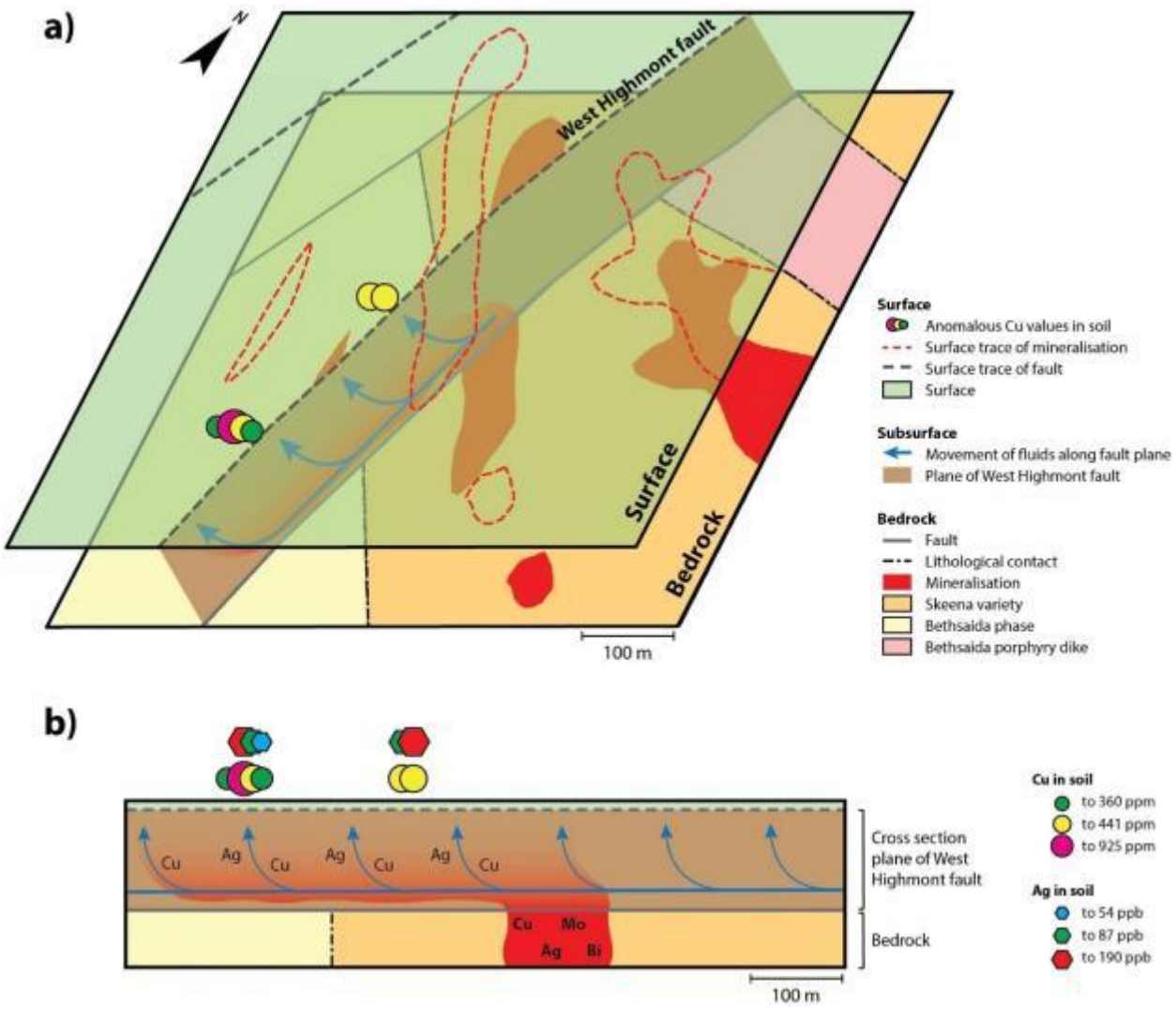

Figure 6-7. Model for hydraulic pumping of groundwater in contact with bedrock mineralisation upwards through fractures associated with West Highmont fault. The mobility of Cu and Ag in soil is highest in acidic and oxidising conditions (Kabata-Pendias, 2010), such as those along a fault pathway. Bedrock and surface topography not shown. Copper and Ag results from aqua regia digest ICP-MS of upper B horizon soil samples. Surficial geology is modified from Plouffe and Ferbey (2015b), using the GSC's data model for surficial geology, version 1.2 (Deblonde et al., 2012); ice-flow direction from Plouffe and Ferbey (2015b); buried mineralisation outlines from Teck (pers. comm., Teck, 2017); bedrock geology and structure based on work completed in August 2016 by Teck and CMIC, modified from McMillan et al. (2009).

Major faults in the Highmont South field area have surficial expressions in the form of elongated depressions in the till blanket. These small stream valleys channel the movement of surface water, with the presence of actively moving streams in wet seasons.

The soil samples in transect two in which the anomalous fault signature were identified, are located in the S-SE down-ice direction (Plouffe and Ferbey, 2015b) from the westernmost body of mineralisation. Concentrations of elements which are more mobile in acidic and oxidising conditions (e.g. Cu, Ag) are elevated in soil overlying the West Highmont fault (Figure 6-7), while other anomalous elements which are less mobile in these conditions (e.g. Mo, Bi, As) remain at local background concentrations. Molybdenum is primarily mobile as an oxyanion complex, essentially immobile in acidic environments (Kabata-Pendias, 2010). The mobility of Bi in soil is generally low and the element tends to form insoluble salts (Kabata-Pendias, 2010). Arsenic has limited mobility in soil and is most mobile in alkaline and reducing conditions (Schwedt, 2001). This supports the concept of metal-bearing fluid migration along the fault rather than a glacially transported clastic signature.

6.2.3 Anomaly in clay rich waterlogged terrain

Aqua regia ICP-MS results for (<180 microns) soils sampled from within waterlogged depositional clay units in the Highmont South area are elevated in Cu, Ag, Ni, Co, Fe, As, Sr, Ca, Cr, Mg, Ba, Al, Na, Sc, Hg, Be, Li, and REE (La, Ce, Y, U, Th) compared to those sampled overlying till blanket material. The main factors hypothesized to result in elevated metal concentrations in clay units are:

- the high CEC of clay which causes the adsorption of cations to negatively charged clay particles; and
- the increased permanent porewater in the material which prevents the drainage and hence leaching of metal-bearing waters.

The soils sampled from these clay units have high buffering capacity, with Eh and pH conditions that allow for the stability of $CaCO_{3(s)}$. The constant and elevated (more alkaline) pH of soils with high capacity to buffer acids can limit metal mobility by preventing leaching by acids (Helios-Rybicka et al., 1994; Rieuwerts et al., 1998).

Although organic matter is generally low in all surficial material at Highmont South, the CEC associated with soil organic matter is pH dependant. A soil with a pH of ~7 will have a higher organic-related CEC than a soil with a more acidic pH (e.g. pH 5), given the same organic content (Ketterings et al., 2007). Therefore the soil in the clay units, with a median pH of 6.7 and median C_{org} of 1.19%, should have a higher organic-related CEC than soil in the dry till blanket units, with a median pH of 5.7 and median C_{org} of 1.09%.

The elevated metal concentrations in the depositional clay units is considered a false positive and not part of the surficial footprint of bedrock mineralisation at Highmont South. The sampling and geochemical characterisation of this material highlights the potential of variability in surficial materials to produce false positives in a surficial survey; the importance of consistently sampling within a single surficial material unit when possible; and the importance of surficial mapping.

6.2.4 Hydrocarbon footprint in AGI Samplers

Normal alkane hydrocarbons in the C_{12}-C_{15} range were detected in soil overlying bedrock mineralisation and the trace of the West Highmont fault in the southern sampling transect (transect two). Microbial populations in the subsurface may play a part in the generation of these hydrocarbon anomalies (Luca et al., 2008). The biodiversity of microbial populations in soil is interconnected with soil physical and chemical properties such as Eh, pH, aeration, and quantity of organic matter (Delgado and Gomez, 2016). Microorganisms are known to produce a range of

different organic compounds as part of their natural life cycle (Sutherland, 2015). The types of microbially derived hydrocarbons present in soil are therefore variable depending on the soil conditions, soil chemistry, and microbial populations present (Delgado and Gomez, 2016). Physicochemical measurements (e.g. soil pH, ORP, EC) did not indicate any changes in conditions in soils overlying mineralisation. The long-chain hydrocarbon anomalies are coincident with anomalous soil Cu and Ag concentrations. More research is required to define microbial populations in soils at Highmont South and their role in the production of long-chain hydrocarbon anomalies spatially related to buried mineralisation.

The analysis of AGI Samplers installed in soil above the buried Deerhorn Cu-Au porphyry prospect in central BC showed a depletion of carbon disulphide, propane, cyclopentane, and 1-ethyl-2/3-methylbenzene over the mineralised bedrock (Rich, 2016). No depletion in these compounds was observed over mineralisation at Highmont South.

6.2.5 Conclusions

Geochemical exploration tools were successful at detecting the surficial footprint of the Highmont South target, a zone of porphyry Cu-Mo mineralised bedrock beneath 2 to 10 metres of till blanket at Highland Valley Copper. Results from the various exploration methodologies applied in this study indicate that the surficial geochemical footprint is generated by a combination of:

- glacial transport of fragments of local bedrock mineralisation containing significant Cu, Mo, Ag, Bi, Sb, As, and W concentrations above background levels;
- migration of Cu, Ag, Sb, W, Pb, Cd, and Zn in solution in groundwater through West Highmont fault crosscutting mineralisation and subsequent accumulation at surface; and

- vegetation uptake and cycling of Mo from groundwater in contact with bedrock mineralisation as well as clastic molybdenite fragments dispersed within the till.

6.3 Surficial geochemistry of J.A.

There is no evidence for a surficial geochemical response to deeply buried porphyry Cu-Mo mineralised bedrock at J.A. Surficial geochemistry is controlled by differences in several surficial material types, both glacial and post-glacial, as well as hydromorphic processes and potentially anthropogenic influences.

Aqua regia digest ICP-MS results for upper B horizon soil samples returned values up to 2,432 ppm Cu, 205 ppm Mo, and 305 ppb Ag. These element concentrations are significantly higher than any response expected in upper B horizon soil above deeply buried mineralisation (e.g. Heberlein, 2010; Heberlein and Samson, 2010). Aqua regia ICP-MS results for upper B horizon soil samples over zones of mineralisation concealed by up to 25 metres of glaciofluvial sediments and till at the Mount Milligan porphyry Cu-Au deposit in north-central BC identified a response of up to 345 ppm Cu, 1.2 ppb Au, 3.1 ppb Ag, and 4.1 ppm Mo (Heberlein, 2010). The same approach at the buried Kwanika porphyry Cu-Au 'Central Zone' target in northern BC failed to detect a surficial response to known mineralisation (Heberlein and Samson, 2010). Similar to the J.A. target at HVC, the Central Zone mineralised bedrock at Kwanika is situated at the bottom of a broad, flat-bottomed valley beneath 20–40 metres of glacial till and outwash sediments and up to 300 metres of post-mineral sedimentary sequences which consist of conglomerates, sandstones, and siltstones (Heberlein and Samson, 2010). In addition to aqua regia digest of Ah, upper B, lower B, and C horizon soil, other soil analysis methods tested at this site are:

- sodium pyrophosphate leach (Ah horizon),
- cold aqua regia (upper B horizon),
- both hot and cold hydroxylamine hydrochloride leach (upper B horizon),
- deionised water leach (upper B horizon),
- Ionic Leach™ (upper B horizon),
- Bioleach™ (upper B horizon),
- Enzyme Leach™ (upper B horizon),
- Spatiotemporal Geochemical Hydrocarbons™ (upper B horizon), and
- Mobile Metal Ions™ (‘10 to 25 centimetres below top of mineral soil’).

None of these methods were successful at identifying a surficial footprint of buried mineralisation using B horizon soil (Heberlein and Samson, 2010). Aqua regia digest and sodium pyrophosphate leach of Ah horizon material were reported to identify responses for elements such as Cu, Au, Ag, and As (Heberlein and Samson, 2010). The subsequent study performed at Mt. Milligan concluded that soil disturbance and potential anthropogenic inputs at sites like Mt. Milligan negate the detection of a response from Ah horizon material (Heberlein, 2010). The Kwanika study site was reported to have well-preserved soil profiles and minimal anthropogenic activities (Heberlein and Samson, 2010). Therefore it is hypothesised that despite the reported success using Ah horizon soil at Kwanika, which has similar cover to that of J.A., the use of Ah horizon material at J.A. would not be successful due to disturbance of soil profiles and potential anthropogenic influences. Additionally there were very few observed Ah horizons in the soil profiles at J.A.

6.3.1 Impediments to a surficial footprint

Clastic material derived from the J.A. target cannot be present in glacial materials from the most recent glaciation due to the pre-Quaternary cover shielding the mineralised bedrock from glacial erosion (Plouffe and Ferbey, 2015). A potential surficial signal generated by ion migration from underlying bedrock mineralisation at J.A. could be confounded by the following factors:

- thickness of cover;
- low porosity of pre-glacial sequences at base of cover, difficult to permeate;
- glacially transported porphyry material from other mineralised centres;
- post-glacial alluvially transported porphyry material from other mineralised centres obscuring the signal;
- high variability of surficial material types; and/or
- anthropogenic influences.

Oxidisation of sulphide ore minerals is weak to nonexistent at the surface of mineralised bedrock in contact with pre-Quaternary cover, determined by visual inspection of an intersection of drill core produced in 2016 by CMIC and Teck (pers. comm., Robert Lee, 2016). This indicates that the pre-Quaternary cover may act to shield the mineralised bedrock surface from oxidisation and weathering. The pre-Quaternary cover is probably equally able to prevent the transport away from source of the small quantity of ore-related elements potentially released by oxidisation and weathering of the sulphide mineralisation.

6.3.2 Surficial response to surrounding mineralisation

Transported porphyry material was identified in soil samples collected from J.A. A small post-glacial alluvial fan in the southwest of the field area was deposited by a stream which can be traced back to the main Highmont deposits. It is hypothesised that weathered porphyry material was transported downstream and deposited within the alluvial fan. Sampled upper B horizon soils developed over the alluvial fan sediments are elevated in Cu, Ag, Cd, Sb, Bi, La, Ba, and Y compared to those sampled from other surficial units. The Cu:S ratios in all soil samples from the alluvial fan unit are close to that of the ore mineral bornite (Cu_5FeS_4). Other soil samples in which the Cu:S ratio closely matches that of ore minerals bornite (Cu_5FeS_4) or chalcopyrite ($CuFeS_2$) are all spatially associated with Witches Brook and a main drainage channel which had ponded surface water post-glacially, depositing lacustrine sediments. Sequential extraction conducted on a soil sample from the alluvial fan unit indicates a significant portion of the Cu and Bi is associated with an amorphous iron oxide soil phase. The majority of Ag is associated with more robust mineral phases such as crystalline iron oxides or residual sulphides.

6.3.3 Conclusions

Geochemical exploration tools were not successful in the detection of a surficial footprint of the deeply buried J.A. target, a zone of porphyry Cu-Mo mineralised bedrock underlying up to 300 metres of various types of pre-glacial and glacial overburden at Highland Valley Copper. A number of factors are hypothesised to contribute to the prevention of a surficial footprint including the thickness of cover, low porosity and permeability of preglacial cover in contact

with mineralised bedrock, high variability of surficial material types, transported geochemical signatures from surrounding mineralisation, and potentially anthropogenic influences.

While the surficial footprint at Highmont South, where cover is only 2–10 metres of subglacial till, is in a large part driven by clastic dispersal of glacially eroded porphyry material, this situation is not possible at J.A. due to preglacial sequences shielding mineralised bedrock during the last glaciation (Plouffe and Ferbey, 2015). Probable clastic responses are identified in upper B horizon soil samples at J.A. which are attributed to other porphyry centres such as the Bethlehem deposits, directly up-ice from J.A., which were exposed to erosion during the last glaciation (Plouffe and Ferbey, 2015).

Despite the reported success of anomaly identification using Ah horizon soil at the Kwanika Central Zone, a porphyry Cu-Au target at the base of a partially buried valley similar to J.A., beneath up to 300 metres of sedimentary rocks and 20–40 metres of glacial sediments (Heberlein and Samson, 2010), this would not be successful at J.A. due to disturbance of soil profiles, lack of Ah horizon soil, and anthropogenic influences.

6.4 General conclusions

6.4.1 Geochemical footprint of HVC

Based on available datasets the surficial geochemical footprint of the Highland Valley camp is a broad halo of elevated Cu (reaches approximately 10 kilometres from mineralised centres) and Mo (approx. 5 km) in till and stream sediments (Arne and Bluemel, 2011; Plouffe and Ferbey, 2015; Ferbey et al., 2016b; pers. comm., Robert Lee, 2017). High counts of chalcopyrite fragments in till occur up to 10 kilometres in the S-SE down-ice direction from HVC (Ferbey et al., 2016b; Arne and Bluemel, 2011).

6.4.2 Geochemical footprint of Highmont South

The geochemical footprint of Highmont South is attributed to glacially transported clastic material (Cu, Mo, Ag, Bi, Sb, As, W), supplemented by Mo cycled from vegetation. There is no evidence in support of ion transfer from mineralised bedrock. Secondary responses are evident above the West Highmont fault which crosscuts mineralisation (Cu, Ag, Sb, W, Cd, Pb, Zn, Mn).

6.4.3 Geochemical footprint of J.A.

There is no evidence to indicate the presence of a geochemical footprint above J.A. in response to the deeply buried mineralisation.

Chapter 7: Exploration implications and recommendations for future work

7.1 Implications for exploration strategy

This research highlights surficial geochemical exploration techniques that can continue to be applied in the exploration for buried mineral deposits in glaciated and till-covered terrain. Implications and suggestions to refine future exploration strategies are presented herein.

7.1.1 Surficial mapping

Prior to any surficial geochemical survey, detailed surface mapping of the field area is critical. This facilitates a more intimate understanding of the site which helps the design the most efficient and appropriate survey, and serves as context for which geochemical data acquired can be spatially interpreted. Many map layers should be produced, including those which focus on surficial material types, landform evolution and geomorphology, vegetation zonation, and anthropogenic influences. A good exploration geologist/geochemist is observant of every aspect of their environment. An abrupt change in vegetation species, for example, could indicate a corresponding change in the subsurface. Data must be integrated with this information during interpretation.

7.1.2 Surficial geochemical sampling

Prior to sampling, a survey must be carefully designed which considers background knowledge and all relevant variables identified during the mapping exercise. Consistency is key in every aspect of geochemical sampling. Depending on the estimated target size and observed variety and distribution of surficial materials, samples may be collected along transects or in a grid pattern. It is important to extend sampling into areas that are determined not to host mineralisation, to establish 'background' conditions with which to compare potentially anomalous samples. If multiple media types are to be sampled, it is important to sample these at the same locations in order to layer and integrate all geochemical data. Examples of survey forms can be found in Appendix A.

7.1.2.1 Soil sampling

Results from this research indicate that the best target horizon for soil samples is the upper B horizon in areas of weak brunisolic soil development over glacially transported material. Samples from horizons closer to the soil-air interface with higher organic matter content have much higher potential to contain anthropogenic inputs.

It is important to obtain samples from within the same surficial material type, with the same relative moisture, wherever possible. Detailed notes and photos are invaluable when irregularities arise during data interpretation. Retaining a small portion of each sample in labelled chip tray slots provides a valuable visual reference for soil characteristics along each sampling transect.

7.1.2.2 Biogeochemical sampling

Similar to any surficial geochemical sampling survey, it is important to conduct sufficient prior research in order to assure that the media type being sampled is indeed fit for purpose. Element concentrations vary not only between different plant species, but between the different tissues within a single species (Dunn, 2007). In retrospect it would have been more appropriate to analyse the lodgepole pine twigs rather than the needles. The twigs of conifers generally have higher Mo concentrations than the foliage (Dunn, 2007). Twigs and needles were collected together, however there were no remaining resources to justify the analysis of an additional tissue. Dunn (2007) suggests that the outer bark is the best sampling medium for lodgepole pine trees, however this was avoided in this particular area due to the propensity of outer bark to sequester airborne anthropogenic inputs.

Do not collect vegetation samples in plastic zip-locking bags (e.g. classic polypropylene sample bags). The samples will get moldy. Use woven polypropylene bags (or paper bags) to allow the samples to dry and take proper precautions to prevent contamination.

7.1.2.3 Dendrochemical sampling to decouple mineralisation and anthropogenic signals

Tree core sampling and analysis has been a useful tool for defining and decoupling relative anthropogenic inputs to a mineralised environment (e.g. Kyser et al., 2015; van Geffen et al., 2012; Kozuskanich et al., 2009). Most dendrochemical studies over buried mineralisation focus on uranium deposits, specifically targeting radiogenic Pb isotope ratios, and to a lesser extent VMS deposits. The method has not yet been successfully applied at a porphyry Cu deposit. In order to maximise chances of success for the relatively expensive study, careful research and planning must be completed beforehand. Vegetation mapping and test-sampling may determine

that dendrochemistry is simply not feasible in some areas (e.g. silvicultural practices or tree death due to infestation). The behaviour of trace elements in vegetation is variable between species and even between different tissues of a single species. The uptake and retention of trace elements is further influenced by local environmental factors such as drainage, climate, and substrate. Considerable research has gone into determining the behaviour and relative mobility of trace elements in vegetation (much of which is compiled in Dunn's 2007 *Biogeochemistry in Mineral Exploration*). There remain many opportunities for refinement in our understanding of the behaviour of trace elements in different types and tissues of vegetation and the use of this knowledge in the search for buried mineral deposits.

Through much trial and error in the dendrochemical sampling and analysis involved in this project, the author has a long list of suggestions for other first-time tree-corers and encourages anyone who is interested to contact her.

7.1.3 Analysis methods of soil samples

The results of this study indicate that aqua regia digest coupled with multi-element ICP-MS instrumental finish is the best digestion method for soils developed above glacially transported materials in an anthropogenically-influenced area. The author does not suggest using a deionised water extraction for soil samples from areas with anthropogenic disturbances.

The use of a pXRF device at its current level of technology could provide a time- and cost-effective method of surficial geochemical surveying depending on the resolution and quality of data desired by the operator and its expected concentration levels. A fast B horizon soil survey using a pXRF in 'soil mode' targeting Cu and Mo concentrations would be successful in an area of suspected porphyry Cu-Mo mineralisation at the concentrations seen at Highmont South. This

would require detailed mapping of the surficial environment, visual estimation of organic content in the soil, and would greatly benefit from measurement of soil physicochemical conditions.

7.1.4 Interpretation of surficial geochemical data

A multi-element approach to the interpretation of surficial geochemical data allows the identification of potential processes which resulted in an anomalous chemical signature. An example is the 'clastic' Cu-Mo-Ag-Bi signature detected at Highmont South, which was differentiated from the 'fault' Cu-Ag signature. The location of the Cu-Ag anomaly over the West Highmont fault in transect two was initially interpreted as a clastic signature due to its position directly down-ice from one of the mineralised targets. Knowledge of the relative solubilities of trace elements in soil and the multi-element interpretation approach allowed the identification of different mechanisms of anomaly formation.

7.2 Recommendations for future research

Based on the conclusions from this research, the following recommendations are made for future studies:

- A more in-depth investigation of the origins of anomalous long-chain hydrocarbon responses from AGI Samplers in soils overlying the Highmont South mineralised targets is suggested.
- Additional upper B horizon soil sampling at Highmont South could verify the difference between the surficial signatures attributed to clastic transport and to element migration through the West Highmont fault.

- Future biogeochemical sampling could target a non-arboreal species, due to the silvicultural practises in the area. Labrador tea has been used as a medium for vegetation sampling in other studies and this species has good spatial coverage in the areas traversed by the author.
- The science and application of dendrochemistry (and biogeochemistry as a whole) has the potential to be vastly improved and streamlined by the improvement of communication and cross-pollination between the geological and biological disciplines, especially within universities.
- A geochemical survey of groundwater in the research area could identify a geochemical signature of groundwater flowing through fault pathways, and well as groundwater in contact with bedrock mineralisation. Anomalous concentrations of elements including Cu, Mo, Ag, Sb, As, W, Zn, and Mn were detected in the Pebble porphyry Cu-Au-Mo deposit area where glacial sediment cover reaches up to 50 metres in thickness (Eppinger et al., 2012).

References

Agriculture Canada, 1998. The Canadian System of Soil Classification, Third Edition. Research Branch, Agriculture and Agri-Food Canada Publication, NRC Research Press, Ottawa, 187 pages.

Anderson, H., 2006. Amplified geochemical imaging: an enhanced view to optimize outcomes. First Break, 24(8), 77–81.

Anderson, R.G., Plouffe, A., Ferbey, T., Dunn, C.E., 2012. The search for surficial expressions of buried Cordilleran porphyry deposits: background and progress in a new Targeted Geoscience Initiative 4 activity in the souther Canadian Cordillera, British Columbia. Geological Survey of Canada, Current Research 2012-7, 15 pages.

Arne, D.C., Bluemel, E.B., 2011. Catchment analysis and interpretation of stream sediment data from QUEST-South, British Columbia. Geoscience BC Report 2011-5, 25 pages.

Asael, D., Matthews, A., Bar-Matthews, M., Halicz, L., Ehrlich, S., Teplyakov, N., 2005. Redox fractionation of copper isotopes in sedimentary conditions. Geochimica et Cosmochimica Acta, 69, A216.

Aspandiar, M.F., Anand, R.R., Gray, D.J., 2008. Geochemical dispersion mechanisms through transported cover: Implications for mineral exploration in Australia. CRC LEME Restricted Report 230, 84 pages. (Reissued as Open File Report 246, CRC LEME, Perth, 2008).

Balistrieri, L.S., Borrok, D.M., Wanty, R.B., Ridley, W.I., 2008. Fractionation of Cu and Zn isotopes during adsorption onto amorphous Fe(III) oxyhydroxide: Experimental mixing of acid rock drainage and ambient river water. Geochimica et Cosmochimica Acta, 72, 311–328.

Bezbaruah, A.N., Zhang, T.C., 2004. pH, redox, and oxygen microprofiles in rhizosphere of bulrush (Scirpus validus) in a constructed wetland treating municipal wastewater. Biotechnology and Bioengineering, 88, 60–70.

Bigalke, M., Weyer, S., Wilcke, W., 2010b. Stable copper isotopes: A novel tool to trace copper behavior in hydromorphic soils. Soil Science Society of America Journal, 74, 60–73.

Bigalke, M., Weyer, S.., Wilcke, W., 2011. Stable Cu isotope fractionation in soils during oxic weathering and podsolization. Geochimica et Cosmochimica Acta, 75, 3119–3134.

Bissig, T., Heberlein, D.R., Dunn, C., 2013. Geochemical techniques for detection of blind porphyry copper-gold mineralisation under basalt cover, Woodjam property, south-central British Columbia (NTS 093A/03, /06). Geoscience BC Report 2013-17, 49 pages.

Blaine, F.A., Hart, C.J.R., 2011. Geochemical-exploration models for porphyry deposits in British Columbia; *in* Geoscience BC Summary of Activities 2011, Geoscience BC, Report 2012-1, p. 29–40.

Blaser, P., Zimmermann, S., Luster, J., Shotyk, W., 2000. Critical examination of trace element enrichments and depletions in soils: As, Cr, Cu, Ni, Pb, and Zn in Swiss forest soils. Science of the Total Environment, 249(1–3), 157–280.

Bluemel, B., Dunn, C., Hart, C., Leijd, M., 2015. Biogeochemical expressions of buried REE mienralization at Norra Kärr, southern Sweden, *in* Simandl, G.J. and Neetz, M. (eds.), Symposium on Stategic and Critical Materials Proceedings, November 13-14, 2015, Victoria, British Columbia. British Columbia Ministry of Energy and Mines, British Columbia Geological Survey, Paper 2015-3, 231–239.

Bobrowsky, P.T., Kerr, D.E., Sibbick, S.J., Newman, K., 1993. Drift exploration studies, Valley Copper pit, Highland Valley Copper mine, British Columbia: stratigraphy and sedimentology (92I/6, 7, 10 and 11): *in* Geological Fieldwork 1992, British Columbia Ministry of Energy, Mines and Petroleum Resources, British Columbia Geological Survey, Paper 1993-1, 427–437.

Bobrowsky, P., Cathro, M., Paulen, R., 2002. Quaternary geology reconnaissance studies (92I/2 and 7); *in* Geological Fieldwork 2001, British Columbia Geological Survey, Paper 2002-1, 397–402.

Bolviken, B., Logn, O., 1975. An electrochemical model for element distribution around sulfide bodies, *in:* Elliott, I.L., and Fletcher, W.K. (eds.), Geochemical Exploration 1974, Association of Exploration Geochemists Special Publications, 2, 631–648.

Borrok, D.M., Ridley, W.I., Wanty, R.B., 2008. Isotopic fractionation of Cu and Zn during adsorption onto bacterial surfaces. Geochimica et Cosmochimica Acta, 72, A99.

Bowen, H.J.M., 1982. Environmental Chemistry, Volume 2. Royal Society of Chemistry, Special Periodical Reports, 204 pages.

British Columbia Ministry of Forests and Range, 2006. Biogeoclimatic zones of British Columbia [map]. BC Ministry of Forests and Range, Victoria, URL: https://www.for.gov.bc.ca/hre/becweb/downloads/Downloads_BGCmaps/BGCzones8x11 (accessed 12/8/2017).

Brockley, R.P., 2001. Fertilization of lodgepole pine in western Canada. Proceedings of Enhanced Forest Management: Fertilization & Economics Conference, 43–54.

Brooks, R.R., Dunn, C.E., Hall, G.E.M., 1995. Biological Systems in Mineral Exploration and Processing. Ellis Horwood, Hemel Hempstead (UK), Toronto, New York, 538 pages.

Park, Y.J., Fray, D.J., 2009. Recovery of high purity precious metals from printed circuit boards. Journal of Hazardous Materials, 164, 1152–1158.

Brushett, D., 2014. Prospecting under cover: Using knowledge of glacial processes in mineral exploration. CIM Professional Short Course, presented November 5, 2014, Newfoundland and Labrador, 25 pages.

Byrne, K., Stock, E., Ryan, J., Johnson, C., Nisenson, J., Alva Jimenez, T., Lapointe, M., Stewart, H., Grubisa, G., Sykora, S., 2013. Porphyry Cu-(Mo) deposits in the Highland Valley district, south central British Columbia; *in* Porphyry Systems of Central and Southern BC: Tour of Central BC Porphyry Deposits from Prince George to Princeton, Logan, J., Schroeter, T. ,(eds.), Society of Economic Geologists, Guidebook Series 44, 99–116.

Cameron, E.M., Hamilton, S.M., Leybourne, M.I., Hall, G.E.M., McClenaghan, M.B., 2004. Finding deeply buried deposits using geochemistry. Geochemistry: Exploration, Environment, Analysis, 4, 7–32.

Canadell, J., Jackson, R.B., Ehleringer, J.B., Mooney, H.A., Sala, O.E., Schulze, E.-D., 1996. Maximum rooting depth of vegetation types at a global scale. Oecologia, 108(4), 583–595.

Caron, L., 2007. Grid work, soil geochemistry and geophysics on the Galaxxy property located in the Afton area. British Columbia Ministry of Energy and Mines, Assessment Report 29628, 88 pages, URL: http://aris.empr.gov.bc.ca/ARISReports/29628.PDF.

Carr, J.M., 1966. Geology of the Bethlehem and Craigmont copper deposits; *in* A symposium on the tectonic history and mineral deposits of the western Cordillera, Vancouver, BC, 1964: Canadian Institute of Mining and Metallurgy Special, 8, 321–328.

Carroll, A.L., Régnière, J., Logan, J.A., Taylor, S.W., Bentz, B.J., Powell, J.A., 2006. Impacts of climate change on range expansion by the mountain pine beetle. Mountain Pine Beetle Initiative Working Paper 2006-14, 20 pages.

Casselman, M.J., McMillan, W.J., Newman, K.M., 1995. Highland Valley porphyry copper deposits near Kamloops, British Columbia: A review and update with emphasis on the Valley deposit; *in* Porphyry deposits of the Northwestern Cordillera of North America, Schroeter, T.G., (ed.), Canadian Institute of Mining and Metallurgy, 46, 161–191.

Chao, T.T., 1984. Use of partial dissolution techniques in geochemical exploration. Journal of Geochemical Exploration, 20, 101–135.

Chouinard, R.L., Winterburn, P.A., Ross, M., Lee, R.G., 2017. Surficial geochemical footprint of buried porphyry Cu-Mo mineralisation at the Highland Valley Copper operations, south-central

British Columbia: Project update. Geoscience BC Summary of Activities, Report 2017-01, 125–131.

Clague, J.J., (compiler), 1989. Quaternary geology of the Canadian Cordillera, *in* Fulton, R.J., (ed.), Quaternary geology of Canada and Greenland. Geological Survey of Canada, Geology of Canada, 1, 15–96.

Clague, J.J., Ward, B.C., 2013. Pleistocene glaciations of British Columbia; *in* Quaternary Glaciations – extent and chronology, Ehlers, J., Gibbard, P.L., Hughes, P.D., (eds.), Developments in Quaternary Science, 15, 563–573.

Clayton, R.E., Hudson-Edwards, K.A., Houghton, S.L., 2005. Isotopic effects during Cu sorption onto goethite. Geochimica et Cosmochimica Acta, 69, A216.

Cohen, D.R., Hoffman, E.L., Nichol, I., 1987. Biogeochemistry: A geochemical method for gold exploration in the Canadian Shield. Journal of Geochemical Exploration, 29, 49–73.

Dalrymple, I., 2007. An approach to the optimization of partial extractions for use in geochemical exploration (Doctoral thesis). The University of New South Wales, Sydney, Australia, 273 pages.

D'Angelo, M., 2016. Geochemistry, petrography and mineral chemistry of the Guichon Creek and Nicola batholiths, southcentral British Columbia (Master's thesis). Lakehead University, Thunder Bay, Ontario, Canada, 421 pages.

D'Angelo, M., Alfaro, M., Hollings, P., Byrne, K., Piercey, S., Creaser, R.A., 2017. Petrogenesis and magmatic evolution of the Guichon Creek batholith: Highland Valley porphyry Cu ± (Mo) district, south-central British Columbia. Economic Geology, 112, 1857–1888.

Deblonde, C., Plouffe, A., Boisvert, É., Buller, G., Davenport, P., Everett, D., Huntley, D., Inglis, E., Kerr, D., Moore, A., Paradis, S.J., Parent, M., Smith, I.R., St. Onge, D., Weatherston, A., 2014. Science language for an integrated Geological Survey of Canada data model for surficial geology maps, version 2.0. Geological Survey of Canada, Open File 7631, 464 pages.

Delgado, A., Gomez, J.A., 2016. The soil. Physical, chemical and biological properties, *in:* Villalobos, F.J., Fereres, E. (eds.), Principles of Agronomy for Sustainable Agriculture, Springer International, 555 pages.

Domenico, P.A., Schwartz, F.W., 1998. Physical and Chemical Hydrogeology, 2nd Edition. Wiley, New York, Chichester, Weinheim, Brisbane, Toronto, Singapore, 528 pages.

Drake, L.D., 1983. Ore plumes in till. Journal of Geology, 91, 707–713.

Dunn, C.E., 1995. Mineral exploration beneath temperate forests: The information supplied by trees. Exploration Mining Geology, 4(3), 197–204.

Dunn, C.E., 2007. Biogeochemistry in Mineral Exploration. Handbook of Exploration and Environmental Geochemistry, Volume 9, Elsevier Science, 480 pages.

Dunn, C.E., Balma, R.G., Sibbick, S.J., 1996. Biogeochemical survey using lodgepole pine bark: Mount Milligan, central British Columbia (parts of 93N/1 and 93O/4). Geological Survey of Canada, Open File 3290, 115 pages.

Dunn, C.E., Hastings, N.L., 2000. Biogeochemical survey of the Nechako River area using outer back of Lodgepole pine (NTS 93 F/9, 93 F/10, 93 F/15, 93 F/16 and parts of 93 F/11, 93 F/14, 93 K/1 and 93 K/2), central British Columbia: digital data release for Open Files 3594a-c. Geological Survey of Canada, Open File 3594d.

Dunn, C.E., Cook, S.J., Hall, G.E.M., 2007. Halogens in surface exploration geochemistry: evaluation and development of methods for detecting buried mineral deposits. Geoscience BC, Report 2007-10, 62 pages.

Ehrlich, S., Butler, I., Halicz, L., Rickard, D., Oldroyd, A., Matthews, A., 2004. Experimental study of the copper isotope fractionation between aqueous Cu(II) and covellite, CuS. Chemical Geology, 209, 259–269.

Eppinger, R.G., Fey, D.L., Giles, S.A., Kelley, K.D., Smith, S.M., 2012. An exploration hydrogeochemical study at the giant Pebble porphyry Cu-Au-Mo deposit, Alaska, USA, using high resolution ICP-MS. Geochemistry: Exploration, Environment, Analysis, 12, 221–226.

Etiope, G., Martinelli, G., 2002. Migration of carrier and trace gases in the geosphere: an overview. Physics of the Earth and Planetary Interiors, 129, 185–204.

Evans, D.J.A, Phillips, E.R., Hiemstra, J.F., Auton, C.A., 2006. Subglacial till: formation, sedimentary characteristics and classification. Earth Science Reviews, 78, 115–176.

Favre, F., Tessier, D., Abdelmoula, M., Génin, J.M., Gates, W.P., Boivin, P., 2002. Iron reduction and changes in cation exchange capacity in intermittently waterlogged soil. European Journal of Soil Science, 53(2), 175–183.

Ferbey, T., Arnold, H., Hickin, A.S., 2013. Ice-flow indicator compilation, British Columbia. British Columbia Ministry of Energy and Mines, British Columbia Geological Survey Open File 2013-06, scale 1:1,650,000.

Ferbey, T., Plouffe, A., Anderson, R.G., 2014. An integrated approach to search for buried porphyry-style mineralisation in central British Columbia using geochemistry and mineralogy: a TGI-4 project. Geological Survey of Canada Current Research 2014-2, 12 pages.

Ferbey, T., Plouffe, A., Bustard, A.L., 2016. Geochemical, mineralogical, and textural data from tills in the Highland Valley Copper mine area, south-central British Columbia. British Columbia Geological Survey, GeoFile 2016-11, Geological Survey of Canada Open File 8119, 15 pages.

Ferbey, T., Plouffe, A., Bustard, A.L., 2016b. Porphyry indicator minerals in tills of the Highland Valley copper-molybdenum mine area, south-central British Columbia. Poster presented at the Association for Mineral Exploration British Columbia Roundup conference, Vancouver, British Columbia, January 25–28, 2016.

Fiedler, S., Vepraskas, M.J., Richardson, J.L., 2007. Soil redox potential: Importance, field measurements, and observations. Advances in Agronomy, Vol. 94, Elsevier, 54 pages.

Flint, R.F., 1971. Glacial and Quaternary Geology. John Wiley and Sons Inc., New York, 892 pages.

Freeze, R.A., Cherry, J.A., 1979. Groundwater. Prentice-Hall, Englewood Cliffs, 624 pages.

Fulton, R.J., 1965. Silt deposition in late-glacial lakes of southern British Columbia. American Journal of Science, 263, 553–570.

Fulton, R.J., 1967. Deglaciation studies in Kamloops region, an area of moderate relief, British Columbia. Geological Survey of Canada, Bulletin 154, 36 pages.

Fulton, R.J., 1969. Glacial lake history, southern Interior Plateau, British Columbia. Geological Survey of Canada, Paper 69-37, 14 pages.

Fulton, R.J., 1975. Quaternary geology and geomorphology, Nicola-Vernon area, British Columbia (82 L W 1/2 and 92 I E 1/2). Geological Survey of Canada, Memoir 380, 50 pages.

Fulton, R.J., Irving, E., Wheadon, P.M., 1992. Stratigraphy and paleomagnetism of Brunhes and Matuyama (>790 ka) Quaternary deposits at Merritt, British Columbia. Canadian Journal of Earth Sciences, 29, 76–92.

Geoscience BC, 2010. QUEST South regional geochemical data, southern British Columbia. Geoscience BC, Report 2010-13, 18 pages.

Gillham, R.W., 1984. The capillary fringe and its effect on water-table response. Journal of Hydrogeology, 67, 307–324.

Government of British Columbia, 1997. Riparian areas protection act. Statute of British Columbia 1997, ch. 21, [URL: http://www.bclaws.ca/Recon/document/ID/freeside/00_97021_01] (accessed 06/20/2017).

Hale, M., Plant, J.A., 1994. Drainage geochemistry. Handbook of Exploration Geochemistry, Elsevier, Amsterdam, 6, 766 pages.

Hall, G. E., Vaive, J. E., Beer, R. Hoashi, M., 1996a. Selective leaches revisited, with emphasis on the amorphous Fe oxyhydroxide phase extraction. Journal of Geochemical Exploration, 56, 59–78.

Hamilton, S.M., 1998. Electrochemical mass transport in overburden: a new model to account for the formation of selective leach geochemical anomalies in glacial terrain. Journal of Geochemical Exploration, 63, 155–172.

Hamilton, S.M., 1999. Summary of Fieldwork and Other Activities, 1999. Ontario Geological Survey, Open File Report 6000, 421–426.

Hamilton, S.M., 2000. Spontaneous potentials and electrochemical cells, *in*: M. Hale (ed.) Geochemical Remote Sensing of the Subsurface, Handbook of Exploration Geochemistry, 7, 81–119.

Hamilton, S.M., 2007. Major advances in soil geochemical exploration methods for areas of thick glacial drift cover, *in:* Milkereit, B. (ed.), Proceedings of Exploration 07: Fifth Decennial International Conference on Mineral Exploration, Paper 13, 263–280.

Heberlein, D.R., Samson, H., 2010. An assessment of soil geochemical methods for detecting copper-gold porphyry mineralisation through Quaternary glaciofluvial sediments at the Kwanika Central Zone, north-central British Columbia. Geoscience BC Report 2010-03, 89 pages.

Heberlein, D.R., 2010. An assessment of soil geochemical methods for detecting copper-gold porphyry mineralisation through Quaternary glaciofluvial sediments at the WBX-MBX and 66 Zones, Mt. Milligan, north-central British Columbia. Geoscience BC report 2010-08, 68 pages.

Helios-Rybicka, E., Wilson, M.J., McHardy, W.J., 1994. Chemical and mineralogical forms and mobilisation of Cu and Pb in soils from a Cu-smelting area in Poland. Journal of Environmental Science and Health, A29, 531–546.

Hooke, R.L., Cummings, D.I., Lesemann, J.-E., Sharpe, D.R., 2013. Genesis of dispersal plumes in till. Canadian Journal of Earth Sciences, 50, 847–855.

Horton, J.L., Hart, S.C., 1998. Hydraulic lift: a potentially important ecosystem process. TREE, 13(6), 232–235.

Johnsen, T.F., Brennand, T.A., 2004. Late-glacial lakes in the Thompson Basin, British Columbia: paleogeography and evolution. Canadian Journal of Earth Sciences, 41, 1367–1383.

Jouvin, D., Louvat, P., Marechal, C., Benedetti, M.F., 2008. Fractionation of copper isotopes in plants. Geochimica et Cosmochimica Acta, 72, A441.

Jumikis, A.R., 1967. Introduction to Soil Mechanics. D. van Nostrand Company, New York, 436 pages.

Kabata-Pendias, A., 2010. Trace elements in soils and plants, fourth edition. CRC Press, 548 pages.

Kerr, D.E., Sibbick, S.J., Belik, G.D., 1993. Preliminary results of glacial dispersion studies on the Galaxy property, Kamloops, BC (92I/9). British Columbia Geological Survey, Geological Fieldwork 1992, paper 1993-1, p. 439–443.

Ketterings, Q., Reid, S., Roa, R., 2007. Cation exchange capacity (CEC). Agronomy Fact Sheet Series #22. Deportment of Crop and Soil Sciences, College of Agriculture and Life Sciences, Cornell University, 2 pages.

Kozuskanich, J.C., Kyser, T.K., MacFarlane, W.R., Hamilton, S.M., 2009. Dendrochemical variation over the Cross Lake VMS mineralisation – a tool for mineral exploration and decoupling anthropogenic input from background signals. Geochemistry: Exploration, Environment, Analysis, 9, 151–157.

Kyser, K., Lahusen, L., Drever, G., Dunn, C., Leduc, E., Chipley, D., 2015. Using Pb isotopes in surface media to distinguish anthropogenic sources from undercover uranium sources. Comptes Rendus Geoscience, 347, 215–226.

Lee, R.G., Byrne, K., Alfaro, M., D'Angelo, M., Hart, C.J.R., Hollings, P., Gleeson, S.A., 2017. Assessing the zircon compositional evolution from the Guichon Creek Batholith and Highland Valley Copper: Proceedings of the 14th Biennial SGA Meeting, 20-23 August 2017, Quebec City, Canada, v. 3, p. 1087–1090.

Lesage, G., Byrne, K., Lee, R.G., Hart, C.J.R., 2016. Characterizing the district-scale alteration surrounding a large poprhyry Cu system: The footprint of Highland Valley Copper, British Columbia: GAC-MAC Abstracts, June 1-3, 2016, Whitehorse, Canada, v. 39, p. 52.

Lesage, G., Byrne, K., Lee, R.G., Hart, C.J.R., 2017. District-scale porphyry-related hydrothermal alteration and the quantitative use of feldspar staining: the case of Highland Valley Copper, British Columbia. Poster presented at the Association for Mineral Exploration Roundup conference, Vancouver, British Columbia, January 23–26, 2017.

Lett, R., Jackaman, W., Englund, L., 2000. Stream geochemical exploration for pluton-related quartz-vein gold deposits in southern British Columbia. British Columbia Geological Survey Open File 2000-23, 22 pages.

Lett, R.E., 2001. Geochemical signatures around massive sulphide deposits in southern British Columbia, Canada, *in*: McCleneghan, M.B., Bobrowsky, P.T., Hall, G.E.M., Cook, S.J., (eds.), Drift Exploration in Glaciated Terrain, Geological Society of London, Special Publications, 185, 301–321.

Lett, R.E., 2002. Geochemical Exploration Models, Volume 2: shale hosted Pb-Zn-Hg deposits in north-eastern British Columbia. British Columbia Geological Survey, Open File 2001-7, 70 pages.

Lett, R.E., 2011. GeoFile 2011-12 surficial geochemistry of the Galaxy porphyry copper-gold deposit, Kamloops, BC (NTS 092I/09). British Columbia Geological Survey, Ministry of Energy and Mines, GeoFile 2011-12, 5 pages.

Li, D., Liu, S.-A., Li, S., 2015. Copper isotope fractionation during adsorption onto kaolinite: Experimental approach and applications. Chemical Geology, 396, 74–82.

Logan, J.M., Mihalynuk, M.G., 2014. Tectonic controls on early Mesozoic paired alkaline porphyry deposit belts (Cu-Au ± Ag-Pt-Pd-Mo) in the Canadian Cordillera. Economic Geology, 109, 827–858.

Logan, J.M., Schroeter, T.G., 2013. Porphyry systems of central and southern British Columbia: Tour of Central BC Porphyry Deposits from Prince George to Princeton. Society of Economic Geologists, Guidebook Series 44, 1–45.

Logan, J.M., Schroeter, T.G., 2016. Porphyry systems of central and southern British Columbia; Riedell, K.B., Putnam, B.R. and Taylor, R.D. (eds.), Society of Economic Geologists, Guidebook Series 52, 110 pages.

Luca, R., Townley, B., Escobar, B., Vargas, T., 2008. Formation of hydrocarbon gaseous compounds during bioleaching of copper sulphide minerals with mesophilic microorganisms. Hydrometallurgy, 94(1), 54–57.

Mann, A.W., Birrell, R.D., Fedikow, M.A.F., de Souza, H.A.F., 2005. Vertical ionic migration: mechanisms, soil anomalies, and sampling depth for mineral exploration. Geochemistry: Exploration, Environment, Analysis, 5, 201–210.

Mathur, R., Fantle, M.S., 2015. Copper isotopic perspectives on supergene processes: implications for the global Cu cycle. Elements, 11, 323–329.

Mathur, R., Ruiz, J., Titley, S., Liermann, L., Buss, H., Brantley, S., 2005. Cu isotopic fractionation in the supergene environment with and without bacteria. Geochimica et Cosmochimica Acta, 69, 5233–5246.

Mathur, R., Titley, S., Barra, F., Brantley, S., Wilson, M., Phillips, A., Munizaga, F., Maksaev, V., Vervoort, J., Hard, G., 2009. Exploration potential of Cu isotope fractionation in porphyry copper deposits. Journal of Geochemical Exploration, 102, 1–6.

McCleneghan, M.B., Thorleifson, L.H., DiLabio, R.N.W., 1997. Till geochemical and indicator mineral methods in mineral exploration, *in:* Gubins, A.G. (ed.), Proceedings of Exploration 97, Fourth Decennial International Conference on Mineral Exploration, Paper 31, 233–248.

McMillan, W.J., Anderson, R.G, Chan R., Chow, W., 2009. Geology and mineral occurrences (MINFILE), the Guichon Creek Batholith and Highland Valley porphyry copper district, British Columbia. Geological Survey of Canada, Open File 6079, 2 sheets.

McMillan, W.J., Panteleyev, A., 1995. Porphyry copper deposits of the Canadian Cordillera; *in* Porphyry copper deposits of the American Cordillera, Pierce, F.W. and Bolm, J.G. (eds.), Arizona Geological Society Digest, 20, 203–218.

McMillan, W.J., 1976. J.A.; *in* Porphyry Deposits of the Canadian Cordillera, Sutherland Brown, A., (ed.), Canadian Institute of Mining, Metallurgy and Petroleum, 15, 144–162.

Miller, J.K., 1984. Model for clastic indicator train in till, *in:* Prospecting in Areas of Glaciated Terrain, Institution of Mining and Metallurgy, London, 69–77.

National Resources Canada, 2013. NRCan certification information and examination preparation booklet – operator of portable XRF analyzers version 4. Government of Canada, 65 pages.

Navarette, J.U., Borrok, D.M., Viveros, M., Ellzey, J.T., 2011. Copper isotope fractionation during surface adsorption and intracellular incorporation by bacteria. Geochimica et Cosmochimica Acta, 75, 784–799.

Padilla, K.L., Anderson, K.A., 2002. Trace element concentration in tree-rings biomonitoring centuries of environmental change. Chemosphere, 49, 575–585.

Nur, A., 1974. Matsushiro, Japan, earthquake swarm: confirmation of dilatancy-fluid diffusion model. Geology, 2, 217–221.

Petit, J.C.J., De Jong, J., Chou, L., Mattielli, N., 2008. Development of Cu and Zn isotope MC-ICP-MS measurements: Application to suspended particulate matter and sediments from the Scheldt Estuary. Geostandards Geoanalytical Research, 32, 149–166.

Piercey, S.J., Devine, M.C., 2014. Analysis of powdered reference materials and known samples with a benchtop, field portable X-ray fluorescence (pXRF) spectrometer: evaluation of performance and potential applications for exploration lithogeochemistry. Geochemistry: Exploration, Environment, Analysis, 14, 139–148.

Plouffe, A., Anderson, R.G., Dunn, C.E., 2011. Till composition and biogeochemistry near a porphyry Cu-Mo deposit: Gibraltar Mine, British Columbia. Geological Survey of Canada, Open File 6755, 31 pages.

Plouffe, A., Bednarski, J.M., Huscroft, C.A., Anderson, R.G., McCuaig, S.J., 2011. Late Wisconsinan glacial history in the Bonaparte Lake map area, south central British Columbia: implications for glacial transport and mineral exploration. Canadian Journal of Earth Sciences, 48, 1091–1111.

Plouffe, A., Ferbey, T., Anderson, R.G., Hashmi, S., Ward, B.C., 2013a. New TGI-4 till geochemistry and mineralogy results near the Highland Valley, Gibraltar, and Mount Polley mines, and Woodjam District: An aid to search for buried porphyry deposits; Geological Survey of Canada, Open File 7473, 58 pages.

Plouffe, A., Ferbey, T., Anderson, R.G., Hashmi, S., Ward, B.C., Sacco, D.A., 2013b. The use of till geochemistry and mineralogy to explore for buried porphyry deposits in the Cordillera - preliminary results from a TGI-4 intrusion-related ore systems project. Geological Survey of Canada, Open File 7367, poster.

Plouffe, A., Ferbey, T., 2015a. Till composition near Cu-porphyry deposits in British Columbia: Highlights for mineral exploration: *in* TGI 4 – Intrusion Related Mineralisation Project" New Vectors to Buried Porphyry-Style Mineralisation, (ed.) N. Rogers; Geological Survey of Canada, Open File 7843, 15–37.

Plouffe, A., Ferbey, T., 2015b. Surficial geology, Gnawed Mountain area, British Columbia (Parts of NTS 92-I/6, NTS 92-I/7, NTS 92-I/10, and NTS 92-I/11). Geological Survey of Canada, Canadian Geoscience Map 214 (preliminary), British Columbia Geological Survey, Geoscience Map 2015-3, scale 1:50 000.

Plouffe, A., Ferbey, T., 2016. Till geochemistry, mineralogy and textural data near four Cu porphyry deposits in British Columbia; Geological Survey of Canada, Open File 8038, British Columbia Ministry of Energy and Mines, British Columbia Geological Survey, GeoFile 2016-10, 1 .zip file.

Pohl, W.L., 2011. Economic Geology: Principles and Practice. John Wiley and Sons Inc., New York, 680 pages.

Pokrovsky, O.S., Viers, J., Emnova, E.E., Kompantseva, E.I., Freydier, R., 2008. Copper isotope fractionation during its interaction with soil and aquatic microorganisms and metal oxy(hydr)oxides: possible structural control. Geochimica and Cosmochimica Acta, 72, 1742–1757.

Pourbaix, M., 1974. Atlas of electrochemical equilibria in aqueous solutions. National Association of Corrosion Engineers, Houston, Texas, 644 pages.

Proffett, J.M., 2009. High Cu grades in porphyry Cu deposits and their relationship to emplacement depths of magmatic sources. Geology, 37, 675–678.

Reed, A., Jambor, J., 1976. Highmont: linearly zoned copper-molybdenum porphyry deposits and their significance in the genesis of the Highland Valley ores; *in* Porphyry Deposits of the Canadian Cordillera, Sutherland Brown, A., (ed.), Canadian Institute of Mining, Metallurgy and Petroleum, 15, 163–181.

Reimann, C., Birke, M., Demetriades, A., Filzmoser, P., O'Connor, P., 2014. Chemistry of Europe's agricultural soils, part B: General background information and further analysis of the GEMAS data set. *Schweizerbart´sche* Verlagsbuchhandlung, 352 pages.

Reman, A., Ross, M., Lee, R.G., 2017. Towards a 3D Quaternary and Neogene stratigraphic model of the Highland Valley Copper mine area, south-central British Columbia. Poster presented at the Association for Mineral Exploration Roundup conference, Vancouver, British Columbia, January 23–26, 2017.

Rich, S.D., 2016. Geochemical mapping of porphyry deposits and associated alteration through transported overburden (Master's thesis). The University of British Columbia, Vancouver, British Columbia, Canada, 494 pages.

Rieuwerts, J.S., Thornton, I., Farago, M.E., Ashmore, M.R., 1998. Factors influencing metal bioavailability in soils: preliminary investigations for the development of a critical loads approach for metals. Chemical Speciation and Bioavailability, 10(2), 61–75.

Ryder, J.M., 1976. Terrain inventory and Quaternary geology Ashcroft, British Columbia. Geological Survey of Canada, Paper 74-49, 17 pages.

Ryder, J.M., Fulton, R.J., Clague, J.J., 1991. The Cordilleran ice sheet and the glacial geomorphology of southern and central British Columbia. Géographie physique et Quaternaire, 45, 365–377.

Safranyik, L., Carroll, A.L., 2006. The biology and epidemiology of the mountain pine beetle in lodgepole pine forests, *in* The Mountain Pine Beetle: A Synthesis of Biology, Management, and Impacts on Lodgepole Pine, Safranyik, L., Wilson, W.R. (eds.). Natural Resources Canada, Canadian Forest Service, Pacific Forestry Centra, Victoria, British Columbia, 304 pages.

Sato, M., Mooney, H.M., 1960. The electrochemical mechanism of sulphide self-potentials. Geophysics, 25, 226–249.

Savard, M.M., Begin, C., Parent, M., Marion, J., Smirnoff, A., 2006. Dendrogeochemical distinction between geogenic and anthropogenic emissions of metals and gases near a copper smelter. Geochemistry: Exploration, Environment, Analysis, 6, 237–247.

Schneider, A.R., Cancès, B., Breton, C., Ponthieu, M., Morvan, X., Conreux, A., Marin, B., 2016. Comparison of field portable XRF and aqua regia/ICPAES soil analysis and evaluation of soil moisture influence of FPXRF results. Journal of Soils and Sediments, 2, 438–448.

Schwedt, G., 2001. The essential guide to environmental chemistry. John Wiley & Sons, 268 pages.

Scott, K.M., 2005. Rutile geochemistry as a guide to porphyry Cu-Au mineralisation, Northparkes, New South Wales, Australia. Geochemistry: Exploration, Environment, Analysis, 5, 247–253.

Seneshen, D.M., 1997. The applicability of partial extractions to mineral exploration in areas of transported overburden (Doctoral thesis). Queen's University, Kingston, Ontario, Canada, 406 pages.

Shiel, A.E., Barling, J., Orians, K.J., Weis, D., 2009. Matrix effects on the multi-collector inductively coupled plasma mass spectrometric analysis of high-precision cadmium and zinc isotope ratios. Analytica Chimica Acta, 633, 29–37.

Shields, W.R., Dildich, S.S., Garner, E.L., Murphy, T.J., 1965. Natural variations in the abundance ratio and the atomic weight of copper. Journal of Geophysical Research, 70(2), 479–491.

Simandl, G.J., Stone, R.S., Paradis, S., Fajber, R., Reid, H.M., Grattan, K., 2014. An assessment of a handheld X-ray fluorescence instrument for use in exploration and development with an emphasis on REEs and related specialty metals. Mineralium Deposita, 49(8), 999–1012.

Smee, B.W., 1979. A theoretical estimation of ion mobilities through glaciolacustrine sediments: diffusion down a concentration gradient. Current Research, Part A, Geological Survey of Canada, Bulletins and Open Reports, 79-1A, 367–374.

Smee, B.W., 1983. Laboratory and field evidence in support of the electrochemically enhanced migration of ions through glaciolacustrine sediment. Journal of Geochemical Exploration, 19, 277–304.

Smee, B.W., 1998. A new theory to explain the formation of soil geochemical responses over deeply covered gold mineralisation in arid environments. Journal of Geochemical Exploration, 61, 149–172.

Smee, B.W., 2003. Theory behind the use of soil pH measurements as an inexpensive guide to buried mineralisation, with examples. Explore, 118, 1 page.

Stevenson, R.W., 1959. Kennco Explorations, (Western) Ltd. report on the geological, geochemical and geophysical surveys on the Gnawed Mountain group, east and west slopes of Gnawed Mountain, Highland Valley area, 50° 120° SW, 50° 121° SE. Ministry of Energy and Mines, ARIS Assessment Report 00286, 25 pages.

Stumpf, A.J., Broster, B.E., Levson, V.M., 2000. Multiphase flow of the Late Wisconsinan Cordilleran ice sheet in western Canada. Geological Society of America Bulletin 112, 1850–1863.

Swift, M.J., Anderson, J.M., 1994. Biodiversity and ecosystem function in agricultural systems *in* Biodiversity and Ecosystem Function, Schulze, E.-D., Mooney, H.A. (eds.), 15–41.

Sutherland, D., 2015. Spatiotemporal Geochemical Hydrocarbons, Actlabs Geochemical Workshop, Vancouver Convention Centre, presented the 21st of January.

Swift, M.J., Anderson, J.M., 1994. Biodiversity and ecosystem function in agricultural systems *in* Biodiversity and Ecosystem Function, Schulze, E.-D., Mooney, H.A. (eds.), 15–41.

Teck Resources Limited, 2018. 2017 Annual Information Form, URL: [http://www.teck.com/media/2017-AIF.pdf] accessed 2018/03/01.

Tipper, H.W., 1971a. Multiple glaciations in central British Columbia. Canadian Journal of Earth Sciences, 8, 743–752.

Tipper, H.W., 1971b. Glacial geomorphology and Pleistocene history of central British Columbia. Geological Survey of Canada, Bulletin 196, 89 pages.

Townley, B., Puig, A., Ojeda, G., Luca, R., Vargas, T., LeRoux, J., 2007. Understanding real time processes behind the development of surface geochemical expressions from ore bodies beneath cover: source to surface and detection by means of collector devices. Geochemical Case Histories & Geochemical Exploration Methods Paper 88, *in* Proceedings of Exploration 07: Fifth Decennial International Conference on Mineral Exploration, 1019–1021.

United States Department of Agriculture, 2014. Kellogg soil survey laboratory methods manual. Soil Survey Investigations Report 42(5), R. Burt and Soil Survey Staff (eds.), Natural Resources Conservation Service, 1001 pages.

van Bemmelen, J.W., 1890. Über die Bestimmung des Wassers, des Humus, des Schwefels, der in den colloïdalen Silikaten gebundenen Kieselsäure, des Mangans u. s. w. im Ackerboden. Die Landwirthschaftlichen Versuchs-Stationen, 37, 279–290

van Geffen, P.W.G., Kyser, T.K., Oates, C.J., Ihlenfeld, C., 2012. Till and Vegetation geochemistry at the Talbot VMS Cu-Zn prospect, Manitoba, Canada: implications for mineral exploration. Geochemistry: Exploration, Environment, Analysis, 12, 67–88.

van Geffen, P.W.G., Kyser, T.K., Oates, C.J., Ihlenfeld, C., 2014. Evaluation of partial digestions for soils to detect a deeply buried VMS Cu-Zn prospect in boreal forests. Geochemistry: Exploration, Environment, Analysis, 15(1), 27–38.

Violante, A., Cozzolino, V., Perelomov, L., Caporale, A.G., Pigna, M., 2010. Mobility and bioavailability of heavy metals and metalloids in soil environments. Journal of Soil Science and Plant Nutrition, 10(3), 268–292.

Vodyanitskii, Y.N., Savichec, A.T., 2012. Lanthanides in soils: X-ray determination, spread in background and contaminated soils in Russia, ch. 16 *in* Panagiotaras, D. (ed.), Geochemistry – Earth's System Processes, InTech, available from: https://www.intechopen.com/books/geochemistry-earth-s-system-processes/lantanides-in-soils-x-ray-determination-spread-in-background-and-contaminated-soils-in-russia.

Waters, B.M., Armbrust, L.C., 2013. Optimal copper supply required for normal plant iron deficiency responses. Plant Signaling and Behaviour, 8(12), 5 pages.

Watmough, S.A., 1997. An evaluation of the use of dendrochemical analyses in environmental monitoring. Environmental Reviews, 5, 181–201.

Watmough, S.A., 1999. Monitoring historical changes in soil and atmospheric trace metal levels by dendrochemical analysis. Environmental Pollution, 106, 391–403.

Winterburn, P.A., Noble, R.R.P., Lawie, D., 2017. Advances in exploration geochemistry, 2007 to 2017 and beyond, *in:* Tschirhart, V, and Thomas, M.D. (eds.), Proceedings of Exploration 17: Sixth Decennial International Conference on Mineral Exploration, Paper 34, 495–505.

Witte, K.M., Wanty, R.B., Ridley, W.I., 2004. Engelmann Spruce (Picea engelmannii) as a biological monitor of changes in soil metal loading related to past mining activity. Applied Geochemistry, 19, 1367–1376.

Weinstein, C., Moynier, F., Wang, K., Paniello, R., Foriel, J., Catalano, J., Pichat, S., 2011. Cu isotopic fractionation in plants. Chemical Geology, 286, 266–271.

White, W.M., 2013. Geochemistry. Wiley-Blackwell, Hoboken, New Jersey, 668 pages.

Yong, R.N., Phadungchewit, Y., 1993. pH influence on selectivity and retention of heavy metals in some clay soils. Canadian Geotechnical Journal, 30, 821–833.

Zhu, X.K., Guo, Y., Williams, R.J.P., O'Nions, R.K., Matthews, A., Belshaw, N.S., Canters, G.W., de Waal, E.C., Weser, U., Bergess, B.K., Salvatio, B., 2002. Mass fractionation processes of transition metal isotopes. Earth and Planetary Science Letters, 200, 47–62.

Zhu, X.K., Li, S.Z., Luo, Y.M., Wu, L.H., 2010. Copper isotope fractionation by higher plants. Geochimica et Cosmochimica Acta, 74, A1234.